



Mechanisms of serotonergic control in fear-related neural circuits and behaviour

Ayesha Sengupta

Queen's College
Departments of Pharmacology & Experimental Psychology
University of Oxford

National Institutes of Health

This dissertation is submitted for the degree of
Doctor of Philosophy
2017

To my parents, Amit and Anuradha,
to Alexei,
for supporting me on my quest to conquer fear

"*To conquer fear is the beginning of wisdom.*" - Bertrand Russell

"*The brave man is not he who does not feel afraid, but he who conquers that fear.*" - Nelson Mandela

"*Remember, if you ever need a helping hand, it's at the end of your arm; as you get older, remember you have another hand: The first is to help yourself, the second is to help others.*"

- Audrey Hepburn

Acknowledgements

There are many people all over the world to whom I am eternally grateful; without their guidance, friendship, and inspiration, I would have no thesis.

I will not question the enormous amount of luck that brought me not to one, not to two, but to *three* wonderful supervisors. I admire them for being brilliant scientists, but also because they are genuinely good people. The final sentence of my thesis is a tribute to the many things my supervisors have taught me, because what better way to prove I have learned something than by deliberately doing the exact opposite? To Trevor – a first person narrative; to David – a one-sentence paragraph; to Andrew – an awkward alliteration.

I want to thank Prof. Trevor Sharp for being the kind of professor who comes into the lab to fix an HPLC machine with his bare hands (i.e. *sans* gloves), for going to the animal facility with me when I was a scared first-year PhD student and doing the cervical dislocations for my experiment. For pushing me to be the best version of myself and not letting me settle for any less. And for using “alas” and “take a chill pill” in the same email.

I want to thank Prof. David Bannerman for having the patience and kindness to sit down and draw out basic statistical concepts on scrap paper for a twenty-something year old who, to paraphrase George R. R. Martin, knows nothing. That lesson has had a butterfly effect and passed itself onto other people. For trans-Atlantic Skype sessions in the middle of the night (and my sincerest apologies for waking up Brenda with our nature vs. nurture debate). For pursuing the good science. For meetings about almost everything except science (sports I have never heard of; shows/books; politics; emotions, both scientific and personal).

I want to thank Dr. Andrew Holmes for being empowering and helping me figure out how to be, or not to be, a scientist. For the few but precious moments of praise. For somehow managing to return documents thousands of words long within hours with useful feedback. For some of the most random emails from my PhD experience. For appreciating my rather Germanic senses of organisation and humour (which can sometimes be the same thing).

I would also like to thank Prof. Marco Capogna for giving me the exciting opportunity to work in his lab and for making my first paper happen.

I would like to thank Marco B for being my Yoda, Obi-Wan, and Qui-Gon rolled into one. For being an inspiration, for being brilliant but kind, and for making impossible things possible.

For a valuable lesson he taught me about science and life: “You don’t have to ask, you have to demand!” For everything does a Padawan him thank, and most of all, for friendship.

I would like to thank the Sharp lab for two amazing years in person, and two more in spirit. Judith S, without whom this thesis would literally and figuratively not be submitted. Chris, Florence, Julia, and Katharina for their help and friendship.

I also want to thank the Bannerman lab and BNU community, especially Amy, Katie H, Katie J, and Steve M.

I am deeply grateful for the incredible people I got to know in Oxford. I would like to thank them for their friendship and invaluable support. I treasure the time we were able to spend together. Anna K, Dimi, Lydia, Nora, Santi, Sarah H, Sebas, Sophie, Vasileios.

I want to thank the Holmes lab for being a family. Lindsay, Lucas, Mio, Olena, and Ozge, who prove that it really is possible to do everything. Shana, for being my graduate soul sister. Aaron, Abby L, Abby P, Adrina, and Emma, for all the late nights and weekends eating takeout in lab and pondering the meaning of life.

I would like to thank the BSB (especially Angela Cooke, Carol Broadbent, Debbie Cobley, Richard Corderoy, and the Level 2 staff) and FLAC (especially Dr. Andrea Barnes, Angela Szwec, Charles Evans, Hector Aguirre, Jorge Medrano, Kenneth Ayisi, and Dr. Raouf Kechrid) for taking such great care of my mice and me.

I want to thank Dr. Phil Burnet, Mary Walker, and Li Chen for helping me genotype what must have been over a thousand earclips. I also want to thank Katie Whitworth for her support.

I am thankful to the Wellcome Trust and NIH for giving me the chance to do this research.

I want to thank Alexei for being even better than expected. For understanding me when I didn’t make sense (and especially when I did). For being my best friend, my partner, and my inspiration. For having a big brain and an even bigger heart.

I would like to thank my parents, Amit and Anu, for helping me find resilience, for being with me through the best and worst times, and for love that transcends borders and barriers. For giving me all the opportunities in life, for protecting me, for being the kind of people I hope to be. For their infallible courage and for taking the road less travelled. I will always look up to them. They are my heroes.

Declaration

I hereby declare that no part of this thesis has been accepted or is currently being submitted for any degree, diploma or certificate or other qualification in this university or elsewhere. This dissertation contains less than 50,000 words including appendices, references, and tables, and has less than 250 figures. I confirm that all results presented in the thesis are wholly my own work, with the following exceptions.

Dr. Marco Bocchio prepared the brain sections (including staining), acquired the images, and created the panels for Figure 5.1A, B, C, E; Figure 5.2A; Figure 5.5A (pp. 130, 133, 140). Dr. Bocchio also quantified ChR2/5-HT overlap in section 5.3.1 (p. 129). Dr. Bocchio, Dr. Linda Katona, and Dr. Gunes Unal carried out VGluT3 staining, imaging, and panel arrangement of VGluT3-expressing 5-HT axons for Figure 5.2F, G (p. 133).

Abstract

Serotonin (5-HT) neurotransmission is strongly implicated in affective psychopathologies, with first-line drugs selectively targeting the 5-HT system. Further evidence for the role of 5-HT as an important regulator of emotional states comes from human gene association studies. These have identified polymorphic variants of the 5-HT transporter (5-HTT) gene with reduced transcription efficacy. Lower 5-HTT expression associates with susceptibility to affective disorders and heightened amygdala reactivity to fearful stimuli. The mechanisms by which 5-HTT gene variation leads to altered amygdala function and fear-related behaviour are unknown. The experiments presented in this thesis study these associations in tractable animal models that allow temporal- and circuit-specific control over 5-HT signalling. Specifically, a translationally relevant mouse model of 5-HTT expression variation and an optogenetic approach are used to probe how changes in 5-HT transmission shape fear-related behaviours.

Using an array of behavioural tests, it was found that 5-HTT overexpressing (OE) mice exhibit a low-fear/anxiety phenotype that is already established in adolescence, indicating a possible neurodevelopmental trajectory. Acute pharmacological blockade of the 5-HTT at the time of behavioural testing did not rescue the low-fear phenotype in adolescent 5-HTT OE mice, whereas 5-HTT blockade during an early postnatal period did reverse it. These results identify a developmental origin of the fear-related phenotype associated with 5-HTT expression variation.

Next, *in vivo* optogenetic tools were employed during a fear learning task to control neuromodulation of the basal amygdala (BA) by 5-HT neurons arising from the dorsal raphe (DRN). Photoexcitation of the DRN-BA 5-HT projection pathway enhanced fear learning and impaired fear extinction, while photoinhibition caused a fear learning deficit and facilitated fear extinction. Thus, a bidirectional functional role in fear learning for the BA-targeting 5-HT pathway was characterised.

The effect of optogenetic photoexcitation of the DRN-BA 5-HT pathway on BA single unit and network activity during the fear learning task was then recorded *in vivo*. The study revealed that 5-HT projection activation promoted a neurophysiological state (both in terms of individual neuron activity and network oscillations) in the BA that has previously been associated with fear expression.

Ex vivo electrophysiology experiments then explored the effect of optogenetic activation of the DRN-BA 5-HT pathway on the BA microcircuitry. These latter experiments identified clear evidence of 5-HT and glutamate co-transmission within the BA, which functioned in a cell type-specific and frequency-dependent manner.

Finally, a combination of retrograde tracing and immunohistochemistry was applied to analyse the neurochemical identity of DRN neurons that project to the BA. The majority of these neurons were found to co-express markers for 5-HT and glutamate. To evaluate the contribution of 5-HT transmission from DRN-BA 5-HT projections to fear learning, optogenetics was combined with local infusion of 5-HT receptor antagonists. This experiment demonstrated that photoexcitation-induced enhancement of fear learning was mediated by 5-HT-dependent mechanisms.

In summary, this thesis presents new evidence that DRN-BA 5-HT projections exert circuit-, temporal-, and 5-HT receptor-specific regulation of fear-related behaviour. These results highlight the importance of elucidating precise actions of 5-HT transmission in moving towards a more accurate understanding of how the 5-HT system influences emotional states.

Table of contents

LIST OF FIGURES XVIII
LIST OF TABLES XXI
ABBREVIATIONS XXII
CHAPTER 1 GENERAL INTRODUCTION 1
1.1 Measurements of fear-related behaviour 2
1.1.1 Fear learning tasks 3
1.1.1.1 Neural networks of fear learning *4*
1.1.2 Anxiety tasks 5
1.1.3 Optogenetic control of circuits 6
1.2 The amygdala 8
1.2.1 Subnuclei of the amygdala 8
1.2.2 Efferent and afferent connectivity of the amygdala 10
1.2.3 The amygdala and fear learning 11
1.2.3.1 Synaptic plasticity *13*
1.2.3.2 Oscillations *13*
1.3 The central 5-HT system 14
1.3.1 Efferent and afferent connectivity of midbrain 5-HT neurons 14
1.3.2 5-HT synthesis and metabolism 18
1.3.3 5-HT receptors 19
1.3.4 The 5-HTT 21
1.3.5 Amygdala 5-HT transmission in fear-related behaviour 22
1.4 Aims of this thesis 26
CHAPTER 2 DEVELOPMENTAL ORIGIN OF FEAR-RELATED PHENOTYPES OF 5-HT TRANSPORTER OVEREXPRESSING MICE 29
2.1 Introduction 29
2.1.1 The human 5-HTT and its influence on negative emotionality and the amygdala 29
2.1.2 The rodent 5-HTT and its association with fear-related behaviours and neural circuits 31

2.1.3 Impact of altered 5-HT transmission in early life 34
2.1.4 Aims of this chapter 35
2.2 Materials and methods 36
2.2.1 Experimental animals 36
2.2.2 Behavioural protocols 36
2.2.2.1 Elevated plus maze 37
2.2.2.2 Hyponeophagia 37
2.2.2.3 Locomotor activity 37
2.2.2.4 Fear learning 38
2.2.3 High-performance liquid chromatography 39
2.2.4 Drug treatment 40
2.2.5 Statistical analysis 40
2.3 Results 41
2.3.1 Characterisation of adolescent 5-HTT OE anxiety phenotype 41
2.3.2 Characterisation of adolescent 5-HTT OE fear phenotype 42
2.3.3 Measurement of adolescent 5-HTT OE body weight and locomotor activity 44
2.3.4 Characterisation of adolescent 5-HTT OE neurochemical phenotype 44
2.3.5 Effect of acute citalopram treatment during conditioning on fear phenotype of adolescent 5-HTT OE mice 45
2.3.6 Effect of postnatal citalopram treatment on anxiety phenotype of adolescent 5-HTT OE mice 48
2.3.7 Effect of postnatal citalopram treatment on the fear phenotype of adolescent 5-HTT OE mice 49
2.3.8 Effect of postnatal citalopram treatment on body weight and locomotor activity of adolescent 5-HTT OE mice 52
2.4 Discussion 53
2.4.1 Developmental trajectory of fear-related phenotypes in adolescent 5-HTT OE mice 54
2.4.2 Altered 5-HT transmission in adolescent 5-HTT OE mice 55
2.4.3 Control of distinct emotional behaviours by the 5-HT system 56

2.4.4 Comparing adolescent and adult 5-HTT OE phenotypes 57

2.4.5 Functional relationship between variation in 5-HTT expression and corresponding phenotypes 58

2.4.6 Conclusions 59

CHAPTER 3 5-HT NEURONS INFLUENCE FEAR LEARNING BY MODULATING THE BASAL AMYGDALA 60

3.1 Introduction 60

3.1.1 Impact of the 5-HT system on the amygdala and fear 60

3.1.2 5-HT innervation of the amygdala from the DRN 62

3.1.3 5-HT in the amygdala and its impact on fear 63

3.1.4 Aims of this chapter 64

3.2 Methods 65

3.2.1 Experimental animals 65

3.2.2 Viral transfection and optic fibre implantation 65

3.2.3 Behavioural testing and optogenetic stimulation 66

3.2.4 Histology 67

3.2.5 Statistical analysis 68

3.3 Results 68

3.3.1 Selective manipulation of BA 5-HT projections during fear behaviour 68

3.3.2 Optogenetic excitation of BA 5-HT projections during fear conditioning 69

3.3.3 Optogenetic inhibition of BA 5-HT projections during fear conditioning 72

3.3.4 Optogenetic manipulations of BA 5-HT projections during fear extinction 73

3.4 Discussion 77

3.4.1 5-HT projection activity in the BA bidirectionally regulates fear learning 77

3.4.2 5-HT projection activity in the BA disrupts fear extinction 79

3.4.3 Functional considerations of 5-HT neuromodulation in the BA 80

3.4.4 Conclusions 82

CHAPTER 4 5-HT NEURONS ALTER BASAL AMYGDALA ACTIVITY DURING FEAR LEARNING 83

4.1 Introduction 83

4.1.1 Human amygdala activation during fear 83

4.1.2 Activity of rodent amygdala neurons in fear 84

4.1.3 Network activity of rodent amygdala in fear 86

4.1.4 5-HT and its influence on amygdala activity in fear 86

4.1.5 Aims of this chapter 88

4.2 Methods 88

4.2.1 Experimental animals 88

4.2.2 Viral transfection and optrode-array implantation 89

4.2.3 Behavioural testing and optogenetic stimulation 90

4.2.4 *In vivo* neuronal recordings 91

4.2.5 Histology 92

4.2.6 Statistical analysis 93

4.3 Results 94

4.3.1 Selective excitation of 5-HT projections and recording of BA neuronal activity during fear 94

4.3.2 Fear conditioning: BA single unit activity during optogenetic excitation of DRN-BA 5-HT projections 97

4.3.3 Fear conditioning: BA network activity during optogenetic excitation of DRN-BA 5-HT projections 100

4.3.4 Fear retrieval: BA single unit activity after optogenetic excitation of DRN-BA 5-HT projections 101

4.3.5 Fear retrieval: BA network activity after optogenetic excitation of DRN-BA 5-HT projections 105

4.3.6 Extinction retrieval: BA single unit activity after optogenetic excitation of DRN-BA 5-HT projections 108

4.3.7 Extinction retrieval: BA network activity after optogenetic excitation of DRN-BA 5-HT projections 111

4.4 Discussion 114

4.4.1 5-HT projection excitation alters BA neuronal activity *in vivo* 114

4.4.2 5-HT projection excitation during conditioning alters BA single unit activity during fear retrieval and extinction retrieval 116

4.4.3 5-HT projection excitation during conditioning changes network activity in the theta and delta ranges 117

4.4.4 Functional implications for 5-HT modulation of BA activity in fear learning 119

4.4.5 Conclusions 120

CHAPTER 5 5-HT NEURONS MODULATE THE BASAL AMYGDALA VIA 5-HT AND GLUTAMATE CO-TRANSMISSION 121

5.1 Introduction 121

5.1.1 Functional importance of 5-HT transmission in the amygdala 121

5.1.2 5-HT signalling in the BLA 122

5.1.3 Aims of this chapter 123

5.2 Materials and methods 123

5.2.1 Animals 123

5.2.2 Viral transfection 124

5.2.3 Electrophysiological recordings 124

5.2.4 Data analysis 126

5.2.5 Immunohistochemistry 127

5.2.6 Quantification of 5-HT immunoreactive ChR2/YFP-transfected neurons 128

5.2.7 Drugs 128

5.2.8 Statistical analysis 128

5.3 Results 129

5.3.1 Selective targeting of ChR2 expression to 5-HT neurons 129

5.3.2 Responses evoked in BA INs upon photoexcitation of DRN-BA 5-HT projections 131

5.3.3 Heterogeneity of BA IN responses to photoexcitation of DRN-BA 5-HT projections 136

5.3.4 Responses evoked in BA PNs upon photoexcitation of DRN-BA 5-HT projections 138

5.4 Discussion 141

5.4.1 Optogenetic control of 5-HT release 141

5.4.2 Release of glutamate from 5-HT neurons 143

5.4.3 Frequency-dependent modulation of BA INs by 5-HT 144

5.4.4 Functional implications 146

5.4.5 Conclusions 147

CHAPTER 6 NEUROCHEMICAL CHARACTERISATION OF BASAL AMYGDALA MODULATION BY 5-HT NEURONS DURING FEAR LEARNING 148

6.1 Introduction 148

6.1.1 Neurochemical identities of DRN neurons 148

6.1.2 Co-transmission of glutamate from 5-HT neurons 152

6.1.3 Ascending projections of the DRN 154

6.1.4 Aims of this chapter 155

6.2 Methods 156

6.2.1 Experimental animals 156

6.2.2 Retrograde tracing and immunohistochemistry 156

6.2.2.1 CTb with 5-HT/VGluT3/c-fos 156

6.2.2.2 CTb with GAD2 or DAT 157

6.2.2.3 Dopamine beta-hydroxylase 157

6.2.3 Quantification of co-localisation with CTb 158

6.2.4 Viral transfection and cannulation 158

6.2.5 Infusions and optogenetic stimulation 159

6.2.6 Behavioural testing 160

6.2.7 Histology 161

6.2.8 Drugs 161

6.2.9 Statistical analysis 162

6.3 Results 162

6.3.1 Identification of BA-projecting neurons in the DRN 162

6.3.2 Neurochemical identities of BA-projecting DRN neurons 163
6.3.3 Optogenetic excitation of BA 5-HT projections and pharmacological antagonism of local 5-HT receptors 168
6.4 Discussion 170
6.4.1 Fear conditioning preferentially recruits BA-projecting DRN neurons that co-express markers for 5-HT and glutamate 171
6.4.2 Co-localisation of neurochemical markers in DRN neurons 172
6.4.3 5-HT projections to the BA regulate fear via 5-HT transmission 174
6.4.4 Conclusions 176
CHAPTER 7 GENERAL DISCUSSION 177
7.1 Thesis background and aims 177
7.2 Short summary of results 178
7.3 Summary of main findings 179
7.4 Discussion of main findings 183
7.4.1 Activation of BA-projecting DRN 5-HT neurons during fear conditioning 183
7.4.2 Mechanisms of 5-HT modulation in the BA 185
7.4.3 5-HT and glutamate co-transmission 186
7.4.4 Neurodevelopmental formation of the 5-HT transmission system 188
7.5 Technical limitations and future directions 190
7.5.1 Achieving temporally precise measurements of BA 5-HT projection activity 191
7.5.2 Probing modulation of BA information processing by 5-HT transmission 192
7.5.3 Achieving precise manipulation of VGluT3 function 194
7.5.4 Towards a study of circuit dysfunction in psychopathology 195
7.6 Conclusions 197
REFERENCES 199

List of figures

Figure 1.1 – Projection pathways to and from the amygdala that mediate different behaviours 2

Figure 1.2 – Optogenetic tools enabling photoexcitation and photoinhibition of neurons 7

Figure 1.3 – Subnuclei of the amygdaloid complex 9

Figure 1.4 – The amygdala as part of a network underlying conditioned fear and extinction 13

Figure 1.5 – Efferent 5-HT projections of midbrain raphe nuclei 16

Figure 1.6 - Afferent projections to the midbrain raphe nuclei 18

Figure 1.7 – 5-HT innervation of the amygdala 24

Figure 1.8 –5-HT receptor localisation in BLA circuit 24

Figure 1.9 – Schematic of thesis chapters 28

Figure 2.1 – Schematic representation of 5-HT synaptic terminal 31

Figure 2.2 – Adolescent 5-HTT OE mice show reduced anxiety on unconditioned tasks compared to WTs 42

Figure 2.3 – Adolescent 5-HTT OE mice show reduced fear in a cued fear conditioning task 43

Figure 2.4 – Weight change and locomotor activity in adolescent 5-HTT OE mice 44

Figure 2.5 – Adolescent 5-HTT OE mouse brains contain lower 5-HT levels in the DRN and BLA 45

Figure 2.6 – Acute citalopram treatment does not rescue cued fear learning in adolescent 5-HTT OE mice but enhances fear in WT mice 47

Figure 2.7 – Postnatal citalopram treatment increases anxiety in adolescent 5-HTT OE mice 49

Figure 2.8 – Postnatal citalopram treatment rescues the fear phenotype of adolescent 5-HTT OE mice 51

Figure 2.9 – Postnatal citalopram treatment does not affect the weight change or locomotor activity of adolescent 5-HTT OE mice 53
Figure 3.1 – Optogenetic manipulation of 5-HT projections during fear conditioning or extinction 69
Figure 3.2 – Optogenetic excitation of BA 5-HT projections during fear conditioning enhances fear 71
Figure 3.3 - Optogenetic inhibition of BA 5-HT projections during fear conditioning reduces learned fear 73
Figure 3.4 - Optogenetic manipulations of BA 5-HT projections during fear extinction influence learned fear 76
Figure 4.1 – Optogenetic excitation of DRN-BA 5-HT projections during fear conditioning alters BA activity 96
Figure 4.2 - Optogenetic excitation of DRN-BA 5-HT projections during fear conditioning alters BA neuronal activity 100
Figure 4.3 - Optogenetic excitation of DRN-BA 5-HT projections during fear conditioning alters BA network activity 101
Figure 4.4 – Optogenetic excitation of DRN-BA 5-HT projections during fear conditioning alters BA neuronal activity during fear retrieval 105
Figure 4.5 - Optogenetic excitation of DRN-BA 5-HT projections during fear conditioning alters BA network activity during fear retrieval 108
Figure 4.6 - Optogenetic excitation of DRN-BA 5-HT projections during fear conditioning alters BA single unit activity during extinction retrieval 110
Figure 4.7 - Optogenetic excitation of DRN-BA 5-HT projections during fear conditioning alters BA network activity during extinction retrieval 114
Figure 5.1 - Expression of ChR2 in dorsal raphe 5-HT neurons 130
Figure 5.2 - 5-HT neurons release glutamate onto BA INs 133
Figure 5.3 - 5-HT neurons modulate BA INs bidirectionally via 5-HT release 135
Figure 5.4 - 5-HT neurons differentially modulate BA INs 137

Figure 5.5 - 5-HT neurons inhibit BA PNs via 5-HT_{1A} receptors and enhanced GABA release 140

Figure 6.1 – Anatomy of the DRN and MRN 150

Figure 6.2 – 5-HT neurons in the DRN and MRN 150

Figure 6.3 – Glutamate neurons in the DRN and MRN 151

Figure 6.4 – GABA and dopamine neurons in the DRN 152

Figure 6.5 – Retrograde labelling of BA-projecting DRN neurons 163

Figure 6.6 – DRN neurons that project to the BA are 5-HT and glutamatergic 165

Figure 6.7 – DRN neurons that project to the BA are not GABAergic, dopaminergic, or noradrenergic 167

Figure 6.8 - Optogenetic excitation of BA 5-HT projections during fear conditioning enhances fear via 5-HT transmission 170

Figure 7.1 – Schematic of DRN-BA 5-HT pathway 183

List of tables

Table 1.1 – Characteristics of fear *versus* anxiety 3

Table 1.2 – Summary of 5-HT receptors in the mammalian brain 20

Table 1.3 – Summary of behavioural effects of 5-HT interventions in the amygdala 25

Table 2.1 – Pre-planned statistical individual pairwise comparisons..... 41

Table 2.2 – Unconditioned responses to the shock during fear conditioning 43

Table 2.3 - Unconditioned responses to the shock during fear conditioning training with acute citalopram.....47

Table 2.4 - Unconditioned responses to the shock during fear conditioning training with acute citalopram..... 51

Abbreviations

5-HIAA	5-hydroxyindoleacetic acid
5-HT	5-hydroxytryptamine, serotonin
5-HTT	5-HT transporter, SERT
5-HTT KO	5-HTT knockout
5-HTT OE	5-HTT overexpressing
5-HTTLPR	5-HTT-linked polymorphic region
ACSF	artificial cerebrospinal fluid
a.u.	arbitrary units
BA	basal amygdala, basal and basomedial nuclei of the amygdala
BLA	basolateral amygdala, basolateral complex of the amygdala
ChR2	channelrhodopsin-2
CR	conditioned response
CS	conditioned stimulus
CTb	cholera toxin subunit B
DAT	dopamine transporter
DMSO	dimethyl sulfoxide
DRN	dorsal raphe nucleus
EPSC	excitatory postsynaptic current
GABA	γ-aminobutyric acid
GAD	glutamate decarboxylase
GFP	green fluorescent protein
HPLC	high-performance liquid chromatography
iC++	chloride-conducting channelrhodopsin
IPSC	inhibitory postsynaptic current
ISI	inter-spike interval
i.p.	intraperitoneal

IN	interneuron
IQR	interquartile range
LA	lateral amygdala, lateral nucleus of the amydgala
MRN	median raphe nucleus
NA	numerical aperture
PBS	phosphate-buffered saline
PFA	paraformaldehyde
PN	principal neuron
PTSD	post-traumatic stress disorder
s.c.	subcutaneous
SEM	standard error of the mean
sIPSC	spontaneous inhibitory postsynaptic current
SSRI	selective serotonin reuptake inhibitor
Tph	tryptophan hydroxylase
UR	unconditioned response
US	unconditioned stimulus
VGluT	vesicular glutamate transporter
WT	wild-type
YFP	yellow fluorescent protein

Chapter 1 General introduction

"Better to be feared than loved," Niccolo Machiavelli wrote in the 16th century, and he made a reasonable point because like his work, fear memories can be powerful and enduring. Fear is an emotion crucial for survival; it can help individuals learn rapidly about threats in their environment. However, fear can also become maladaptive and debilitating, a cornerstone of affective psychopathology.

It is important to understand the neural mechanisms of emotional memory formation that become dysregulated when fear becomes excessive in affective disorders such as anxiety, phobias, and post-traumatic stress disorder (PTSD). Different theories aim to explain the neural mechanisms of how learning is strengthened by emotional salience. The emotional tagging theory posits that salient experiences activate the amygdala, which, in turn, moderates synaptic plasticity in brain regions that encode memories (Bergado et al., 2011). The amygdala seems to be a vital anatomical target for pathological fear, because lesions of the amygdala in humans impair innate and learned fear expression (Bechara et al., 1995; LaBar et al., 1995; Adolphs, 1997)

The amygdala is a limbic structure that is part of a wider network involved in mediating a range of emotional behaviours (Figure 1.1). Its role in emotional regulation has garnered much scientific interest in the past decades, with the number of publications dedicated to the amygdala steadily rising since the 1960's (Janak and Tye, 2015). Across species, the amygdala receives dense serotonergic (5-hydroxytryptamine, 5-HT) innervation

(Asan et al., 2013). In the treatment of affective disorders, first-line drugs selectively target the 5-HT system (Nemeroff and Owens, 2002). This forms part of the evidence that 5-HT transmission is an important regulator of amygdala function and emotionality, although the details of this modulation are not completely understood. This thesis uses a translationally relevant genetic mouse model and optogenetic approaches to dissect 5-HT mechanisms of negative affect, particularly in the amygdala, on a temporally- and circuit-specific scale.

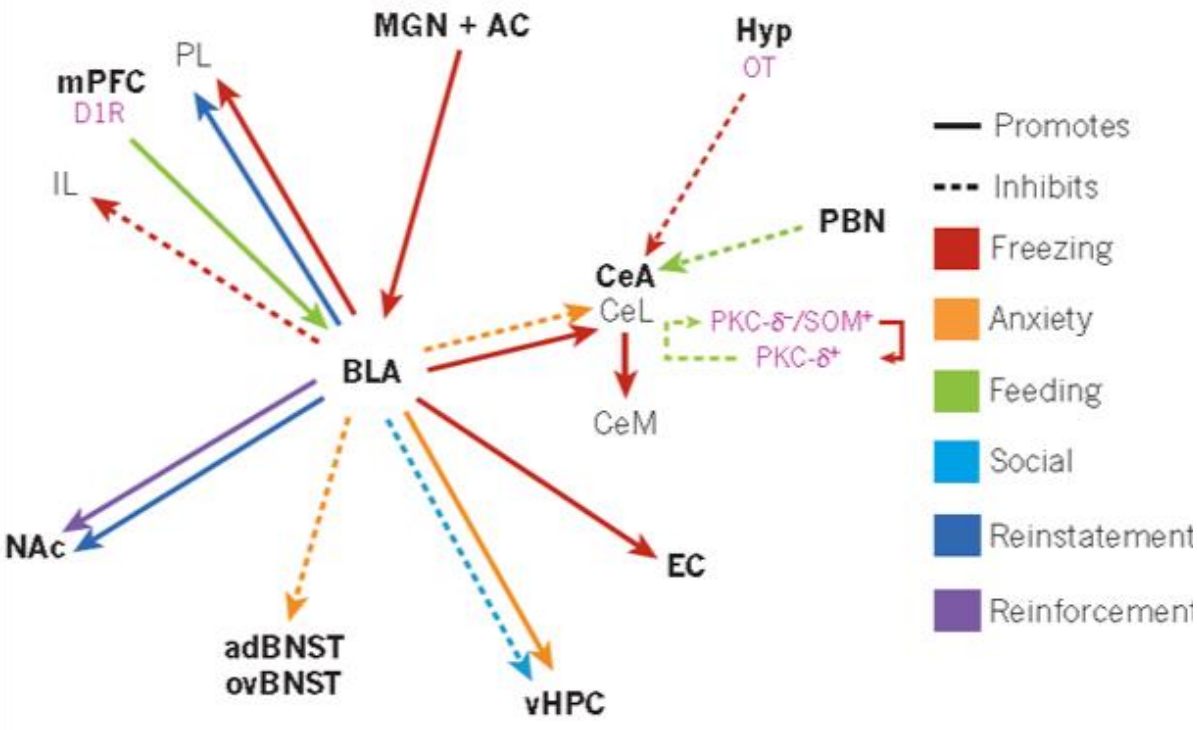


Figure 1.1 – Projection pathways to and from the amygdala that mediate different behaviours
Simplified schematic representation of efferent and afferent pathways of the amygdala that control particular behaviours, as demonstrated through opto- and pharmacogenetics studies. Solid and dashed lines indicate promotion and inhibition of behaviours, respectively. For simplicity, this schematic does not include all anatomically and electrophysiologically validated projection pathways. AC, auditory cortex; adBNST, anterodorsal bed nucleus of the stria terminalis; CeA, central nucleus of the amygdala; CeL, lateral CeA; CeM, medial CeA; D1R, dopamine 1 receptor; EC, entorhinal cortex; Hyp, hypothalamus; IL, infralimbic; MGN, medial geniculate nucleus; mPFC, medial prefrontal cortex; NAc, nucleus accumbens; OT, oxytocin; ovBNST, oval nucleus of the BNST; PBN, parabrachial nucleus; PKC, protein kinase C; PL, prelimbic; SOM, somatostatin; vHPC, ventral hippocampus. Adapted from Janak and Tye (2015).

1.1 Measurements of fear-related behaviour

Several paradigms of animal behaviour aim to model fear and anxiety in rodents (Griebel, 1995). Although both are defined by emotional states of negative affect, fear and anxiety derive from threats of different natures (Table 1.1). Whereas fear is targeted towards

the presence of a specific environmental threat, anxiety arises more diffusely from the possibility of a potential threat in the future (Sylvers et al., 2011). Thus, behavioural protocols to test fear behaviour are often based on conditioned responses to stimuli predictive of noxious stimuli, while anxiety-like behaviour is commonly considered through performance on unconditioned ethological tasks.

Table 1.1 – Characteristics of fear *versus* anxiety
Adapted from Sylvers et al. (2011).

Dimension	Fear	Anxiety
Emotional valence	Negative	Negative
Temporal focus	Present	Future
Duration of arousal	Phasic/brief	Tonic/sustained
Defensive direction	Avoidance/escape	Approach/avoidance
Specificity of threat	Specific	Diffuse
Pain perception	Blunted	Enhanced

1.1.1 Fear learning tasks

Fear learning can be measured in mice using classical (Pavlovian) conditioning (Fendt and Fanselow, 1999). An initially neutral conditioned stimulus (CS, e.g. an auditory tone) is paired with an unconditioned stimulus (US, e.g. an electric shock), which evokes an instinctive unconditioned response (UR, e.g. burst of activity). As mice learn the association between the CS and the US, the CS elicits a conditioned response (CR, e.g. freezing). Thus, the freezing response can be taken as a measurement for fear expression. Because mice form fear memories, not only with the CS cue but also with the conditioning context, the degree of learning to the discrete CS is usually measured in a different context.

A typical fear learning task might involve a fear conditioning session, followed by a fear retrieval test after 24 hours. In this arrangement, the task only evaluates the stages of acquisition and retrieval of a fear memory. In another configuration, the fear learning task entails a fear conditioning session, followed by fear extinction training 24 hours later, and finally an extinction retrieval test another 24 hours later (Milad and Quirk, 2012). In the

latter version, the task also assesses the stages of acquisition and retrieval of an extinction memory.

Rodent fear learning paradigms can be translated to human studies (Delgado et al., 2006). In humans, the CS activates a different type of CR (typically skin conductance). When fear learning becomes maladaptive, fear retrieval may be excessive or extinction impaired, as is likely to be the case for phobias or PTSD. Importantly, research across species demonstrates that the amygdala is a key neural correlate across all stages of fear learning, whereas the prefrontal cortex is involved in fear extinction in particular (LaBar et al., 1998; Milad et al., 2007; Sierra-Mercado et al., 2011) (see section 4.1.1 for a discussion of human functional imaging studies).

1.1.1.1 Neural networks of fear learning

Fear conditioning involves interplay between several different neural structures that together encode emotional memories (Davis, 1992; Maren and Quirk, 2004; Fanselow, 2010). In rodents, evidence suggests that the fear memory acquisition stage requires the basolateral (BLA) and central amygdala, as well as the periaqueductal grey (Muller et al., 1997; De Oca et al., 1998; Akirav et al., 2006; Wilensky et al., 2006). In fact, the periaqueductal grey likely relays instructive information to the amygdala during fear conditioning (Johansen et al., 2010). Data from a range of sources suggest that the amygdala mediates both cued and contextual fear conditioning, while the hippocampus is needed only for contextual fear conditioning (Kim and Fanselow, 1992; Phillips and LeDoux, 1992). Fear expression during cued retrieval is also likely mediated by the BLA and central amygdala, as well as the periaqueductal grey and prelimbic cortex (De Oca et al., 1998; Wilensky et al., 2006; Sierra-Mercado et al., 2011). Interestingly, activation of the infralimbic cortex impairs fear expression (Vidal-Gonzalez et al., 2006).

Fear extinction, rather than being an erasure of a previous memory, is the formation of a new one. This is reflected in the neural correlates of extinction memories, which, though located within the same brain structures as those of fear memories, involve distinct neuronal circuits (Herry et al., 2010). Based on a combination of electrophysiological recordings with lesion or pharmacological inactivation in rodents, studies show that fear extinction requires the BLA, ventral hippocampus, periaqueductal grey, and infralimbic cortex (Milad and Quirk, 2002; Maren and Quirk, 2004; McNally et al., 2004; Sierra-Mercado et al., 2011), as well as inhibition of the prelimbic cortex (Vidal-Gonzalez et al., 2006). Extinction involves distinct neurons of the BLA from those that represent fear memories, and is impaired by inactivation of the BLA by muscimol infusion (Herry et al., 2008).

Taken together, previous studies clearly indicate that the amygdala plays a key role in fear conditioning, expression, and extinction (for reviews, see Davis, 1992; LeDoux, 2003; Kim and Jung, 2006; Milad and Quirk, 2012), though different neurons may be involved in distinct functions. Similarly, the prelimbic and infralimbic areas of the prefrontal cortex likely mediate opposite effects, with the prelimbic favouring fear and the infralimbic extinction.

1.1.2 Anxiety tasks

Unconditioned anxiety can be tested using a range of tasks. In this thesis, experiments using the elevated plus maze and hyponeophagia tests are presented. The elevated plus maze comprises two open and two closed arms arranged in a plus formation, raised above the ground. The test draws on the conflict between the drive to explore new environments and find rewards (e.g. food or mates) as opposed to the drive to avoid danger (e.g. exposure to predators or heights). Therefore, the open arms are more aversive to mice and normally less explored than the closed arms (Handley and Mithani, 1984; Pellow et al., 1985). Highly anxious mice would experience a stronger drive to avoid danger and thus avoid the open arms, preferring to remain in the sheltered closed arms instead. The opposite would be true

for less anxious mice. The validity of the elevated plus maze has been demonstrated using drugs known to influence anxiety in humans. Anxiolytic (e.g. benzodiazepines, barbiturates) and anxiogenic (e.g. adrenocorticotropin, picrotoxin) drugs increase and decrease exploration of open arms, respectively.

The hyponeophagia test assesses the latency of a mouse to initiate eating a novel food in an unknown environment. This test also draws on the conflict between the drives to find food and to avoid unfamiliar, possibly dangerous situations. Highly anxious mice would hesitate to seek food, while less anxious mice would obtain the food more quickly. The task has been validated with anxiolytic (e.g. benzodiazepines) and anxiogenic (e.g. picrotoxin) drugs, which decrease and increase the latency to eat food, respectively (Shephard and Broadhurst, 1982).

Anxiety-like behaviour across both tasks is mediated by a common neural structure. Ventral hippocampus lesions increase open arm exploration on the elevated plus maze and reduce latency to begin eating in the hyponeophagia test (Bannerman et al., 2002). In contrast to the ventral hippocampus, lesions in the amygdala do not affect anxiety-like behaviour, indicating that these brain regions contribute distinct roles to anxiety (McHugh et al., 2004). An optogenetic study has demonstrated that BLA projections to the central amygdala could influence anxiety-like behaviour on the elevated plus maze, suggesting that the precise function of the amygdala in anxiety is still up for debate (Tye et al., 2011).

1.1.3 Optogenetic control of circuits

Genetically encoded, light-sensitive ion channels originally derived from microbes have been recently combined with gene delivery systems to control the activity of neurons with high temporal and spatial specificity (Bernstein and Boyden, 2011). Because these ion channels are genetically encoded and optically gated, the general approach is often referred to as optogenetics. The ion channels are analogous to transmembrane opsins involved in light

transduction in the mammalian eye, and passively or actively conduct cations (Na^+, H^+, K^+, Ca^{2+}) or anions (Cl^-) across the cell membrane to influence the excitability of neurons when light stimulation is delivered (Figure 1.2). Examples of such opsins include the cation-permeable channelrhodopsin-2 (ChR2) (Bernstein and Boyden, 2011) or chloride-conducting mutated channelrhodopsin (iC++) (Wiegert et al., 2017).

Currently, the optogenetic approach is being widely used in neuroscience to study the roles of particular neurons in behaviour. One way to achieve cell type-specific targeting of the opsins is through viral delivery combined with the Cre-recombinase (Cre) system (Atasoy et al., 2008). In this arrangement, the expression of virally-delivered genetic constructs encoding the opsins is dependent on recombination executed by the Cre enzyme. The Cre-dependent constructs can be introduced into transgenic mice expressing Cre under the control of a given promoter.

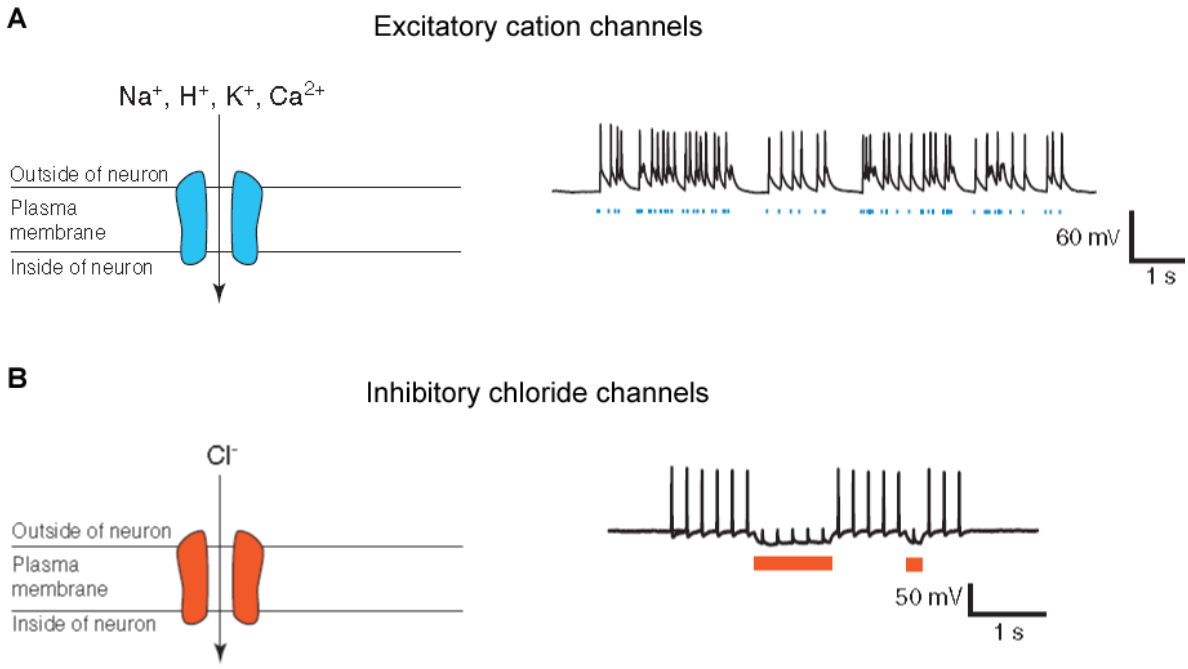


Figure 1.2 – Optogenetic tools enabling photoexcitation and photoinhibition of neurons
A. Opsin that conducts cations (left) and excites neuronal activity upon light stimulation (shown in blue) (right) **B**. Opsin that conducts chloride ions (left) and inhibits neuronal activity upon light stimulation (shown in orange) (right). Adapted from (Bernstein and Boyden, 2011).

1.2 The amygdala

The amygdala is a brain structure long considered important for emotional processing, and is highly conserved across species (Sah et al., 2003). Located in the temporal lobe, it comprises multiple interconnected subnuclei. The amygdala is connected with several other structures that, together, are involved in emotional regulation (Figure 1.1).

1.2.1 Subnuclei of the amygdala

The amygdala complex can be classified into three main groups: the BLA, cortical, and centromedial (Figure 1.3; Sah et al., 2003; Pape and Pare, 2010; Duvarci and Pare, 2014). In addition, there are also the intercalated cell masses and amygdalohippocampal area. These divisions are based on cytoarchitecture, immunohistochemistry, connectivity, and developmental origin.

The BLA complex contains the lateral (LA), basal, and basomedial subnuclei. For the scope of this thesis, the basal amygdala (BA) refers to the basal and basomedial subnuclei combined. The cytoarchitecture of the BLA complex has been likened to that of the cortex because the majority of neurons are glutamatergic principal neurons (PNs) (McDonald, 1982a). Unlike the cortex and hippocampus, however, the PNs in the BLA are not arranged in a laminar structure, but instead organised randomly (McDonald, 1984). The remaining minority of BLA neurons are local GABAergic interneurons (INs) (McDonald, 1982a). PNs and INs can be distinguished by their electrophysiological, neurochemical, and synaptic connection properties, and numerous classes of INs have been identified (Sah et al., 2003).

Neurons in the central amygdala are homogeneously distributed. Most of the projection neurons, unlike in the BLA, are GABAergic and peptidergic (Cassell and Gray, 1989; Sun and Cassell, 1993). Thus, central amygdala neurons are also morphologically distinct from BLA neurons, and are more similar to striatal neurons in their morphology (McDonald, 1982b).

The intercalated cell masses are made up of GABAergic cell clusters and located between subnuclear borders (Millhouse, 1986; Paré and Smith, 1993). The medial amygdala has only one cell type similar to one found in the central amygdala, while the amygdalohippocampal and cortical nuclei resemble the cytoarchitecture of the BLA (Sah et al., 2003).

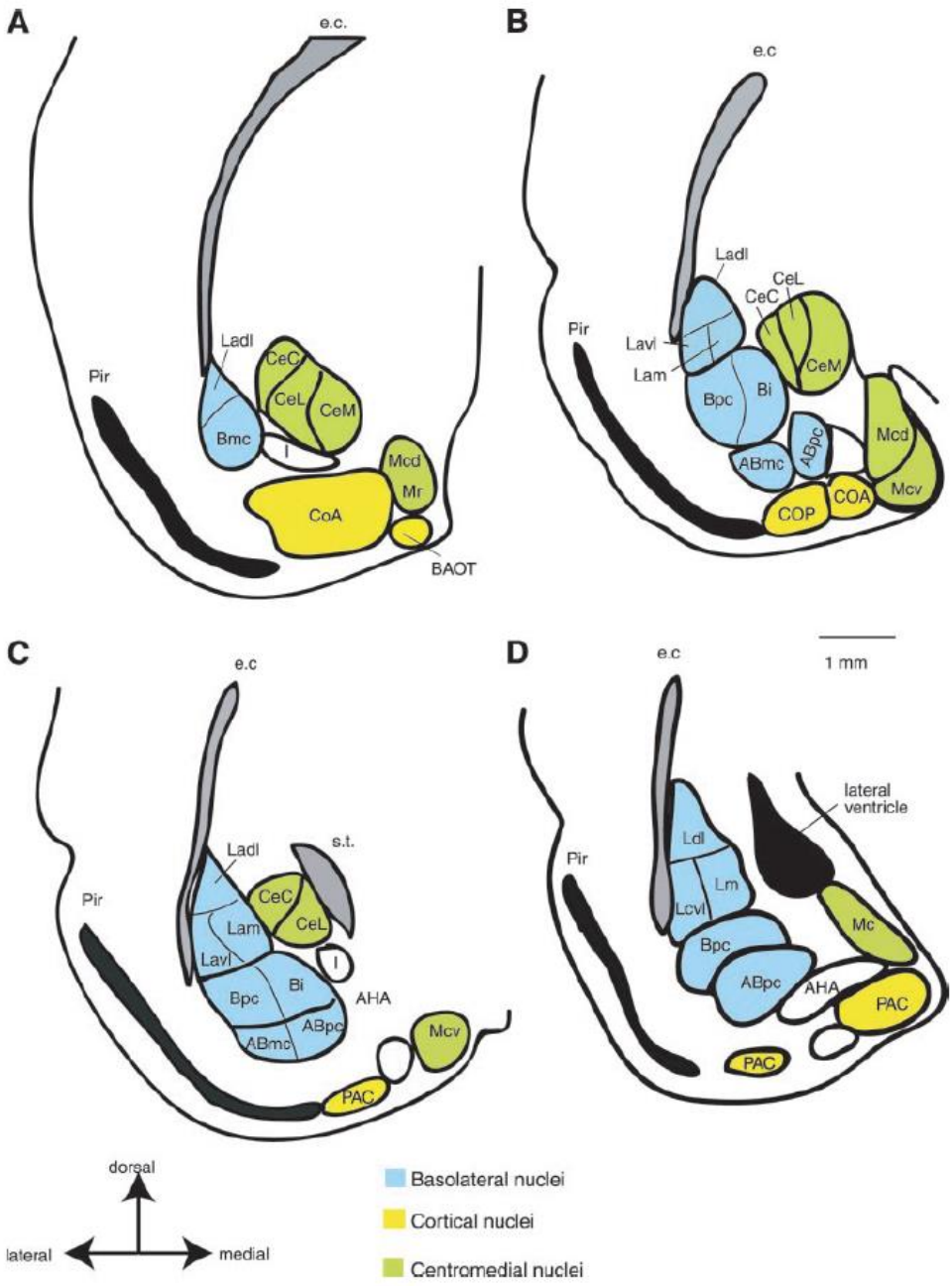


Figure 1.3 – Subnuclei of the amygdaloid complex
Coronal schematics from rostral (**A**) to caudal (**D**) rat amygdala. Areas in blue form the basolateral group, yellow the cortical group, and green the centromedial group. ABmc, accessory basal magnocellular subdivision; ABpc, ac- cessory basal parvicellular subdivision; Bpc, basal nucleus magnocellular subdivision; e.c., external capsule; Ladl, lateral amygdala medial subdivision; Lam, lateral amygdala medial subdivision; Lavl, lateral amygdala ventrolateral subdivision; Mcd, medial amygdala dorsal subdivision; Mcv, medial amygdala ventral subdivision;

Mr, medial amygdala rostral subdivision; Pir, piriform cortex; s.t., stria terminalis. Adapted from Sah et al. (2003).

1.2.2 Efferent and afferent connectivity of the amygdala

The amygdala is connected with numerous brain regions, positioning it optimally to contribute to a diverse range of functions (Figure 1.1). As mentioned earlier, amygdala subnuclei can be distinguished by their projection targets. BLA projections tend to favour cortical and striatal structures, while the central amygdala largely contacts brain stem nuclei responsible for executing behaviour (Krettek and Price, 1977; Hopkins and Holstege, 1978; LeDoux et al., 1988). Projections of the BLA and central amygdala do overlap in targeting the lateral hypothalamus and basal forebrain (Krettek and Price, 1978a). The amygdala also projects to neuromodulatory systems in the midbrain and brain stem; for instance, the central amygdala projects to dopamine, noradrenaline, and acetylcholine neurons, whereas 5-HT neurons in the raphe are less densely targeted (Hopkins and Holstege, 1978; Price and Amaral, 1981; Pollak Dorocic et al., 2014).

The amygdala receives numerous extrinsic inputs from cortical, thalamic, and subcortical sources. These ensure that the amygdala has access to sensory information of all modalities (Pape and Pare, 2010). Importantly, these projections do not originate directly from primary sensory areas, but rather from associative cortical and multimodal thalamic areas. Though sensory afferents from the cortex predominantly target the LA, the central nucleus and also BA receive inputs from thalamic and pre-thalamic regions (Turner and Herkenham, 1991; McDonald, 1998). The BLA complex is also reciprocally connected with the hippocampus, which is thought to provide contextual information during fear learning (Pitkänen et al., 2000). The BLA is also subjected to regulation by ascending and local transmitter systems, including 5-HT, dopamine, noradrenaline, and acetylcholine (Rainnie, 1999; LaLumiere et al., 2004).

The amygdala is a structure distinguished by its high degree of inter- and intra-nuclear connectivity. Inter-nuclear amygdala connections display evidence of preferential

directionality. In the BLA complex, information is thought to be transmitted dorsoventrally, from the LA to the BA (Pitkänen et al., 1997). The LA and BA nuclei project to the central amygdala, but these projections are not thought to be reciprocal. In particular, the LA projects preferentially to the centrolateral nucleus, while the BA nuclei project to both the centromedial and centrolateral (Krettek and Price, 1978b). This topographical segregation has important implications for the function of different subnuclei in fear regulation, because the centromedial nucleus is more strongly connected to brainstem effector neurons compared to the centrolateral (Hopkins and Holstege, 1978). Furthermore, BLA neurons project preferentially to the intercalated masses (Royer et al., 1999). These projections are also arranged topographically, with lateral and BA projections targeting distinct medial intercalated clusters. The medial intercalated cells also project to the central amygdala, while lateral intercalated cells project to the BLA (Marowsky et al., 2005). Connections also exist between different medial intercalated cell masses, with preferential directionality rather than reciprocal projections (Royer et al., 1999).

As previously mentioned, intra-nuclear connections in the amygdala are also strong. Within intercalated cell clusters, neurons form non-reciprocal GABAergic synapses with other neurons (Geracitano et al., 2007). In the central amygdala, centrolateral neurons project to the centromedial nucleus, but not vice versa (Jolkkonen and Pitkänen, 1998). Axons of BLA glutamatergic PNs often form dense *en passant* synapses with other BLA neurons (Smith and Paré, 1994). In parallel, central amygdala neurons are also interconnected, but via GABAergic synapses (Lopez de Armentia and Sah, 2004).

1.2.3 The amygdala and fear learning

Circuit dynamics of the amygdala have been found to be crucial in the fear learning process (Pape and Pare, 2010; Duvarci and Pare, 2014). A simplified circuit model proposes that sensory information is relayed to the lateral nucleus (LA) from the thalamus and cortex (Sigurdsson et al., 2007). These inputs are glutamatergic projections and form weak

connections onto LA PNs to begin with. According to the model, CS-representing inputs to particular PN ensembles are potentiated when the CS and US are paired together (McKernan and Shinnick-Gallagher, 1997; Rogan et al., 1997). The LA then transmits information to the BA, and both of these nuclei project to the central amygdala. Central amygdala projections, in turn, regulate brain stem nuclei to coordinate defensive responses, such as the periaqueductal grey for freezing behaviour (LeDoux et al., 1988; Ciocchi et al., 2010). Hence, potentiated synapses in the LA are thought to underlie the CS-evoked freezing CR following fear conditioning.

This model places the BLA as a critical relay point between sensory inputs and behavioural outputs. Accordingly, variation in BLA volume has been associated with differences in fear and other emotional behaviours in mice (Yang et al., 2008). Within the BLA, local regulation by INs is also important for shaping circuit dynamics during fear learning (Ehrlich et al., 2009). The BA shares reciprocal connectivity with prefrontal cortex circuits that are known to be essential for determining fear behaviour (Figure 1.4; Vidal-Gonzalez et al., 2006; Cho et al., 2013; Arruda-Carvalho and Clem, 2015). Moreover, the BA is necessary for fear expression, identifying it as a critical structure of emotional regulation (Anglada-Figueroa and Quirk, 2005). The LA, on the other hand, is the recipient of sensory inputs and appears to be a locus of synaptic plasticity.

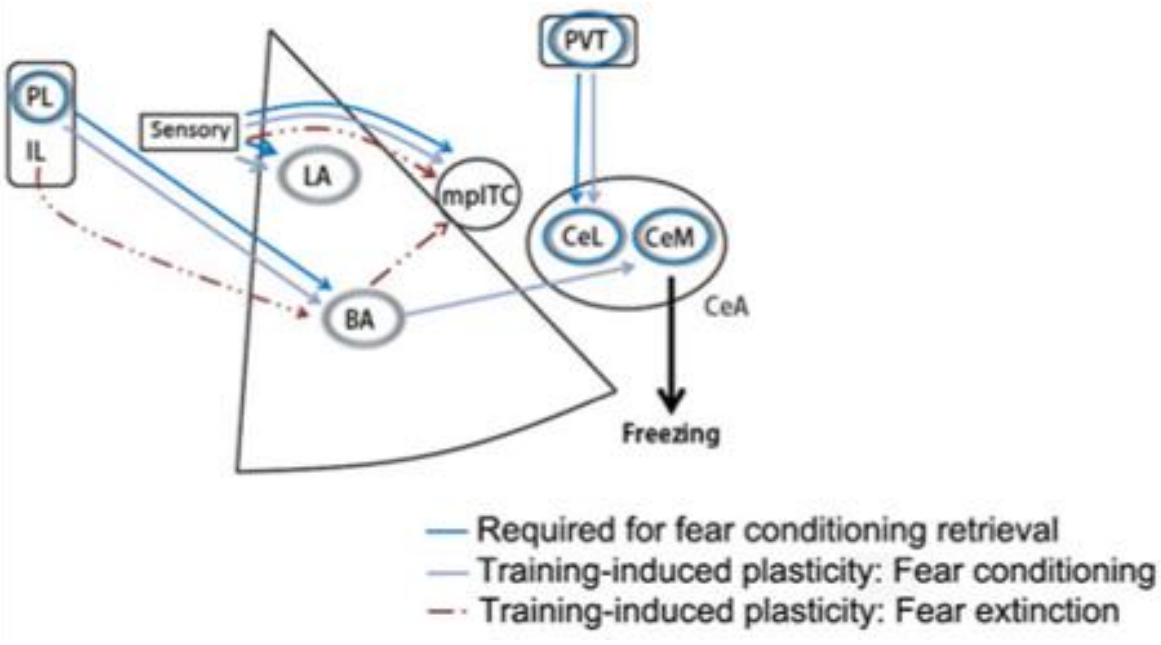


Figure 1.4 – The amygdala as part of a network underlying conditioned fear and extinction
Schematic depicting brain regions (circles) or projection pathways (arrows) involved in fear conditioning or extinction, as expressed 24 h after fear or extinction training. Designation of regions and pathways required for retrieval is based on opto- or chemogenetic manipulations. Designation of pathways displaying training-associated synaptic plasticity is based on *ex vivo* brain slice recordings obtained 24 h after fear conditioning or extinction. BA, basal amygdala; CeA, central amygdala; CeL, lateral division of the central amygdala; CeM, medial division of the central amygdala; IL, infralimbic cortex; LA, lateral amygdala; mpITC, medial paracapsular intercalated cells; PL, prelimbic cortex; PVT, paraventricular thalamus. Adapted from Arruda-Carvalho and Clem (2015).

1.2.3.1 Synaptic plasticity

Evidence for the involvement of long-term plasticity in the BLA in fear learning has been growing. These plastic changes are thought to represent memory formation and storage (Bocchio et al., 2017). The study of plasticity has been focussed on LA synapses. Changes in synaptic strength, such as by long-term potentiation or depression, are thought to be cellular substrates of emotional memory. For example, exposure to CS-US pairings increases electrophysiological measures of synaptic efficacy at CS inputs to the BLA (McKernan and Shinnick-Gallagher, 1997; Rogan et al., 1997), whereas fear extinction reduces such measures in the BLA (Maren and Quirk, 2004; Cho et al., 2013). However, a caveat of these studies is that they often use supra-physiological stimuli to induce plasticity and may not reflect natural phenomena (Bocchio et al., 2017). Local GABAergic INs in the BLA gate heterosynaptic plasticity (i.e. strength of other synapses) and are moderated by neuromodulators such as 5-HT, dopamine, and noradrenaline (Rainnie, 1999; Bissière et al., 2003; Tully et al., 2007; Bazelot et al., 2015).

1.2.3.2 Oscillations

In the amygdala, neural network activity in the form of oscillatory power at a given frequency can correspond to a particular behavioural state, such as freezing or sleep (Karalis et al., 2016; Bocchio et al., 2017). Amygdala network oscillations arise from the synchronised, rhythmic voltage fluctuations of PNs and can be monitored through local field potential recordings. Amygdala oscillations occur at multiple frequency bands: delta (0.5 – 4 Hz), theta

(4 – 12 Hz), beta (12 – 30 Hz), and gamma (30 – 120 Hz). The amygdala exhibits oscillatory activity at theta frequency during fear behaviour, and this is likely driven by intrinsic neuronal resonance, local phase-locking, and synchrony with or entrainment from other regions (Pape and Driesang, 1998; Likhtik et al., 2013; Karalis et al., 2016). Importantly, ectopic neural synchrony in the amygdala is associated with human psychopathology (e.g. schizophrenia, epilepsy, autism, Alzheimer's disease, Parkinson's disease) and cognitive dysfunction. Local field potentials could therefore offer an important translational measure in animal models (Uhlhaas and Singer, 2006).

1.3 The central 5-HT system

5-HT neurons in the brain were first visualised using formaldehyde-induced fluorescence and are organised into 9 discrete cell groups (B1-B9) in the midbrain and brainstem (Dahlström and Fuxe, 1964). Subsequent studies utilised a combination of tracing, immunohistochemistry, and autoradiography approaches to map the 5-HT system (Aghajanian and Bloom, 1967; Descarries et al., 1975; Azmitia and Segal, 1978; Jacobs et al., 1978; Steinbusch et al., 1978; Steinbusch, 1981). The raphe nuclei of the brain stem medulla oblongata contain the more caudal 5-HT cell groups (B1-B3) (Steinbusch, 1981), while the more rostral 5-HT cell groups are located in the midbrain median (MRN) and dorsal (DRN) raphe nuclei (B7-B9), and in the supralemniscal region (B9).

Within the DRN, the majority of neurons are thought to contain 5-HT (Wiklund et al., 1981). However, other transmitters and peptides are also produced by DRN neurons (Hokfelt et al., 2000). Importantly, multiple neurotransmitters can be co-localised in the same cells.

1.3.1 Efferent and afferent connectivity of midbrain 5-HT neurons

5-HT efferents project extensively to widespread targets across the central nervous system. Brain stem 5-HT neurons (B1-B3) give rise to descending projections to the spinal

cord, whereas midbrain 5-HT neurons (B7-B9) primarily innervate the forebrain with ascending projections (Bowker et al., 1982; Törk, 1990). The remaining 5-HT cell groups (B4-B6) send both descending and ascending projections. Midbrain 5-HT pathways ascend via the medial forebrain bundle to innervate areas of the limbic system, cerebral cortex, basal ganglia, and diencephalon (Figure 1.5; Steinbusch, 1981; Törk, 1990). Retrograde labelling of 5-HT cells demonstrates that the BLA receives projections predominantly from the DRN and some from the MRN (Steinbusch, 1981; Abrams et al., 2005). Anatomically separate 5-HT projection pathways are thought to contribute to distinct processes, suggesting that the topographical organisation of 5-HT cells could have a functional significance (Graeff et al., 1996; Lucki, 1998).

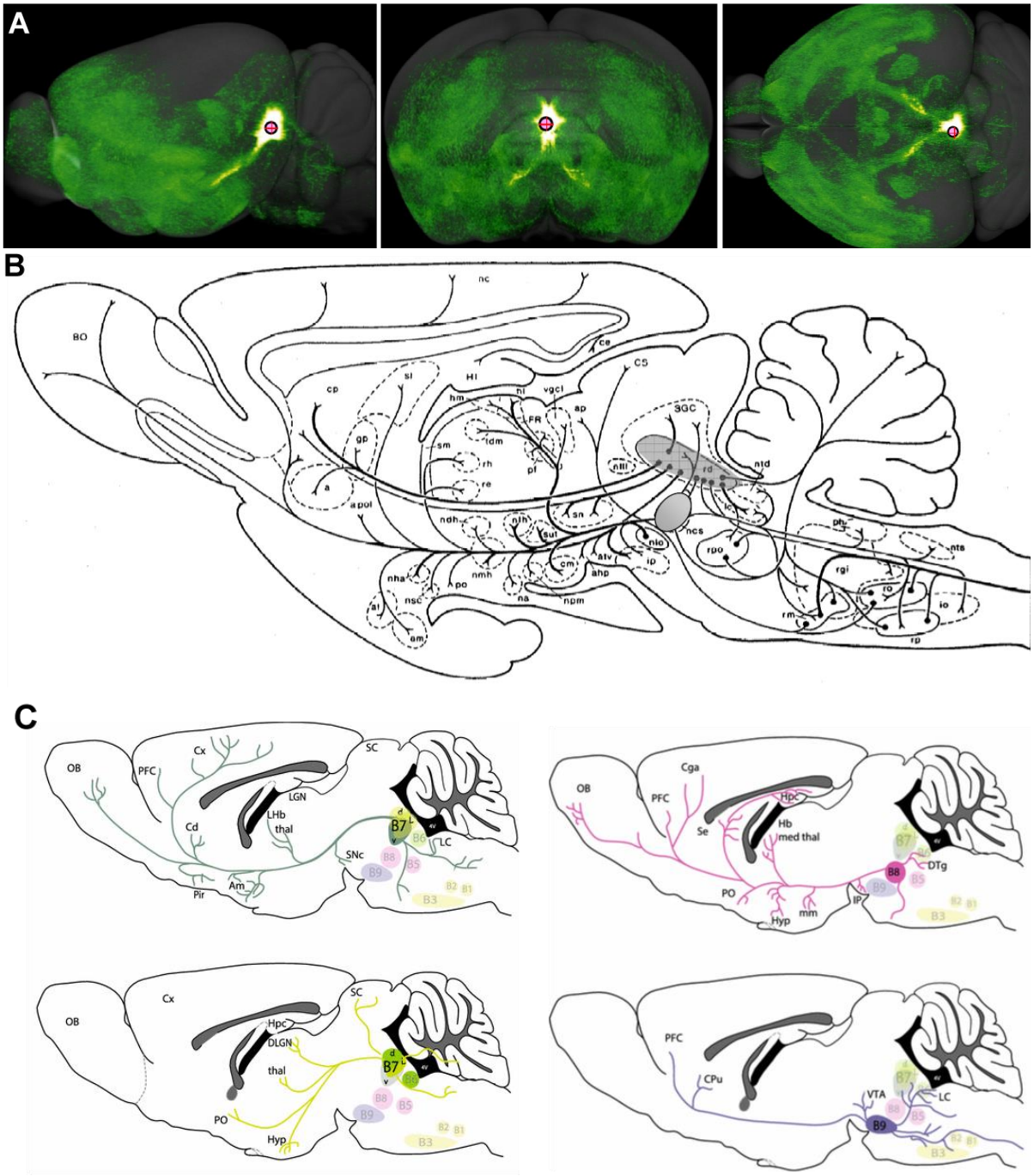


Figure 1.5 – Efferent 5-HT projections of midbrain raphe nuclei
A. 3-D sagittal (left), coronal (middle), and horizontal (right) visualisation of 5-HT neurons by injection of a Cre-dependent anterograde tracer (rAAV2/1.hSynapsin.EGFP.WPRE.bGH) into the DRN (red crosshair) of 5-HTT-Cre mice. **B**. Schematic sagittal section of the efferent projections of the midbrain raphe nuclei in the rat brain. The DRN and MRN are shaded. n, nucleus; a, n. accumbens; ahp, area hypothalami posterior; al, n. amygdaloideus lateralis; am, n. amygdaloideus medialis; ap, area pretectalis; a pol, area preopticus lateralis; BO, bulbus olfactorius; ce, cortex entorhinalis; cm, n. centromedianus thalami; cp, n. caudatus putamen; CS, colliculus superios; FR, fasciculus retroflexus; gp, globus pallidus; HI, hippocampus; hl, n. habenulae lateralis; hm, n. habenulae medalis; io, n. olivaris inferior; ip, n. interpenduncularis; na n. arcuatus; nc, neocortex; ncs, n. centralis superior; ndh, n. dorsalis hypothalami; nf n. fastiguus; nha, n. hypothalami anterior; nlh, n. lateralis hypothalami; nlo, n. lineris oralis; nmh, n. medianus hypothalami; npd, n. parabrachialis dorsalis; npm, n. premammalaris; npv, n. paraventricular hypothalami; ntd, n. tegmentalis; nts, n. tractus solitaruis; nIII, n. motoruis nervi oculomotori; pf, n. parafascicularis; PF, cortex prefrontalis; ph, n. prepositus hypoglossi; po, n. pontis; pv, n. periventricularis thalami; rd, n. raphe dorsalis; re, n. reunions; rgi, n. reticularis gigantocellularis; rh, n. rhomboideus; rm, n. raphe magnus; ro, n. raphe obscurus; rp, n. raphe pallidus; rpo, n. raphe pontis; rpoo, n. reticularis pontis oralis; SGC, substantia grisea. **C.** Summary scheme of the principal targets of the main B7–

B9 5-HT cell subgroups, as observed by the viral delivery of a Cre-dependent anterograde tracer under the control of the 5-HTT promoter. Am, amygdala; Cd, caudate nucleus; Cga, anterior cingulate cortex; CPu, caudate-putamen nucleus; Cx, cortex; DLGN, dorsal lateral geniculate nucleus; DTg, dorsal tegmental nucleus of Gudden; Hpc, hippocampus; Hyp, hypothalamus; IP, interpeduncular nucleus; LC, locus coeruleus; LGN, lateral geniculate nucleus; LHb, lateral habenula; med thal, medial thalamus; mm, mammillary bodies; OB, olfactory bulb; PFC, prefrontal cortex; Pir, piriform cortex; PO, preoptic area; SC, superior colliculus; Se, septum; SNC, substantia nigra, compact part; thal, thalamus; VTA, ventral tegmental area. Adapted from Allen Mouse Brain Connectivity Atlas (Oh et al., 2014), experiment 114155190, website: © 2017 Allen Institute for Brain Science, available from: http://connectivity.brain-map.org (**A**), Steinbusch and Nieuwenhuys (1983), courtesy of Burnham (2009) (**B**), and Muzerelle et al., (2016) (**C**).

Earlier pathway tracing studies established that midbrain 5-HT neurons receive dense inputs from the hypothalamus, midbrain, and brainstem, and are also targeted by cortical, basal ganglia, and amygdala projections. This connectivity has recently been confirmed and extended by utilising rabies virus tracing strategies, in combination with cell-type-specific Cre-driver mouse lines (Ogawa et al., 2014; Pollak Dorocic et al., 2014; Weissbourd et al., 2014). Inputs to DRN and MRN 5-HT cells are spatially segregated in the forebrain, with the MRN receiving projections from a medial stream and the DRN from an intermediate stream (Ogawa et al., 2014). Projections from the prefrontal cortex and lateral habenula are glutamatergic, whereas amygdala and striatal inputs are GABAergic (Pollak Dorocic et al., 2014; Weissbourd et al., 2014). Importantly, the GABAergic amygdala projections to raphe nuclei arise primarily from the central amygdala. Within the DRN, 5-HT neurons are preferentially targeted by prefrontal cortex projections, whereas GABA neurons receive more inputs from the central amygdala (Weissbourd et al., 2014). Intra-DRN mapping revealed extensive 5-HT-to-5-HT and GABA-to-5-HT connectivity with a topographic organisation (Figure 1.6; Weissbourd et al., 2014). These input patterns suggest a polysynaptic feedback loop between 5-HT neurons and the amygdala, via 5-HT projections to the BA, central amygdala, DRN GABA cells, and finally back to 5-HT neurons.

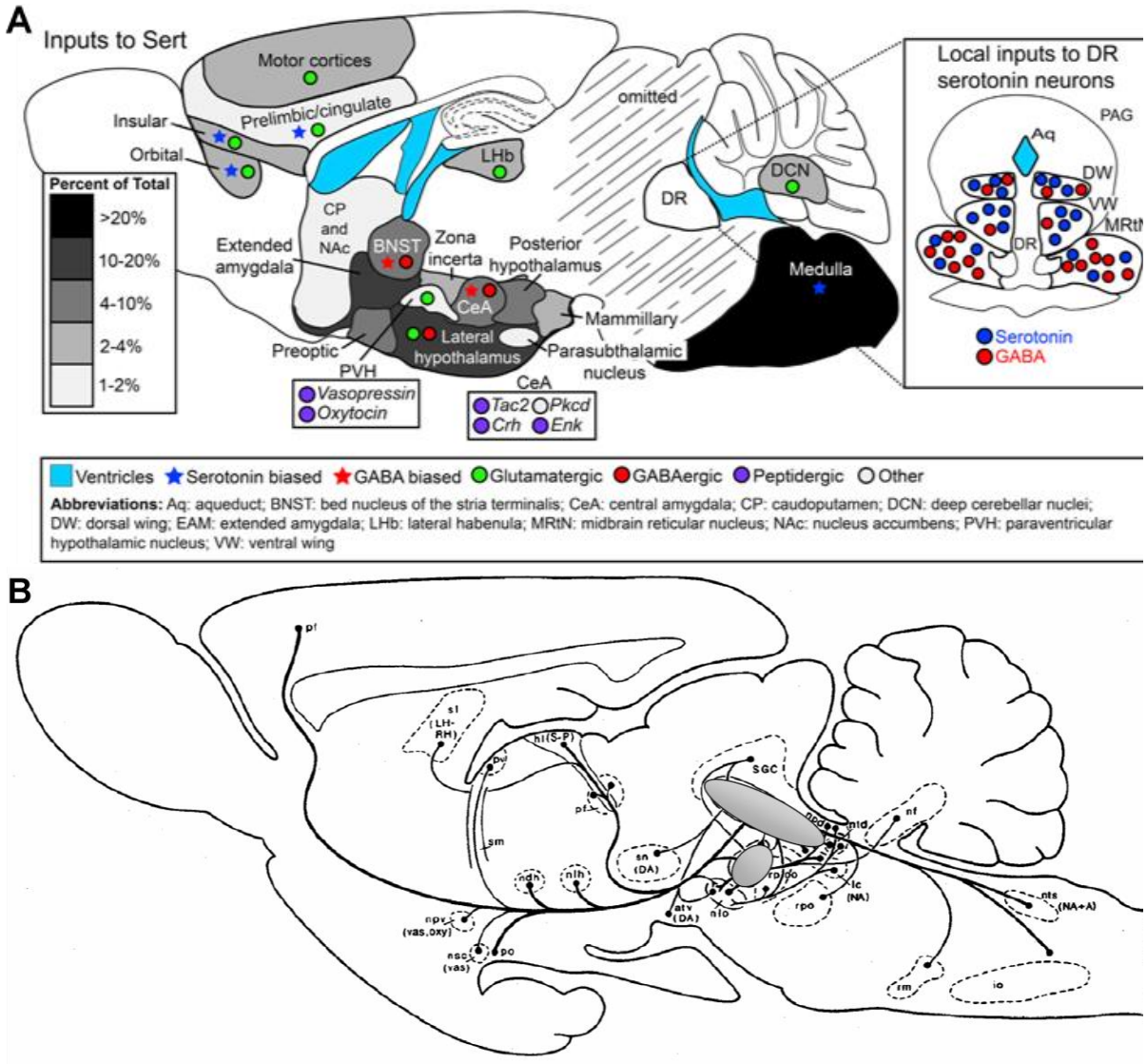


Figure 1.6 - Afferent projections to the midbrain raphe nuclei
A. Summary of inputs to the DRN on a schematic sagittal section showing regions containing >1% of total inputs. Percentage of total input is coded by grey scales (inset). Stars indicate biased input to DRN 5-HT (blue) or GABA (red) neurons. The primary neurotransmitters expressed by input regions are shown as small circles as indicated in the inset. **B**. Schematic sagittal section of the afferent projections to the midbrain raphe nuclei in the rat brain. The DRN and MRN are shaded. Abbreviations as Figure 1.5B and: vas, vasopressin; oxy, oxytocin; SP, substance P; DA, dopamine; NA, noradrenaline; A, adrenaline; GABA, γ-aminobutyric acid. Adapted from Weissbourd et al. (2014) (**A**) and Steinbusch and Nieuwenhuys (1983), courtesy of Burnham (2009) (**B**).

1.3.2 5-HT synthesis and metabolism

The 5-HT synthesis pathway requires the precursor, the amino acid L-tryptophan, which is hydroxylated by the enzyme tryptophan hydroxylase (Tph) to form 5-hydroxytryptophan (Hamon and Glowinski, 1974). This is the initial and rate-limiting reaction of the pathway. Tph exists as two variants, with Tph2 expressed to a greater extent than Tph1 in raphe nuclei (Patel et al., 2004). The second and rapid reaction involves the

decarboxylation of 5-hydroxytryptophan to 5-HT by the enzyme aromatic L-amino acid decarboxylase. Similar to other transmitters, 5-HT is packaged into vesicles, where it is stored until release (Tamir and Gershon, 1990). Vesicular packaging of 5-HT in neurons is mediated by vesicular monoamine transporter 2 (Erickson et al., 1996). 5-HT that is not sequestered into vesicles is rapidly metabolised by the enzyme monoamine oxidase to 5-hydroxyindoleacetic acid (5-HIAA).

1.3.3 5-HT receptors

Released 5-HT exerts its effects through its actions on 5-HT receptors. To date, at least 14 identified subtypes have been characterised by structural (amino acid sequence), transductional (signalling pathway), and operational (pharmacology) properties (Humphrey et al., 1993; Barnes and Sharp, 1999). A summary of 5-HT receptor subtypes and their distribution in the brain can be found in Table 1.2. These subtypes are categorised into 7 families ($5\text{-HT}_{1\text{-}7}$) that are typically located in both the central and peripheral nervous systems. However, particular receptor subtypes often display specialised distributions and have been implicated in certain functions (Hoyer et al., 2002). It is therefore vital to dissect the role of distinct receptor types in a circuit-specific manner to achieve a precise understanding of 5-HT function and dysfunction in emotional psychopathology. This could be important for the optimisation of first-line affective disorder pharmacotherapies, many of which still have inconsistent effects on patients (Vasa et al., 2006).

Table 1.2 – Summary of 5-HT receptors in the mammalian brain
Distribution and localisation is in rodents. Information collated from Barnes and Sharp (1999), Hannon and Hoyer (2008), Holmes (2008), Asan et al. (2013), and Bocchio et al. (2016).

Receptor subtype	Mechanism	Distribution in the brain	Neuronal localisation
5-HT_{1A}	$G_{i/o}$	Hippocampus, lateral septum, cortex, raphe nuclei, **amygdala**	Somatodendritic (autoreceptors), presynaptic, postsynaptic, extra-synaptic
5-HT_{1B}	$G_{i/o}$	Basal ganglia, raphe nuclei, hippocampus	Presynaptic (auto- and heteroreceptors), postsynaptic
5-HT_{1D}	$G_{i/o}$	Basal ganglia, hippocampus, cortex, nucleus accumbens, dorsal raphe nucleus, locus coeruleus	Presynaptic (auto- and heteroreceptors)
5-ht_{1E}	$G_{i/o}$	Cortex, caudate-putamen, claustrum, hippocampus, **amygdala**, hypothalamus	Postsynaptic
5-HT_{1F}	$G_{i/o}$	Cortex, hippocampus, claustrum, caudate-putamen, **amygdala**, nucleus accumbens, olfactory bulb, olfactory nucleus, hypothalamus, thalamus, mammillary nuclei, geniculate nucleus, ventral tegmental area, vestibular nucleus, cochlear nucleus, spinal tract	-
5-HT_{2A}	$G_{q/11}$	Cortex, claustrum, **amygdala**, endopiriform nucleus, brainstem, caudate nucleus, nucleus accumbens, olfactory bulb, olfactory tubercle, hippocampus	Presynaptic, postsynaptic, extra-synaptic
5-HT_{2B}	$G_{q/11}$	Cerebellum, lateral septum, hypothalamus, **amygdala**	Postsynaptic
5-HT_{2C}	$G_{q/11}$	Choroid plexus, cortex, hippocampus, **amygdala**, nucleus accumbens, olfactory nucleus, endopiriform nucleus, basal ganglia, thalamus, habenula, brainstem, central grey, raphe nuclei (?)	Presynaptic (?), postsynaptic
5-$HT_{3A/B/C/D/E}$	ionotropic (cation influx)	Brainstem, hippocampus, **amygdala**, cortex, basal ganglia, nucleus accumbens	Presynaptic, postsynaptic
5-HT_4	G_s	Olfactory tubercle, basal ganglia, hippocampus, **amygdala**,	Postsynaptic
5-HT_{5A}	$G_{i/o}$	Cortex, hippocampus, cerebellum, hypothalamus, thalamus, brainstem, basal ganglia, olfactory bulb	Postsynaptic
5-ht_{5B}	$G_{i/o}$ (?)	Hippocampus, hypothalamus, habenula, dorsal raphe nucleus, olfactory bulb, cortex	-
5-HT_6	G_s	Basal ganglia, **amygdala**, nucleus accumbens, hippocampus, cortex, olfactory tubercle, hypothalamus, thalamus, cerebellum, choroid plexus, raphe nuclei (?)	Postsynaptic, extrasynaptic
5-HT_7	G_s	Suprachiasmatic nucleus, thalamus, cortex, basal ganglia, hypothalamus, hippocampus, **amygdala**, central grey, dorsal raphe nucleus	Postsynaptic

1.3.4 The 5-HTT

The 5-HTT is a member of a family of transmembrane transporter proteins that includes transporters for dopamine, noradrenaline, and GABA (Blakely et al., 1991; Nelson, 1998). It is expressed exclusively in 5-HT neurons during adulthood (Blakely et al., 1994; Torres and Amara, 2007). The 5-HT transporter (5-HTT) terminates 5-HT neurotransmission by reuptake of released 5-HT from the extracellular space. This role puts the 5-HTT in a key position to control the magnitude and duration of 5-HT signals.

Human gene association studies have identified a polymorphism in the 5-HTT gene (5-HTT-linked polymorphic region, 5-HTTLPR) that results in a long or short allele variant. The short allele has been linked to decreased transcriptional efficacy compared to the long allele, which leads to reduced 5-HTT expression, less 5-HT reuptake, and thus elevated extracellular 5-HT levels (Greenberg et al., 1999). The short allele has also been associated with susceptibility to anxiety traits and with heightened amygdala reactivity to fearful stimuli (Lesch et al., 1996; Hariri et al., 2002). Although altered amygdala function has not been replicated by all studies, meta-analyses have confirmed the association, albeit with a marginal effect size (Munafò et al., 2008; Murphy et al., 2013).

The links between 5-HTT expression variation, fear-related phenotypes, and amygdala function have been corroborated in transgenic rodents (Holmes et al., 2003a; Barkus et al., 2014) (see Chapter 2 for more detail). Thus, translationally relevant animal models exist that emphasise the critical relationship between the 5-HT system, the amygdala, and fear behaviour. Intriguingly, non-constitutive manipulations of 5-HT signalling at distinct time periods of the animal's life lead to differential behavioural effects (Thakker et al., 2005; Ansorge et al., 2008; Homberg et al., 2011). Namely, the impact on depressive and fear-related behaviours can vary depending on whether a particular 5-HT manipulation occurs during early life or adulthood. This indicates that there might be a crucial temporal window in which 5-HTT activity shapes behavioural phenotypes. However, a critical time period remains to be identified in a constitutive model of altered 5-HTT expression.

It should be noted that variation in 5-HTT expression has also been linked to over 50 phenotypes other than increased emotionality (for reviews, see Murphy and Lesch, 2008; Murphy et al., 2008). The short 5-HTTLPR allele, for example, has been associated with improved cognition (Homberg and Lesch, 2011). Although this thesis focusses on fear-related behaviours, the functional spectrum of 5-HTT variation encompasses a much wider range of psychological and physiological traits.

1.3.5 Amygdala 5-HT transmission in fear-related behaviour

5-HT signalling in the amygdala has been strongly implicated in the regulation of fear-related behaviours (for reviews, see Davis et al., 1994; Holmes, 2008; Asan et al., 2013; Bocchio et al., 2016); however, the precise role of 5-HT in this region is uncertain (see Chapter 3 for more detail). Table 1.3 summarises the sometimes contradictory behavioural results of studies in which 5-HT transmission has been pharmacologically manipulated through local drug administration into the amygdala. For example, 5-HT_{1A} agonism in the amygdala during behaviour has resulted in increased anxiety or no behavioural effect at all. Furthermore, social anxiety is reduced by 5-HT_{2B} activation in the amygdala, but enhanced by 5-HT_{2C} receptor agonism. 5-HT axon depletion in the amygdala has been shown to both elevate and decrease anxiety-like behaviours. These inconsistencies could be explained by a number of factors; different amygdala subnuclei are thought to mediate distinct functions in fear behaviour (section 1.2.3), 5-HT receptor subtypes are localised on particular amygdala cell types (Figure 1.8), 5-HT transmission could modulate distinct behaviours differentially, and pharmacological approaches may not accurately represent physiological 5-HT signalling mechanisms. Therefore, it is necessary to study the role of 5-HT in fear-related behaviours using more physiological approaches, keeping in mind that 5-HT mechanisms likely operate in a circuit- and receptor-specific manner.

As described earlier, DRN 5-HT neurons send projections to the amygdala, with particularly dense innervation of the BA (Figure 1.7). For this reason, the experiments of this

thesis are concentrated on 5-HT transmission in the BA. While recent technical advances have enabled the study of circuit-specific projection pathways, these approaches have not yet been fully exploited to investigate 5-HT afferents in amygdala nuclei. Indeed, since intra-amygdala pharmacological 5-HT perturbations yield different results compared to systemic manipulations (Li et al., 2006; Cornélio and Nunes-de-Souza, 2007; Matsuzaki et al., 2011), circuit-specific dissection of 5-HT projections to the amygdala is needed to clarify the role of amygdala 5-HT transmission in fear behaviour. Such analysis is crucial for accurately elucidating the neural mechanisms that underpin fear learning and which become maladaptive in affective disorders.

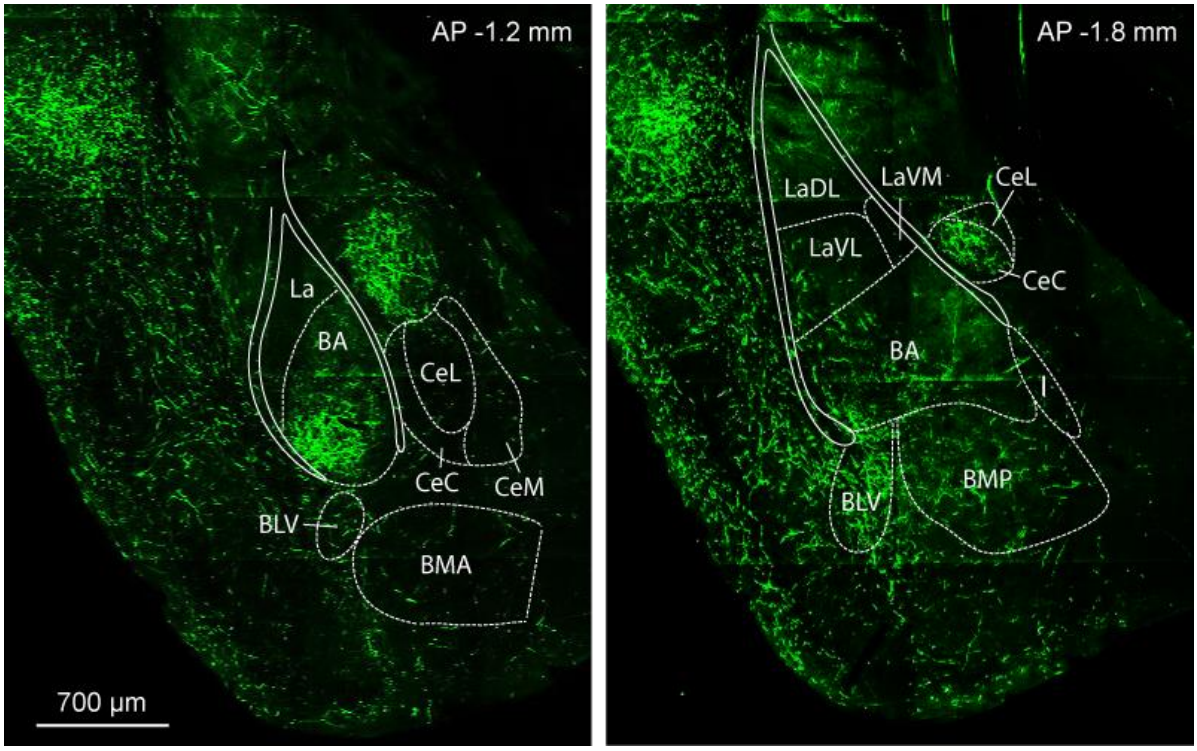


Figure 1.7 – 5-HT innervation of the amygdala
Coronal images of anterior (left) and caudal (right) amygdala with 5-HT projections labelled by injection of a Cre-dependent anterograde tracer (rAAV2/1.hSynapsin.EGFP.WPRE.bGH) into the DRN of 5-HTT-Cre mice. AP, anterioposterior coordinates from bregma. Adapted from Allen Mouse Brain Connectivity Atlas (Oh et al., 2014), experiment 114155190, website: © 2017 Allen Institute for Brain Science, available from: http://connectivity.brain-map.org.

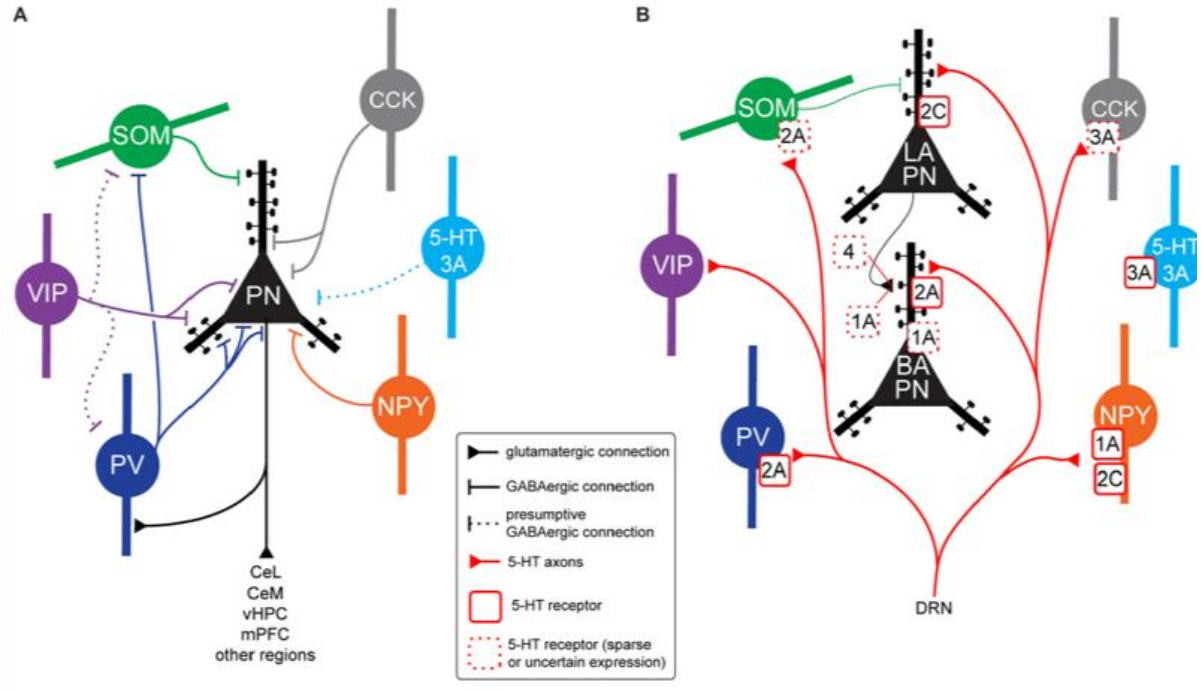


Figure 1.8 –5-HT receptor localisation in BLA circuit
A. Connectivity between BLA PN and IN populations in rodents. **B**. Expression of 5-HT receptor subtypes in neuron types of the BLA in rodents. CCK, cholecystokinin; CeL, centrolateral amygdala; CeM, centromedial amygdala; mPFC, medial prefrontal cortex; NPY, neuropeptide Y; PV, parvalbumin; SOM, somatostatin; vHPC, ventral hippocampus; VIP, vasoactive intestinal peptide.

Table 1.3 – Summary of behavioural effects of 5-HT interventions in the amygdala
Studies consider fear-related behaviours in rodents.

5-HT system target	Manipulation	Location	Behavioural effect	References
5-HT_{1A} receptors	Agonism	Basolateral amygdala	No exploratory anxiety effect	Gonzalez et al., 1996
5-HT_{1A} receptors	Agonism	Basolateral amygdala	↑ Social anxiety	Gonzalez et al., 1996
5-HT_{1A} receptors	Agonism	Amygdala	↓ Conditioned avoidance	Liang, 1999
5-HT_{1A} receptors	Agonism	Amygdala	↓ Contextual fear	Li et al., 2006; Matsuzaki et al., 2011
5-HT_2 receptors	Antagonism	Basolateral amygdala	↑ Conditioned place aversion	Macedo et al., 2007
5-HT_2 receptors	Agonism	Central amygdala	No exploratory anxiety effect	Campbell and Merchant, 2003
5-HT_{2B} receptors	Agonism	Medial amygdala	↓ Social anxiety	Duxon et al., 1997
5-HT_{2C} receptors	Agonism	Basolateral amygdala	↑ Exploratory anxiety	Campbell and Merchant, 2003
5-HT_{2C} receptors	Antagonism	Basolateral amygdala	↓ Stress-potentiated social anxiety	Christianson et al., 2010
5-HT_{2C} receptors	Agonism	Basolateral amygdala	↑ Social anxiety	Christianson et al., 2010
5-HT_{2C} receptors	Antagonism	Basolateral amygdala	↑ Stress-potentiated cued fear	Baratta et al., 2016
5-$HT_{2A/C}$ receptors	Agonism	Basolateral amygdala	↑ Exploratory anxiety	De Mello Cruz et al., 2005
5-$HT_{2B/C}$ receptors	Agonism	Amygdala	↑ Exploratory anxiety	Cornélio and Nunes-de-Souza, 2007
5-HT_3 receptors	Agonism	Amygdala	↑ Exploratory anxiety	Costall et al., 1989
5-HT_3 receptors	Antagonism	Amygdala	↓ Social anxiety	Higgins et al., 1991
5-HT_3 receptors	Agonism	Amygdala	↑ Social anxiety	Higgins et al., 1991
5-HTT	Inhibition	Amygdala	↓ Contextual fear	Inoue et al., 2004
5-HT axons	Lesion/depletion	Amygdala	↑ Social anxiety	File et al., 1981
5-HT axons	Lesion/depletion	Lateral amygdala	↑ Fear-potentiated startle	Tran et al., 2013
5-HT axons	Lesion/depletion	Basolateral amygdala	↑ Exploratory anxiety	Izumi et al., 2012
5-HT axons	Lesion/depletion	Basolateral amygdala	↓ Contextual fear	Izumi et al., 2012
5-HT axons	Lesion/depletion	Basolateral amygdala	↓ Social anxiety	Johnson et al., 2015
5-HT axons	Lesion/depletion	Basolateral amygdala	↓ Cued fear	Johnson et al., 2015

1.4 Aims of this thesis

Based on the evidence discussed above, probing the critical time windows and specific circuits through which 5-HT neurotransmission regulates fear-related behaviours is a necessary step in clarifying the precise 5-HT mechanisms that moderate emotional processing. In this thesis, the temporally- and circuit-specific roles of 5-HT signalling will be explored (chapter schematic in Figure 1.9). This will be done in a translationally relevant mouse model whose phenotypes have previously only been studied in adulthood, or using an optogenetic approach that has not yet been applied to an amygdala-targeting 5-HT pathway.

Chapter 2 aims to characterise the behavioural phenotype of adolescent 5-HTT overexpressing mice to test whether the low-fear-related phenotypes of adult 5-HTT OE mice are already established at this younger age (Jennings et al., 2006; Line et al., 2014). If the phenotypes are present, pharmacological 5-HTT inhibition will be administered either acutely during behaviour or chronically during postnatal neurodevelopment to assess which time period is essential for bringing about the low-fear phenotype associated with 5-HTT OE animals.

Chapter 3 aims to test the role of the 5-HT pathway projecting specifically from the DRN to the BA in fear learning. The 5-HT pathway will be selectively targeted using optogenetic tools. This will enable the much-needed temporal- and circuit-specific control of BA 5-HT afferent activity *in vivo*, since previous pharmacological manipulations of 5-HT transmission in the amygdala have yielded conflicting behavioural results (Table 1.3).

The normal activity of individual neurons and network oscillations in the amygdala have previously been described during the fear learning process (Herry et al., 2008; McHugh et al., 2014). *Chapter 4* aims to investigate the impact of optogenetic excitation of DRN-BA 5-HT projections on BA activity during fear learning. To this end, *in vivo* recordings will be conducted in the BA during a behavioural task.

Chapter 5 aims to dissect the physiological mechanisms through which DRN 5-HT neurons modulate BA neurons. Previous research has made use of exogenous

pharmacological agents to assess the influence of 5-HT signalling on amygdala circuits (Rainnie, 1999). In the current study, the DRN-BA 5-HT pathway will be selectively excited using optogenetics in *ex vivo* brain slices to analyse the effects of endogenous 5-HT transmission on BA neurons.

Individual DRN 5-HT neurons have previously been shown to contain multiple transmitters (Johansson et al., 1981; Gras et al., 2002). *Chapter 6* aims to evaluate the neurochemical identities of DRN neurons that project to the BA using a combination of retrograde tracing and immunohistochemistry.

The central hypothesis is that 5-HT transmission operates in a temporally- and circuit-specific manner to regulate fear behaviour. The thesis will test whether 5-HT transmission during neurodevelopment is vital for shaping the fear-related phenotypes of altered 5-HTT expression later in life and whether the BA is a key site for 5-HT neuromodulation during fear behaviour.

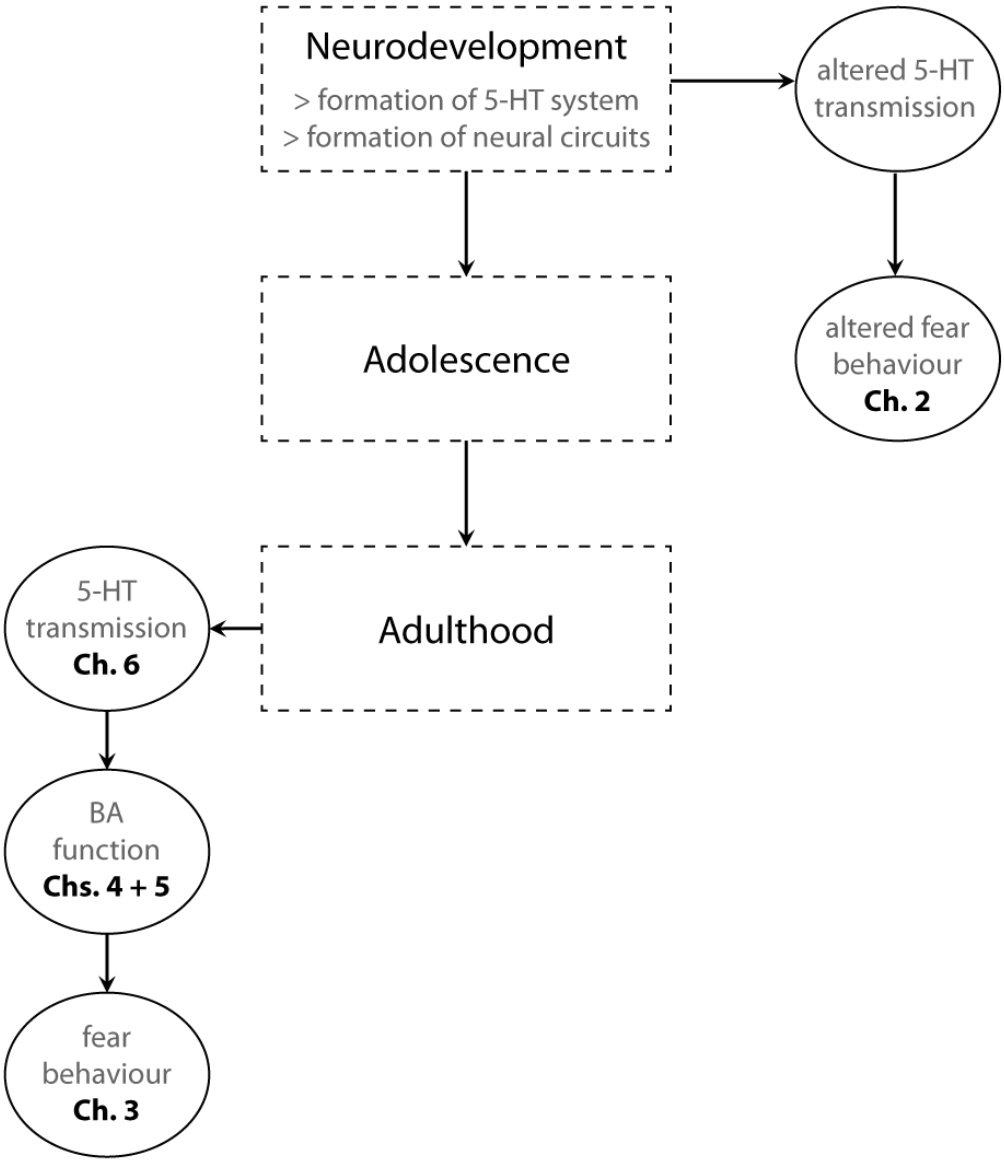


Figure 1.9 – Schematic of thesis chapters

Chapter 2 Developmental origin of fear-related phenotypes of 5-HT transporter overexpressing mice

2.1 Introduction

2.1.1 The human 5-HTT and its influence on negative emotionality and the amygdala

The 5-HTT reuptakes extracellular 5-HT (Figure 2.1) and thus regulates the availability of 5-HT. It therefore determines the magnitude and duration of 5-HT signalling (Iversen, 1971; Blakely et al., 1991; Torres and Amara, 2007). Over 20 functional variants of the human 5-HTT gene have been identified and associated with a variety of phenotypes (for review, see Murphy and Moya, 2011). The earliest discovered and most extensively studied is a polymorphism in the promoter region, the 5-HTTLPR, generated by a 44 base pair insertion/deletion that gives rise to long and short allele variants. The long allele is associated with a three-fold higher efficacy of transcription (Heils et al., 1996), and thus with greater expression and consequent reuptake activity of the 5-HTT (Greenberg et al., 1999).

The variation in 5-HTT expression has been linked to emotional regulation, as evidenced by human gene association studies (Hariri and Holmes, 2006). Carriers of the short allele have a greater risk for anxious personality traits (Lesch et al., 1996) and PTSD (Lee et al., 2005). Carriers of the short allele also acquire fear memories more easily (Garpenstrand et al., 2001), have a greater acoustic startle response (Brocke et al., 2006),

and exhibit enhanced fear-potentiated startle (Lonsdorf et al., 2009). Impaired fear extinction and heightened anxiety and depression symptoms have also been observed in humans with a polyadenylation polymorphism due to which 5-HTT expression is reduced (Hartley et al., 2012). 5-HTTLPR short allele carriers have a greater susceptibility to depression, especially when combined with exposure to traumatic events (Caspi et al., 2003; Uher and McGuffin, 2010). This provides evidence for a gene × environment interaction between the 5-HTTLPR and emotionally salient life experiences. The 5-HTTLPR-mediated gene × environment interaction has not been found in all studies (Risch et al., 2009), but Murphy and Moya (2011) posit that these have been few and commonly based on self-reports rather than on objective measures.

5-HTT expression variation has also been associated with changes in amygdala function, with carriers of the short allele displaying a greater activation of the amygdala in response to fear-related stimuli (Hariri et al., 2002). This relationship has been replicated in a number of different cohorts (for review, see Hariri and Holmes, 2006), including in patients with social phobia (Furmark et al., 2004), panic disorder (Domschke et al., 2006), and depression (Dannlowski et al., 2008), as well as in healthy subjects without a history of psychiatric illness (Hariri et al., 2005). However, this link has also faced issues of non-replication. Nevertheless, meta-analyses have revealed that there is a connection between the 5-HTTLPR and amygdala reactivity, although the effect size is smaller than reported in some earlier accounts (Munafò et al., 2008; Murphy et al., 2013).

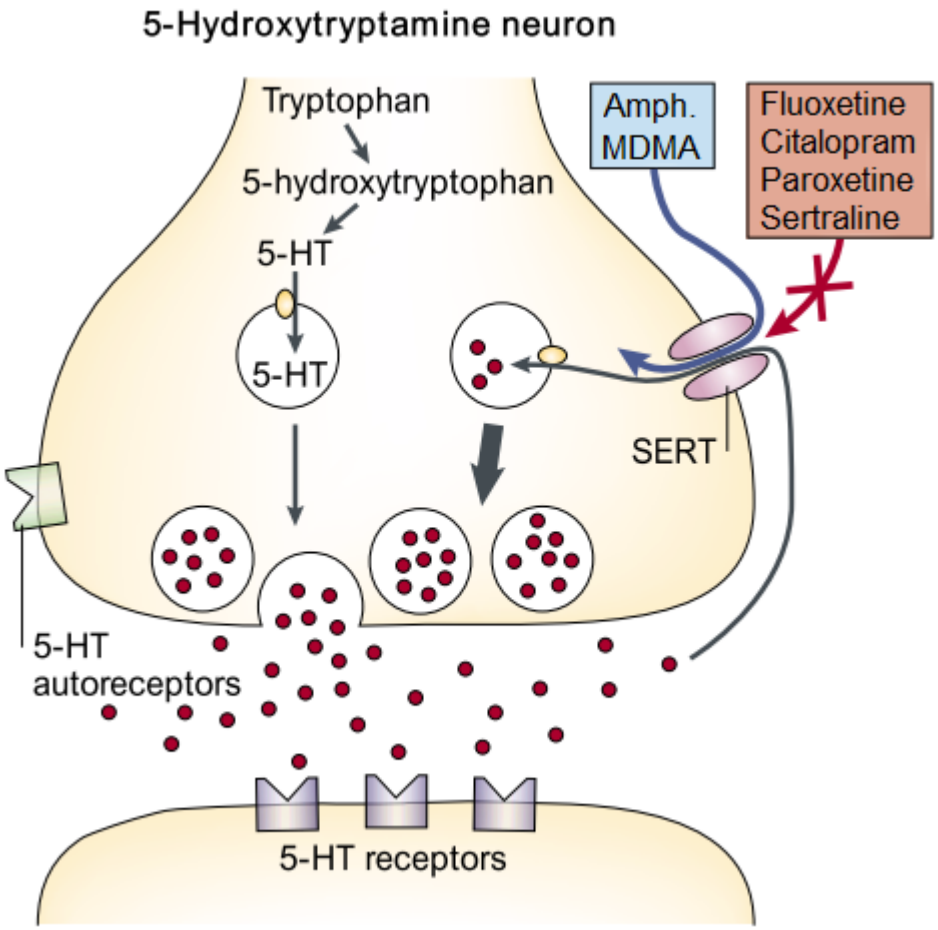


Figure 2.1 – Schematic representation of 5-HT synaptic terminal
The 5-HTT (SERT) is located perisynaptically. Its reuptake activity is important both for termination of 5-HT signals, as well as for storage of 5-HT in the presynapse. Amphetamine (Amph.) and (+)-3,4-methylenedioxymethamphetamine (MDMA), acting as substrates, are competitive inhibitors of the 5-HTT. SSRIs such as fluoxetine, citalopram, paroxetine, and sertraline block the activity of the 5-HTT. Adapted from Torres et al., 2003.

2.1.2 The rodent 5-HTT and its association with fear-related behaviours and neural circuits

In spite of the care previous studies have taken to screen subjects and control for variables, human research faces the complication of diverse demographic and environmental factors that could obfuscate the relationship being investigated (for review, see Caspi et al., 2010). The neurobiological effects of 5-HTT expression variation can be interrogated in the more controlled settings afforded by animal models. To this end, multiple rodent models of altered 5-HTT expression have been developed, in which the 5-HTT gene is either knocked

out (KO) or overexpressed (OE) (Bengel et al., 1998; Jennings et al., 2006; Smits et al., 2006; Zhao et al., 2006). On the one hand, adult 5-HTT OE mice have lower extracellular 5-HT levels (Jennings et al., 2006, 2010), are deficient in acquiring fear memories (Barkus et al., 2014; Line et al., 2014; Bocchio et al., 2015; McHugh et al., 2015), and exhibit reduced anxiety (Jennings et al., 2006; Line et al., 2011). On the other hand, adult 5-HTT KO rodents have higher extracellular levels of 5-HT (Mathews et al., 2004; Homberg et al., 2007; Jennings et al., 2010), are impaired in extinguishing fear memories (Wellman et al., 2007; Nonkes et al., 2012), and display heightened anxiety (Holmes et al., 2003b; Zhao et al., 2006; Olivier et al., 2008b; Line et al., 2011). Therefore, the phenotypes of mice with altered 5-HTT expression strongly resemble those of humans varying in 5-HTT expression (for reviews, see Murphy and Lesch, 2008; Murphy et al., 2008).

Studies in altered 5-HTT rodent models have corroborated associations that have been controversial in human experiments and revealed potential underpinning physiological mechanisms (for reviews, see Holmes et al., 2003a; Caspi et al., 2010). The debated 5-HTT-mediated gene × environment interaction has been demonstrated in 5-HTT KO rats that exhibit impaired fear extinction only when housed in open, exposed but not closed, individually ventilated cages (Nonkes et al., 2012; Shan et al., 2014). Furthermore, differences in anxiety-like behaviour between 5-HTT KO and WT rats are abolished in animals raised in stressful conditions (Schipper et al., 2011). Control 5-HTT KO mice display impaired extinction and do not change their fear behaviour following social defeat; in contrast, wild-type (WT) mice that have experienced social defeat exhibit deficient extinction learning compared to their controls (Narayanan et al., 2011). Gene × environment interactions have not just been described behaviourally, but also on a molecular level; early life stress by maternal separation differentially affects corticoid receptor expression in rats with altered 5-HTT expression (van der Doelen et al., 2014). Furthermore, variation in amygdala activity has also been linked to 5-HTT expression. 5-HTT KO rodents display heightened amygdala activity during a task in which an aversive stimulus is used to devalue a rewarded cue, and increased theta synchrony between the amygdala and prefrontal cortex

during impaired extinction retrieval (Nonkes et al., 2010; Narayanan et al., 2011). In contrast, 5-HTT OE mice show decreased amygdala reactivity and theta oscillations in response to a CS during fear retrieval (Barkus et al., 2014). 5-HTT variation could lead to altered amygdala function via a number of mechanisms, including those involving 5-HT receptors, 5-HT homeostasis, growth factors, corticosteroid receptors, neuroplasticity, and neuronal morphology (Li et al., 2000; Homberg et al., 2007, 2011; Wellman et al., 2007; Karpova et al., 2009; van der Doelen et al., 2014; Bocchio et al., 2015). Hence, the 5-HT system can moderate the impact of environmental events on the emotionality of animals, as well as the function of underlying neural circuits, such as the amygdala.

For example, rodents with 5-HTT expression variation exhibit altered 5-HT homeostasis. 5-HTT KO rodents have abnormal 5-HT turnover rates and 5-HT_{1A} receptor function *in vivo* (Kim et al., 2005; Homberg et al., 2008; Olivier et al., 2008a). The DRN, a primary source of 5-HT neurons, contains fewer and lower-firing 5-HT neurons in 5-HTT KO mice (Gobbi et al., 2001; Lira et al., 2003). Moreover, tissue levels of 5-HT and its main metabolite, 5-HIAA, are altered throughout the brains of 5-HTT KO and OE rodents (Kim et al., 2005; Jennings et al., 2006; Zhao et al., 2006; Homberg et al., 2007; Line et al., 2014). These findings highlight the significant influence of 5-HTT variation on shaping the 5-HT transmission system itself.

5-HTT expression variation could give rise to its phenotypes through the ongoing activity of the 5-HTT. There is some support for the ability of acute pharmacological interventions in adulthood to reverse the phenotypes generated by altered 5-HTT expression. Acute administration of a 5-HT_{1A} receptor antagonist reversed the passive coping behaviour of 5-HTT KO mice in a swim stress task (Soiza-Reilly et al., 2015). Similarly, on the elevated plus maze, acute blockade of 5-HT_{1A} receptors rescued the high-anxiety 5-HTT KO phenotype (Holmes et al., 2003b). The elevated plus maze test has also been used to study 5-HTT OE mice, with acute 5-HTT inhibition reversing the low-anxiety phenotype (Jennings et al., 2006). Thus, the activity of the 5-HTT at the time of the behaviour could underlie the phenotypes associated with altered 5-HTT expression.

2.1.3 Impact of altered 5-HT transmission in early life

In healthy humans, the 5-HTTLPR has been linked to differences in amygdala activation as early as adolescence (Lau et al., 2009). A gene × environment interaction of the 5-HTTLPR has also been reported in childhood, with evidence that short allele carriers are more emotionally susceptible to both positive and negative parenting experiences (Hankin et al., 2011). In support of the importance of the 5-HTT gene's interaction with early life environmental events, an increased risk of recurrent depression was found in adult carriers of the short allele who were exposed to maltreatment in their childhood (Uher et al., 2011). In addition, when their mothers reported anxiety during pregnancy, infant carriers of the short allele were reported more prone to negative emotionality (Pluess et al., 2011). Taken together, these studies indicate that the effects of 5-HTT expression variation might have developmental origins.

The possibility of a developmental mechanism underpinning phenotypic effects of 5-HTT gene variation in adults is in accordance with several rodent studies that report that perturbation of 5-HT signalling in early life produces altered emotionality in adulthood (for reviews, see Gaspar et al., 2003; Homberg et al., 2010; Teissier et al., 2017). Such manipulations have pharmacologically blocked or genetically knocked down 5-HT_{1A} receptors, 5-HT_{2A} receptors, or the 5-HTT, for example (Hansen et al., 1997; Gross et al., 2002; Ansorge et al., 2004; Ribas et al., 2008; Noorlander et al., 2008; Jiang et al., 2009a; Karpova et al., 2009; Benekareddy et al., 2011; Olivier et al., 2011; Smit-Rigter et al., 2012; Freund et al., 2013; Rebello et al., 2014; Sarkar et al., 2014; Garcia-Garcia et al., 2017). Indeed, 5-HT manipulations often evoke different behavioural effects when administered during postnatal or adolescent development rather than during adulthood (Gross et al., 2002; Thakker et al., 2005; Ansorge et al., 2008; Norcross et al., 2008; Popa et al., 2008; Homberg et al., 2011; Garcia-Garcia et al., 2016). This can account for the apparent paradox that 5-HTT KO increases negative emotionality while selective serotonin reuptake inhibitors (SSRIs) are used clinically as antidepressants and anxiolytics (Nemeroff and Owens, 2002). Early life 5-HT manipulations not only alter emotional behaviour in later life, but also change

molecular, structural, and functional properties of neural circuits across the brain (Homberg et al., 2011; Olivier et al., 2011; Guidotti et al., 2012; Rebello et al., 2014). These results identify a developmental trajectory through which phenotypes of altered 5-HT transmission appear to be established.

The fact that there are overlapping features of the 5-HTT KO phenotype and the effects of pharmacological 5-HT signalling manipulation in early life suggests that neurodevelopmental mechanisms may be a cause of the KO phenotype (Olivier et al., 2013). One drawback of the 5-HTT KO model is that it is not straightforward to rescue the 5-HTT during a specific time window and thereby investigate the developmental origin of the behavioural phenotype directly. In an effort to circumvent this problem, pharmacological agents have been used to target other 5-HT signalling mechanisms at developmental time points. For example, by postnatal administration of a 5-HT synthesis inhibitor (P5-P19) or 5-HT_{1A} receptor antagonist (P5-P33), Alexandre et al. (2006) rescued the depressive behaviour of 5-HTT KO mice and thereby characterised a crucial time window in which the phenotype develops. In another study, the impaired cortical response of 5-HTT KO mice to sensory stimuli, as measured by local glucose utilisation, was restored by postnatal (P0-P1) inhibition of 5-HT synthesis (Esaki et al., 2005). However, the 5-HTT OE model is perhaps more amenable to direct pharmacological manipulation through the use of SSRIs to inhibit the 5-HTT, and has the advantage of reflecting a more physiological range of variation in 5-HTT expression (two/three-fold increase) (Malison et al., 1998; Mann et al., 2000; Jennings et al., 2006). However, a study of the effects of early life administration of an SSRI on the behavioural phenotype of 5-HTT OE mice has not yet been conducted.

2.1.4 Aims of this chapter

This chapter investigated the developmental trajectory of 5-HTT expression variation by using a translationally relevant mouse model in which the 5-HTT is overexpressed. First, the behavioural and neurochemical phenotypes of adolescent 5-HTT OE mice were

characterised to assess whether the adult phenotypes of reduced fear, anxiety, and tissue 5-HT were already established in adolescence (Jennings et al., 2006; Line et al., 2014). Second, acute (in adolescence at the time of behavioural testing) or postnatal pharmacological 5-HTT blockade was administered to identify the critical time point during which altered 5-HTT expression shapes the fear-related phenotypes.

2.2 Materials and methods

2.2.1 Experimental animals

5-HTT OE mice (University of Oxford) and WT littermates were maintained on a CBAxC57BL/6J background. The founders of this transgenic line were generated by using a yeast artificial chromosome to introduce the human 5-HTT gene into mice, which resulted in a three-fold increase in 5-HTT expression (Jennings et al., 2006). Animals were bred by mating 5-HTT OE males with CBAxC57BL/6J females (Charles River, UK) to generate heterozygous 5-HTT OE or WT mice. Genotyping was performed using polymerase chain reaction.

5-HTT OE mice were housed with WT littermates on a 12/12 h light/dark cycle (lights on at 7.00 A.M.) at constant temperature and humidity. Mice had *ad libitum* access to food (standard lab chow) and water unless otherwise stated. Environmental enrichment was provided in the form of nesting material and cardboard dome homes. Mice were group-housed (2-6 per cage). All experiments were conducted using male and female mice, and in compliance with the Animals (Scientific Procedures) Act of 1986 (UK).

2.2.2 Behavioural protocols

Adolescent mice were tested between P25 and P40. Mice were handled for one week prior to testing. Body weight was recorded on the final day of habituation. The experimenter

was blind to genotype and drug treatment while running behavioural tests. Animal cohorts for the adolescent and citalopram studies were assessed on tasks in the order below.

2.2.2.1 Elevated plus maze

The elevated plus maze consisted of two "open" arms and two "closed" arms aligned in a plus formation. The open arms were 29 x 4 cm and made of white plexiglass; the closed arms were 27 x 8 cm, enclosed by 30 cm-high walls, and made of grey plexiglass. The arms were joined in the middle by a central rectangular area onto which mice were placed individually to initiate a trial. The apparatus was elevated 50 cm above the ground. Animals were allowed to explore the maze for 300 s. The amount of time spent in open arms, number of entries into open arms, and latency to first enter an open arm were recorded (Line et al., 2011).

2.2.2.2 Hyponeophagia

Mice were food deprived overnight prior to testing. Mice were presented with a novel food in a novel environment: a white plexiglass base with a food well filled with 50% condensed milk. Mice were placed onto the apparatus facing away from the well and covered with a plastic jug. Latencies to first make contact with the milk and to begin continuous eating were measured. If the mouse did not initiate eating, the experiment was terminated after three trials of 120 s (Line et al., 2011).

2.2.2.3 Locomotor activity

Spontaneous locomotor activity was evaluated by placing mice individually into plastic cages lined with bedding, similar to a home cage environment to reduce anxiety and encourage exploration. The cages were 26 cm long, 16 cm wide, and 17 cm high. Two infrared

beams crossed each cage. Mice were allowed to explore for 2 h, and the total number of beam breaks per 5 min time bin were recorded (Line et al., 2011).

2.2.2.4 Fear learning

Fear learning was conducted in one of two operant chambers (ENV-307A, Med Associated Inc.), each with distinct visual and olfactory cues. The chambers were 17 cm long, 11.5 cm wide, and 20 cm high. The chamber was inside a sound-insulated box. For fear conditioning training, the floor of the chamber consisted of stainless steel bars 8.5 mm apart. Footshocks were delivered through the bars (Med Associated shock generator). Stimulus delivery was controlled by MED-PC (Med Associates). During the experiment, images were captured by a wide-angle video camera attached to the ceiling of the chamber, and stored on a digital video recorder. Fear memory retrieval was tested in a novel context (i.e. a mouse trained in Context A would be tested in Context B). Additionally, a plastic insert was placed above the bars to distinguish the contexts.

Fear learning was conducted over two consecutive days (day 1: conditioning training, day 2: retrieval test). During training, after a 180 s acclimation period, mice received two pairings (180s inter-trial interval) of a 30 s, 80 dB tone cue (CS) and a co-terminating, 0.5 s, 0.3 mA scrambled footshock. The total session lasted 480 s. The retrieval test was conducted without footshocks in a different context, with the same dimensions but novel visual and olfactory cues. After a 180 s acclimation period, mice received two presentations (180 s inter-trial interval) of the 30 s, 80 dB CS tone. The test lasted 480 s (Line et al., 2014).

Movement was monitored using NIH Image (Barkus et al., 2014), which compared consecutive video frames (1 frame per s) to calculate percentage of pixel change. Freezing was detected when the percentage pixel change from one frame to the next was below a set threshold (Richmond et al., 1998). This threshold was calibrated for an absence of movement other than breathing. A freezing difference score was calculated by subtracting the freezing

amount during the pre-tone period from the freezing amount during the tone presentation period. Hence, positive freezing difference scores demonstrate an increase in freezing compared to the 30 s pre-tone period. Unconditioned responses were analysed during the first CS-US pairing on the training day. Shock reactivity was analysed from the last 1 s (movement). Measuring the orienting response to the auditory cue was attempted by considering freezing levels in the first 4 s of the first CS tone presentation. However, there was no freezing during these first 4 s, therefore it was not possible to assess the orienting response.

2.2.3 High-performance liquid chromatography

High-performance liquid chromatography (HPLC) with electrochemical detection was carried out to measure tissue 5-HT levels. Mice were sacrificed by cervical dislocation after completion of behavioural testing. Brains were extracted, snap frozen in isopentane, and stored at -80°C. On the day of HPLC analysis, brains were sectioned into 150 µm slices on a cryostat, and 750 µm diameter tissue punches were rapidly taken and homogenised for 10 s in 100 µL of 0.06 M perchloric acid. Samples were collected as three tissue punches per brain region. The homogenate was centrifuged at 15000 rotations per min for 10 mins. 50 µL samples of the supernatant were loaded onto the HPLC system via the injection port (Rheodyne).

5-HT and 5-HIAA were separated in a 100 x 4.6 mm reverse-phase column with 3 µm C_{18} Microsorb ODS2 particles (Waters Ltd.). The column was perfused at a flow rate of 1ml/min by a degassed mobile phase containing 12.5% (v/v) methanol, 0.13 M $NaH_2PO_4.H_2O$, 0.85 mM EDTA, and 0.025 mM 1-octanesulphonic acid sodium at pH 3.5. The column was eluted with the mobile phase by 2150 HPLC pump (LKB).

Analytes were detected electrochemically (LC-4B amperometric detector, BAS Instruments) using a glassy carbon electrode working at +0.7V and a salt bridge silver/silver

chloride reference electrode (BAS Instruments). The HPLC apparatus was calibrated using external standard solutions containing 5 pmol of each compound of interest in 0.06 M perchloric acid. Peak heights were converted into concentrations by a benchtop integrator (Milton Roy CI4000). Because all samples contained tissue punches of fixed size (0.75 mm diameter x 150 μm thickness), concentrations were reported in pmol.

2.2.4 Drug treatment

Citalopram hydrobromide (Sigma Aldrich) was dissolved in 0.9% saline and injected *i.p.* at a dose of 10 mg/kg (Invernizzi et al., 1992, 1995; Hjorth et al., 1997; Burghardt et al., 2004). The vehicle solution was 0.9% saline. For fear conditioning experiments, adolescent mice were administered an acute *i.p.* injection of citalopram 30 min prior to fear conditioning to inhibit 5-HTT activity during fear memory acquisition. In other behavioural experiments, mice were administered citalopram (*s.c.*) daily during the postnatal period from P4 to P21; this dosing regimen has been used previously on postnatal pups and found to produce changes in emotional behaviour later in life (Ansorge et al., 2008; Popa et al., 2008). Since single injections of citalopram at 10 mg/kg have been shown to elevate extracellular 5-HT levels for over 5 hours, the daily injection regimen likely exposed animals to prolonged elevations of 5-HT levels during the postnatal period (Invernizzi et al., 1992). At least one week was allowed to pass before behavioural experiments, to ensure the clearance of citalopram.

2.2.5 Statistical analysis

Statistical analysis was performed using SPSS (IBM) and GraphPad Prism software. Student's unpaired t-test was used when data were of equal variance and normally distributed. If Levene's test for equality of variance was not passed, Welch's t-test was used. If Shapiro-Wilk's test for normality was not passed, Mann Whitney U test was used. When

using repeated measures ANOVA, the within-subjects variable was checked for sphericity using Mauchly's test. If non-spherical, the Greenhouse-Geisser correction was applied. 2- and 3-way ANOVAs were used to assess main effects and interactions, and Sidak's test was used for multiplicity-corrected pairwise comparisons. N-values refer to the number of animals in an experiment, and degrees of freedom refer to both the number of animals and the number of observations. Due to the robustness and replicability of 5-HTT OE phenotypes (Jennings et al., 2006; Line et al., 2011, 2014; Barkus et al., 2014; Bocchio et al., 2015), the following pairwise comparisons were pre-planned to evaluate the effect of citalopram treatment on these phenotypes (Table 2.1).

Table 2.1 – Pre-planned statistical individual pairwise comparisons

Measurement	Planned pairwise comparisons *a priori*	Prerequisite (to confirm replication of previously reported effects)
Body weight, spontaneous locomotor activity, elevated plus maze, fear retrieval (difference scores)	WT vehicle vs. WT citalopram, OE vehicle vs. OE citalopram	Main effect of genotype (Line et al., 2011)
Fear retrieval	Pre-tone vs. tone for each condition (WT vehicle, WT citalopram, OE vehicle, OE citalopram)	Period × genotype interaction (Line et al., 2014)

2.3 Results

2.3.1 Characterisation of adolescent 5-HTT OE anxiety phenotype

The effect of 5-HTT overexpression on adolescent anxiety was assessed. Thus, adolescent 5-HTT OE mice and WT littermates (P25 – P40) were monitored during ethological, unconditioned anxiety tasks (Figure 2.2A). On the elevated plus maze, compared to WT mice, 5-HTT OE mice spent a greater amount of time in the open arms [Mann Whitney U test, U=86.500, p=0.004] (Figure 2.2B, left) and made a higher number of entries into the open arms [Mann Whitney U test, U=103.000, p=0.014] (Figure 2.4B, middle). 5-HTT OE mice did not display statistically significant differences in latencies to first enter an open arm [Mann Whitney U test, U=127.500, p=0.081] (Figure 2.2B, right). However, an alternative interpretation could also be considered due to the overall difference observed

between the mean latencies; the statistical test may be underpowered with the current sample sizes. Because 5-HTT OE mice explored the anxiogenic open arms to a greater extent, the data indicate that 5-HTT OE mice were less anxious than WT mice. In the hyponeophagia task, OE and WT mice had similar latencies to first make contact with the novel food [2-sample 2-tailed t-test, t(65)=1.055, p=0.248] (data not shown). However, upon having initially made contact with the food, 5-HTT OE mice were significantly quicker to begin eating (latency to eat – latency to contact) [Welch's 2-tailed t-test, t(39.044)=2.316, p=0.026] (Figure 2.2C). The latter finding is also evidence that 5-HTT OE mice were less anxious than WT mice.

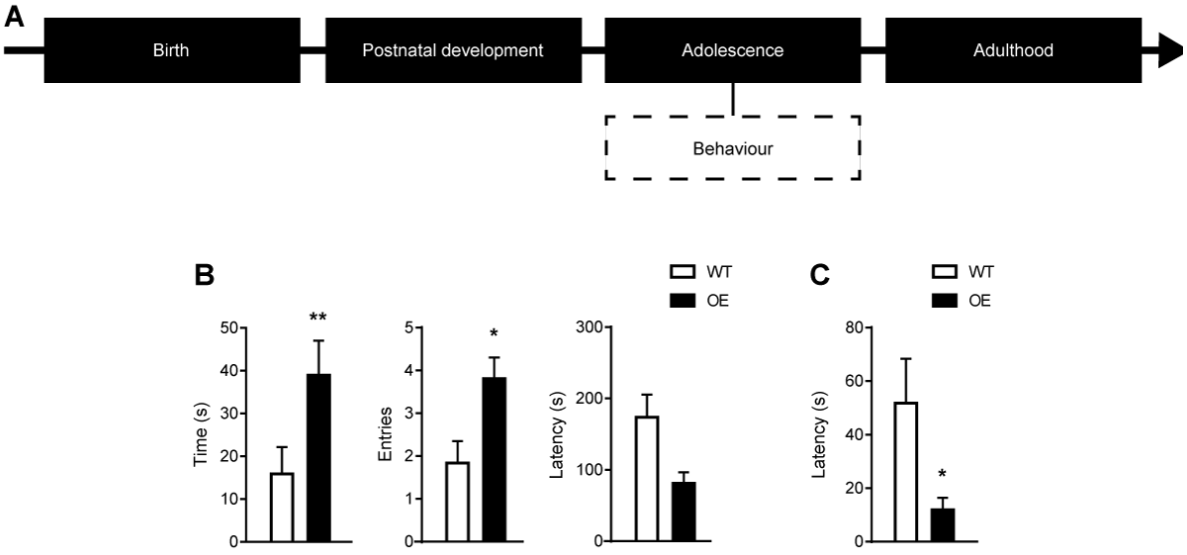


Figure 2.2 – Adolescent 5-HTT OE mice show reduced anxiety on unconditioned tasks compared to WTs

A. Schematic of experiment in which behavioural tests are conducted during adolescence. **B.** Elevated plus maze: time spent in open arms (left), number of entries into open arms (middle), and latency to first enter an open arm (right; WT n=18, OE n=21). **C.** Hyponeophagia: latency to begin eating after approaching and contacting food (eat-contact; WT n=35, OE n=31). Data are expressed as means ± SEM. *p<0.05, **p<0.01.

2.3.2 Characterisation of adolescent 5-HTT OE fear phenotype

Having confirmed the low-anxiety 5-HTT OE phenotype, it was next investigated whether 5-HTT overexpression influences fear learning in adolescence using a standard fear conditioning paradigm with adolescent mice (P25 – P40) (Figure 2.3A). During training, 5-HTT OE and WT mice did not differ significantly in their unconditioned responses to the shock, but 5-HTT OE mice did show a trend towards greater shock reactivity [Welch's 2-

tailed t-test, t(12.975)=2.134, p=0.053] (Table 2.2). During the fear memory retrieval test, 5-HTT OE and WT mice exhibited different levels of freezing to the conditioned tone [repeated measures 2-way ANOVA; main effect of period, F(1,20)=9.795, p=0.005; main effect of genotype, F(1,20)=5.721, p=0.027; period × genotype interaction, F(1,20)=10.497, p=0.004]. Only WT mice showed increased freezing to the conditioned tone compared to the pre-tone period [Sidak's pairwise comparisons: pre-tone vs. tone, WT p=0.001, OE p=0.932] (Figure 2.3B). A freezing difference score was calculated (tone freezing – pre-tone freezing), and this was lower for 5-HTT OE mice compared to WTs [Welch's 2-tailed t-test, t(8.393)=2.702, p=0.026] (Figure 2.3C). This result suggests that fear learning is impaired in adolescent 5-HTT OE mice.

Table 2.2 – Unconditioned responses to the shock during fear conditioning
Inter-genotype comparison of unconditioned reaction to the first shock (arbitrary units of movement, a.u.) (WT n=9, OE n=13). Data are expressed as medians and interquartile ranges (IQR).

	First shock reactivity (a.u.)
WT	6.0 (IQR 4.3 – 7.6)
OE	9.2 (IQR 5.9 – 15.6)

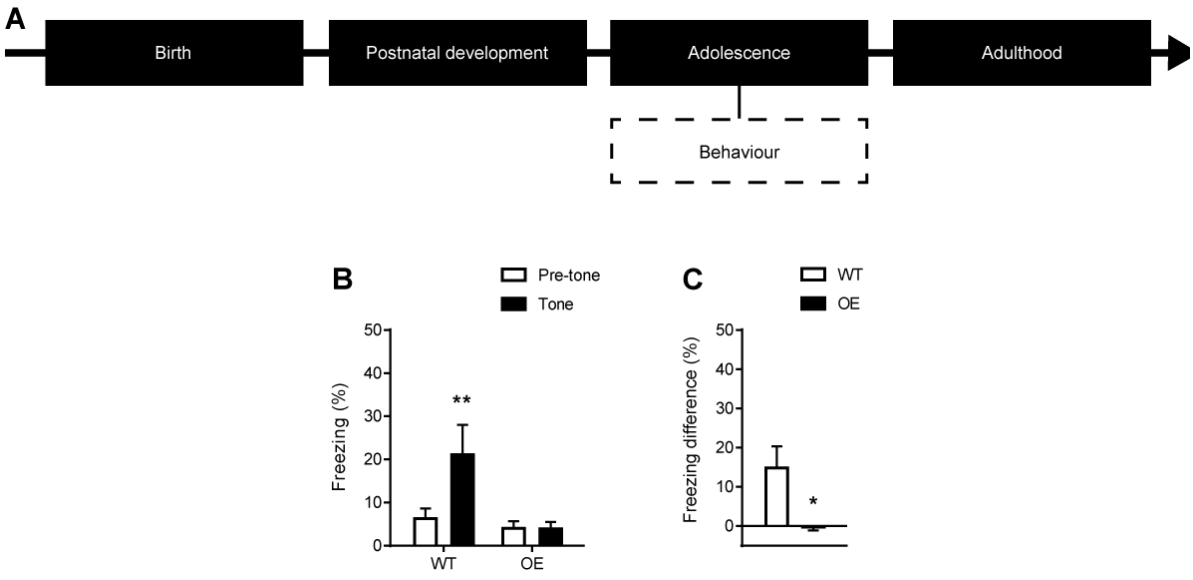


Figure 2.3 – Adolescent 5-HTT OE mice show reduced fear in a cued fear conditioning task
A. Schematic of experiment in which behavioural tests are conducted during adolescence. **B.** Percentage time spent freezing to a CS tone and in the pre-tone period during fear retrieval (WT n=9, OE n=13). **C.** Pre-tone freezing subtracted from tone-evoked freezing during fear retrieval (WT n=9, OE n=13). Data are expressed as means ± SEM. *p<0.05, ***p<0.001.

2.3.3 Measurement of adolescent 5-HTT OE body weight and locomotor activity

Adolescent 5-HTT OE mice and WT littermates (P25 – P40) were weighed and monitored for spontaneous locomotor activity (Figure 2.4A). OE mice were lighter than WT littermates [2-sample 2-tailed t-test, $t(91)=2.984$, $p=0.004$] (Figure 2.4B). However, OE and WT mice did not display differences in spontaneous locomotor activity [repeated measures 2-way ANOVA; main effect of time with Greenhouse-Geisser correction, $F(8.631, 379.785)=94.672$, $p<0.001$; main effect of genotype, $F(1,44)=0.539$, $p=0.467$; time × genotype interaction with Greenhouse-Geisser correction, $F(8.631, 379.785)=0.632$, $p=0.763$] (Figure 2.4C). This shows that adolescent 5-HTT OE mice, compared to WTs, had lower body weights but similar locomotor activity, which should therefore not have contributed to performance on other tasks (i.e. anxiety tests and fear conditioning).

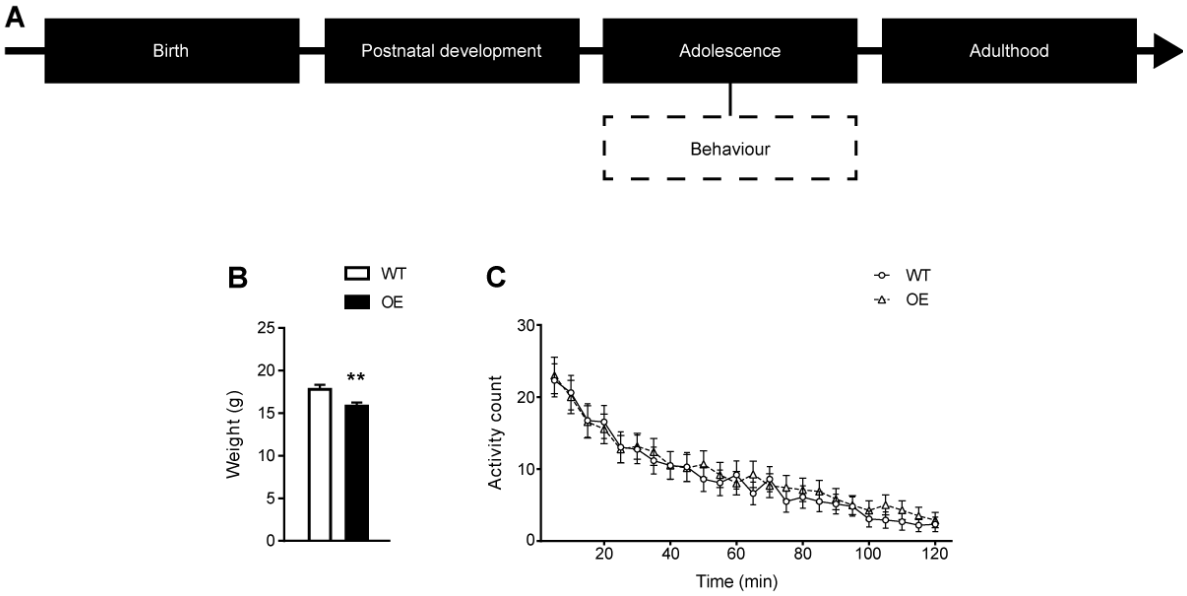


Figure 2.4 – Weight change and locomotor activity in adolescent 5-HTT OE mice
A. Schematic of experiment in which behavioural tests are conducted during adolescence. **B.** Weights of mice (WT n=41, OE n=52). **C.** Locomotor activity measured as photocell beam breaks per 5 min block in a novel environment (WT n=25, OE n=21). Data are expressed as means ± SEM. **p<0.01.

2.3.4 Characterisation of adolescent 5-HTT OE neurochemical phenotype

Characterisation of the behavioural phenotypes was followed up by a neurochemical analysis, for which tissue punches were taken from the DRN and BLA of adolescent 5-HTT OE mice and WT littermates (P35 – P40) (Figure 2.5A,B). The neurochemical phenotype of

5-HTT overexpression was characterised by measuring amounts of 5-HT and its main metabolite, 5-HIAA, using HPLC with electrochemical detection. In 5-HTT OE mice, both the DRN [2-sample 2-tailed t-test, t(9)=3.328, p=0.009] and BLA [2-sample 2-tailed t-test, t(9)=3.202, p=0.011] contained lower levels of 5-HT compared to the respective regions in WT mice (Figure 2.5C). In contrast, 5-HIAA levels were similar in 5-HTT OE and WT mice, both in the DRN [2-sample 2-tailed t-test, t(9)=1.603, p=0.143] and BLA [2-sample 2-tailed t-test, t(9)=0.610, p=0.557] (Figure 2.5D). These data indicate that overexpression of the 5-HTT leads to lower tissue 5-HT levels in the DRN and amydgala.

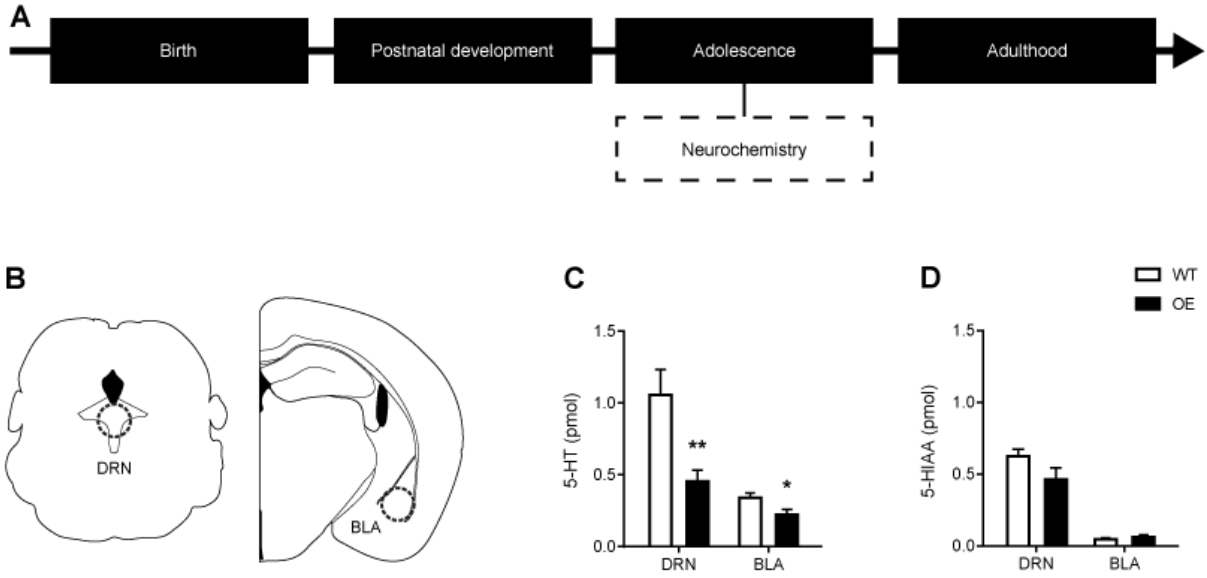


Figure 2.5 – Adolescent 5-HTT OE mouse brains contain lower 5-HT levels in the DRN and BLA
A. Schematic of experiment in which neurochemical analyses are conducted at adolescence. **B.** Tissue punch (3 per sample, 750 µm diameter × 150 µm thickness) locations in the DRN (left) and BLA (right) depicted by the dashed circle. **C.** Tissue 5-HT levels in brain punches taken from the DRN (WT n=5, OE n=6) and BLA (WT n=5, OE n=6). **D.** Tissue 5-HIAA levels in brain punches taken from the DRN (WT n=5, OE n=6) and BLA (WT n=5, OE n=6). Data are expressed as means ± SEM. *p<0.05, **p<0.01.

2.3.5 Effect of acute citalopram treatment during conditioning on fear phenotype of adolescent 5-HTT OE mice

Since the behavioural and neurochemical phenotypes of 5-HTT overexpression were already established during adolescence, the following experiment tested whether the low-fear phenotype of adolescent 5-HTT OE mice is driven by the ongoing activity of the 5-HTT at the time of behavioural testing. To this end, adolescent mice (P25 – P40) were administered

citalopram (10 mg/kg) 30 min prior to fear conditioning training to block the 5-HTT specifically during fear conditioning training (Figure 2.6A).

During training, neither genotype nor drug treatment significantly affected unconditioned responses to the shock. However, 5-HTT OE mice tended towards a reduced shock reactivity in this particular experiment (note: the opposite was seen in section 2.3.2) [2-way ANOVA; main effect of genotype, $F(1,50)=3.646$, $p=0.062$; main effect of drug, $F(1,50)=0.002$, $p=0.961$; genotype × drug interaction, $F(1,50)=0.001$, $p=0.972$] (Table 2.3).

During the fear retrieval test, only WT mice exhibited increased freezing to the conditioned tone compared to the pre-tone period (Figure 2.6B). This was evidenced by a significant main effect of genotype and the period × genotype interaction [repeated measures 3-way ANOVA; main effect of period, $F(1,50)=17.395$, $p<0.001$; main effect of genotype, $F(1,50)=11.074$, $p=0.002$; main effect of drug, $F(1,50)=3.324$, $p=0.074$; period × genotype interaction, $F(1,50)=20.859$, $p<0.001$]. There were also significant period × drug, and, crucially, genotype × drug interactions, though the period × genotype × drug interaction was not significant [period × drug interaction, $F(1,50)=4.392$, $p=0.041$; genotype × drug interaction, $F(1,50)=5.391$, $p=0.024$; period × genotype × drug interaction, $F(1,50)=2.411$, $p=0.127$]. Further exploration of the genotype × drug interaction by pairwise comparisons revealed that there was a significant effect of citalopram in WT but not 5-HTT OE mice [Sidak's pairwise comparisons: vehicle vs. citalopram, WT $p=0.009$, OE $p=0.704$]. These effects appear to be driven almost exclusively by the freezing responses during the tone presentations, and pre-planned individual pairwise comparisons (Table 2.1) confirmed that there was significant fear learning in both of the WT groups but neither of the 5-HTT OE groups, consistent with the genotype × period interaction [Sidak's pairwise comparisons: pre-tone vs. tone, WT vehicle $p=0.019$, WT citalopram $p<0.001$, OE vehicle $p=0.618$, OE citalopram $p=0.936$].

Pre-planned pairwise comparisons (Table 2.1) were made to individually analyse freezing difference scores and evaluate the effect of citalopram treatment on the two

genotype groups. 5-HTT OE mice retained their low-fear phenotype compared to WTs (see above). In addition, only WT mice had higher freezing difference scores when administered citalopram [Sidak's pairwise comparisons: vehicle vs. citalopram, WT p=0.020, OE p=0.679] (Figure 2.6C). These results suggest that citalopram administration enhanced fear learning in WT but not 5-HTT OE mice. Therefore, 5-HTT OE mice exhibited no fear learning in the presence or absence of the SSRI. Hence, acute citalopram treatment failed to rescue the low-fear phenotype of these mice.

Table 2.3 - Unconditioned responses to the shock during fear conditioning training with acute citalopram

Inter-genotype comparison of unconditioned reaction to the first shock (arbitrary units of movement, a.u.) (WT vehicle n=12, WT citalopram n=11, OE vehicle n=15, OE citalopram n=16). Data are expressed as medians and interquartile ranges (IQR).

	First shock reactivity (a.u.)
WT vehicle	6.1 (IQR 3.8 – 7.3)
WT citalopram	4.7 (IQR 3.0 – 9.2)
OE vehicle	3.1 (IQR 1.7 – 6.7)
OE citalopram	3.6 (IQR 1.5 – 5.5)

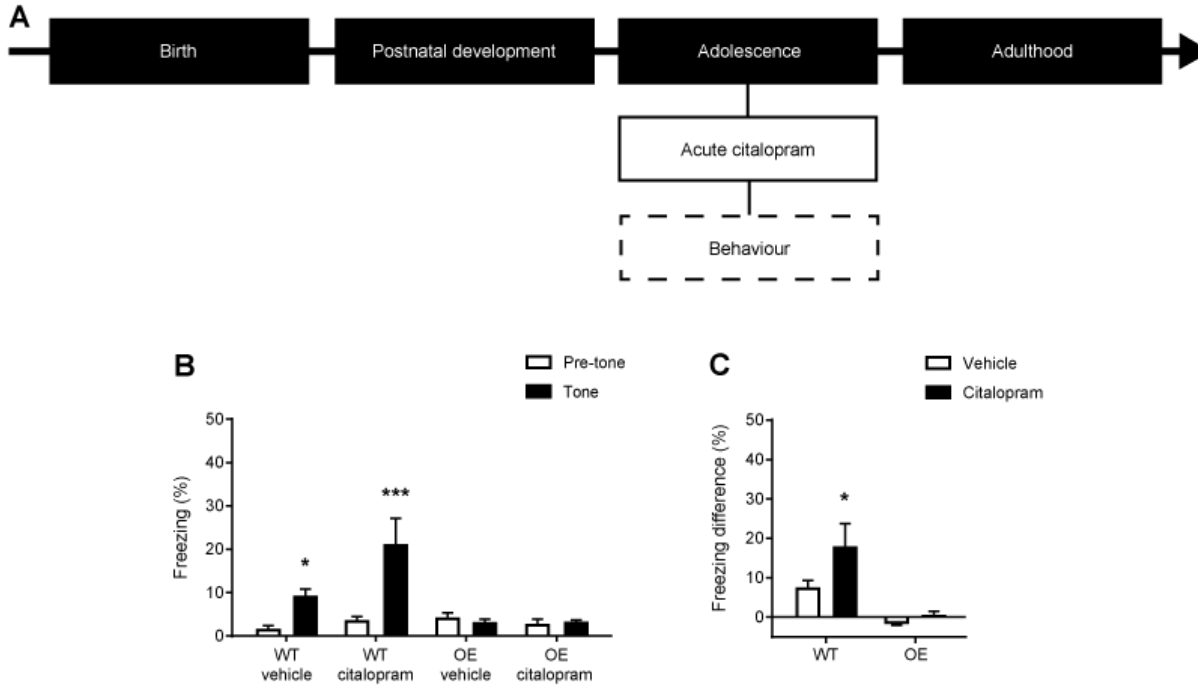


Figure 2.6 – Acute citalopram treatment does not rescue cued fear learning in adolescent 5-HTT OE mice but enhances fear in WT mice

A. Schematic of experiment in which acute citalopram treatment is given immediately before conditioning during adolescence. **B.** Percentage time spent freezing to a CS tone and in the pre-tone period during fear retrieval (WT vehicle n=12, WT citalopram n=11, OE vehicle n=15, OE citalopram n=16). **C.** Pre-tone freezing subtracted from

tone-evoked freezing during fear retrieval (WT vehicle n=12, WT citalopram n=11, OE vehicle n=15, OE citalopram n=16; * compared to WT vehicle). Data are expressed as means ± SEM. *p<0.05, ***p<0.001.

2.3.6 Effect of postnatal citalopram treatment on anxiety phenotype of adolescent 5-HTT OE mice

Because the low-fear phenotype of adolescent 5-HTT OE mice could not be reversed with acute administration of citalopram to these mice during behavioural testing in adolescence, the effect of postnatal citalopram on the behavioural phenotype of adolescent 5-HTT OE mice was investigated next. To this end, the influence of postnatal citalopram on the low-anxiety phenotype of 5-HTT OE mice was tested. 5-HTT OE and WT mice were administered citalopram (10 mg/kg) or vehicle over the early postnatal period (P4 – P21), and then mice were tested on the elevated plus maze as adolescents (P28 – P40) (Figure 2.7A). Hence, the 5-HTT was blocked over a key period during postnatal development, but not during adolescence while mice performed in behavioural tasks.

In the elevated plus maze task, 5-HTT OE mice again spent more time in open arms [2-way ANOVA; main effect of genotype, $F(1,53)=12.336$, $p=0.001$; main effect of drug, $F(1,53)=2.495$, $p=0.120$, genotype × drug interaction, $F(1,53)=2.553$, $p=0.116$]. Pre-planned pairwise comparisons (Table 2.1) were made for citalopram treatment, which did not influence WT mice but resulted in OE mice spending less time in open arms [Sidak's pairwise comparisons: vehicle vs. citalopram, WT $p=0.989$, OE $p=0.038$] (Figure 2.7B, left). WT mice were presumably unaffected due to the high levels of anxiety evident even with vehicle treatment, which may have resulted in a floor effect and obscured the possibility of seeing any further increase in anxiety (i.e. any further reduction in time spent in open arms). OE mice also made more entries into open arms [2-way ANOVA; main effect of genotype, $F(1,53)=4.572$, $p=0.037$; main effect of drug, $F(1,53)=0.777$, $p=0.382$; genotype × drug interaction, $F(1,53)=0.354$, $p=0.554$]. (Figure 2.7B, middle). Pre-planned pairwise comparisons (Table 2.1) revealed that citalopram treatment did not affect entries of either genotype [Sidak's pairwise comparisons: vehicle vs. citalopram, WT $p=0.831$, OE $p=0.327$].

Importantly, there were no differences in the number of entries into closed arms, indicating that overall locomotor activity was similar across conditions [2-way ANOVA; main effect of genotype, $F(1,53)=0.023$, $p=0.880$; main effect of drug, $F(1,53)=0.061$, $p=0.806$; genotype × drug interaction, $F(1,53)=1.299$, $p=0.259$] (data not shown). Neither genotype nor drug treatment appeared to have significant effects on latencies to first enter an open arm [2-way ANOVA; main effect of genotype, $F(1,53)=3.437$, $p=0.069$; main effect of drug, $F(1,53)=0.963$, $p=0.331$; genotype × drug interaction, $F(1,53)=1.594$, $p=0.212$] (Figure 2.7B, right). Overall, these results suggest that postnatal citalopram treatment may reverse the low-anxiety phenotype of 5-HTT OE mice, with the proviso that the genotype × drug interaction was not statistically significant.

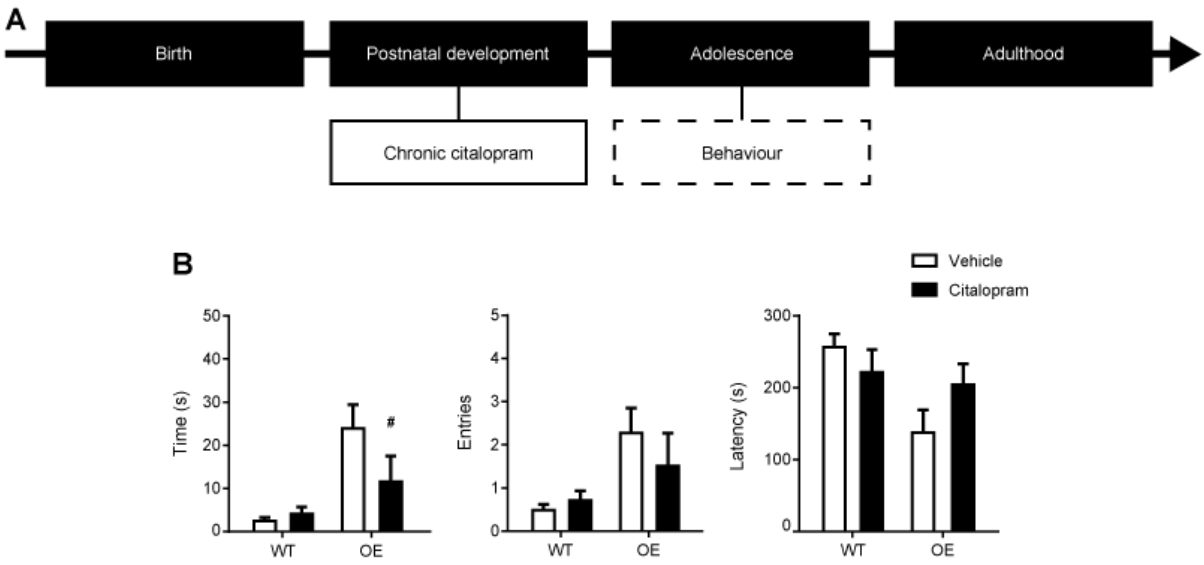


Figure 2.7 – Postnatal citalopram treatment increases anxiety in adolescent 5-HTT OE mice
A. Schematic of experiment in which chronic citalopram treatment is given during postnatal development and behavioural tests are conducted during adolescence. **B.** Elevated plus maze: time spent in open arms (left), number of entries into open arms (middle left), latency to first enter an open arm (middle right; WT vehicle n=17, WT citalopram n=13, OE vehicle n=11, OE citalopram n=14; # compared to OE vehicle), and number of entries into closed arms (right). Data are expressed as means ± SEM. #$p<0.05$.

2.3.7 Effect of postnatal citalopram treatment on the fear phenotype of adolescent 5-HTT OE mice

Given the above evidence that postnatal citalopram reverses the low-anxiety phenotype of 5-HTT OE mice, further experiments tested the influence of this treatment on the low-fear phenotype of these mice. Thus, 5-HTT OE and WT mice were administered

citalopram (10 mg/kg) or vehicle over the early postnatal period (P4 – P21), and then mice were tested in the fear conditioning paradigm in adolescence (P28 – P40) in the absence of any drug treatment (Figure 2.8A).

Shock reactivity during training was analysed. Neither genotype nor prior citalopram treatment influenced unconditioned responses to the shock [2-way ANOVA; main effect of genotype, $F(1,41)=1.746$, $p=0.194$; main effect of drug, $F(1,41)=0.086$, $p=0.771$; genotype × drug interaction, $F(1,41)=0.018$, $p=0.894$] (Table 2.4).

During the fear retrieval test, both vehicle- and citalopram-treated WT mice exhibited increased freezing to the conditioned tone compared to the pre-tone period, as well as 5-HTT OE mice given citalopram treatment. There was a main effect of drug, and drug did not significantly interact with genotype or period [repeated measures 3-way ANOVA; main effect of period, $F(1,41)=26.216$, $p<0.001$; main effect of genotype, $F(1,41)=3.323$, $p=0.076$; main effect of drug, $F(1,41)=7.208$, $p=0.010$]. This suggests that mice given citalopram treatment postnatally exhibited enhanced fear irrespective of genotype or period. Nevertheless, citalopram treatment seemed to increase freezing particularly in WT mice independently of tone presentation [Sidak's pairwise comparisons: vehicle vs. citalopram, WT $p=0.017$; OE $p=0.197$]. There were also significant two-way interactions with period [period × genotype interaction, $F(1,41)=5.368$, $p=0.026$; period × drug interaction, $F(1,41)=6.152$, $p=0.017$; genotype × drug interaction, $F(1,41)=0.649$, $p=0.425$; period × genotype × drug interaction, $F(1,41)=0.629$, $p=0.432$]. Pre-planned individual pairwise comparisons (Table 2.1) were carried out to verify that postnatal citalopram could rescue the low-fear phenotype of 5-HTT OE mice [pre-tone vs. tone, WT vehicle $p=0.005$, WT citalopram $p<0.001$, OE vehicle $p=0.825$, OE citalopram $p=0.003$] (Figure 2.8B). This result indicates that there was significant fear learning in citalopram-treated 5-HTT OE mice, which suggests a rescue of the low-fear phenotype specifically by postnatal 5-HTT inhibition.

Pre-planned pairwise comparisons (Table 2.1) were also made of freezing difference scores to evaluate the impact of postnatal citalopram treatment on fear behaviour. Notably,

citalopram-treated 5-HTT OE mice had higher freezing scores compared to vehicle-treated 5-HTT OE mice [Sidak's pairwise comparisons: vehicle vs. citalopram, WT p=0.234, OE p=0.027] (Figure 2.8C). These data indicate that postnatal citalopram administration enhanced fear learning in 5-HTT OE mice, thereby restoring a normal fear phenotype. However, it should be noted that the genotype × drug interaction was not statistically significant.

Table 2.4 - Unconditioned responses to the shock during fear conditioning training with acute citalopram

Inter-genotype comparison of unconditioned reaction to the first shock (arbitrary units of movement, a.u.) (WT vehicle n=12, WT citalopram n=12, OE vehicle n=10, OE citalopram n=12). Data are expressed as medians and interquartile ranges (IQR).

	First shock reactivity (a.u.)
WT vehicle	8.5 (IQR 2.4 – 11.1)
WT citalopram	7.8 (IQR 4.1 – 10.3)
OE vehicle	5.0 (IQR 1.8 – 6.9)
OE citalopram	5.3 (IQR 1.5 – 8.5)

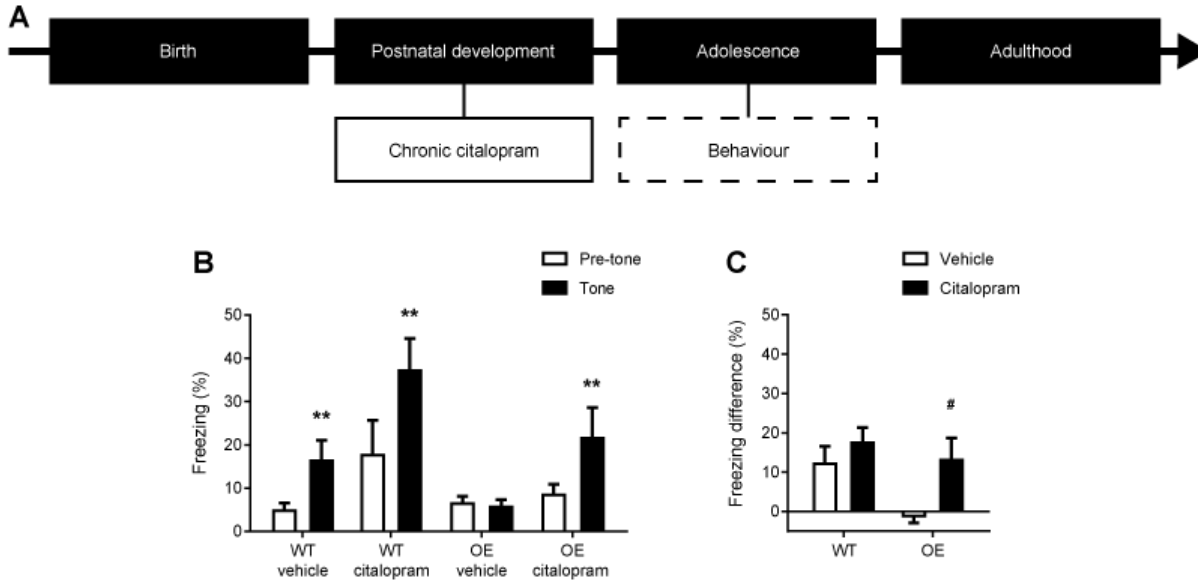


Figure 2.8 – Postnatal citalopram treatment rescues the fear phenotype of adolescent 5-HTT OE mice

A. Schematic of experiment in which chronic citalopram treatment is given during postnatal development and behavioural tests are conducted during adolescence. **B.** Percentage time spent freezing to a CS tone and in the pre-tone period during fear retrieval (WT vehicle n=12, WT citalopram n=12, OE vehicle n=10, OE citalopram n=12). **C.** Pre-tone freezing subtracted from tone-evoked freezing during fear retrieval (WT vehicle n=12, WT citalopram n=12, OE vehicle n=10, OE citalopram n=12; * compared to WT vehicle, # compared to OE vehicle). Data are expressed as means ± SEM. #p<0.05, **p<0.01.

2.3.8 Effect of postnatal citalopram treatment on body weight and locomotor activity of adolescent 5-HTT OE mice

Finally, the effect of postnatal citalopram treatment on the body weight and locomotor activity of adolescent 5-HTT OE mice was assessed. 5-HTT OE and WT mice were administered citalopram (10 mg/kg) or vehicle over the early postnatal period (P4 – P21). Mice were then weighed and monitored for spontaneous locomotor activity during adolescence (P28 – P40) in the absence of any drug treatment (Figure 2.9A).

5-HTT OE mice were lighter than WT littermates but there was no effect of the prior postnatal drug treatment [2-way ANOVA; main effect of genotype, $F(1,55)=12.714$, $p=0.001$; main effect of drug, $F(1,55)=1.842$, $p=0.180$; genotype × drug interaction, $F(1,55)=0.573$, $p=0.452$]. Pre-planned pairwise comparisons (Table 2.1) of the drug treatment were made, but were found not to influence body weight in either genotype, reflecting the lack of main effect of drug [Sidak's pairwise comparisons: vehicle vs. citalopram, WT $p=0.661$, OE $p=0.155$] (Figure 2.9B).

OE and WT mice did not display differences in spontaneous locomotor activity, and this was not changed by prior drug treatment [repeated measures 3-way ANOVA; main effect of time with Greenhouse-Geisser correction, $F(7.465, 283.656)=69.464$, $p<0.001$; main effect of genotype, $F(1,38)=2.019$, $p=0.164$; main effect of drug, $F(1,38)=0.054$, $p=0.818$]. There were also no significant interactions [time × genotype interaction with Greenhouse-Geisser correction, $F(7.465, 283.656)=1.929$, $p=0.060$; time × drug interaction, $F(7.465, 283.656)=0.637$, $p=0.735$; genotype × drug interaction, $F(1,38)=0.249$, $p=0.620$] (Figure 2.9C). These findings demonstrate that postnatal citalopram treatment does not affect body weight or locomotor activity of OE mice. Hence, differences in locomotor activity should not contribute to performance on other tasks.

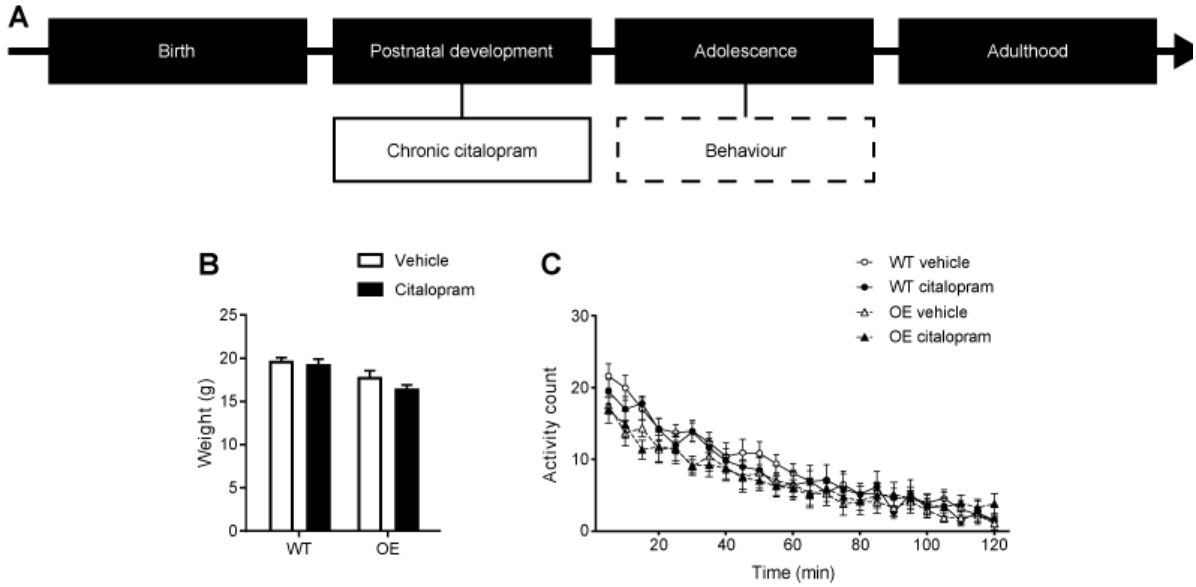


Figure 2.9 – Postnatal citalopram treatment does not affect the weight change or locomotor activity of adolescent 5-HTT OE mice
A. Schematic of experiment in which chronic citalopram treatment is given during postnatal development and behavioural tests are conducted during adolescence. **B.** Weights of mice (WT vehicle n=19, WT citalopram n=13, OE vehicle n=12, OE citalopram n=15; * compared to WT vehicle, † compared to WT citalopram). **C.** Locomotor activity measured as photocell beam breaks per 5 min block (WT vehicle n=13, WT citalopram n=8, OE vehicle n=10, OE citalopram n=11). Data are expressed as means ± SEM.

2.4 Discussion

Evidence from human studies and rodent models suggests that variation in 5-HTT gene expression in early life shapes emotional phenotypes in the adult. The 5-HTT OE model, rather than ablating the 5-HTT gene, relies on overexpressing the 5-HTT to an extent similar to the physiological range observed in humans (Malison et al., 1998; Mann et al., 2000; Jennings et al., 2006), and these mice have striking low-anxiety and -fear phenotypes in adulthood. However, the developmental trajectory of the behavioural phenotype of the 5-HTT OE mouse has yet to be studied. The current study investigated anxiety- and fear-related behaviour in 5-HTT OE mice in adolescence. First, it was observed that the low-anxiety and -fear phenotypes previously reported in adult 5-HTT OE mice were already established in adolescence. This could indicate that the mechanisms giving rise to the phenotypes have a developmental origin. Next, it was found that pharmacological blockade of the 5-HTT by citalopram treatment at the time of behavioural testing did not reverse the deficit in fear learning of adolescent 5-HTT OE mice, suggesting that this behavioural phenotype was not

linked to ongoing increased 5-HTT expression. However, pharmacological inhibition of the 5-HTT in an early postnatal period did reverse the low-anxiety/fear phenotype of 5-HTT OE mice, thereby identifying 5-HTT overexpression during this period as critical to phenotype generation.

2.4.1 Developmental trajectory of fear-related phenotypes in adolescent 5-HTT OE mice

Postnatal (P4-P21) administration of citalopram reversed both the low-anxiety and low-fear phenotypes of adolescent 5-HTT OE mice. It must be noted that these results should be interpreted with caution because some of the pre-planned comparisons did not have statistically significant interactions. Nevertheless, the finding is in accordance with previous studies in which postnatal SSRI treatment increased fear, anxiety-, and depression-like behaviours later in the life of WT animals (Hansen et al., 1997; Ansorge et al., 2004, 2008; Popa et al., 2008; Ribas et al., 2008; Jiang et al., 2009a; Karpova et al., 2009; Rebello et al., 2014; Sarkar et al., 2014; for review, see Kepser and Homberg, 2015). One such study reported that neither postnatal noradrenaline transporter blockade nor transient adult 5-HTT inhibition alter fear-related behaviour in mice, indicating that the behavioural effects are specific to developmental 5-HT transmission (Ansorge et al., 2008). Another study that points towards a developmental trajectory of the 5-HTT in driving emotional behaviour demonstrates that knockdown of the 5-HTT by RNA interference in adult mice, similar to chronic SSRI administration, produces an antidepressant-like effect, which is the opposite behavioural effect from constitutive 5-HTT KO (Thakker et al., 2005).

The 5-HT system is known to modulate numerous aspects of neural maturation, including axonal growth, synaptogenesis, cell differentiation, cytoarchitectural morphology, neuronal connectivity, GABAergic transmission, synaptic plasticity, growth factor expression, and raphe neuron excitability (Haydon et al., 1984; Lauder, 1990; Gaspar et al., 2003; Homberg et al., 2010; Guidotti et al., 2012; Calabrese et al., 2013; Miceli et al., 2013; Teissier

et al., 2017). Importantly, until the third postnatal week, the 5-HTT is expressed ectopically in non-5-HT neurons of structures relevant for emotional regulation, including the hippocampus, amygdala, cortex, thalamus, and septum (Lebrand et al., 1998). This could explain why the number and density of 5-HT fibres has been observed to transiently increase during postnatal development; the 5-HTT takes up extracellular 5-HT into non-5-HT axons (Fujimiya et al., 1986; Lebrand et al., 1996). Although the functions of this internalised 5-HT are not known, it has been hypothesised that it could contribute to intraneuronal maturation or to extraneuronal signalling as a "borrowed" transmitter (Lebrand et al., 1996). Thus, several mechanisms of neurodevelopment and 5-HT signalling could be affected specifically during the postnatal period by physiological variation in 5-HTT expression, thereby shaping behavioural phenotypes in later life.

In adolescent WT mice, postnatal citalopram treatment elevated overall freezing levels during conditioned fear retrieval, but not in a tone-specific manner. This could reflect a high-fear state that persisted throughout the entire fear retrieval session, and is supported by studies showing that fearful mice continue to exhibit freezing responses in between tone trials, including the pre-tone period (Seo et al., 2015; Glover et al., 2017). The overall increased fear observed in citalopram-treated mice, regardless of genotype, appeared to parallel previous work showing that postnatal SSRI administration heightens anxiety-like behaviour in adult animals (Ansorge et al., 2008; Karpova et al., 2009; Sarkar et al., 2014).

2.4.2 Altered 5-HT transmission in adolescent 5-HTT OE mice

Acute 5-HTT inhibition in adolescent WT mice increased fear learning, but did not alter the behaviour of 5-HTT OE mice. These results should be interpreted with caution because the comparisons were pre-planned, but some of the interactions were not statistically significant. Nevertheless, the enhanced fear learning of WT mice treated with acute citalopram is in agreement with previous findings (Burghardt et al., 2004). The observations suggest an impairment of 5-HT transmission mechanisms in the neural fear

circuits of 5-HTT OE animals, resulting in deficient behavioural control by the 5-HT system. This could be due to fundamental aspects of 5-HT transmission becoming disrupted in 5-HTT OE mice, which is reflected in the reduced tissue 5-HT levels detected in the DRN and BLA. Support for this is also provided by previous reports of altered 5-HT_{2A} receptor function (Jennings et al., 2008; Bocchio et al., 2015) and loss of ability for 5-HT neurons to control extracellular 5-HT levels through firing rate in 5-HTT OE mice (Jennings et al., 2010). Importantly, in *ex vivo* slices, these functional deficits in 5-HT signalling mechanisms cannot be rescued by acute perfusion of citalopram (Jennings et al., 2010; Bocchio et al., 2015). Furthermore, even in human functional imaging studies, acute citalopram treatment has different effects on neural excitability in long *versus* short 5-HTTLPR carriers (Eichhammer et al., 2003; Smith et al., 2004). This has crucial clinical implications, because SSRIs can have variable efficacy based on the natural range of 5-HTT expression in patients (Serretti et al., 2005; Hu et al., 2007).

In the current study, the 5-HTT was pharmacologically inhibited during either the postnatal period or adolescence. The low-fear phenotype of 5-HTT OE mice was sensitive to postnatal but not acute 5-HTT function. It would therefore be useful to verify whether the neurochemical phenotype (low tissue 5-HT) and acute citalopram sensitivity are also rescued by postnatal 5-HTT blockade.

2.4.3 Control of distinct emotional behaviours by the 5-HT system

Acute 5-HTT blockade, in spite of increasing fear in WT mice, did not change the low-fear phenotype of adolescent OE mice in the fear conditioning task. In contrast, a previous study reported that the low-anxiety phenotype of adult 5-HTT OE mice was reversed in the elevated plus maze test without any change to the WT phenotype by acute administration of the SSRI paroxetine (Jennings et al., 2006). This discrepancy likely arises from the fact that distinct brain regions contribute dissociable functions to emotional behaviour; for example, hippocampal lesions reduce anxiety while amygdala lesions impair fear learning (Phillips and

LeDoux, 1992; McHugh et al., 2004; but see also Tye et al., 2011). This is particularly relevant because 5-HT transmission in different neural targets is also thought to be involved in separate aspects of emotional behaviour (Graeff et al., 1996; Liu et al., 2014). Fear and anxiety-like behaviours, mediated by distinct brain areas and 5-HT mechanisms, might therefore be affected in different ways by 5-HTT overexpression.

In addition, both acute and postnatal SSRI treatment seem to reverse the low-anxiety phenotype of 5-HTT OE mice in the elevated plus maze task (Jennings et al., 2006), whereas only postnatal administration rescues the low-fear behaviour. This provides a neurobiological parallel for the psychological disparity between fear and anxiety-like behaviour, as described in Chapter 1. Anxiety, as shown in Table 1.1, is driven by a diffuse threat and promotes a sustained arousal state. In contrast, fear is a more specific, phasic emotion. If these characteristics are reflected in the underlying neural mechanisms, it would make sense for 5-HT transmission to influence anxiety in a generalised, tonic manner. Fear learning, in contrast, could require a particular formation and action of the 5-HT system and relevant circuits.

2.4.4 Comparing adolescent and adult 5-HTT OE phenotypes

The present study observed reduced fear and anxiety-like behaviour, as well as decreased body weights and tissue 5-HT levels, in adolescent 5-HTT OE mice. These results are largely in accordance with previous findings, in that the same phenotypic effects reported in adult 5-HTT OE mice were already in place during adolescence (Jennings et al., 2006; Line et al., 2011, 2014; Barkus et al., 2014; Bocchio et al., 2015; McHugh et al., 2015). Adult 5-HTT OE mice also exhibit lower spontaneous locomotor activity, which was not found in adolescent animals. This suggests that the differences in fear and anxiety-like behaviours in adolescence were not confounded by alterations in locomotor activity.

It should be noted that due to overarching similarities between adolescent and adult 5-HTT OE phenotypes, the discussion of this chapter uses findings from both ages to compare aspects of 5-HTT expression variation. However, care should be taken not to overlook differences between adolescent and adult animals. While adolescent and adult rodents exhibit similar fear-related behaviour after transient chronic 5-HTT inhibition, they display differences in depression-like behaviour, wakefulness, and acoustic startle (Norcross et al., 2008; Homberg et al., 2011).

2.4.5 Functional relationship between variation in 5-HTT expression and corresponding phenotypes

Adolescent 5-HTT OE mice displayed reduced fear, anxiety, and body weights, similar to adult OE mice that, in addition, have been shown to have decreased extracellular 5-HT (Jennings et al., 2006, 2010, Line et al., 2011, 2014; Barkus et al., 2014; Bocchio et al., 2015; McHugh et al., 2015). This mirrors the adult 5-HTT KO phenotypes, which are characterised by elevated fear, anxiety, and body weights, as well as increased extracellular 5-HT (Holmes et al., 2003b, 2003c; Lira et al., 2003; Jennings et al., 2010; Line et al., 2011). This would suggest a linear relationship between 5-HTT expression, 5-HT release, and emotional behaviour. However, there are other aspects of the behavioural and neurochemical phenotypes associated with variation in 5-HTT expression that are decidedly non-linear. For instance, both 5-HTT OE and KO mice display diminished spontaneous locomotor activity compared to WT mice (Line et al., 2011). Moreover, tissue 5-HT levels are lower in both 5-HTT OE and KO animals (Kim et al., 2005; Jennings et al., 2006; Zhao et al., 2006; Homberg et al., 2007; Line et al., 2014). The fidelity with which extracellular 5-HT signal magnitudes follow the frequency of 5-HT neuron stimulation *ex vivo* is also lost in both OE and KO mice (Jennings et al., 2010). Thus, there is not always a linear relationship between the extent of 5-HTT expression, 5-HT signalling mechanisms, and behavioural phenotypes.

The amygdala, which is necessary for normal fear behaviour, seems to be a vital target of the 5-HT system (Phillips and LeDoux, 1992). The current study found reduced tissue 5-HT in the amygdala of 5-HTT OE mice, and there are several previous reports of altered amygdala structure or function as a result of 5-HTT manipulations. For example, altered 5-HTT expression or activity leads to changes in 5-HT_{1A} receptor expression, 5-HT_{2A} receptor function, tissue 5-HT levels, BDNF expression, corticosteroid receptor expression, neuroplasticity markers, and dendritic spine density in the amygdala (Li et al., 2000; Homberg et al., 2007, 2011; Wellman et al., 2007; Karpova et al., 2009; van der Doelen et al., 2014; Bocchio et al., 2015). 5-HT neuromodulation of amygdala circuits is therefore likely to be important for fear regulation.

2.4.6 Conclusions

The data presented in this chapter identified a developmental origin of the fear-related behaviours associated with variation in 5-HTT expression using a translationally relevant mouse model. Consideration was given to the possibility that altered development of the 5-HT system and particular neural circuits drives the fear phenotype. This highlights the precise actions of 5-HT neurotransmission in fear regulation and the need to study 5-HT pathways with anatomical specificity. In the following chapters, a circuit-specific dissection of 5-HT neuromodulation in the amygdala during fear leaning will be conducted.

Chapter 3 5-HT neurons influence fear learning by modulating the basal amygdala

3.1 Introduction

In Chapter 2, the effects of transgenically engineered 5-HTT overexpression on fear- and anxiety-related behaviours were investigated. In addition to identifying a developmental origin for the reduced fear-related phenotype of 5-HTT OE mice, the findings discussed in Chapter 2 raised the question of the neural locus of these effects and, specifically, the potential role of 5-HT signalling in the amygdala in the regulation of fear. The current chapter explores this question in greater detail using an *in vivo* optogenetics approach to address the causal contribution of 5-HT inputs to the BA in fear.

3.1.1 Impact of the 5-HT system on the amygdala and fear

Both genetic and pharmacological evidence in humans suggests that the 5-HT system mediates fear and anxiety states, at least partly, through modulation of the amygdala (for review, see Holmes, 2008). As described in Chapter 2, variations in 5-HTT expression have been associated with affective disorder susceptibility, anxiety trait expression, and changes in functional responses of the amygdala to aversive stimuli (Lesch et al., 1996; Hariri et al., 2002). In addition, acute pharmacological blockade of the 5-HTT produces altered functional amygdala reactivity to emotionally salient stimuli (Bigos et al., 2008; Murphy et al., 2009).

However, results from human findings have been inconsistent, with some gene association studies finding smaller or no effects (Munafò et al., 2008; Murphy et al., 2013), and drug studies reporting opposite functional imaging observations in the amygdala (Bigos et al., 2008; Murphy et al., 2009). These discrepancies may arise from variation across human studies, including demographic, functional imaging, task design, and analysis factors (for review, see Caspi et al., 2010).

Links between the 5-HTT, amygdala function, and fear behaviour have also been reported in rodents. Rodents provide tractable model systems, given that environmental and genetic factors can be more reliably controlled than in human subjects. 5-HTT KO rodents exhibit impaired fear extinction, abnormal neuronal morphology in the BLA, and reduced tissue 5-HT levels in the amygdala (Homberg et al., 2007; Wellman et al., 2007; Narayanan et al., 2011; Nonkes et al., 2012). 5-HTT OE mice, on the other hand, display impaired fear conditioning (Line et al., 2014; Bocchio et al., 2015; McHugh et al., 2015; Chapter 2), enhanced amygdala haemodynamic reactivity to fear cues (Barkus et al., 2014), and lower tissue 5-HT levels in the BLA, as shown in Chapter 2.

In Chapter 2, further evidence was provided in support of the hypothesis that acute 5-HTT blockade increases fear learning in WT mice (Burghardt et al., 2004). Pharmacological studies in rats have demonstrated that acute 5-HTT blockade elevates 5-HT levels in the amygdala (Bosker et al., 2001), while chronic 5-HTT blockade alters expression of neuroplasticity markers in the amygdala (Homberg et al., 2011). Thus, systemic 5-HTT manipulations appear to affect both amygdala function and fear behaviour, and the former is likely causative of the latter because acute 5-HTT blockade specifically in the BLA alters conditioned fear expression (Inoue et al., 2004; Ruiz Martinez et al., 2007). In particular, heightened fear states seem to be favoured by reduced 5-HTT activity and elevated 5-HT levels in the amygdala, though not all studies confirm this relationship (Inoue et al., 2004).

3.1.2 5-HT innervation of the amygdala from the DRN

The amygdala is a brain region containing multiple nuclei that together are involved in the regulation of fear learning (Duvarci and Pare, 2014; Janak and Tye, 2015). 5-HT immunoreactivity across amygdala nuclei is not uniform, with especially dense innervation in the BA compared to the central and LA nuclei (Steinbusch, 1981). Lesions or pharmacological inactivation of the BA impair fear expression (Anglada-Figueroa and Quirk, 2005; Amano et al., 2011); 5-HT inputs to the BA could therefore influence fear behaviour by modulating BA circuits. Pathway tracing and immunohistochemistry data from rodents demonstrate that the majority of 5-HT innervation in the amygdala arises from the midbrain DRN (Azmitia and Segal, 1978; Jacobs et al., 1978; Abrams et al., 2005; Asan et al., 2013).

Putative 5-HT neurons in the DRN increase their firing during wakefulness and are quiescent during sleep (Sakai, 2011). This is mirrored by the elevated brain extracellular 5-HT levels detected during activity compared to rest (Portas et al., 1998). Investigations of DRN 5-HT neuron responses to emotionally salient stimuli have produced less consistent results. In *in vivo* electrophysiology or calcium imaging experiments, aversive stimuli such as electric shocks and airpuffs to the eye excite most 5-HT neurons in rodents (Schweimer and Ungless, 2010; Cohen et al., 2015; Matias et al., 2017). Similarly, C-fos expression is also enhanced in DRN 5-HT neurons in the rat from exposure to inescapable shocks (Grahn et al., 1999; Takase et al., 2004; Spannuth et al., 2011). However, significant responses during shocks have not been detected in DRN processes as determined by fibre photometry measurements of calcium signals in genetically identified 5-HT neurons (Li et al., 2016). Moreover, conditioned cues that predict airpuffs have not been found to elicit significant responses in DRN 5-HT neurons (Cohen et al., 2015; Matias et al., 2017). The necessity of DRN 5-HT neurons has been tested through optogenetic silencing, which impairs fear learning when coupled to CS-US presentations during conditioning, but only in previously stressed mice (Baratta et al., 2016). The latter study photoinhibits neurons in the DRN rather than isolating a 5-HT pathway targeted to a specific anatomical structure. Together, the

existing literature does not fully clarify the precise function of 5-HT neurons in fear regulation.

3.1.3 5-HT in the amygdala and its impact on fear

In spite of discrepancies observed in electrophysiological and calcium imaging investigations of the DRN, aversive stimuli have been consistently shown to heighten 5-HT transmission in the amygdala. Neurochemical studies have reported elevated 5-HT release in the BLA from inescapable shocks (Amat et al., 1998; Christianson et al., 2010), vicarious observance of shock exposure (Kawahana et al., 1993), and cues predictive of shocks (Zanoveli et al., 2009; Baratta et al., 2016). Furthermore, the 5-HT_{2C} gene is overexpressed in the amygdala of stressed rodents (Harada et al., 2008; Baratta et al., 2016). Thus, there is evidence that 5-HT neurons are in a position to influence fear behaviour by potentiating 5-HT signalling in the amygdala.

The involvement of 5-HT transmission in the amygdala during fear processing has been corroborated by pharmacologically targeting 5-HT receptors and consequently affecting fear behaviour. Non-specific agonism of 5-HT receptors in the amygdala promotes suppression of punished reward-seeking without affecting behaviour in rewarded or neutral situations, whereas 5-HT_2 receptor antagonism impairs punished suppression (Hodges et al., 1987). 5-HT_2 antagonism in the BLA also impairs conditioned aversion (De Mello Cruz et al., 2005; Macedo et al., 2007), while 5-HT_2 agonism is anxiogenic in exploratory tasks (Campbell and Merchant, 2003). Specifically, 5-HT_{2C} agonism in the amygdala increases anxiety-like behaviour (Cornélio and Nunes-de-Souza, 2007) and 5-HT_{2C} antagonism in the BLA prevents stress-potentiated fear and anxiety-related behaviours (Christianson et al., 2010; Baratta et al., 2016). Although these results indicate that 5-HT signalling via 5-HT_2 receptors in the amygdala favours fearful states, other manipulations have yielded opposite results. 5-HT_{2B} agonism in the medial amygdala during a social interaction task, for example, has an anxiolytic-like impact (Duxon et al., 1997).

Studies of other 5-HT receptor subtypes have also revealed some conflicting findings. 5-HT_{1A} agonism in the amygdala reduces both conditioned fear expression (Li et al., 2006; Matsuzaki et al., 2011) and retention in an avoidance task (Liang, 1999), yet is anxiogenic-like in social interaction (Gonzalez et al., 1996). In contrast, 5-HT_3 agonism in the amygdala increases anxiety-like behaviour in the light-dark test (Costall et al., 1989) and also in the social interaction test (Higgins et al., 1991). Overall, the relationship between 5-HT receptor activation in the amygdala and fearful states appears to be complex, possibly due to differential effects on distinct receptor types, behaviours, and amygdala subnuclei.

The necessity of 5-HT inputs to the amygdala for fear behaviour has been established in rodent models using a chemical lesion approach. Pharmacological depletion of 5-HT in the amygdala by 5,7-dihydroxytryptamine reduces the number of 5-HT fibres and the concentration of tissue 5-HT (Tran et al., 2013). In the BLA, 5-HT lesions impair both fear conditioning and fear retrieval (Izumi et al., 2012; Johnson et al., 2015). In contrast, 5-HT depletion in the LA enhances fear-potentiated startle responses (Tran et al., 2013). The effect of 5-HT lesions in the amygdala on social interaction has been contradictory, with studies observing both anxiogenic (File et al., 1981) and anxiolytic (Johnson et al., 2015) effects. These findings have been pivotal in identifying the involvement of 5-HT afferents in the amygdala during fear regulation, yet the exact role of 5-HT projections has not yet been fully characterised. In particular, 5-HT pathways to amygdala subnuclei have not been examined during the fear learning process with the circuit and temporal specificity offered by more recently developed techniques such as optogenetics.

3.1.4 Aims of this chapter

The aim of the study described in this chapter was to investigate the role of 5-HT neurotransmission in the BA in the regulation of fear. An *in vivo* optogenetics approach was employed to selectively interrogate endogenous DRN 5-HT inputs in the BA by photostimulation of 5-HT fibres transfected with light-gated opsins.

3.2 Methods

3.2.1 Experimental animals

5-HTT-Cre+/- mice (MMRRC, B6.Cg-Tg(Slc6a4-cre)Et33Gsat, stock number 031028-UCD) of either sex, genotyped by Transnetyx (Cordova, TN), were singly housed after surgeries to maintain the integrity of intracranial implants, with *ad libitum* access to food and water in a 12/12 h light/dark cycle (lights on 6am). Experiments were performed in compliance with the National Institutes of Health *Guide for the Care and Use of Laboratory Animals* and approved by the local National Institute on Alcohol Abuse and Alcoholism Animal Care and Use Committee.

3.2.2 Viral transfection and optic fibre implantation

To selectively transfect 5-HT neurons with viral optogenetic constructs, Cre-inducible recombinant viral vectors (AAV2-EF1a-DIO-hChR2(E123T/T159C)-EYFP or AAV-EF1a-DIO-iC++-EYFP; UNC Vector Core) were stereotaxically injected (1 µl at 100 nL/min) into the DRN (coordinates (mm) according to bregma and the brain surface; anterior-posterior -4.1; dorso-ventral -2.5, -2.2, -1.9) of 5-HTT-Cre mice (2 to 4 months) anaesthetised using 1-2 % isoflurane in oxygen (2 L/min). The viral constructs encoded one of two opsins, either a floxed excitatory ultrafast (E123T/T159C) light-gated cation channel ChR2, or a floxed inhibitory light-gated chloride channel iC++, fused with yellow fluorescent protein (YFP). As a control construct, a Cre-dependent vector (AAV-EF1a-DIO-EYFP; UNC Vector Core) containing only YFP was used. Optic fibres of 200 mm diameter (numerical aperture (NA) 0.39) and affixed to ferrules (Thorlabs, Inc., USA) were bilaterally positioned at the BA (coordinates (mm) according to bregma; anterior-posterior -1.8; medio-lateral ±3.22; dorso-ventral -4.65) and chronically implanted by attaching to the skull using dental cement (Coralite Dental Products). On recovery from surgery, mice were administered 5 mg/kg ketoprofen (s.c.) for post-operative analgesia. Mice were left undisturbed for 5 to 6 weeks to allow for recovery and virus expression before behavioural testing. The selectivity of Cre-

dependent opsin expression for 5-HT neurons in 5-HTT-Cre mice is quantified in Chapter 5

.

3.2.3 Behavioural testing and optogenetic stimulation

Prior to behavioural testing, mice were handled for 2 min a day for 6 days and habituated to being connected to optic fibre cables in the home cage for 45 min a day for 3 days. On the first testing day, fear conditioning was conducted in a 30 × 25 × 25 cm chamber with a metal rod floor, metal walls, and a distinctive vanilla olfactory cue (context A). After 180 s acclimation, mice received three pairings (60 to 90 s inter-trial interval) of a 30 s, 80 dB white noise cue (CS) and a co-terminating, 0.5 s, 0.6 mA scrambled footshock (US).

On the second day, fear extinction training was conducted in a different room, in a 27 × 27 × 14 cm chamber with transparent walls, a floor covered with wooden chips, and a distinctive acetic acid olfactory cue (context B). After 180 s acclimation, 50 × 30 s CS presentations (5 s inter-CS interval) were delivered. On the third day, after 180 s of acclimation, extinction retrieval was tested in context B with 5 × 30 s CS presentations (5 s inter-CS interval). On the fourth day, for a context test, mice were returned to Context A for 5 min (Bukalo et al., 2015).

CS and US presentations were controlled by the Med Associates Video Freeze or MedPC system (Med Associates Inc., St. Albans, VT). Freezing was defined as the absence of visible movement, excluding respiration, and was scored as present or not present at 5 s intervals by an observer blind to genotype. Freezing was converted to a percentage [(number of freezing observations/total number of observations) × 100] for analysis. On conditioning day, freezing was analysed per CS presentation. On extinction (training) day, CS presentations were grouped into blocks of 5, and the first and last block were compared. On extinction retrieval day, the 5 CS presentations were grouped into one block. Movement velocity was measured around the first CS-US pairing of the fear conditioning session using

the Ethovision videotracking system (Noldus Information Technology Inc., Leesburg, VA), during the last 30 s of baseline, 29.5 s of pre-shock CS and light stimulation, 0.5 s shock, and the first 30 s post-shock of the inter-trial interval.

To photoexcite or -inhibit 5-HT axons in the BA, a blue laser (λ = 473 nm) was bilaterally shone onto ChR2- or iC++-transfected fibres in the BA. The power of the blue laser was adjusted to ~10 mW from the tip of the optic fibre, calculated based on the transmission efficiency of individual optic fibre-ferrules. Laser power was calibrated before testing each mouse by measuring the power at the tip of the patch cord with a PM100D optical power metre with a S120C sensor (Thorlabs, Inc., USA). Optogenetic manipulations were made throughout the duration of 30 s CS presentations continuously (for iC++), or at 20 Hz (for ChR2) to match the physiological activity of 5-HT neurons during arousal (Cohen et al., 2015; Li et al., 2016). Laser stimulation was delivered in this manner during either the fear conditioning or extinction (training) session (Figure 3.1D).

3.2.4 Histology

To verify virus expression and optic fibre-ferrule placements, mice were terminally overdosed with pentobarbital at the completion of behavioural testing. Mice were then transcardially perfused with phosphate-buffered saline (PBS), followed by 4% paraformaldehyde (PFA). After overnight suspension in 4% PFA at 4°C, 50 μm coronal sections were cut with a vibratome (Classic 1000 model, Vibratome). Brain sections were incubated in blocking solution (10% normal goat serum (Vector Laboratories) and 2% bovine serum albumin (MP Biomedicals) in 0.05 M PBS with 0.3% Triton X-100] for 90 min at room temperature and then incubated at 4°C overnight in chicken anti-green fluorescent protein (GFP) (1:3000 dilution, Abcam cat. no. 13970) primary antibody to enhance visualisation of opsins. The next day, sections were incubated in goat anti-chicken Alexa 488 secondary antibody (1:1000 dilution, Abcam cat. no. 150169). The sections were mounted onto glass slides and coverslipped with Vectashield HardSet mounting medium (Vector Laboratories

Inc.). Sections were imaged using an Olympus BX41 microscope (Olympus) and a Zeiss LSM 700 confocal microscope (Carl Zeiss Microscopy).

3.2.5 Statistical analysis

Statistical analysis was performed using GraphPad Prism software. The effects of opsin group and period on freezing were analysed using 2-way ANOVA. Subsequently, Sidak's *post-hoc* pairwise comparisons were made. Student's unpaired t-tests were used to analyse freezing during the context test when data were normally distributed (based on Shapiro-Wilk's test for normality).

3.3 Results

3.3.1 Selective manipulation of BA 5-HT projections during fear behaviour

To control 5-HT projections in the BA arising from the DRN, viral vectors carrying either the floxed light-gated excitatory opsin ChR2, or the floxed light-gated inhibitory opsin iC++, were stereotaxically injected into the DRN of 5-HTT-Cre mice (Figure 3.1A). Both opsins were tagged with the YFP reporter. 5 weeks after injections, brains of 5-HTT-Cre mice contained a distribution of ChR2/YFP+ or iC++/YFP+ fibres in the DRN (Figure 3.1B), with particularly dense innervation of the BA in the amygdala. Light stimulation was delivered to the 5-HT projections in the BA during behaviour through chronically implanted optic fibres (Figure 3.1C).

5 to 6 weeks after injections, separate cohorts of mice underwent fear testing with optogenetic manipulations performed at different phases. In one experiment, light was delivered during each CS presentation on the fear conditioning day only (Figure 3.1D, top left). A second experiment comprised a control "conditioning" day, in which light was paired with the CS, but without any presentation of the US during the session (Figure 3.1D, top

right). In the third experiment, light was delivered during each CS presentation in the extinction (training) session only (Figure 3.1D, bottom).

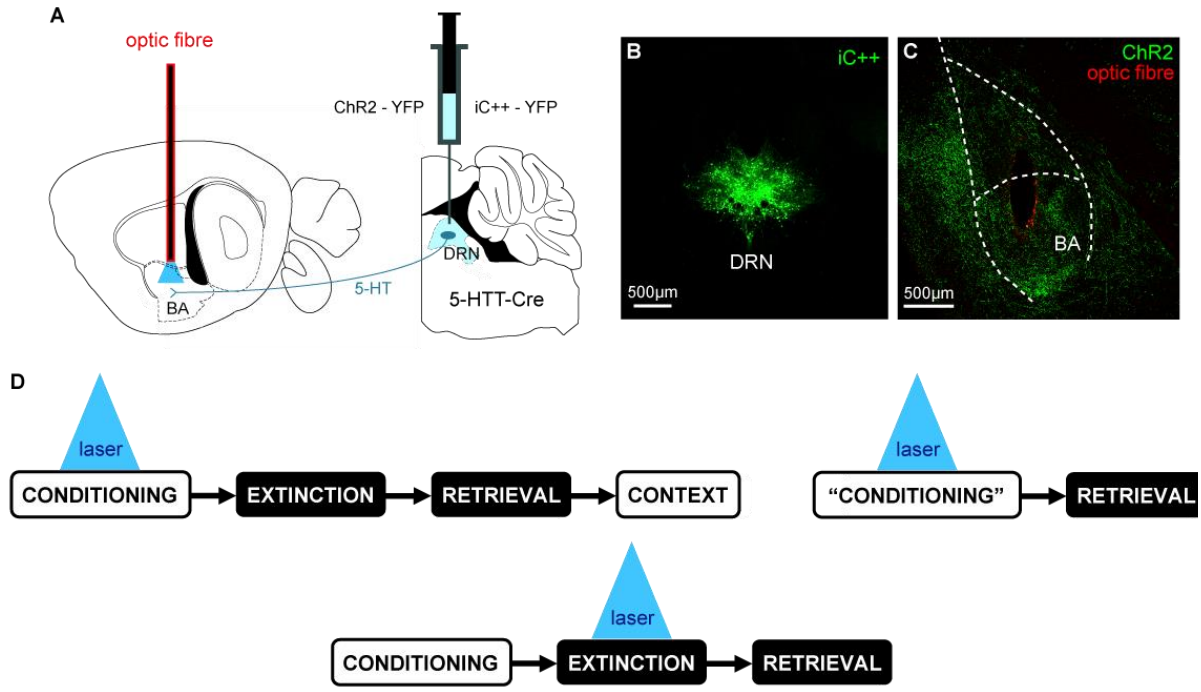


Figure 3.1 – Optogenetic manipulation of 5-HT projections during fear conditioning or extinction **A.** Sagittal schematic showing delivery of viral vectors containing optogenetic constructs for either ChR2 or iC++into the DRN under control of the 5-HTT promoter. Photoexcitation (ChR2) or -inhibition (iC++) of 5-HT projections in the BA through light stimulation. **B.** Coronal image of 5-HT neurons in the DRN expressing iC++. **C.** Coronal image of an optic fibre implanted into the BA to deliver light stimulation to 5-HT projections expressing ChR2. **D.** Schematic showing optogenetic manipulations during fear learning tasks. Light stimulation delivered during fear conditioning (top left), during a control fear "conditioning" session without electric shocks (top right), or during fear extinction (bottom).

3.3.2 Optogenetic excitation of BA 5-HT projections during fear conditioning

In order to investigate the influence of 5-HT projections to the BA on fear behaviour, DRN 5-HT afferents were photoexcited in ChR2-expressing mice during fear conditioning in the first experiment (Figure 3.2A, top). Light was delivered during the CS-US presentations.

On the fear conditioning day, ChR2-expressing mice exhibited significantly greater freezing responses [repeated measures 2-way ANOVA; main effect of opsin $F(1,18)=8.008$, $p=0.011$; main effect of period, $F(3,18)=51.79$, $p<0.001$; opsin × period interaction, $F(3,18)=8.385$, $p<0.001$] to the second and third CSs, as compared to YFP-expressing controls [Sidak's pairwise comparisons: YFP vs. ChR2, BL $p=1.000$, CS1 $p=0.999$, CS2 $p<0.001$, CS3 $p=0.001$] (Figure 3.2A, bottom left). Movement velocity was also monitored

during the pre-CS baseline and first CS-US pairing of the conditioning session, but no effects of photoexcitation were detected [repeated measures 2-way ANOVA; main effect of opsin $F(1,14)=0.1694$, $p=0.687$; main effect of period, $F(3,14)=16.81$, $p<0.001$; opsin × period interaction, $F(3,14)=0.1839$, $p=0.907$] (Figure 3.2B).

One day later, in a novel context, ChR2-expressing mice again showed enhanced freezing during CS presentation in an extinction training session [repeated measures 2-way ANOVA; main effect of opsin $F(1,18)=4.602$, $p=0.046$; main effect of period, $F(2,18)=76.77$, $p<0.001$; opsin × period interaction, $F(2,18)=2.211$, $p=0.124$] (Figure 3.2A, bottom middle-left). Although the interaction did not reach statistical significance, pairwise comparisons were made to evaluate whether freezing during specific CS bins drove the main virus group effect. The increased freezing of ChR2-expressing mice was present during the first five CSs of extinction, reflecting fear memory retrieval, but not during the baseline period or the last five CSs [Sidak's pairwise comparisons: YFP vs. ChR2, BL $p>0.999$, CS1-5 $p=0.029$, CS46-50 $p=0.281$]. One day later, during extinction retrieval, ChR2-expressing mice continued to display elevated freezing to the CS [repeated measures 2-way ANOVA; main effect of opsin $F(1,18)=16.15$, $p<0.001$; main effect of period, $F(1,18)=110.5$, $p<0.001$; opsin × period interaction, $F(1,18)=18.19$, $p<0.001$; Sidak's pairwise comparisons: YFP vs. ChR2, BL $p=0.998$, CS1-5 $p<0.001$] (Figure 3.2A, bottom middle-right).

As a comparison with CS-evoked fear, freezing responses to the original conditioning context were also assessed, but there were no differences between YFP- and ChR2-expressing mice [unpaired t-test, $t(18)=1.407$, $p=0.177$] (Figure 3.2B, bottom right). Taken together, the results suggest that photoexcitation of 5-HT projections in the BA enhanced cued fear learning.

In a control experiment, fear "conditioning" was conducted in the absence of the US, such that only light stimulation was paired with CS-alone presentations (Figure 3.2C, top). No freezing responses were observed during "conditioning," or one day later, during a fear retrieval test. Freezing behaviour was similar between YFP- and ChR2-expressing mice, and did not differ from baseline to CS period [repeated measures 2-way ANOVA; main effect of

opsin F(1,16)=0.6706, p=0.425; main effect of period, F(1,16)=1.233, p=0.283; opsin × period interaction, F(1,16)=0.1826, p=0.675] (Figure 3.2C, bottom). Thus, increasing transmission in the DRN-BA 5-HT pathway was not sufficient to generate a conditioned fear response.

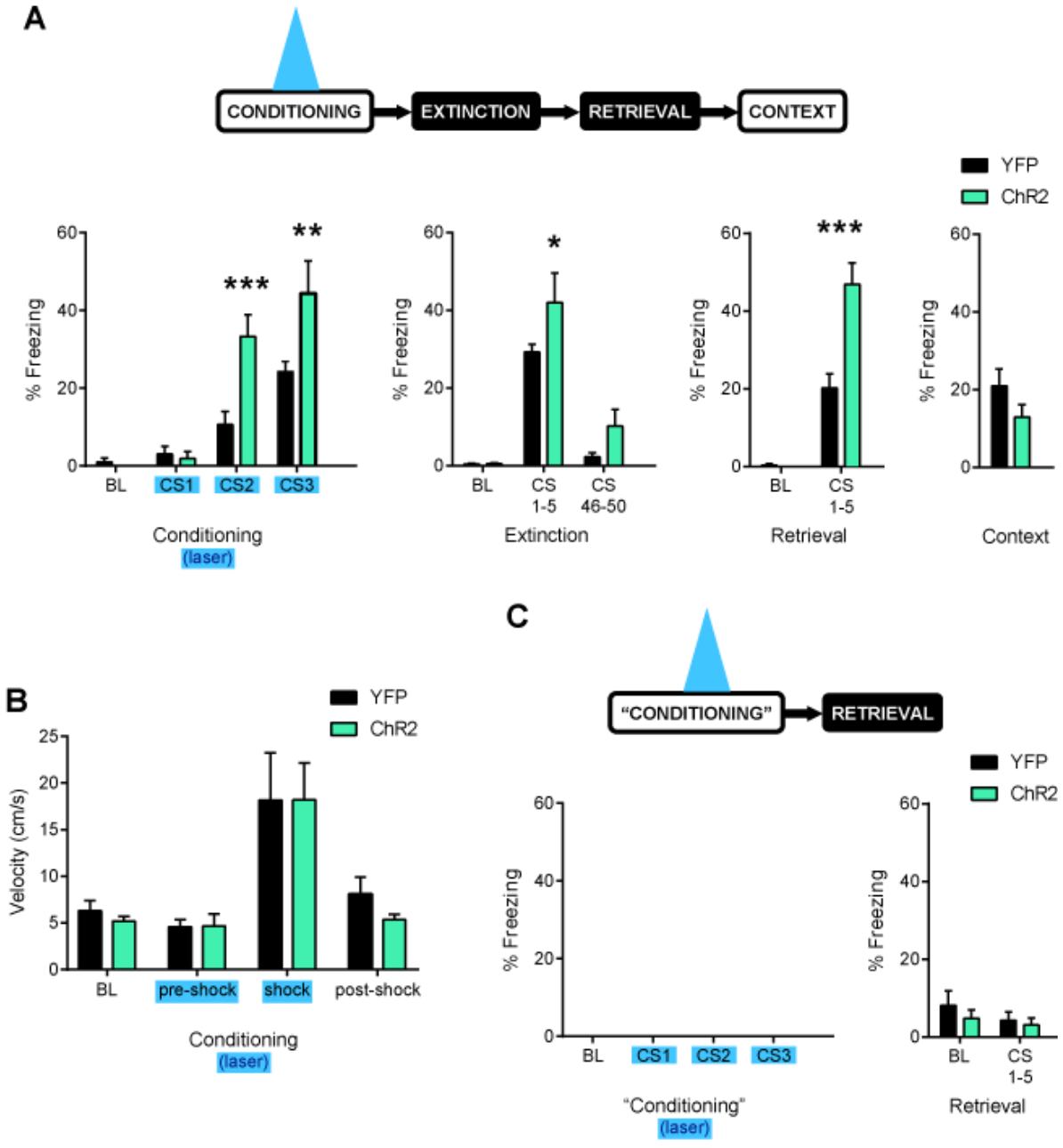


Figure 3.2 – Optogenetic excitation of BA 5-HT projections during fear conditioning enhances fear

A. Optogenetic excitation during conditioning session of a fear learning task (top). Percentage time spent freezing in the baseline (BL) period and to the CS during fear conditioning, extinction, retrieval, and context sessions (bottom; YFP n=11, ChR2 n=9). **B.** Movement velocity during BL and first CS of the fear conditioning session (YFP n=8, ChR2 n=8). **C.** Optogenetic excitation during the "conditioning" session of a fear learning task, in which shocks were absent (top). Percentage time spent freezing at BL and to a CS during fear "conditioning" and

retrieval sessions (bottom; YFP n=9, ChR2 n=9). Data are expressed as means ± SEM. *p<0.05, **p<0.01, ***p<0.001.

3.3.3 Optogenetic inhibition of BA 5-HT projections during fear conditioning

Next, the necessity of DRN 5-HT projections to the BA was assessed by inhibiting 5-HT inputs in iC++-expressing mice during fear conditioning (Figure 3.3A, top). Light was delivered during the presentation of the CS and co-terminating US.

No significant differences in freezing responses were found in YFP- and iC++-expressing mice on the conditioning day [repeated measures 2-way ANOVA; main effect of opsin $F(1,15)=0.2662$, $p=0.613$; main effect of period, $F(3,15)=20.93$, $p<0.001$; opsin × period interaction, $F(3,15)=1.756$, $p=0.169$] (Figure 3.3A, bottom left). During the baseline period and first CS-US pairing, photoinhibition did not affect movement velocity [repeated measures 2-way ANOVA; main effect of opsin $F(1,13)=0.0033$, $p=0.955$; main effect of period, $F(3,13)=29.51$, $p<0.001$; opsin × period interaction, $F(3,13)=1.601$, $p=0.205$] (Figure 3.3B).

One day later, in a novel context, iC++-expressing mice displayed reduced freezing responses compared to YFP controls during fear extinction training [repeated measures 2-way ANOVA; main effect of opsin $F(1,15)=7.012$, $p=0.018$; main effect of period, $F(2,15)=74.89$, $p<0.001$; opsin × period interaction, $F(2,15)=6.108$, $p=0.006$] (Figure 3.3A, bottom middle-left). This effect was driven by differences during the first five CSs of extinction, which represent fear retrieval, rather than the baseline period or the last five CSs [Sidak's pairwise comparisons: YFP vs. ChR2, BL $p=1.000$, CS1-5 $p<0.001$, CS46-50 $p=0.827$]. A day later, during extinction retrieval, iC++-expressing mice again demonstrated attenuated freezing behaviour during CS presentations [repeated measures 2-way ANOVA; main effect of opsin $F(1,15)=4.655$, $p=0.048$; main effect of period, $F(1,15)=57.19$, $p<0.001$; opsin × period interaction, $F(1,15)=5.478$, $p=0.034$; Sidak's pairwise comparisons: YFP vs. ChR2, BL $p=0.972$, CS1-5 $p=0.007$] (Figure 3.3A, bottom middle-right).

Freezing responses to the conditioning context were monitored, but as with ChR2-expressing mice, there were no differences between YFP- and iC++-expressing mice

[unpaired t-test, t(15)=0.2954, p=0.772] (Figure 3.3A, bottom right). Together, these results indicate that inhibition of DRN 5-HT inputs in the BA attenuated cued fear learning.

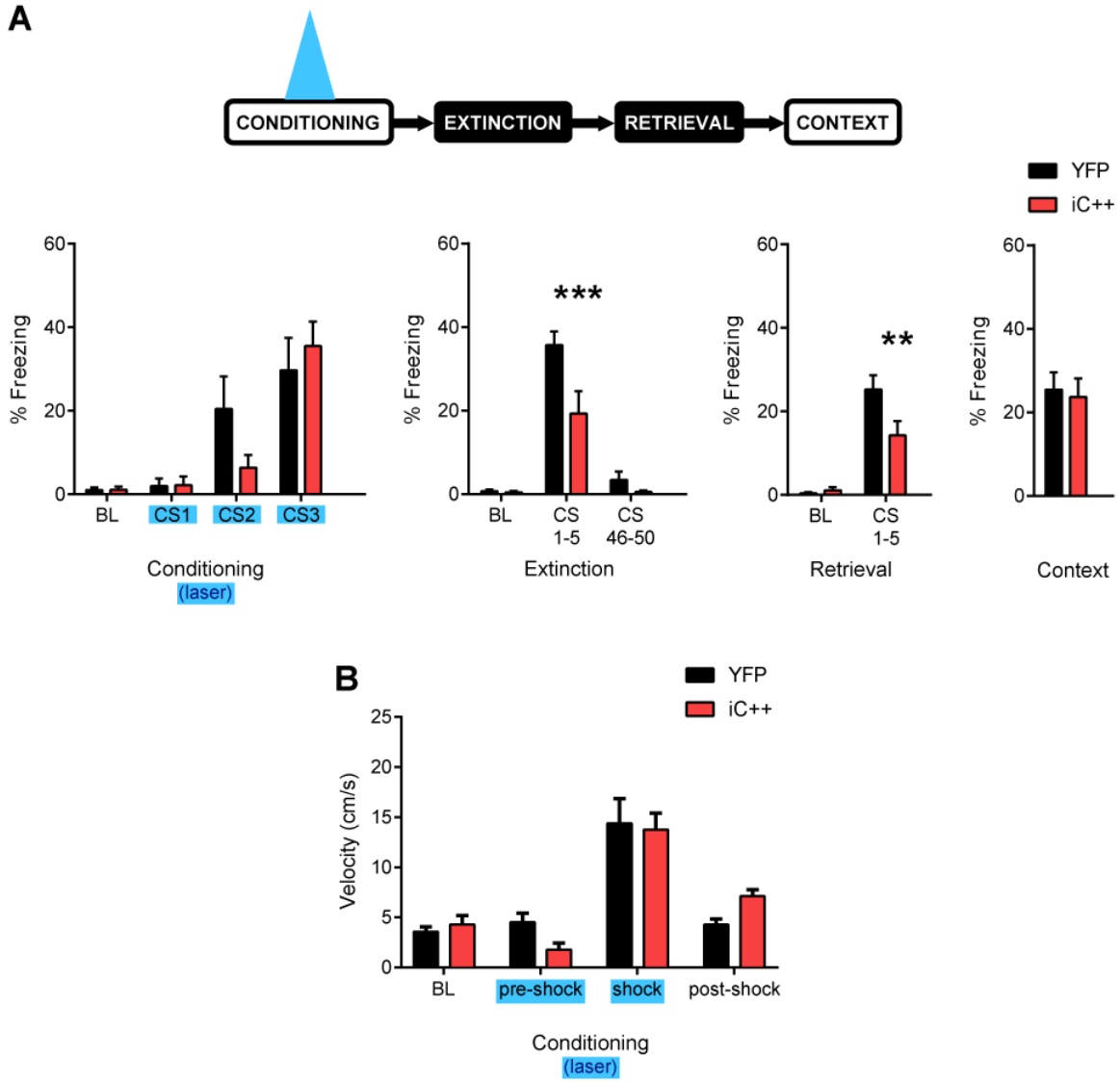


Figure 3.3 - Optogenetic inhibition of BA 5-HT projections during fear conditioning reduces learned fear
A. Optogenetic inhibition during the conditioning session of a fear learning task (top). Percentage time spent freezing in the baseline (BL) period and to the CS during fear conditioning, extinction, retrieval, and context sessions (bottom; YFP n=9, iC++ n=8). **B.** Movement velocity during BL and the first CS of the fear conditioning session (YFP n=9, iC++ n=8). Data are expressed as means ± SEM. **p<0.01, ***p<0.001.

3.3.4 Optogenetic manipulations of BA 5-HT projections during fear extinction

In the previous experiments, optogenetic manipulations focussed on the conditioning session, when fear memories are acquired. Next, the ability of BA 5-HT projections to affect the retrieval and extinction of the fear memory was explored by optogenetically manipulating

DRN 5-HT projection activity in the BA of ChR2- or iC++-expressing mice during fear extinction training. Light stimulation was delivered during the presentation of all CSs of the extinction training session.

5-HT projections were photoexcited in mice with ChR2 during fear extinction training (Figure 3.4A, top). Before photoexcitation, on conditioning day, there were no differences in the freezing behaviour of ChR2-expressing mice and YFP controls [repeated measures 2-way ANOVA; main effect of opsin $F(1,15)=1.069$, $p=0.318$; main effect of period, $F(3,15)=73.4$, $p<0.001$; opsin × period interaction, $F(3,15)=0.9708$, $p=0.415$] (Figure 3.4A, bottom left). During fear extinction training, ChR2- and YFP-expressing mice froze to similar extents [repeated measures 2-way ANOVA; main effect of opsin $F(1,15)=1.269$, $p=0.278$; main effect of period, $F(2,15)=40.85$, $p<0.001$; opsin × period interaction, $F(2,15)=1.248$, $p=0.670$] (Figure 3.4A, bottom middle). During extinction retrieval (no light stimulation) one day later, ChR2-expressing mice displayed increased freezing behaviour compared to YFP controls [repeated measures 2-way ANOVA; main effect of opsin $F(1,15)=10.71$, $p=0.005$; main effect of period, $F(1,15)=71.64$, $p<0.001$; opsin × period interaction, $F(1,15)=10.7$, $p=0.005$] (Figure 3.4A, bottom right). In particular, ChR2-expressing mice froze more during the CSs [Sidak's pairwise comparisons: YFP vs. ChR2, BL $p=0.999$, CS1-5 $p<0.001$]. These data show that excitation of 5-HT projections in the BA during fear extinction did not affect fear retrieval or short-term extinction training, but impaired long-term extinction memory formation.

In a separate experiment, 5-HT projections were inhibited in iC++ expressing mice during fear extinction (Figure 3.4B, top). On conditioning day, prior to inhibition, there were no differences in the freezing responses of iC++- and YFP-expressing mice [repeated measures 2-way ANOVA; main effect of opsin $F(1,19)=0.3773$, $p=0.546$; main effect of period, $F(3,19)=30.38$, $p<0.001$; opsin × period interaction, $F(3,19)=0.2972$, $p=0.827$] (Figure 3.4B, bottom left). One day later, in a novel context, during fear extinction training with photoinhibition, iC++-expressing mice exhibited reduced freezing compared to YFP controls [repeated measures 2-way ANOVA; main effect of opsin $F(1,19)=4.288$, $p=0.052$;

main effect of period, $F(2,19)=18.66$, $p<0.001$; opsin × period interaction, $F(2,19)=6.348$, $p=0.004$] (Figure 3.4B, bottom middle). The effect was driven by freezing differences during the first five CSs, which represents fear retrieval [Sidak's pairwise comparisons: YFP vs. iC++, BL $p>0.999$, CS1-5 $p<0.001$, CS46-50 $p=0.966$]. During extinction retrieval one day later, iC++-expressing mice continued to show reduced freezing relative to YFP-expressing mice [repeated measures 2-way ANOVA; main effect of opsin $F(1,19)=15.92$, $p<0.001$; main effect of period, $F(1,19)=197.9$, $p<0.001$; opsin × period interaction, $F(1,19)=25.41$, $p<0.001$] (Figure 3.4B, bottom right). During the CS presentations, iC++-expressing mice froze less than YFP controls [Sidak's pairwise comparisons: YFP vs. iC++, BL $p=0.975$, CS1-5 $p<0.001$]. Thus, inhibition of DRN 5-HT projections in the BA during fear extinction training reduced fear memory expression and facilitated the long-term

extinction of fear.

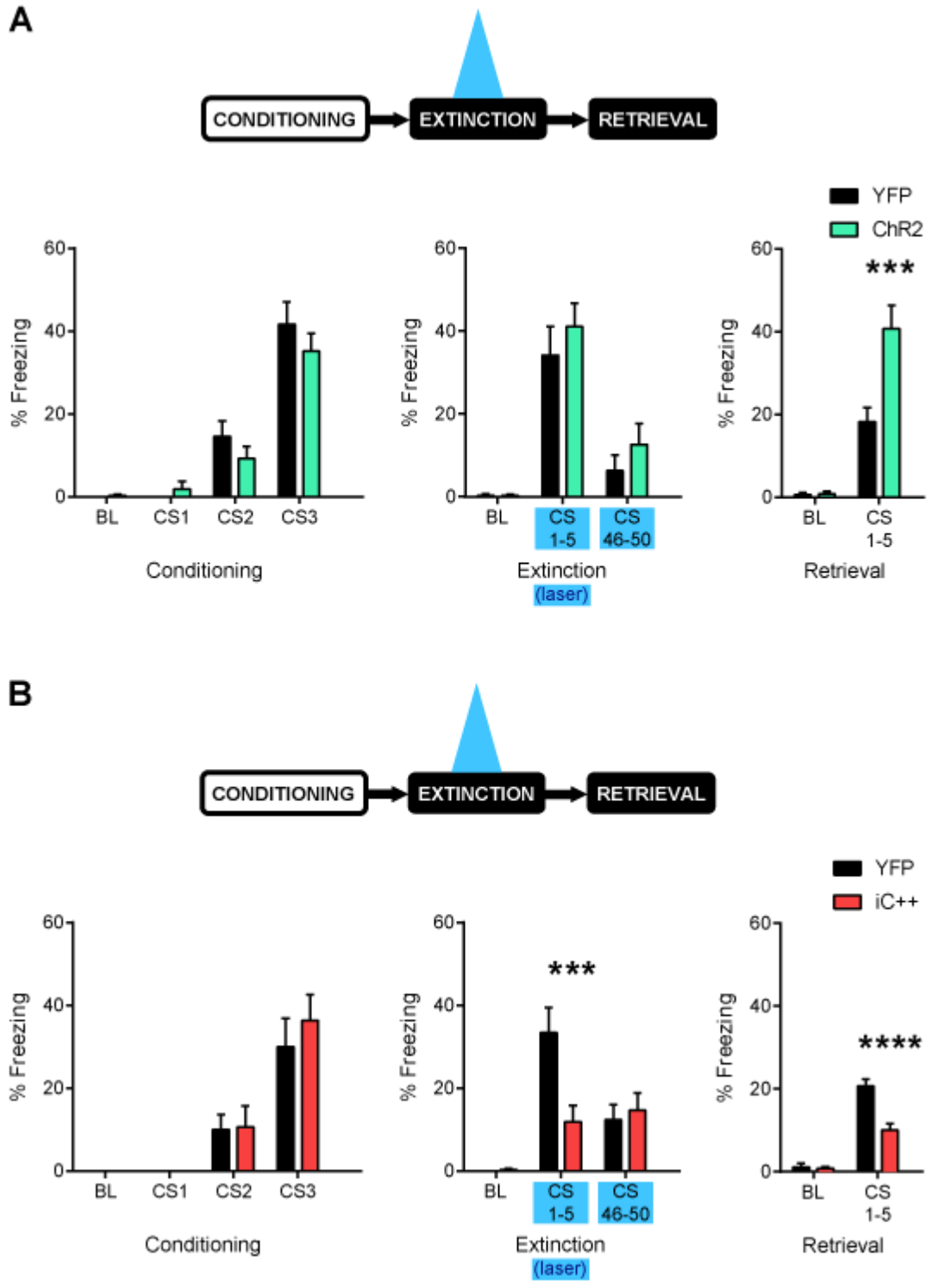


Figure 3.4 - Optogenetic manipulations of BA 5-HT projections during fear extinction influence learned fear

A. Optogenetic excitation during the extinction session of a fear learning task (top). Percentage time spent freezing in the baseline (BL) period and to the CS during fear conditioning, extinction, and retrieval sessions (bottom; YFP n=8, ChR2 n=9). **B.** Optogenetic inhibition during the extinction session of a fear learning task (top). Percentage time spent freezing at BL and to the CS during fear conditioning, extinction, and retrieval sessions (bottom; YFP n=10, iC++ n=11). Data are expressed as means ± SEM. ***p<0.001.

3.4 Discussion

The current study provides the first account of behavioural effects of optogenetically manipulated DRN 5-HT projections in the amygdala during fear and extinction memory formation and subsequent retrieval. Cre-driven optogenetic constructs allowed for circuit-specific excitation or inhibition of 5-HT axons from the DRN targeting the BA. Evidence for the bidirectional influence of 5-HT inputs to the BA was provided. Namely, excitation of 5-HT projections during either conditioning or extinction enhanced fear expression, whereas inhibition attenuated fear. Notably, fear memories could not be generated by 5-HT fibre excitation alone without exposure to the US.

3.4.1 5-HT projection activity in the BA bidirectionally regulates fear learning

Excitation of 5-HT fibres in the BA during the CS presentations of fear conditioning increased freezing responses to the CS short-term during conditioning, and long-term on following extinction training and retrieval. In addition, inhibition of 5-HT axons during fear conditioning produced reduced freezing responses long-term on following extinction and extinction retrieval days. These findings suggest that fear learning is favoured by increased 5-HT transmission in the BA. This is in agreement with data from Chapter 2 and previous studies showing that acute 5-HTT blockade during fear conditioning, which elevates extracellular 5-HT, heightens fear learning (Bosker et al., 2001; Burghardt et al., 2004). Moreover, reduced 5-HT levels of 5-HTT OE mice, as well as 5-HT depletion in the BLA, disrupt fear conditioning (Barkus et al., 2014; Line et al., 2014; Johnson et al., 2015; McHugh et al., 2015, Chapter 2).

While these results are in accordance with reports associating increased 5-HT signalling in the amygdala and extended structures with elevated conditioned fear expression (Macedo et al., 2007; Ruiz Martinez et al., 2007; Zanoveli et al., 2009; Johnson et al., 2015; Baratta et al., 2016; Marcinkiewcz et al., 2016), other studies describe an inverse relationship between amygdala 5-HT transmission and conditioned fear, such that increased 5-HT is

associated with decreased fear (Liang, 1999; Inoue et al., 2004; Li et al., 2006; Matsuzaki et al., 2011). Most of the latter studies focus on amygdala 5-HT_1 receptors. Activation of 5-HT_1 receptors is known to suppress local 5-HT release (Bosker et al., 1997a, 1997b), desensitise within the course of minutes (Harrington et al., 1994), and suppress anxiolytic effects of acute 5-HTT blockade (Hashimoto et al., 1997; Bosker et al., 2001). It is therefore possible that in these studies, selective 5-HT_{1A} agonism exerts its effects on fear learning through the reduction of 5-HT release or the desensitisation of 5-HT_{1A} receptors, rather than through 5-HT signalling *per se*. Hence, higher 5-HT levels in the amygdala could still give rise to greater cued fear learning during conditioning through actions on other receptor types.

Manipulations of BA 5-HT transmission did not influence contextual fear retrieval, however. This does not match with the elevated cued and contextual fear retrieval observed after a similar excitation of 5-HT projections in the extended amygdala during fear conditioning (Marcinkiewcz et al., 2016). Although this could be due to distinct roles of 5-HT-modulated circuits in the BA and bed nucleus of the stria terminalis, it is possible that extinction training, even when conducted in a different context, affected the representation of the conditioning context for mice. Thus, to assess contextual fear retrieval more accurately, it should be tested immediately after fear conditioning.

Furthermore, since amygdala neurons process the CS and US differentially (Wolff et al., 2014), BA modulation by 5-HT afferents may exert distinct effects on fear learning depending on its precise timing. In a paradigm of stress-potentiated fear conditioning, DRN 5-HT neuron activity during either the CS-US pairing or the US alone was necessary for normal cued fear learning (Baratta et al., 2016). Here, 5-HT manipulations in the BA occurred during both the CS and co-terminating US. With the temporal specificity afforded by optogenetic methods, it would be useful to also investigate the effects of 5-HT manipulations in the BA during the US only.

Recently, an examination of inhibitory opsins demonstrated that under some conditions, their biophysical effects could be different from those intended (Mahn et al.,

2016). These disparities seem to vary between opsins, and the study tested archaerhodopsin, halorhodopsin, and chloride-conducting GtACR1, but not iC++. Given the bidirectional behavioural effects brought about by iC++ and ChR2, it is not likely that, in the conditions of this study, iC++ was increasing neuronal excitability. To verify the reliability of iC++, *ex vivo* voltammetry experiments could be done to monitor the levels of extracellular 5-HT during photoinhibition via iC++.

3.4.2 5-HT projection activity in the BA disrupts fear extinction

Excitation of DRN 5-HT projections in the BA during the CS presentations of fear extinction training increased freezing responses to the CS, while inhibition of 5-HT axons reduced freezing. Behavioural differences were observed at the start of extinction, representing retrieval of the fear memory, and during extinction retrieval; freezing responses at the end of extinction were similar across opsin and control groups. These findings suggest that increased 5-HT transmission in the BA during extinction favours retrieval of the fear memory rather than of the extinction memory. This is supported by the impaired fear extinction retrieval of 5-HTT KO mice (Wellman et al., 2007), whose extracellular 5-HT levels in the brain are increased (Jennings et al., 2010). It is also in agreement with 5-HT depletion in the amygdala attenuating conditioned fear retrieval (Izumi et al., 2012).

5-HT manipulations during fear extinction are of translational interest because in affective disorders, the acquisition of fear memories is often in the past and not amenable to treatment. Fear and anxiety disorders are commonly treated through exposure therapy to extinguish fear memories (Bisson et al., 2013) or with drugs such as SSRIs (Ipser et al., 2006). Importantly, the combination of behavioural and pharmacological approaches is more effective than either on its own, both in humans and in mouse models (Pampallona et al., 2004; Karpova et al., 2011). Here, one specific physiological aspect of the pharmacotherapy, namely changes in BA 5-HT transmission, was studied during the fear extinction process. In the future, longer-term retrieval, renewal, and spontaneous recovery of fear memories should

be tested to provide more translationally relevant insight into the impact of BA 5-HT transmission during extinction. At least in the short-term, 5-HT manipulations in the BA influenced the efficacy of behavioural extinction of a fear memory.

The increased fear retrieval brought about by elevated BA 5-HT transmission does not fit readily with findings from SSRI administration experiments. Specifically, chronic systemic SSRI treatments in rodents reduce fear retrieval (Burghardt et al., 2004; Karpova et al., 2011), in spite of raising extracellular 5-HT levels (Moret and Briley, 1996). Nevertheless, effects of chronic systemic SSRI administration are thought to be brought about by the desensitisation of 5-HT_{1A} (Moret and Briley, 1996; Le Poul et al., 2000), 5-HT_{2A} (Yamauchi et al., 2006), and 5-HT_{2C} (Yamauchi et al., 2004) receptors over time. Importantly, some findings report the opposite fear-enhancing effect of acute systemic SSRI treatment (Burghardt et al., 2004; Chapter 2), although this is not corroborated by all studies (Hashimoto et al., 1997). Even with acute infusions of SSRIs into the amygdala, both increases (Ruiz Martinez et al., 2007) and decreases (Inoue et al., 2004) in conditioned fear expression have been observed. These inconsistencies could arise from differences in task design, SSRI specificity, or infusion procedure. Notably, both acute and chronic SSRI infusions into the amygdala lead to desensitised 5-HT_{1A} receptors, albeit to different extents (Bosker et al., 2001); this may be an amygdala-specific mechanism underpinning the discrepancies between the pharmacological and optogenetic approaches, the latter operating with greater temporal precision and possibly being less susceptible to receptor desensitisation.

3.4.3 Functional considerations of 5-HT neuromodulation in the BA

A novel investigation of 5-HT inputs to the BA was enabled in this study by the application of a Cre-dependent optogenetic approach. Isolating this particular pathway is critical for its characterisation with respect to fear behaviour because 5-HT projections to different anatomical targets have distinct roles (Graeff et al., 1996). This is highlighted by the

fact that pharmacological manipulations of the 5-HT system have yielded discrepant behavioural results when delivered to the amygdala instead of systemically (Hodges et al., 1987; Cornélio and Nunes-de-Souza, 2007; Matsuzaki et al., 2011) or even to distinct nuclei of the amygdala (Campbell and Merchant, 2003). It could also explain why excitation of DRN 5-HT neurons does not alter standard, as opposed to stress-potentiated, fear learning (Baratta et al., 2016), while changing the activity of 5-HT projections to the BA in particular appears to do so. This is supported by the finding that the elimination of a subset of 5-HT neurons expressing Pet1 largely spares innervation of the BLA, but increases fear learning (Kiyasova et al., 2011).

The current study indicates that heightened or reduced 5-HT transmission in the BA during solely the CS was sufficient to regulate the CS-associated fear memory. However, in microdialysis experiments, extracellular 5-HT levels in the amygdala reportedly remain elevated for several minutes during and after fear memory retrieval (Yokoyama et al., 2005; Zanoveli et al., 2009) and may be involved in multiple aspects of fear learning, such as attention or memory consolidation, depending on the timing. For instance, 5-HT neuromodulation during the inter-trial intervals might contribute to fear learning. This could be one reason that, with the current paradigm, no effects on contextual fear emerged in spite of pharmacological manipulations of amygdala 5-HT signalling producing altered contextual fear responses in other accounts (Inoue et al., 2004; Li et al., 2006; Ruiz Martinez et al., 2007; Matsuzaki et al., 2011). It would be useful to utilise optogenetic manipulations to dissociate and compare between the CS and inter-trial interval periods.

Light stimulation for the optogenetic excitation of 5-HT projections was delivered at 20 Hz for the duration of the CS. Although DRN 5-HT neurons generally fire at slow rates (0.5-5 Hz) (Allers and Sharp, 2003; Schweimer and Ungless, 2010; Sakai, 2011), they also fire in a manner that decreases with rest and increases with arousal (Veasey et al., 1995; Sakai, 2011). Opto-tagging studies in awake mice indicate that the firing of DRN 5-HT neurons increases markedly (15-20 Hz) in response to aversive or rewarding stimuli (Cohen et al.,

2015; Li et al., 2016). The 20 Hz laser stimulation protocol used here attempted to emulate 5-HT neuron activity during emotionally salient events.

The current study also showed that optogenetic excitation of 5-HT axons in the BA, in the absence of footshocks, was insufficient to produce unconditioned fear or establish a 'false' fear memory. This indicates that 5-HT neurotransmission does not generate the aversive signal itself, but rather modulates US-dependent information transmitted by other inputs to the BA. In fact, pharmacological perturbations of 5-HT transmission in the BLA alter aversive information encoded by the periaqueductal grey (Ruiz Martinez et al., 2007) and inferior colliculus (Macedo et al., 2007). Through volume transmission and appositions onto other presynaptic terminals in the amygdala, 5-HT projections have the ability to modulate heterosynaptic inputs to the BA (Muller et al., 2007; Belmer et al., 2017).

3.4.4 Conclusions

In summary, the research findings described in this chapter explored the behavioural regulation exerted by 5-HT afferents in the BA during fear and extinction. The potential role of 5-HT inputs was briefly discussed in the context of BA circuit function. To better understand how 5-HT transmission influences information processing in the BA, it is necessary to consider the physiological impact of 5-HT signalling on BA neuronal activity. To address this, the next chapter will investigate the effects of 5-HT modulation on single unit and network activity in the BA during fear learning.

Chapter 4 5-HT neurons alter basal amygdala activity during fear learning

4.1 Introduction

In Chapter 3, the behavioural regulation exerted by BA 5-HT transmission was investigated using an *in vivo* optogenetic approach. A bidirectional effect on fear was described, in that the activity of DRN 5-HT projections in the BA was necessary for normal fear learning and retrieval, and was also sufficient to enhance fear. Thus, it was established that 5-HT neuromodulation of BA activity mediates fear at the behavioural level. In this chapter, the role of 5-HT inputs in shaping the *in vivo* neuronal encoding of fear in the BA is explored.

4.1.1 Human amygdala activation during fear

During fear conditioning and retrieval in humans, the amygdala becomes activated on presentations of a CS, as shown by functional magnetic resonance imaging (Büchel et al., 1998; LaBar et al., 1998; Phelps et al., 2004; Linnman et al., 2011; Dejean et al., 2015; but see Knight et al., 1999). Importantly, high resolution functional imaging revealed that within the amygdala, activation of the BLA subregion is particularly associated with CS presentations (Boll et al., 2013). The degree of amygdala activation correlates with a physiological marker of fear expression, namely skin conductance responses (CR). Correspondingly, over the

course of fear memory extinction, amygdala activation diminishes (LaBar et al., 1998; Phelps et al., 2004). Building on these findings, studies have analysed how activation of different brain regions correlate with each other during fear memory retrieval. These have identified coupled activation between the amygdala and orbitofrontal cortex during fear retrieval, and between the ventromedial prefrontal cortex and amygdala or hippocampus during extinction retrieval (Milad et al., 2007; Alvarez et al., 2008). In addition to the amygdala, prefrontal cortex, and hippocampus, the anterior cingulate and anterior insular cortices are also involved in fear learning (Büchel et al., 1998).

Amygdala reactivity is dysfunctional in affective disorders that involve maladaptive fear. PTSD patients, when recalling traumatic memories, experience heightened amygdala and lower prefrontal cortex activation in functional imaging experiments (Bremner et al., 1999; Liberzon et al., 1999; Shin et al., 2014). Moreover, following fear conditioning, PTSD patients exhibit persistent fear responses, amygdala activation, and a lack of prefrontal cortex and hippocampus activation during extinction or extinction retrieval (Milad et al., 2009; Garfinkel et al., 2014). Indeed, when presented with fearful faces in a passive viewing task, PTSD patients display a reciprocal interaction between heightened amygdala and diminished prefrontal cortex activation (Rauch et al., 2000; Shin et al., 2005). Together, these results indicate an important role for the amygdala in fear regulation, particularly in relation to the prefrontal cortex and hippocampus.

4.1.2 Activity of rodent amygdala neurons in fear

Rodent models of fear enable monitoring the activity of individual neurons *in vivo*, providing greater precision in the interrogation of amygdala fear circuits than is possible in humans. In the amygdala, fear associations are thought to be stored as potentiated synapses in the LA (Rogan et al., 1997; Sigurdsson et al., 2007; Kim and Cho, 2017), which projects to the BA. In the BA, isolated neurons display increased firing to the CS after fear conditioning (Herry et al., 2008; Amano et al., 2011). Importantly, these cells comprise two distinct

functional groups. One group of BA neurons is responsive at the start of extinction but becomes less so over the course of extinction; these cells are thought to encode the fear memory. The second group of BA neurons becomes more responsive through the course of extinction, and is thought to encode the extinction memory (Herry et al., 2008). These groups of neurons are mutually exclusive, because in a fear learning paradigm consisting of an extinguished CS and a non-extinguished CS, extinction neurons were responsive only to the former CS and fear neurons to the latter (Herry et al., 2008). It has been proposed that these BA neuron groups provide context-dependent information to guide fear expression (Vlachos et al., 2011). During freezing episodes, putative PNs in the BLA display higher firing rates (Karalis et al., 2016). In addition, a large proportion of BLA neurons are responsive to the US, but the magnitude of the response is diminished when the US is predicted by a CS (Johansen et al., 2010). Thus, BLA neurons may signal a form of aversive prediction error in fear learning.

BLA neurons are predominantly glutamatergic PNs (McDonald, 1982a), but there are also important IN populations in the BLA complex that have been investigated for their role in fear (Ehrlich et al., 2009). These INs are heterogeneous in their responses to noxious stimuli, with some becoming active (Bienvenu et al., 2012) and others inhibited (Wolff et al., 2014) during fear conditioning. Optogenetic targeting of BLA parvalbumin-positive INs characterised a disinhibitory influence on PNs that is crucial for the formation of a fear memory (Wolff et al., 2014). Furthermore, BLA parvalbumin INs are recruited by and necessary for fear retrieval (Bocchio et al., 2015; Karalis et al., 2016). Interestingly, neuromodulators including 5-HT, dopamine, and noradrenaline have been shown to regulate inhibition exerted by local INs onto PNs in the BLA (Rainnie, 1999; Bissière et al., 2003; Tully et al., 2007; Bocchio et al., 2015). INs may also be important for long-range communication between neural fear circuits, since a class of BLA IN fires in phase with hippocampal theta oscillations (Bienvenu et al., 2012).

4.1.3 Network activity of rodent amygdala in fear

Synchronicity of local field potentials are thought to underpin interactions between distinct networks involved in fear regulation (Herry and Johansen, 2014). For example, theta oscillation synchronisation between the amygdala and the hippocampus is enhanced during fear retrieval (Seidenbecher et al., 2003). During freezing episodes, theta coherence between the BLA and prefrontal cortex is enhanced, and large proportions of both BLA and prefrontal PNs become phase-locked to theta (Karalis et al., 2016). Theta synchrony between the amygdala and prefrontal cortex is prominent in mice able to distinguish between aversive and neutral situations, and could provide a mechanism for top-down regulation of fear behaviour through the entrainment of BLA neuron firing to prefrontal theta oscillations (Likhtik et al., 2013).

Within the amygdala, theta oscillations may encode an aversive prediction error signal. At the start of fear conditioning, the US evokes theta oscillations that gradually shift towards the preceding CS presentation as mice learn the predictive association (McHugh et al., 2014). Correspondingly, an unexpected omission of a US presentation following a predictive CS yields reduced theta power. More prominent theta responses to the US during conditioning are predictive of enhanced behavioural discrimination between an aversive and a neutral CS during retrieval. Therefore, along with the findings of Likhtik et al. (2013), the results suggest that theta oscillations could reflect information processing or attention dedicated to sensory stimuli, strengthening the association between the predictive CS and the US.

4.1.4 5-HT and its influence on amygdala activity in fear

As described in previous chapters, genetic variation of human 5-HTT expression has been linked to altered functional reactivity of the amygdala to aversive stimuli, as well as to susceptibility to fearful traits (Munafò et al., 2008; Murphy et al., 2013). Rodent models in

which expression of the 5-HTT has been genetically changed have been used to study amygdala network activity during fear learning tasks. 5-HTT KO mice, containing higher levels of extracellular brain 5-HT (Jennings et al., 2010), display persistent fear expression and heightened theta synchronisation between the BLA and prefrontal cortex to CS presentations during fear extinction retrieval (Narayanan et al., 2011). Additionally, 5-HTT OE mice, with lower levels of extracellular brain 5-HT (Jennings et al., 2010), exhibit impaired fear conditioning (Line et al., 2014; Bocchio et al., 2015; McHugh et al., 2015; Chapter 2) and reduced theta oscillations in the amygdala during CS presentation (Barkus et al., 2014). Hence, altered 5-HTT expression influences fear and amygdala network activity, though the mechanistic link between the two is not fully established.

In Chapter 2 it was shown that developmental changes brought about by variation in 5-HTT expression are important in shaping the fear phenotype. Moreover, BLA and prefrontal cortex dendritic morphology (Wellman et al., 2007), as well as 5-HT signalling mechanisms (Jennings et al., 2010; Bocchio et al., 2015), appear to be permanently altered by differences in 5-HTT expression. *Ex vivo* slice electrophysiology recordings in WT mouse brains have demonstrated that exogenous 5-HT excites BLA INs and thereby inhibits PNs, but this phenomenon is impaired in 5-HTT OE mice (Rainnie, 1999; Jiang et al., 2009b; Bocchio et al., 2015). Thus, BLA circuit formation, changes in BLA input structures, or compensatory 5-HT transmission mechanisms that occur during development could underlie the distinct BLA theta oscillations in mice with 5-HTT gene variation. However, the normal relationship between 5-HT signalling and neuronal activity in the BA has not been studied *in vivo* during fear behaviour. Thus, to clarify whether there is a connection between 5-HT transmission, fear, and amygdala neuronal activity, 5-HT signalling needs to be manipulated in a reversible, temporally specific manner.

4.1.5 Aims of this chapter

The current chapter investigated the role of 5-HT neurotransmission in altering BA neuronal and network activity *in vivo* during fear. The optogenetic approach validated in Chapter 3 was used to selectively activate DRN 5-HT inputs to the BA during fear conditioning with temporal specificity. In concert, the effects of activating these inputs on the firing rates of isolated BA neurons, as well as on BA neuronal network oscillations, were examined during different stages of fear conditioning and extinction. The data presented in this chapter are restricted to the stages of the fear learning task in which behaviour was affected by BA 5-HT projection photoexcitation during conditioning in Chapter 3. The goal was to establish whether 5-HT signalling influences the neuronal activity of the BA during fear, and whether this could provide a neurophysiological correlate to the behavioural observations described in the previous chapter.

4.2 Methods

4.2.1 Experimental animals

5-HTT-Cre+/- mice (MMRRC, B6.Cg-Tg(Slc6a4-cre)Et33Gsat, stock number 031028-UCD) of either sex, genotyped by Transnetyx (Cordova, TN), were singly housed after surgeries to maintain the integrity of intracranial implants, with ad libitum access to food and water at a 12/12 h light/dark cycle (lights on 6am). Experiments were performed in compliance with the National Institutes of Health Guide for the Care and Use of Laboratory Animals and approved by the local National Institute on Alcohol Abuse and Alcoholism Animal Care and Use Committee.

4.2.2 Viral transfection and optrode-array implantation

To selectively transfect 5-HT neurons with the excitatory light-gated cation channel ChR2, a Cre-inducible recombinant viral vector (AAV-EF1a-DIO-hChR2(E123T/T159C)-EYFP; UNC Vector Core) carrying a floxed ultrafast (E123T/T159C) ChR2 fused with YFP was stereotaxically injected (1 µl at 100 nL/min) into the DRN (coordinates (mm) according to bregma and the brain surface; anterior-posterior -4.1; dorso-ventral -2.5, -2.2, -1.9) of 5-HTT-Cre mice (2 to 4 months) anaesthetised using 1-2 % isoflurane in oxygen (2 L/min). As a control construct, a Cre-dependent vector (AAV-EF1a-DIO-EYFP; UNC Vector Core) containing only YFP was used.

Optrode-arrays were constructed by affixing optic fibres of 200 mm diameter (NA 0.39) and attached to ferrules (Thorlabs, Inc., USA) onto a 8 × 2–row array (200-µm spacing between rows) of tungsten microelectrodes (Innovative Neurophysiology), such that the fibre tip was aligned about 0.5 mm above the electrode tips. Following injection of the viral vector, the array was positioned lengthwise anteroposterior (35-µm diameter electrode tips, 150-µm spacing between electrodes within a row), with counterbalancing for hemispheres. The optrode-array assembly was inserted into the BA unilaterally (coordinates (mm) for the most posterior-lateral electrode of the array according to bregma; anterior-posterior -2.2; medio-lateral ±3.1; dorso-ventral -5.1), counterbalancing for hemispheres. Contralaterally, an optic fibre-ferrule was directed into the BA (coordinates (mm) according to bregma; anterior-posterior -1.8; medio-lateral ±3.22; dorso-ventral -4.65). Implants were attached to the skull using two screws and dental cement (Coralite Dental Products). On recovery from surgery, mice were administered 5 mg/kg ketoprofen (s.c.) for post-operative analgesia. Mice were left undisturbed for 5 to 6 weeks to allow for recovery and virus expression before behavioural testing.

4.2.3 Behavioural testing and optogenetic stimulation

Mice were habituated before testing as described in Chapter 3. Fear conditioning was conducted in a 27 × 27 × 11 cm chamber with a metal rod floor, metal walls, and a distinctive vanilla olfactory cue (context A). After 180 s acclimation, mice received three pairings (60- to 90-s inter-trial interval) of a 30 s, 80 dB white noise pip train (250 ms pips at 1 Hz; CS) and a co-terminating, 0.5 s, 0.6 mA scrambled footshock (US).

The next day, fear extinction training was conducted in a 20 cm diameter Plexiglas cylinder with stripe-patterned walls and a distinctive acetic acid olfactory cue (context B). After 180 s acclimation, 50 × 30 s CS presentations (10 s inter-CS interval) were delivered. The first five CSs provided a measurement for fear memory retrieval. The following day, after 180 s of acclimation, extinction retrieval was tested in context B with 5 × 30 s CS presentations (10 s inter-CS interval).

CS and US presentations were controlled by the Med Associates MedPC system (Med Associates Inc., St. Albans, VT). Cameras were mounted overhead to record behaviour. Freezing was defined as the absence of visible movement for at least 1 s, excluding respiration, and was scored using CinePlex Behavioural Research System software (Plexon, Dallas, TX) by an observer blind to genotype. Freezing was converted to a percentage [(time spent freezing/total time) × 100] for analysis. On conditioning day, freezing was analysed per CS presentation. On extinction (training) day, CS presentations were grouped into blocks of 5, and the first and last block were compared. On extinction retrieval day, the 5 CS presentations were grouped into one block.

5-HT projections in the BA were excited using blue laser light (λ = 473 nm) that was bilaterally shone onto ChR2-transfected fibres in the BA. Optogenetic manipulations were made throughout the duration of 30 s CS presentations at 20 Hz during the fear conditioning session. The power of the blue laser was adjusted to ~10 mW from the tip of the optic fibre, calculated based on the transmission efficiency of individual optic fibre-ferrules. Laser power

was calibrated before testing each mouse by measuring the power at the tip of the patch cord with a PM100D optical power metre with a S120C sensor (Thorlabs, Inc., USA).

4.2.4 *In vivo* neuronal recordings

Neuronal recordings took place during the fear learning task. Data reported is from the CS presentations of the conditioning, extinction and extinction retrieval sessions, but with data obtained during the US presentation during the conditioning session being excluded because of electrical noise. Neural recordings were made using Omniplex Neural Data Acquisition System (Plexon, Dallas, TX).

BA single units were sorted and waveforms isolated manually using principal component analysis on Offline Sorter (Plexon, Dallas, TX). Spikes were included in analyses if they displayed a refractory period of at least 1 ms. Autocorrelograms from simultaneously recorded units were compared to ensure that cells were not counted twice. Single units were analysed by generating perievent histograms of firing rates with 10 ms bins for CS pips, 1 s bins for CS, and 100 ms bins for freezing. Firing rates were considered from 250 ms before pip onset until 250 ms after pip offset, from 10 s before CS onset until 10 s after CS offset, and from 1 s before freezing onset until 3 s after freezing onset using NeuroExplorer 5.0 (Nex Technologies, Madison, AL). Z-score transformations of firing rates were made by normalising to baseline, which was taken over the 250 ms before CS pip onset, 10 s before CS onset, and 1 s before freezing onset. Firing rate responses were considered significant only if they were at least 2.58 standard deviations (during CS pips and freezing events) or 1.96 standard deviations (during CS presentations) above or below baseline firing rates for two consecutive time bins. Standard deviation cut-offs were chosen based on perievent histogram bins, with a higher cut-off to account for shorter time bins (Halladay and Blair, 2015).

Local field potentials were low-pass filtered up to 20 Hz. Perievent spectrograms and power spectral densities of continuous data were generated using fourier transform analyses

on NeuroExplorer 5.0 (Nex Technologies, Madison, AL). Spectrograms displayed local field potentials from 10 s before CS onset until CS offset, and from 1 s before freezing onset until 3 s after freezing onset. Power spectra were calculated for the third CS (conditioning), averaged over the first five CSs (extinction), averaged over all five CSs (retrieval), or calculated for the first s of freezing episodes. Power spectra were normalised and expressed for each frequency bin as a percentage of the total power between 0 and 20 Hz. In particular, theta (4-9 Hz) and delta (1-4 Hz) oscillations were considered (Barkus et al., 2014).

In an experiment to control for the effects of light stimulation *per se*, BA neuronal responses to 5 × 30 s trains of 20 Hz laser stimulation (10 s inter-trial interval) were recorded in behaviourally naïve mice in their home cage. BA neuronal data was analysed as described above, from 10 s before laser onset until 10 s after laser offset, in 1 s bins. Z-score transformations of firing rates were made by normalising to baseline, which was taken over 10 s before laser onset. Units were considered responsive if the firing rate changed by at least 1.96 standard deviations from their pre-laser firing rates for two consecutive time bins. As another control measure, the power spectral density of local field potentials for the last 30 s of the fear extinction baseline period was calculated, as described above, to assess whether baseline network oscillations were altered by optogenetic manipulation after fear conditioning.

4.2.5 Histology

To verify electrode placements, lesions were made at the tips of the recording electrodes by passing currents, typically 40 μA (S48 Stimulator and Model CCU1, Grass Technologies), for 2 s at the completion of behavioural testing. To check virus expression, electrode placements, and optic fibre-ferrule placements, mice were transcardially perfused with PBS, followed by 4% PFA. After overnight suspension in 4% PFA at 4°C, 50 μm coronal (DRN) or sagittal (BA) sections were cut with a vibratome (Classic 1000 model, Vibratome). Bright field images of wet sagittal sections were taken to verify placement of individual

electrodes. Alternate sections were stained with acetylcholinesterase to facilitate visualisation of anatomical structures. Remaining sections were incubated in blocking solution (10% normal goat serum (Vector Laboratories) and 2% bovine serum albumin (MP Biomedicals) in 0.05 M PBS with 0.3% Triton X-100] for 90 min at room temperature and then incubated at 4°C overnight in chicken anti-GFP (1:3000 dilution, Abcam cat. no. 13970) primary antibody to enhance visualisation of opsins. The next day, sections were incubated in goat anti-chicken Alexa 488 secondary antibody (1:1000 dilution, Abcam cat. no. 150169). The sections were mounted onto glass slides and coverslipped with Permount (Fisher Chemical; for acetylcholinesterase-stained sections) or Vectashield HardSet (Vector Laboratories Inc.; for immunostained sections) mounting medium. Sections were imaged using an Olympus BX41 microscope (Olympus).

4.2.6 Statistical analysis

Statistical analysis was performed using GraphPad Prism software. The effects of opsin group and period on freezing were analysed using 2-way ANOVA. Subsequently, Sidak's *post-hoc* pairwise comparisons were made. Z-scored response magnitudes and power spectral densities were also compared between opsin groups using 2-way ANOVAs. Proportions of response type were compared using Fisher's exact test. Student's unpaired t-tests were used to analyse the effect of opsin group on mean delta and theta power, unless data did not pass Shapiro-Wilk's test for normality, in which case the non-parametric Mann Whitney U test was used.

4.3 Results

4.3.1 Selective excitation of 5-HT projections and recording of BA neuronal activity during fear

To investigate the influence of 5-HT projections on BA neuronal activity during fear, DRN-BA 5-HT projections were optogenetically excited and BA activity concomitantly monitored via *in vivo* electrophysiological recordings. As in Chapter 3, 5-HT neurons in the DRN were transfected with viral vectors containing the floxed light-gated excitatory cation channel ChR2, and projections were given laser stimulation through bilateral optic fibres. Multi-electrode arrays were unilaterally implanted into the BA to monitor single unit and network activity during a fear learning task (Figure 4.1A).

To examine BA neuronal responses to photoexcitation *per se* (in the absence of the CS and US), a laser control experiment was carried out. Light stimulation trains were delivered to behaviourally naïve mice in their home cage. For BA cells during light stimulation, units were categorised as responsive if the firing rate changed by at least 1.96 standard deviations from pre-laser firing rates over two consecutive time bins of 1 s each. In ChR2-expressing mice, a significantly greater proportion of BA neurons was excited during photoexcitation compared to YFP controls, although the majority were non-responsive in both groups [Fisher's exact test: YFP vs. ChR2, non-responsive vs. responsive, $p=0.003$] (Figure 4.1B). The response magnitude of BA firing rates was significantly larger in ChR2- than YFP-expressing mice [repeated measures 2-way ANOVA; main effect of opsin $F(1,141)=1.717$, $p=0.193$; main effect of time, $F(29,141)=2.366$, $p<0.001$; opsin × time interaction, $F(29,141)=1.578$, $p=0.025$] (Figure 4.1C). These data indicate that DRN-BA 5-HT projection excitation *in vivo* led to an increase in BA neuron firing when behaviourally naïve mice were in their home cage.

In the fear conditioning session, 5-HT projections in the BA were excited during CS-US presentations (Figure 4.1D, top). During fear conditioning, no significant differences in freezing behaviour were observed between ChR2- and YFP-expressing mice [repeated

measures 2-way ANOVA; main effect of opsin $F(1,15)=0.0094$, $p=0.924$; main effect of period, $F(3,15)=22.83$, $p<0.001$; opsin × period interaction, $F(3,15)=1.549$, $p=0.215$] (Figure 4.1D, bottom left). In a novel context, one day later, ChR2-expressing mice displayed enhanced freezing responses during fear extinction compared to YFP controls [repeated measures 2-way ANOVA; main effect of opsin $F(1,15)=3.308$, $p=0.089$; main effect of period, $F(2,15)=26.98$, $p<0.001$; opsin × period interaction, $F(2,15)=5.341$, $p=0.010$] (Figure 4.1D, bottom middle). This effect was driven by freezing differences during the first five CSs (fear retrieval) [Sidak's pairwise comparisons: YFP vs. ChR2, CS1-5 $p=0.002$] rather than during the baseline period or the last five CSs. After another day, during extinction retrieval, the elevated freezing of ChR2-expressing mice was still present [repeated measures 2-way ANOVA; main effect of opsin $F(1,15)=9.808$, $p=0.007$; main effect of period, $F(1,15)=51.19$, $p<0.001$; opsin × period interaction, $F(1,15)=12.33$, $p=0.003$] (Figure 4.1D, bottom right). ChR2-expressing mice froze more compared to YFP controls during the CSs [Sidak's pairwise comparisons: YFP vs. ChR2, CS1-5 $p<0.001$]. These results replicate the finding from Chapter 3 that excitation of DRN 5-HT projections in the BA during conditioning enhanced fear.

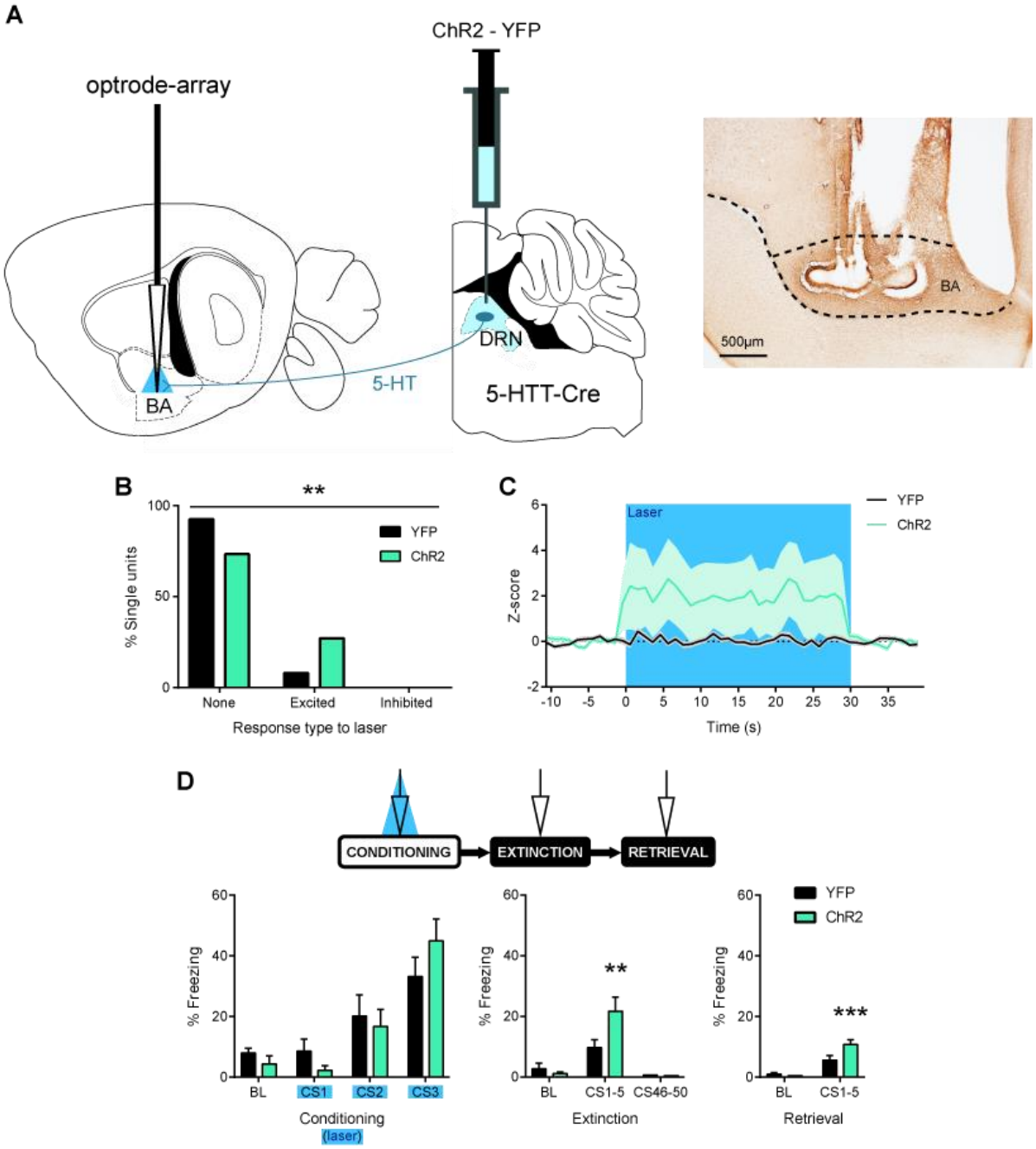


Figure 4.1 – Optogenetic excitation of DRN-BA 5-HT projections during fear conditioning alters BA activity

A. Sagittal schematic showing delivery of a viral vector containing the ChR2 construct into the DRN under control of the 5-HTT promoter, enabling excitation of 5-HT projections in the BA through laser stimulation during *in vivo* recordings (left). Sagittal image of multi-electrode array implanted in BA to record electrophysiological activity *in vivo* (right). **B.** Proportion of responsive BA single unit cells during 30 s laser stimulation in naïve mice in home cage (YFP n=77 cells, 9 mice; ChR2 n=67 cells, 9 mice). **C.** Mean z-score response magnitude of all BA cell firing rates during 30 s laser stimulation in home cage (YFP n=76 cells, 9 mice; ChR2 n=67 cells, 9 mice). **D.** Optogenetic excitation during the conditioning session of a fear learning task, with *in vivo* electrophysiology recordings during conditioning, extinction, and extinction retrieval sessions (top). Percentage time spent freezing in the baseline (BL) period and to a CS during fear conditioning, extinction, and retrieval sessions (bottom; YFP n=9, ChR2 n=8). Data are expressed as means ± SEM. **p<0.01, ***p<0.001.

4.3.2 Fear conditioning: BA single unit activity during optogenetic excitation of DRN-BA 5-HT projections

Although YFP- and ChR2-expressing mice displayed similar fear expression during the conditioning session (Figure 4.1D, bottom left), BA single unit activity was analysed during the three CS presentations to assess the effect of optogenetic excitation of DRN 5-HT projections (Figure 4.2A). BA neuronal responses were examined during 250 ms CS pips and entire 30 s CS presentations.

For BA cells during pips (Figure 4.2B), units were categorised as responsive if the firing rate changed by at least 2.58 standard deviations from the pre-CS pip firing rate over two consecutive time bins of 10 ms each. The proportion of responsive BA cells was comparable between ChR2- and YFP-expressing mice [Fisher's exact test: YFP vs. ChR2, non-responsive vs. responsive, $p=0.187$] (Figure 4.2C). The mean CS pip-response magnitude of BA cell firing in ChR2-expressing mice was significantly lower than that of YFP controls [repeated measures 2-way ANOVA; main effect of opsin $F(1,109)=0.0184$, $p=0.892$; main effect of time, $F(74,109)=3.095$, $p<0.001$; opsin × time interaction, $F(74,109)=2.035$, $p=0.002$; Sidak's pairwise comparisons: YFP vs. ChR2, 0.02 s $p=0.020$] (Figure 4.2D). These results demonstrate that 5-HT projection excitation during fear conditioning reduced the response magnitude of BA neurons to individual CS pips.

For responses over the entire 30 s CS (Figure 4.2E), units were categorised as responsive if the firing rate changed by at least 1.96 standard deviations from pre-CS firing rates over two consecutive time bins of 1 s each. The proportion of responsive BA cells was significantly smaller in ChR2-expressing mice compared to YFP controls [Fisher's exact test: YFP vs. ChR2, non-responsive vs. responsive, $p=0.002$] (Figure 4.2F). The mean response magnitude of BA neuronal firing rates, was not significantly different between ChR2- and YFP-expressing mice during the CS [repeated measures 2-way ANOVA; main effect of opsin $F(1,111)=0.5097$, $p=0.477$; main effect of time, $F(9,111)=1.246$, $p=0.263$; opsin × time

interaction, $F(9,111)=0.5499$, $p=0.838$] (Figure 4.2G). Therefore, 5-HT projection excitation during fear conditioning resulted in a smaller population of CS-responsive BA neurons.

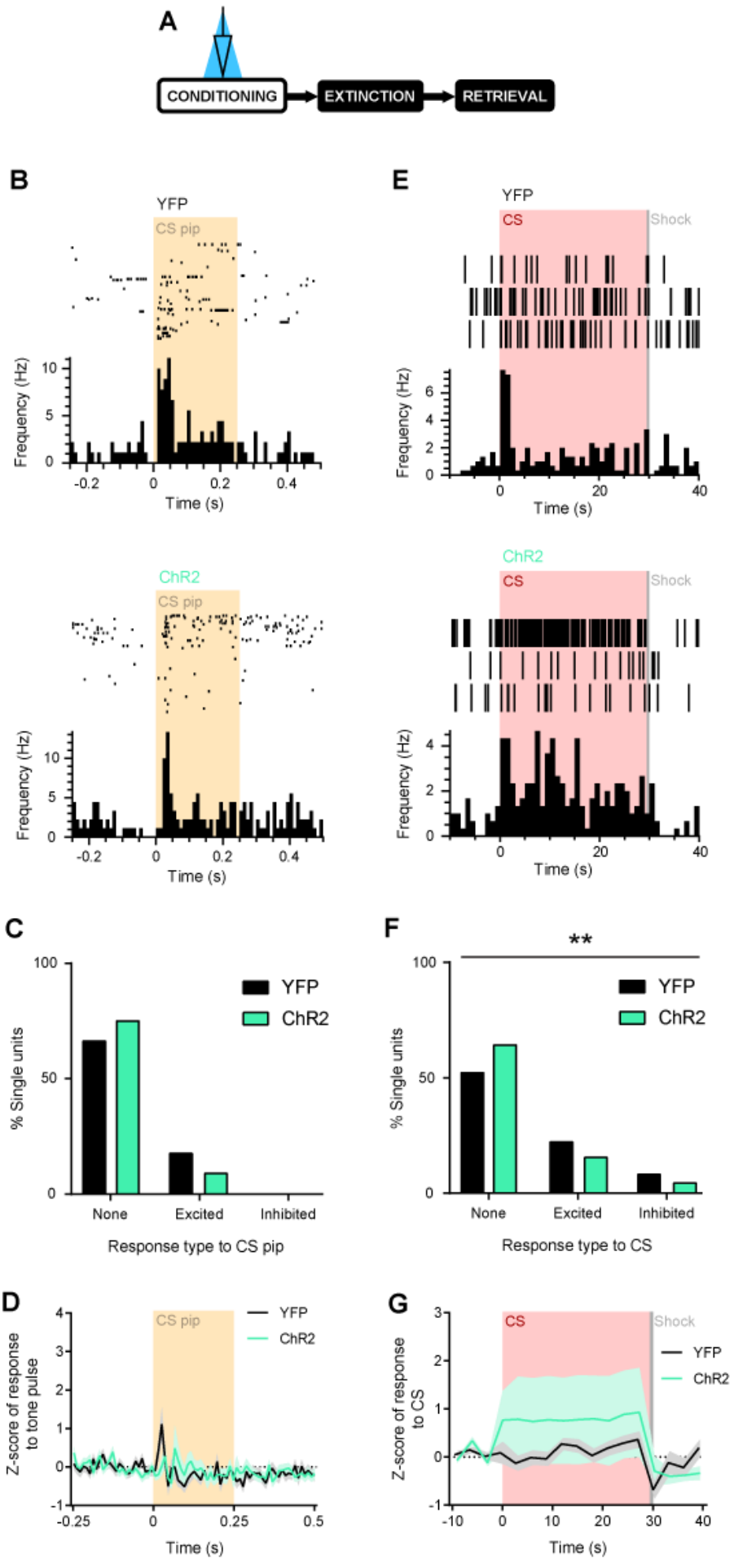

A
CONDITIONING
EXTINCTION
RETRIEVAL
B
YFP
CS pip
Frequency (Hz)
Time (s)
ChR2
CS pip
E
YFP
CS
Shock
ChR2
C
% Single units
YFP
ChR2
None
Excited
Inhibited
Response type to CS pip
F
**
Response type to CS
D
Z-score of response to tone pulse
G
Z-score of response to CS

Figure 4.2 - Optogenetic excitation of DRN-BA 5-HT projections during fear conditioning alters BA neuronal activity
A. During optogenetic excitation in the conditioning session of a fear learning task, *in vivo* electrophysiology recordings during the CS. **B.** Example raster plots of BA single unit cells excited during CS pips in YFP (top) and ChR2 (bottom) mice. **C.** Proportion of responsive BA single unit cells during CS pips (YFP n=53 cells, 9 mice; ChR2 n=58 cells, 9 mice). **D.** Mean z-score response magnitude of all BA cell firing rates during CS pips (YFP n=53 cells, 9 mice; ChR2 n=58 cells, 9 mice). **E.** Example raster plots of BA single unit cells excited during CS in YFP (top) and ChR2 (bottom) mice. **F.** Proportion of responsive BA single unit cells during CS (YFP n=53 cells, 9 mice; ChR2 n=60 cells, 9 mice). **G.** Mean z-score response magnitude of all BA cell firing rates during CS (YFP n=53 cells, 9 mice; ChR2 n=60 cells, 9 mice). Data are expressed as proportions or mean ± SEM. **p<0.01.

4.3.3 Fear conditioning: BA network activity during optogenetic excitation of DRN-BA 5-HT projections

As detailed above, during photoexcitation in the conditioning session (during CS-US pairings), the ChR2 group expressed similar freezing levels to the CS as YFP controls (Figure 4.1D, bottom left). Nonetheless, BA local field potentials respective to the third CS were analysed to evaluate neurophysiological function corresponding to the newly-learned CS (Figure 4.3A).

BA local field potentials were analysed during the entirety of the 30 s CS (Figure 4.3B). Power spectral density distributions indicated BA network activity differences between YFP and ChR2-expressing mice during the CS [repeated measures 2-way ANOVA; main effect of opsin $F(1,16)=0.8421$, $p=0.372$; main effect of frequency, $F(31,16)=55.5$, $p<0.001$; opsin × frequency interaction, $F(31,16)=8.05$, $p<0.001$] (Figure 4.3C). Specifically, delta oscillations were attenuated [unpaired t-test, $t(16)=6.029$, $p<0.001$] and theta oscillations elevated [Mann Whitney U test, $U=11$, $p=0.008$] (Figure 4.3D) in ChR2-expressing mice. This shows that photoexcitation of DRN 5-HT inputs altered BA network activity to the final CS.

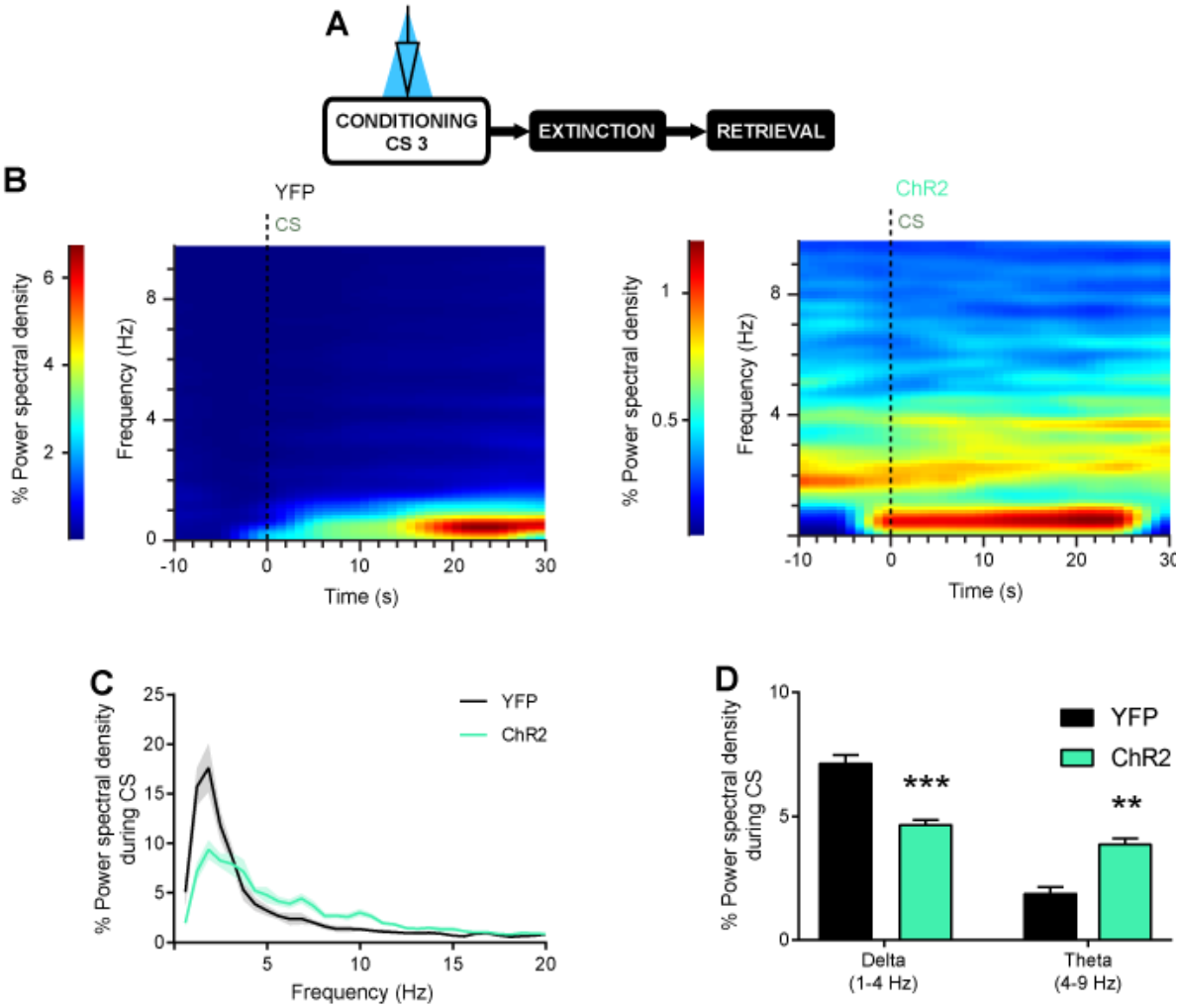


Figure 4.3 - Optogenetic excitation of DRN-BA 5-HT projections during fear conditioning alters BA network activity
A. During optogenetic excitation in the conditioning session of a fear learning task, *in vivo* electrophysiology recordings during the third CS. **B.** Example spectrograms of BA local field potentials during the third CS in YFP (left) and ChR2 (right) mice. **C.** Power spectral density of BA local field potentials during the third CS (YFP n=9, ChR2 n=9). **D.** Mean power of BA delta and theta oscillations during the third CS (YFP n=9, ChR2 n=9). Data are expressed as means ± SEM. **p<0.01, ***p<0.001.

4.3.4 Fear retrieval: BA single unit activity after optogenetic excitation of DRN-BA 5-HT projections

Following DRN 5-HT projection excitation during conditioning, ChR2-expressing mice froze significantly more at the start of the fear extinction session (i.e. during fear memory retrieval) than YFP controls (Figure 4.1D, bottom middle). The corresponding activity of BA single units during these first five CSs of extinction were analysed (Figure 4.4A), respective to the 250 ms CS pips, entire 30 s CS presentations, and freezing episodes that were a minimum of 1 s in duration.

The firing rates of single BA cells monitored during the CS pips (Figure 4.4B) were categorised as responsive if the firing rate changed by at least 2.58 standard deviations from their pre-CS pip firing rates over two consecutive time bins of 10 ms each. The proportion of responsive BA cells was significantly greater in ChR2- than in YFP-expressing controls [Fisher's exact test: YFP vs. ChR2, non-responsive vs. responsive, $p=0.022$] (Figure 4.4C). The mean response magnitude of BA cell firing rates was comparable in the ChR2 and YFP groups during CS pips [repeated measures 2-way ANOVA; main effect of opsin $F(1,157)=0.1169$, $p=0.733$; main effect of time, $F(24,157)=14.79$, $p<0.001$; opsin × time interaction, $F(24,157)=0.5594$, $p=0.958$] (Figure 4.4D). These results demonstrate that DRN-BA 5-HT projection excitation during fear conditioning led to more CS pip-responsive BA neurons on fear retrieval.

BA neuron firing rates analysed during the 30 s CS (Figure 4.4E) were categorised as responsive if the firing rate changed by at least 1.96 standard deviations from pre-CS firing over two consecutive time bins of 1 s each. The proportion of responsive BA cells was not different between ChR2 and YFP groups [Fisher's exact test: YFP vs. ChR2, non-responsive vs. responsive, $p=0.692$] (Figure 4.4F). The mean response magnitude of BA neuron firing rates was also similar between ChR2 and YFP groups during the CS [repeated measures 2-way ANOVA; main effect of opsin $F(1,161)=0.0009$, $p=0.976$; main effect of time, $F(9,161)=2.393$, $p=0.011$; opsin × time interaction, $F(9,161)=1.44$, $p=0.166$] (Figure 4.4G). Therefore, DRN 5-HT projection excitation during fear conditioning did not produce differences in the responsiveness of BA single units to the entire CS during fear retrieval.

Finally, BA cell firing rates during freezing events were monitored (Figure 4.4H); units were categorised as responsive if the firing rate changed by at least 1.96 standard deviations from pre-freezing firing rates over two consecutive time bins of 100 ms each. The proportion of responsive BA neurons was not different between ChR2 and YFP groups [Fisher's exact test: YFP vs. ChR2, non-responsive vs. responsive, $p=0.324$] (Figure 4.4I). The mean response magnitude of BA cell firing rates was higher in the ChR2 group than in YFP controls during freezing [repeated measures 2-way ANOVA; main effect of opsin

F(1,130)=4.206, p=0.042; main effect of time, F(10,130)=3.012, p=0.001; opsin × time interaction, F(10,130)=5.14, p<0.001] (Figure 4.4J). These data show that DRN 5-HT projection excitation during fear conditioning produced greater mean response magnitudes during freezing events on fear retrieval.

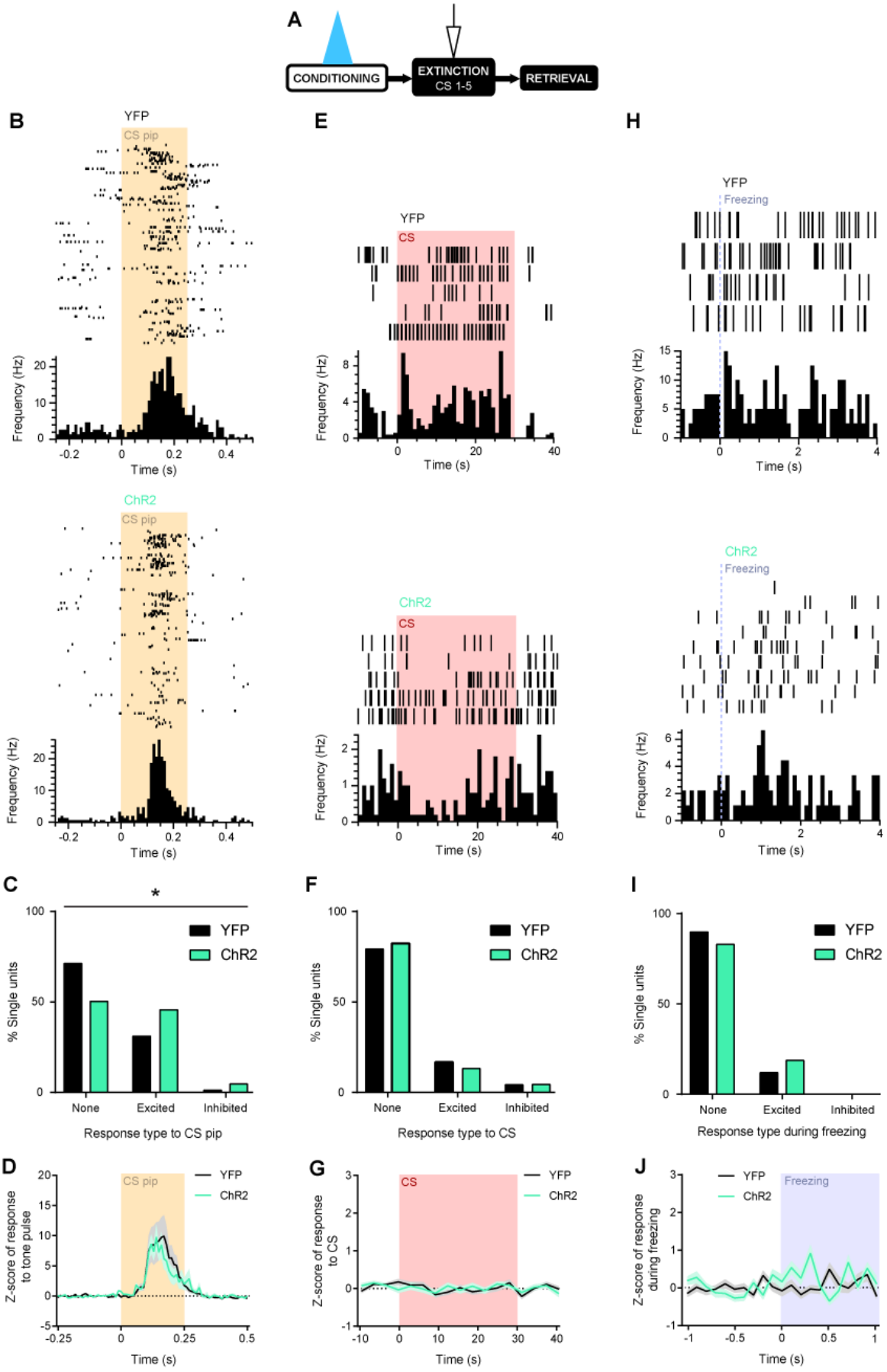

A
CONDITIONING
EXTINCTION
CS 1-5
RETRIEVAL
B
YFP
CS pip
Frequency (Hz)
Time (s)
ChR2
CS pip
E
YFP
CS
ChR2
CS
H
YFP
Freezing
ChR2
Freezing
C
*
% Single units
YFP
ChR2
None
Excited
Inhibited
Response type to CS pip
F
Response type to CS
I
Response type during freezing
D
CS pip
Z-score of response to tone pulse
G
CS
Z-score of response to CS
J
Freezing
Z-score of response during freezing

Figure 4.4 – Optogenetic excitation of DRN-BA 5-HT projections during fear conditioning alters BA neuronal activity during fear retrieval
A. After optogenetic excitation during conditioning session of a fear learning task, *in vivo* electrophysiology recordings were analysed during CS 1 to 5 of the extinction session (fear retrieval). **B.** Example raster plots of BA single unit cells excited during CS pips in YFP (top) and ChR2 (bottom) mice. **C.** Proportion of responsive BA single unit cells during CS pips (YFP n=93 cells, 9 mice; ChR2 n=66 cells, 8 mice). **D.** Mean z-score response magnitude of all BA cell firing rates during CS pips (YFP n=93 cells, 9 mice; ChR2 n=66 cells, 8 mice). **E.** Example raster plots of BA single unit cells excited during CS in YFP (top) and inhibited during CS in ChR2 (bottom) mice. **F.** Proportion of responsive BA single unit cells during CS (YFP n=96 cells, 9 mice; ChR2 n=67 cells, 8 mice). **G.** Mean z-score response magnitude of all BA cell firing rates during CS (YFP n=96 cells, 9 mice; ChR2 n=67 cells, 8 mice). **H.** Example raster plots of BA single unit cells excited during freezing in YFP (top) and ChR2 (bottom) mice. **I.** Proportion of responsive BA single unit cells during freezing (YFP n=71 cells, 9 mice; ChR2 n=61 cells, 8 mice). **J.** Mean z-score response magnitude of all BA cell firing rates during freezing (YFP n=71 cells, 9 mice; ChR2 n=61 cells, 8 mice). Data are presented as proportions or mean ± SEM. *p<0.05, **p<0.01.

4.3.5 Fear retrieval: BA network activity after optogenetic excitation of DRN-BA 5-HT projections

As noted above, after DRN 5-HT projection excitation during conditioning, ChR2-expressing mice froze significantly more at the start of fear extinction (i.e. during fear memory retrieval) (Figure 4.1D, bottom middle). BA local field potentials respective to these first five CS presentations of extinction were analysed (Figure 4.5A).

BA network activity was first examined during the entirety of the 30 s CS (Figure 4.5C). Power spectral density distributions indicated BA network activity differences between the YFP and ChR2 groups during the CS [repeated measures 2-way ANOVA; main effect of opsin $F(1,15)=3.261$, $p=0.091$; main effect of frequency, $F(31,15)=50.34$, $p<0.001$; opsin × frequency interaction, $F(31,15)=5.608$, $p<0.001$] (Figure 4.5D). Specifically, delta oscillations were attenuated [Mann Whitney U test, $U=14$, $p=0.036$] and theta oscillations elevated [unpaired t-test, $t(15)=4.55$, $p<0.001$] (Figure 4.5E) in the ChR2 group. This shows that photoexcitation during fear conditioning altered BA network activity to the CS on fear retrieval.

As a control measure, the power spectral density of BA network activity was also assessed during the baseline (pre-CS) period in the extinction session, when freezing levels were similar between ChR2 and YFP groups, and was found to be no different between groups [repeated measures 2-way ANOVA; main effect of opsin $F(1,15)=3.947$, $p=0.066$;

main effect of frequency, $F(31,15)=45.96$, $p<0.001$; opsin × frequency interaction, $F(31,15)=1.008$, $p=0.457$] (Figure 4.5B). This suggests that the 5-HT projection excitation during fear conditioning did not affect subsequent BA network activity during emotionally neutral baseline conditions.

BA oscillations were also examined during CS-evoked freezing episodes that were a minimum of 1 s (Figure 4.5F). Power spectral densities were similar for the YFP and ChR2 groups during freezing [repeated measures 2-way ANOVA; main effect of opsin $F(1,15)=0.625$, $p=0.442$; main effect of frequency, $F(31,15)=17.4$, $p<0.001$; opsin × frequency interaction, $F(31,15)=0.5202$, $p=0.986$] (Figure 4.5G). Neither delta nor theta oscillations were significantly different [unpaired t-test: delta, $t(15)=0.1755$, $p=0.863$; theta, $t(15)=1.043$, $p=0.313$] (Figure 4.5H). Hence, 5-HT projection excitation during fear conditioning did not affect BA network activity during CS-evoked freezing events during fear retrieval.

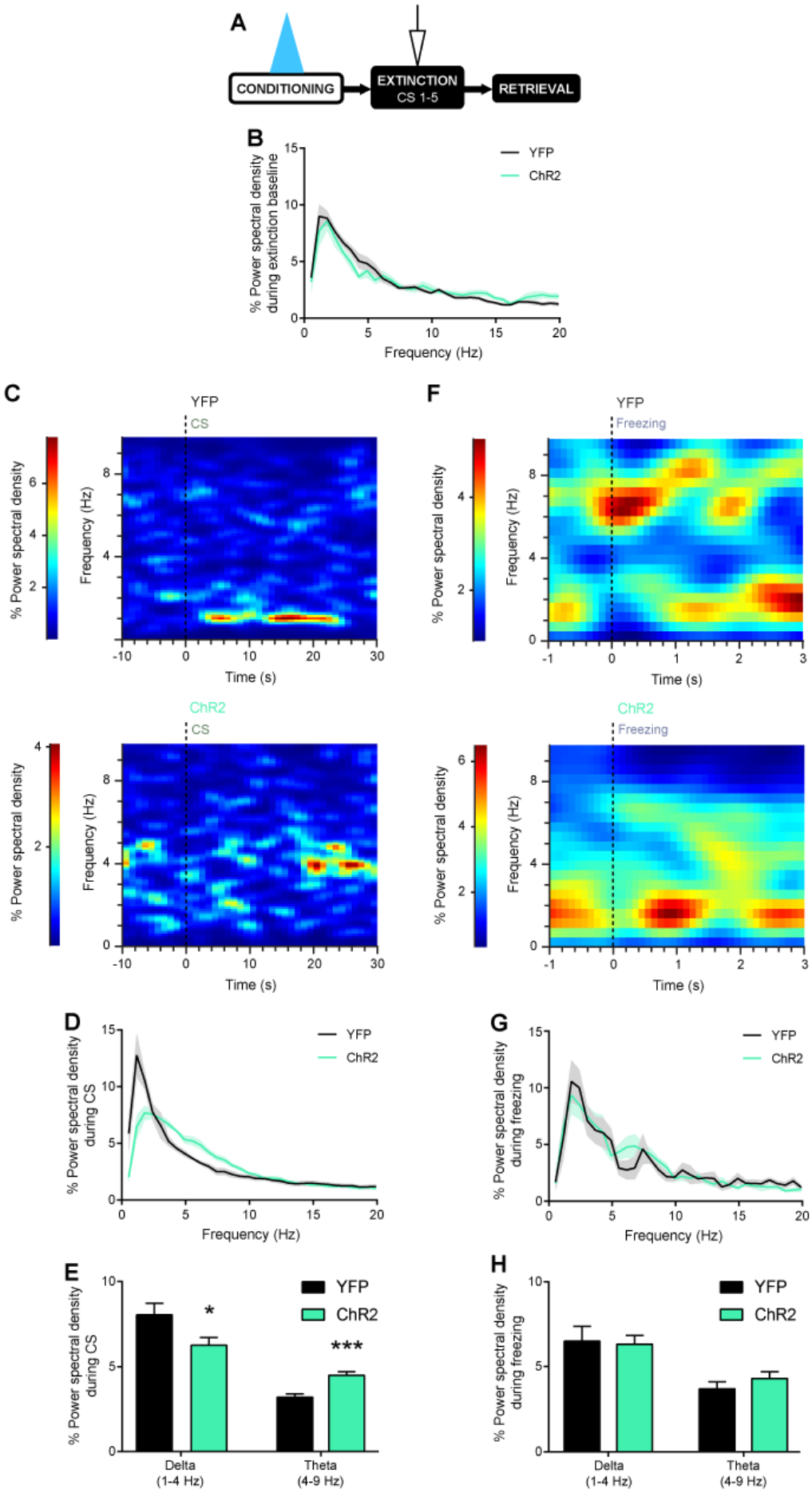

A
CONDITIONING
EXTINCTION
CS 1-5
RETRIEVAL
B
% Power spectral density during extinction baseline
YFP
ChR2
Frequency (Hz)
C
YFP
CS
% Power spectral density
Frequency (Hz)
Time (s)
ChR2
CS
F
YFP
Freezing
ChR2
Freezing
D
% Power spectral density during CS
G
% Power spectral density during freezing
E
*
***
Delta (1-4 Hz)
Theta (4-9 Hz)
H

Figure 4.5 - Optogenetic excitation of DRN-BA 5-HT projections during fear conditioning alters BA network activity during fear retrieval
A. After optogenetic excitation during conditioning session of a fear learning task, *in vivo* electrophysiology recordings were analysed during CS 1 to 5 of the extinction session (fear retrieval). **B**. Power spectral density of BA local field potentials during baseline (BL) period of fear extinction session (YFP n=9, ChR2 n=8). **C.** Example spectrograms of BA local field potentials during CS in YFP (top) and ChR2 (bottom) mice. **D.** Power spectral density of BA local field potentials during CS (YFP n=9, ChR2 n=8). **E.** Mean power of BA delta and theta oscillations during CS (YFP n=9, ChR2 n=8). **F.** Example spectrograms of BA local field potentials during freezing in YFP (top) and ChR2 (bottom) mice. **G.** Power spectral density of BA local field potentials during freezing (YFP n=9, ChR2 n=8). **H.** Mean power of BA delta and theta oscillations during freezing (YFP n=9, ChR2 n=8). Data are expressed as means ± SEM. *p<0.05, ***p<0.001.

4.3.6 Extinction retrieval: BA single unit activity after optogenetic excitation of DRN-BA 5-HT projections

Since ChR2-expressing mice froze significantly more during extinction retrieval following DRN-BA 5-HT photoexcitation during conditioning (Figure 4.1D, bottom right), the corresponding activity of BA neurons was analysed (Figure 4.6A), during 250 ms CS pips, entire 30 s CS presentations, and freezing episodes that were a minimum of 1 s in duration.

For BA neuronal firing rates during CS pips (Figure 4.6B), neurons were categorised as responsive if the firing rate changed by at least 2.58 standard deviations from their pre-CS pip firing rates over two consecutive time bins of 10 ms each. The proportion of responsive BA cells was not different between the ChR2 and YFP groups [Fisher's exact test: YFP vs. ChR2, non-responsive vs. responsive, p=0.724] (Figure 4.6C). The mean response of BA cell firing rates was higher in the ChR2 than the YFP group during CS pips [repeated measures 2-way ANOVA; main effect of opsin $F(1,158)=1.775$, $p=0.185$; main effect of time, $F(24,158)=10.69$, $p<0.001$; opsin × time interaction, $F(24,158)=2.51$, $p<0.001$; Sidak's pairwise comparisons: YFP vs. ChR2, 0.12 s p=0.048, 0.13 s p=0.001] (Figure 4.6D). These results demonstrate that photoexcitation during fear conditioning led to a greater mean BA neuron response magnitude during CS pips on extinction retrieval.

For BA neuronal firing rates analysed during the 30 s CS (Figure 4.6E), neurons were categorised as responsive if the firing rate changed by at least 1.96 standard deviations from pre-CS firing rates over two consecutive time bins of 1 s each. The proportion of responsive BA cells was significantly greater in the ChR2 than the YFP group [Fisher's exact test: YFP vs.

ChR2, non-responsive vs. responsive, p=0.027] (Figure 4.6F). The mean response magnitude of BA neuron firing rates was not different between groups [repeated measures 2-way ANOVA; main effect of opsin $F(1,157)=2.098$, $p=0.150$; main effect of time, $F(9,157)=0.1.195$, $p=0.294$; opsin × time interaction, $F(9,157)=1.524$, $p=0.134$] (Figure 4.6G). Hence, excitation of DRN-BA 5-HT neurons during fear conditioning produced responses to the CS in a greater proportion of BA neurons during extinction retrieval.

Finally, BA firing rates were monitored during freezing events (Figure 4.6H), with units categorised as responsive if the firing rate changed by at least 1.96 standard deviations from pre-freezing firing rates over two consecutive time bins of 100 ms each. The proportion of responsive BA neurons was similar between groups [Fisher's exact test: YFP vs. ChR2, non-responsive vs. responsive, p=0.487] (Figure 4.6I). However, the mean response magnitude of BA cell firing rates was higher in the ChR2 group, as compared to YFP controls [repeated measures 2-way ANOVA; main effect of opsin $F(1,124)=1.222$, $p=0.271$; main effect of time, $F(10,124)=3.076$, $p<0.001$; opsin × time interaction, $F(10,124)=4.93$, $p<0.001$; Sidak's pairwise comparisons, YFP vs. ChR2, 0.3 s $p<0.001$] (Figure 4.6J). These results indicate that photoexcitation increased BA neuronal firing magnitude during freezing events on extinction retrieval.

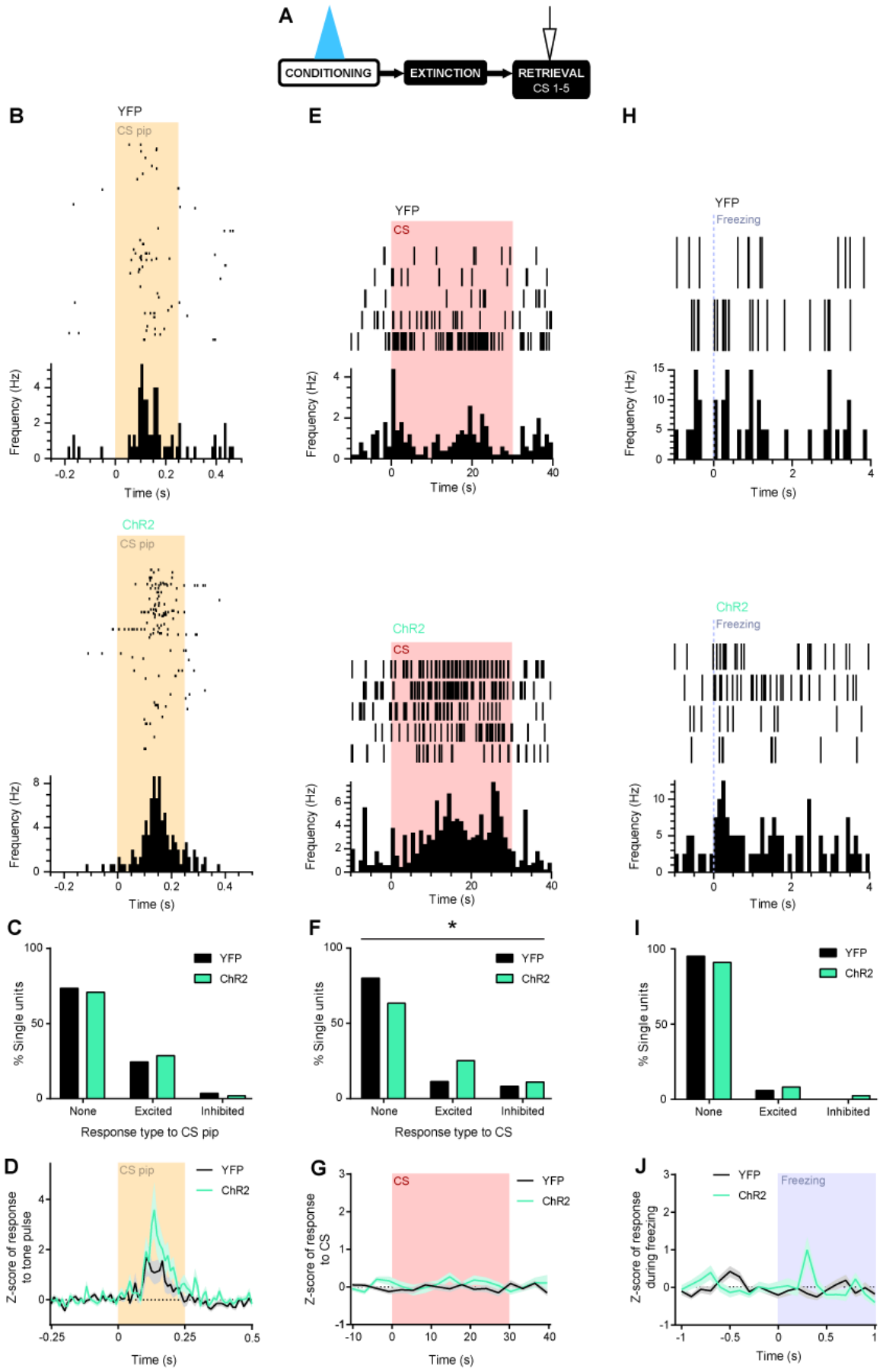


Figure 4.6 - Optogenetic excitation of DRN-BA 5-HT projections during fear conditioning alters BA single unit activity during extinction retrieval

A. After optogenetic excitation during conditioning session of a fear learning task, *in vivo* electrophysiology recordings during CS 1 to 5 of the retrieval session. **B.** Example raster plots of BA single unit cells excited during CS pips in YFP (top) and ChR2 (bottom) mice. **C.** Proportion of responsive BA single unit cells during CS pips (YFP n=96 cells, 9 mice; ChR2 n=64 cells, 9 mice). **D.** Mean z-score response magnitude of all BA cell firing rates during CS pips (YFP n=96 cells, 9 mice; ChR2 n=64 cells, 9 mice). **E.** Example raster plots of BA single unit cells excited during CS in YFP (top) and ChR2 (bottom) mice. **F.** Proportion of responsive BA single unit cells during CS (YFP n=96 cells, 9 mice; ChR2 n=63 cells, 9 mice). **G.** Mean z-score response magnitude of all BA cell firing rates during CS (YFP n=96 cells, 9 mice; ChR2 n=63 cells, 9 mice). **H.** Example raster plots of BA single unit cells not responsive during freezing in YFP (top) and excited during freezing in ChR2 (bottom) mice. **I.** Proportion of responsive BA single unit cells during freezing (YFP n=74 cells, 9 mice; ChR2 n=52 cells, 9 mice). **J.** Mean z-score response magnitude of all BA cell firing rates during freezing (YFP n=74 cells, 9 mice; ChR2 n=52 cells, 9 mice). Data are expressed as means ± SEM. **p<0.01.

4.3.7 Extinction retrieval: BA network activity after optogenetic excitation of DRN-BA 5-HT projections

To reiterate, following excitation of DRN-BA 5-HT neurons during conditioning, ChR2-expressing mice froze significantly more during fear extinction retrieval (Figure 4.1D, bottom right). BA local field potentials respective to the five CS presentations of extinction retrieval were analysed (Figure 4.7A).

BA network activity was first examined during the entirety of the 30 s CS (Figure 4.7B). Power spectral density distributions indicated BA network activity differences between the YFP and ChR2 groups during the CS [repeated measures 2-way ANOVA; main effect of opsin $F(1,16)=0.5275$, $p=0.478$; main effect of frequency, $F(31,16)=62.52$, $p<0.001$; opsin × frequency interaction, $F(31,16)=2.154$, $p<0.001$] (Figure 4.7C). Although delta oscillations were not significantly different [unpaired t-test, $t(16)=0.9522$, $p=0.355$], theta oscillations were elevated in the ChR2 group [unpaired t-test, $t(16)=2.236$, $p=0.040$] (Figure 4.7D). This shows that photoexcitation during fear conditioning altered BA network activity on extinction retrieval.

For BA oscillations examined during freezing episodes that were a minimum of 1 s (Figure 4.7E), power spectral densities were similar between YFP and ChR2 groups [repeated measures 2-way ANOVA; main effect of opsin $F(1,16)=0.6154$, $p=0.444$; main effect of frequency, $F(31,16)=16.64$, $p<0.001$; opsin × frequency interaction, $F(31,16)=0.6992$, $p=0.888$] (Figure 4.7F). Neither delta nor theta oscillations were significantly different

[unpaired t-test: delta, t(16)=0.2464, p=0.809; theta, t(16)=0.0702, p=0.945] (Figure 4.7G), indicating photoexcitation during fear conditioning did not affect BA network activity during extinction retrieval freezing events.

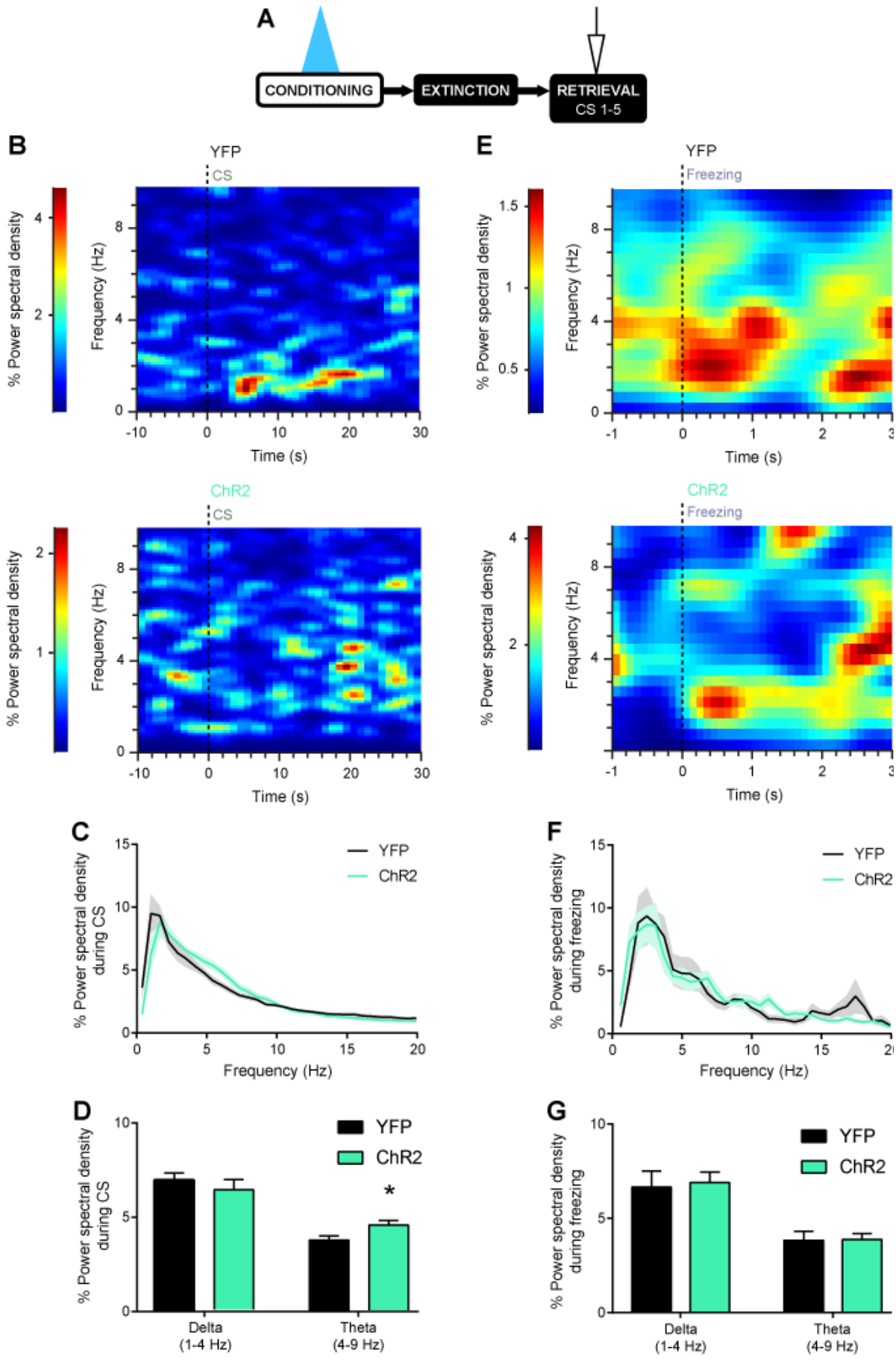

A
CONDITIONING
EXTINCTION
RETRIEVAL
CS 1-5
B
YFP
CS
% Power spectral density
Frequency (Hz)
Time (s)
ChR2
CS
E
YFP
Freezing
ChR2
Freezing
C
YFP
ChR2
% Power spectral density during CS
Frequency (Hz)
F
% Power spectral density during freezing
D
Delta (1-4 Hz)
Theta (4-9 Hz)
*
G

Figure 4.7 - Optogenetic excitation of DRN-BA 5-HT projections during fear conditioning alters BA network activity during extinction retrieval
A. After optogenetic excitation during conditioning session of a fear learning task, *in vivo* electrophysiology recordings were analysed during CS 1 to 5 of the retrieval session. **B.** Example spectrograms of BA local field potentials during CS in YFP (top) and ChR2 (bottom) mice. **C.** Power spectral density of BA local field potentials during CS (YFP n=9, ChR2 n=9). **D.** Mean power of BA delta and theta oscillations during CS (YFP n=9, ChR2 n=9). **E.** Example spectrograms of BA local field potentials during freezing in YFP (top) and ChR2 (bottom) mice. **F.** Power spectral density of BA local field potentials during freezing (YFP n=9, ChR2 n=9). **G.** Mean power of BA delta and theta oscillations during freezing (YFP n=9, ChR2 n=9). Data are expressed as means ± SEM. *p<0.05.

4.4 Discussion

The data in this chapter replicated the results of chapter 3; optogenetically enhancing DRN 5-HT inputs to the BA during CS presentations on fear conditioning led to increased fear on fear retrieval and extinction retrieval tests. Furthermore, it was shown that this behavioural effect was associated with significant alterations in both isolated BA neuron activity and BA neuronal network activity. Specifically, optogenetic photoexcitation of DRN-BA 5-HT fibres during fear conditioning reduced the proportion and magnitude of BA neuronal responses to the CS (Figure 4.2D, F). However, during subsequent fear retrieval and extinction retrieval tests (no light stimulation), prior 5-HT photoexcitation resulted in increased BA neuron activation during the CS or CS-evoked freezing episodes (Figure 4.4C, J; Figure 4.6D, F, J). Furthermore, in all stages of the fear task, 5-HT photoexcitation during conditioning was associated with enhanced CS-related BA theta oscillations Figure 4.3D; Figure 4.5E; Figure 4.7D). CS-related delta oscillations were also attenuated during fear conditioning and fear retrieval (Figure 4.3D; Figure 4.5E). Thus, excitation of DRN-BA 5-HT projections during fear conditioning altered BA neuronal and network activity in tandem with enhanced fear expression.

4.4.1 5-HT projection excitation alters BA neuronal activity *in vivo*

Photoexcitation of DRN 5-HT axons in the BA caused an increase in BA neuronal activity in the home cage, but reduced activity during CS presentations on fear conditioning. This suggests that the influence of 5-HT signalling on BA circuits is likely input- and state-

dependent, with the effects of 5-HT transmission occurring through the modulation of other concurrently active inputs to BA neurons. This is supported by the finding from Chapter 3 that indicated that 5-HT transmission alone was not sufficient to generate a fear memory in the absence of a concomitant CS.

5-HT is a neuromodulator that acts on multiple receptor types, most of which are metabotropic (Barnes and Sharp, 1999), as described in Chapter 1. 5-HT is therefore in a position to change the impact of primary transmitters, namely by altering glutamatergic or GABAergic signals, through both pre- and postsynaptic mechanisms. Evidence suggests that 5-HT reduces glutamate release presynaptically from LA projections onto BA PNs via 5-HT_{1A} or 5-HT_{2} receptors (Cheng et al., 1998; Yamamoto et al., 2012). 5-HT could also modulate inputs to the amygdala from other sources, such as from the prefrontal cortex, hippocampus, or intercalated cells, all of which are thought to provide instructive signals to BA neurons during fear learning (Herry et al., 2008; Sierra-Mercado et al., 2011; Cho et al., 2013; Arruda-Carvalho and Clem, 2014; Asede et al., 2015; Bukalo et al., 2015). A recent study proved this *ex vivo* by demonstrating that 5-HT gates cortical and thalamic inputs to the BLA via 5-HT_{1B} receptors (Guo et al., 2017). 5-HT terminals can form triads onto other synapses of both excitatory or inhibitory nature, and this phenomenon occurs most commonly in the amygdala (Belmer et al., 2017). More 5-HT triads are formed at inhibitory rather than excitatory synapses, and an electrophysiology study in *ex vivo* dissociated BLA neurons demonstrated that 5-HT prevents GABA release presynaptically via 5-HT_{1A} receptors (Koyama et al., 1999), which likely affects transmission from local INs. In the BA, the functional role of the input source would be critical in determining the behavioural impact of 5-HT modulation. Thus, it is important to dissect whether certain synapses in the BA are preferentially regulated by 5-HT transmission.

In addition to presynaptic control, 5-HT can also modulate inputs to the BA at the postsynaptic BA neuron. In the hippocampus, 5-HT and NMDA receptors converge onto the same signalling mechanisms (Gandolfi et al., 1990), and 5-HT transmission regulates phosphorylation of $GABA_A$ receptors in the prefrontal cortex in an activity-dependent

manner (Feng et al., 2001). Although 5-HT modulation mechanisms in the amygdala have not been as precisely characterised, there is support for 5-HT signalling enhancing NMDA receptor-mediated synaptic events in the BLA (Chen et al., 2003). Furthermore, 5-HT neurons might also influence postsynaptic BA neurons through co-release of other transmitters, such as glutamate (Trudeau, 2004). Subsets of BA neurons that are mutually exclusive have been implicated in opposing functions in emotional behaviour (Herry et al., 2008; Lee et al., 2017) and as having distinct anatomical targets (Senn et al., 2014; Cheriyan et al., 2016). Differential modulation of BA cell groups by 5-HT could be important in shaping behaviour, as has been shown recently for orexin signalling (Flores et al., 2017).

4.4.2 5-HT projection excitation during conditioning alters BA single unit activity during fear retrieval and extinction retrieval

During fear retrieval, the proportions of BA neurons responsive to the CS in YFP controls were similar to those reported previously (Herry et al., 2008; Amano et al., 2011). After photoexcitation of DRN-BA 5-HT projections during fear conditioning, BA single units in ChR2-expressing mice displayed increased activity during CS presentations of subsequent fear and extinction retrieval sessions. Additionally, the ChR2-expresing group not only froze more than YFP controls, but also exhibited greater BA neuronal activity during freezing episodes. Increases in BLA neuron firing have been associated with freezing behaviour (Karalis et al., 2016), consistent with the elevated activity of BA neurons being functionally coupled to the increased fear expression observed after DRN-BA 5-HT neuron photoexcitation. As mentioned, previous studies have identified mutually exclusive cell groups that are active either during high fear states after conditioning or low fear states after extinction (Herry et al., 2008; Senn et al., 2014). To map the influence of 5-HT modulation onto this phenomenon, BA neuron responses should be considered separately for each CS during conditioning and extinction sessions, so that changes in activity within the same

individual neurons can be tracked across testing stages. Additionally, it would be informative to consider US-evoked responses (Johansen et al., 2010; McHugh et al., 2014).

Given that increased fear expression and BA single unit activity persisted 1-2 days after photoexcitation, enhancing 5-HT transmission likely affected plasticity in the BA (Chen et al., 2003). 5-HT receptors have the ability to regulate synaptic plasticity by influencing transmitter release (Cheng et al., 1998; Koyama et al., 1999; Mathur et al., 2011), non-5-HT receptor function (Feng et al., 2001), action potential firing rates (Ashby et al., 1992), and membrane conductances (McCormick et al., 1993). Moreover, 5-HT receptors are differentially located on distinct cell types (Asan et al., 2013), which suggests selective modulation of particular synaptic connections. 5-HT transmission may be better equipped to modulate plasticity than to directly drive neuronal firing like glutamate or GABA. 5-HT receptors are located both perisomatically and on distal dendrites (McDonald and Mascagni, 2007). Similar to INs, 5-HT neurons target distinct subcellular compartments and can therefore modulate neurons in a compartment- and input-specific manner. This is important for plasticity because dendritic events can be highly compartmentalised (Chiu et al., 2013) and sometimes more critical than somatic events for controlling the strength of synaptic inputs (Lovett-Barron et al., 2012). It could also explain why, in spite of reducing BA neuron firing during conditioning, enhancing 5-HT transmission seemed to potentiate neuronal activity on subsequent retrieval tests.

4.4.3 5-HT projection excitation during conditioning changes network activity in the theta and delta ranges

Overall, across all stages of fear learning, 5-HT projection excitation enhanced theta oscillations in the BA during CS presentations. This is in agreement with other models of 5-HT manipulation, in which 5-HTT overexpression reduces fear, extracellular 5-HT, and amygdala theta power, whereas 5-HTT KO increases fear, extracellular 5-HT, and theta coherence between the amygdala and prefrontal cortex (Jennings et al., 2010; Narayanan et

al., 2011; Barkus et al., 2014). Interestingly, in both the current data and in a previous study, increased theta power was observed in higher-fear mice with more 5-HT signalling, even in individual sessions when their freezing responses did not differ significantly (Barkus et al., 2014). It is worth noting that the power spectral densities of control mice in the current study seem to reflect those of 5-HTT OE mice displaying low fear described by Barkus et al. (2014), but this may be due to the current fear conditioning paradigm being milder in comparison. Taken together, BA theta power seems to be associated with emotionally salient, aversive experiences rather than with freezing episodes specifically. One way to test this more precisely would be to analyse BA local field potentials during shorter time bins over the course of conditioning and retrieval tests to confirm whether increases in theta power precede freezing events (Karalis et al., 2016).

If theta oscillations in the BA are not directly related to freezing, they could be associated with a different aspect of fear. McHugh et al. (2014) reported that amygdala theta represents an aversive prediction error, and greater theta synchrony between the BLA and prefrontal cortex occurs in mice that can better distinguish between aversive and neutral cues (Likhtik et al., 2013). BA theta oscillations might therefore indicate enhanced top-down information flow from the prefrontal cortex, increased attentional or processing effort directed towards the fear memory, or elevated emotional salience of the predictive CS. In accordance with this, BA delta oscillations, which are slow waves that have been associated with low arousal levels (Bazelot et al., 2015), are attenuated by photoexcitation.

There are a number of mechanisms that could be affected by 5-HT to cause changes in BA theta oscillations. If amygdala theta rhythms are generated in the prefrontal cortex (Likhtik et al., 2013; Karalis et al., 2016), 5-HT transmission might enhance this input to the BA. In the prefrontal cortex and hippocampus, parvalbumin INs have been identified as crucial for regulating theta rhythms (Courtin et al., 2013; Amilhon et al., 2015). In a recent multiplexed study combining electrophysiological recordings with chemogenetics, it has been shown that extinction training generates a 6-12 Hz oscillation that competes with the 3-6 Hz oscillation associated with fear expression in the BLA (Davis et al., 2017). Importantly, this

oscillatory competition is mediated by BLA parvalbumin INs. Since 5-HT is known to modulate parvalbumin INs in the BLA (Bocchio et al., 2015), 5-HT input could also influence local theta. BLA PNs themselves resonate at theta frequencies due to intrinsic membrane conductances (Pape and Driesang, 1998), which could be affected by 5-HT signalling. Theta modulation of the BA regulates heterosynaptic plasticity (Bazelot et al., 2015), which suggests that by enhancing theta power, 5-HT transmission could gate the strength of other inputs to the BA.

4.4.4 Functional implications for 5-HT modulation of BA activity in fear learning

The results from this study raise the question of whether a specific type of information coding in the BA is regulated by 5-HT neurons. BA neurons could encode fear memories through a rate code, which would correspond to the firing frequency of individual neurons, or through a temporal code, which would rely on precisely timed firing of BA neurons. As discussed above, the increase in BA single unit activity and the possibility of underlying plasticity mechanisms suggest a rate code. However, a temporal code would not necessarily be detected by simply monitoring neuronal firing rates. To directly examine this, phase-locking of the neurons to BA theta oscillations might provide more information. Furthermore, BLA single units are often phase-locked to theta oscillations in other brain regions (Bienvenu et al., 2012; Likhtik et al., 2013; Karalis et al., 2016), so a useful experiment would be to monitor local field potentials in the prefrontal cortex or hippocampus in addition to the approach used in this study. Notably, phase-locked BLA neurons are often of a particular cell type, so it would be interesting to use electrophysiological parameters to identify putative BA cell types to monitor whether 5-HT modulates them differentially during fear (Likhtik et al., 2006).

4.4.5 Conclusions

This study is the first to demonstrate that increases in DRN-BA 5-HT transmission during fear conditioning alters the activity of individual BA neurons and BA network activity during all stages of a fear learning task. To better understand how optogenetic photoexcitation of 5-HT projections brought about the effects on BA neuronal activity described in this chapter, it is necessary to characterise the mechanisms through which 5-HT neurons modulate BA circuits. Some possible mechanisms that were mentioned above include activation of specific receptors, heterosynaptic modulation, cell type-specific signalling, and co-release of other transmitters. The next chapter will investigate the control of BA neurons by 5-HT projections and characterise some of the mechanisms of modulation in *ex vivo* slices.

Chapter 5 5-HT neurons modulate the basal amygdala via 5-HT and glutamate co-transmission

5.1 Introduction

Results presented in the previous chapters highlight the functional importance of amygdala modulation by DRN 5-HT neurons during fear behaviour. However, the precise physiological mechanisms through which 5-HT inputs influence BA neurons are still unknown. In this chapter, the control of BA neurons by DRN 5-HT projections is investigated by combining optogenetics with *ex vivo* whole-cell patch-clamp electrophysiology.

5.1.1 Functional importance of 5-HT transmission in the amygdala

The neurotransmitter 5-HT regulates a vast array of brain functions. Among these, 5-HT is strongly implicated in emotional regulation, and in the aetiology and drug treatment of mood and anxiety disorders (Nemeroff and Owens, 2002). Presumably, these behavioural effects arise from the 5-HT modulation of multiple neuronal circuits, but as discussed in previous chapters, 5-HT transmission in the amygdala is likely to play a critical role.

The amygdala is a brain region that comprises multiple nuclei that collectively encode many aspects of emotionality including fear learning and memory (Duvarci and Pare, 2014; Janak and Tye, 2015). Across species, the amygdala is heavily innervated by 5-HT neurons

arising from the DRN in the midbrain (Jacobs et al., 1978; Steinbusch, 1981; Asan et al., 2013). Moreover, selective pharmacological manipulations of 5-HT in the amygdala are reported to have striking effects on fear and anxiety responses in experimental animals (Christianson et al., 2010; Johnson et al., 2015; Baratta et al., 2016).

5.1.2 5-HT signalling in the BLA

The interaction between 5-HT and the amygdala is complex, and takes the form of synaptic and non-synaptic 5-HT terminals that target diverse excitatory and inhibitory 5-HT receptor subtypes distributed across a microcircuitry comprised of many neuron populations (for review, see Asan et al, 2013; Bocchio et al, 2016b). In the BLA complex, further subdivided into BA and LA nuclei, immunohistochemical and in situ hybridisation studies (Aznar et al., 2003; McDonald and Mascagni, 2007) report the presence of both excitatory ($5\text{-}HT_{2A}$) and inhibitory ($5\text{-}HT_{1A}$) 5-HT receptors on glutamatergic PNs, which comprise about 80% of the neurons of the BLA. Similar studies report that these receptors, as well as excitatory ionotropic ($5\text{-}HT_{3A}$) 5-HT receptors, are also distributed across different groups of GABAergic INs in the BLA (Aznar et al., 2003; Mascagni and McDonald, 2007; McDonald and Mascagni, 2007; Bonn et al., 2013).

These receptor localisation studies are supported by investigations of 5-HT receptor function in the BLA. *In vitro* electrophysiological studies find that PNs respond to exogenous 5-HT with $5\text{-}HT_{2C}$ receptor-mediated depolarisation in the LA (Yamamoto et al., 2014) but not in the BA (Rainnie, 1999; Bocchio et al., 2015). Furthermore, 5-HT was found to depolarise BA INs, mainly via $5\text{-}HT_{2A}$ receptors, leading to enhanced GABA release onto PNs (Rainnie, 1999; Jiang et al., 2009; Bocchio et al., 2015).

Despite these advances, it remains crucial to understand how BA neurons respond to physiologically released 5-HT. Virtually all that is known about the action of 5-HT on BA neurons is based on the prolonged application of exogenous 5-HT and 5-HT ligands

(Eidelberg et al., 1967; Rainnie, 1999; Stutzmann and LeDoux, 1999; Jiang et al., 2009; Bocchio et al., 2015). A pitfall of this approach was recently highlighted in a study that found that the response of BA neurons to acetylcholine released physiologically by targeted optogenetic stimulation did not match the canonical response of BA neurons to locally applied acetylcholine (Unal et al., 2015). Differences between such pharmacological and physiological approaches could arise from a mismatch between pharmacological and physiological concentrations of 5-HT, non-physiological activation of extra-synaptic receptors, and the potential role of physiologically released co-transmitters. In the case of 5-HT, co-transmitters include a number of candidate amino acids and neuropeptides (e.g. see Fernandez et al., 2016).

5.1.3 Aims of this chapter

The current study adopted a more physiological approach to investigate the effect of 5-HT on BA neuron subtypes as a follow up of a recent pharmacological 5-HT study (Bocchio et al, 2015). 5-HT axons in the BA were photoexcited by light stimulation of ChR2, which was selectively expressed in DRN 5-HT neurons. The goal was to identify mechanisms of control of amygdala microcircuits by DRN 5-HT neurons.

5.2 Materials and methods

5.2.1 Animals

SERT-Cre+/- mice (MMRRC, B6.Cg-Tg(Slc6a4-cre)Et33Gsat, stock number 031028-UCD) of either sex, genotyped via polymerase chain reaction, were housed with their littermates with *ad libitum* access to food and water at a constant temperature and humidity on a 12/12 h light/dark cycle (lights on 7am). Experiments were performed in compliance with the Animals (Scientific Procedures) Act, 1986 (UK) and approved by local ethical review at the University of Oxford.

5.2.2 Viral transfection

To selectively transfect 5-HT neurons with ChR2, a Cre-inducible recombinant viral vector (AAV-EF1a-DIO-hChR2(E123T/T159C)-EYFP; UNC Vector Core) carrying a floxed ultrafast (E123T/T159C) ChR2 fused with YFP was stereotaxically injected (1 µl at 100 nL/min) into the DRN (coordinates (mm) according to bregma and the brain surface; anterior-posterior -4.1; dorso-ventral -2.5, -2.2, -1.9) of SERT-Cre mice (P30-P75) anesthetised using 1-2 % isoflurane in oxygen (2 L/min). On recovery from surgery, mice were administered 0.3 mg/kg s.c. buprenorphine for post-operative analgesia.

5.2.3 Electrophysiological recordings

Electrophysiological recordings were performed 4 weeks following viral transfection. Mice were deeply anesthetised (4% isoflurane) and brains were rapidly extracted and immersed in an ice-cold cutting solution with the following composition (in mM): 0.5 $CaCl_2$, 10 glucose, 2.5 KCl, 7 $MgCl_2$, 85 NaCl, 25 $NaHCO_3$, 1.25 NaH_2PO_4, and 65 sucrose (all from Sigma-Aldrich) saturated with 95% O_2, 5% CO_2, at pH 7.3. Coronal slices (325 µm) were cut at 4°C at the level of the BLA or DRN using a microtome (Microm HM 650 V, Thermo Fisher). Slices were then incubated at 36°C for 10 min, after which heating was switched off to allow the slices to re-equilibrate to room temperature (18-22 °C, ~1 h). During this period, slices were perfused at a rate of ~5 mL/min with artificial cerebrospinal fluid (ACSF) composed of (in mM): 2 $CaCl_2$, 10 glucose, 3.5 KCl, 2 $MgCl_2$, 130 NaCl, 24 $NaHCO_3$, and 1.25 NaH_2PO_4; saturated with 95 % O_2, 5 % CO_2, at a pH 7.3. Slices were then transferred to a submerged recording chamber mounted on the stage of an upright microscope (Axioskop 2FS, Zeiss, Jena, Germany), secured under a nylon mesh, and continuously perfused with oxygenated ACSF at a rate of ~5 mL/min at 34±1 °C.

Neurons were visualised using a 60× immersion objective (Olympus) coupled with infrared and differential interference contrast optics linked to a video camera (CCD Camera

Orca R2, Hamamatsu, Japan). Somatic whole-cell patch-clamp recordings were made from visually identified BLA or DRN cells. Patch recording electrodes were pulled (DMZ puller; Zeitz-instrumente GmbH, Munich, Germany) from borosilicate glass capillaries (GC120F, 1.2 mm outer diameter, Clarke Electromedical Instruments, Reading, UK) and filled with a filtered solution consisting of (in mM): 140 K-gluconate, 4 KCl, 4 ATP-Mg, 0.3 GTP-Na2, 10 Na2-phosphocreatine, 10 HEPES and 0.5 % w/v biocytin, osmolarity 270–280 mOsmol/L without biocytin, pH 7.3 adjusted with KOH. Patch electrode resistance was 4-6 MΩ. Electrophysiological signals were amplified (EPC9/2 amplifier; HEKA Electronik), acquired using Patchmaster software (HEKA Electronik), low pass filtered at 2.9 kHz, and digitised at 5 or 10 kHz. Recordings were accepted only when the initial seal resistance was greater than 2 GΩ and the series resistance (22.8 ± 0.9 MΩ, range: 11-26 MΩ) did not change by more than 20% throughout the recording. No correction was made for the junction potential between the pipette and the ACSF (14 mV).

Patch-clamp recordings were targeted at the BA subdivision of the BLA, because the BA had the densest ChR2/YFP positive (ChR2/YFP+) projections from the DRN (see later). During light stimulation protocols in voltage clamp mode, PNs were held at -70 mV to test for the presence of fast and slow excitatory postsynaptic currents (EPSCs) and then at -50 mV to monitor both slow 5-HT-evoked inhibitory postsynaptic currents (IPSCs) and spontaneous IPSCs (sIPSCs). The INs were always held at -70 mV, because this allowed study of the kinetics of 5-HT-mediated slow IPSCs and EPSCs at the same time. Importantly, it was verified in a subset of cells (n=8/8) that neurons displaying a significant 5-HT_{1A}-mediated slow IPSCs at -50 mV (see below for criteria of significance) also displayed a significant slow IPSC at -70 mV. This suggests that the holding potential is unlikely to have affected the relative distribution of response types in INs (Figure 5.4A).

Photoexcitation of ChR2-expressing 5-HT afferents in the BLA was performed using an optoLED system (Cairn Research), consisting of 3.5 W LED mounted on a Zeiss Axioskop 2 FS microscope, which delivered pulses of light (470 nm) of 3-5 ms duration and 8 mW/mm2 intensity. The spot size corresponded to the area of slice visualised with a 60×

objective. Single light pulses were delivered at 20 s intervals and repeated at least 10 times. Light stimulation trains consisted of 5 or 30 s trains of light pulses delivered at 1, 10, or 20 Hz. To avoid adaptation of responses due to receptor desensitisation, 10 min. intervals were allowed between subsequent 30s trains.

5.2.4 Data analysis

Analyses of synaptic currents and intrinsic membrane properties were performed using IGOR Pro (Wavemetrics Inc.) and MATLAB (Mathworks, Inc.). The rheobase (pA) was determined as the 50 ms current injection able to generate a spike in 50% of the cases out of ten trials. Instantaneous firing rate (Hz) was defined as the number of action potentials evoked during a 1 s-long depolarizing current pulse of twice the amplitude of the rheobase current. Adaptation index (range: 0-1) was defined as the ratio between the first and last inter-spike interval (ISI, ms) elicited by the same current pulse used to measure instantaneous firing rate. Coefficient of variation of the ISI was calculated from the instantaneous firing rate and was the ratio of the ISI standard deviation and ISI mean.

BA PNs were distinguished from INs according to the following electrophysiological parameters, in line with previous reports (Sosulina et al., 2006; Bocchio et al., 2015): 1) smaller amplitude of fast after-hyperpolarisation and prominent medium after-hyperpolarisation from the second spike in an instantaneous firing rate protocol; 2) adapting ISIs; 3) instantaneous firing rate <20 Hz; 4) lower input resistance (<150 MΩ); 5) longer spike half-width (~1 ms). INs were divided into fast-spiking and non-fast spiking categories according to previous electrophysiological criteria (Rainnie, 1999; Ascoli et al., 2008), with minor adaptations. Specifically, fast-spiking INs had instantaneous firing rates of ≥50 Hz, an adaptation index of ≥0.4, a coefficient of variation of the ISI of <0.8 and a spike half-width of 0.33 ± 0.01 ms, while non-fast spiking neurons had instantaneous firing rates of <50 Hz, an adaptation index of <0.4, a coefficient of variation of the ISI of ≥0.8 and a spike half-width of 0.51 ± 0.03 ms.

Postsynaptic currents were considered significant only if their amplitude was at least two standard deviations above or below the mean baseline current. Current amplitudes were calculated from the difference between the peak and mean baseline current. sIPSCs were detected using TaroTools toolbox for Igor Pro (https://sites.google.com/site/tarotoolsregister). At the end of recordings, some slices were fixed overnight at 4°C in 4 % PFA and 15 % saturated picric acid in 0.1 M PB. After 24 h, slices were embedded in gelatin and re-sectioned (60 µm) with a VT-1000 vibrating microtome (Leica).

5.2.5 Immunohistochemistry

Sections containing biocytin-filled neurons were stained with Cy3-conjugated streptavidin (1:1000-3000, Life Technologies) and visualised using an epifluorescence microscope (AxioImager M2, Zeiss). Confocal stacks of axonal and dendritic fields of labeled neurons were acquired using a laser-scanning confocal microscope (LSM 510, Zeiss).

For immunohistological analysis, mice were perfused transcardially with 0.1 M phosphate buffer (pH 7.3) followed by a fixative solution containing 4% PFA and 15% (v/v) saturated picric acid in 0.1 M phosphate buffer (pH 7.3). Brains were extracted, post-fixed overnight at 4 °C in the same fixative solution, and coronal sections (60 µm) were cut with a VT-1000 vibrating microtome (Leica). Sections were stained with the following antibodies: goat anti-5-HT (1:500 dilution; Immunostar, cat no. 20079), which was visualised with a DyLight 594–conjugated secondary antibody (1:500 dilution; Abcam, cat no. ab96937); rabbit anti-5-HT (1:2500 dilution; kindly provided by Prof. Harry Steinbusch, Maastricht University, the Netherlands), which was visualised with a Cy3-conjugated secondary antibody (1:500 dilution; Jackson Immunoresearch, cat no. 711-165-152); and guinea pig anti-VGLUT3 (1:250 dilution; kindly provided by Prof. Masahiko Watanabe, Hokkaido University Graduate School of Medicine, Sapporo, Japan), which was visualised with the same Cy3-conjugated secondary antibody. To strengthen the endogenous ChR2/YFP

fluorescence (ChR2/YFP+), sections were stained with a chicken anti-GFP antibody (1:1000 dilution; Aves Labs) and Alexa 488-conjugated secondary antibody (Jackson Immunoresearch, cat. no. 703-545-155).

5.2.6 Quantification of 5-HT immunoreactive ChR2/YFP-transfected neurons

To quantify the percentage of ChR2/YFP+ neurons in the DRN that also expressed 5-HT, three evenly spaced coronal sections (rostro-caudal coordinates approximately -5 to -4.3 mm from bregma; from the Franklin and Watson (1997) atlas) were selected and a region of interest within the DRN was defined using a 5× 0.16 NA objective lens. Series of tiled stacked images (10 μm depth) were acquired using a 40× 1.3 NA oil-immersion objective and with 1 μm steps. Counting was performed offline using StereoInvestigator (MBF Bioscience). A neuron was counted only if its immunopositive nucleus came into focus in the optical section. Nuclei already in focus at the top optical section were not counted (West, 1999). Data were exported to Excel (Microsoft) and pooled for further analysis.

5.2.7 Drugs

NBQX, APV, WAY-100635, SR 95531 and CGP54626 were obtained from Tocris Biosciences (UK). Kynurenic acid and MDL-100907 were obtained from Sigma-Aldrich (UK).

5.2.8 Statistical analysis

For electrophysiological data, distributions passing the Shapiro-Wilk test for normality were compared using Student's t-tests. Distributions that did not pass this test were compared using non-parametric tests (Mann Whitney U test, Wilcoxon matched-pairs signed rank test). Comparisons between light stimulation trains of different frequencies were performed with ANOVAs and Bonferroni post-hoc tests. Correlations of response amplitudes

were quantified using Pearson's correlation coefficient. Effects of photoexcitation on firing rate were analysed with Dunnett's multiple comparisons test. Statistical analysis was performed with SPSS (IBM) or GraphPad Prism (Graphpad Software, Inc.).

5.3 Results

5.3.1 Selective targeting of ChR2 expression to 5-HT neurons

To control 5-HT axons arising from the DRN and projecting to the BLA, a viral vector carrying a floxed ChR2 and tagged with YFP was stereotaxically injected into the DRN of SERT-Cre mice (Figure 5.1A). Three weeks after injection of the viral vector, fluorescent microscopy analysis revealed an abundance of ChR2/YFP+ cell bodies within the DRN (Figure 5.1B) that were 5-HT+ (Figure 5.1C). Expression of ChR2/YFP+ was highly targeted in that 100% of ChR2/YFP+ cells (98.7 ± 22.5 ChR2+ cells counted per brain, n=3 brains) were also 5-HT+. Two weeks after injection of the viral vector, the functionality of ChR2 expression was tested by whole-cell patch-clamp recordings from ChR2/YFP+ DRN neurons. Stimulation with pulses of light at 20 Hz reliably evoked inward currents in voltage clamp mode as well as action potentials in current clamp mode (Figure 5.1D), demonstrating selective light-gated control of DRN 5-HT neuron activity.

After four weeks from the injection of the viral vector, brains of SERT-Cre mice displayed a widespread distribution of ChR2/YFP+ fibres, including an extensive innervation of the BLA (Figure 5.1E, F). The expression pattern of ChR2/YFP in the BLA largely overlapped with that of 5-HT (Figure 5.1F), with ChR2+/YFP+ axons being immunoreactive for 5-HT (Figure 5.1G). Since the BA subdivision of the BLA displayed a particularly dense innervation by ChR2/YFP+ fibres compared to the LA (Figure 5.1E, F), subsequent electrophysiological recordings were performed in the former region.

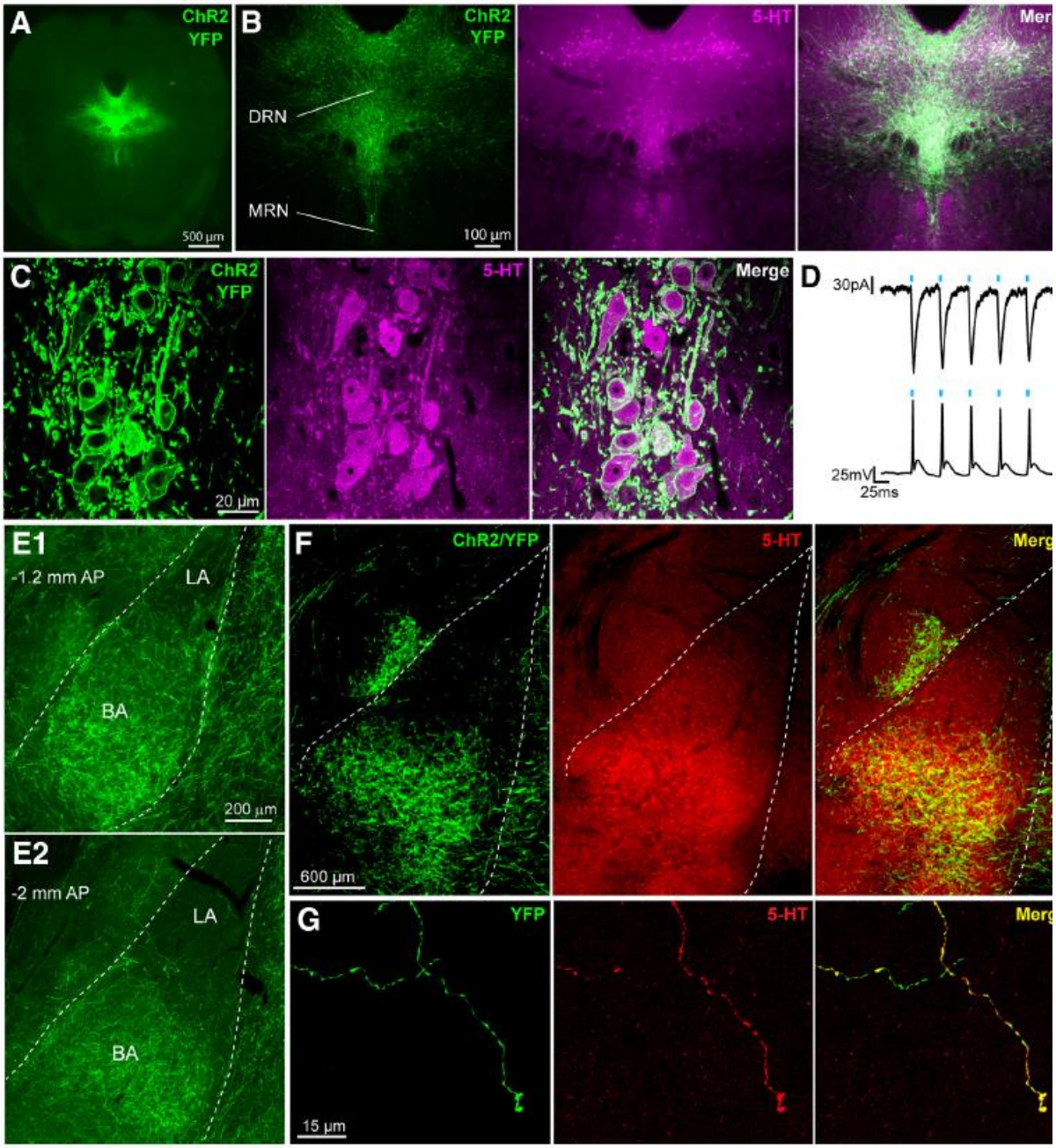


Figure 5.1 - Expression of ChR2 in DRN 5-HT neurons

A. Cre-dependent expression of ChR2/YFP in the DRN of SERT-Cre mice. **B.** Overlap between ChR2/YFP and 5-HT expression in the DRN and lack of ChR2/YFP expression in the median raphe nucleus (MRN). **C.** Maximum-intensity projection (z-stack: 4.2 µm, 0.21 µm optical sections) showing expression of ChR2/YFP in the membrane of 5-HT + DRN neurons. **D.** Light pulses (5 ms) delivered at 20 Hz evoke inward currents in voltage clamp (top) and action potentials in current clamp (bottom) in a DRN neuron expressing ChR2/YFP. **E.** ChR2/YFP+ axons innervating the anterior (E1) and posterior BLA (E2); the BA shows a denser innervation than the LA. *AP* – anteroposterior distance from bregma. **F.** Overlap between 5-HT and ChR2/YFP expression in the BLA. **G.** Representative image showing a 5-HT+ axon in the BA that also expresses ChR2/YFP.

5.3.2 Responses evoked in BA INs upon photoexcitation of DRN-BA 5-HT projections

Patch-clamp recordings were carried out to investigate the mechanisms by which 5-HT axons originating from the DRN influence neurons within the BA microcircuit. BA INs were distinguished from PNs using electrophysiological criteria (see Materials and methods), and the validity of these criteria was confirmed by post hoc histological analysis of cells (six of each type) filled with biocytin. In all cases, putative INs had the expected small, ovoid somata, spine-sparse dendrites, and axons which branched profusely within the BLA (Figure 5.2A). In contrast, putative PNs had larger, pyramidal-shaped somata, thick spiny dendrites, and axons that often projected outside the BLA (Figure 5.5A). Since previous electrophysiological studies suggested that locally applied 5-HT preferentially depolarises BA INs (Rainnie et al., 1999; Jiang et al., 2009; Bocchio et al., 2015), initial experiments investigated the effect of 5-HT neuron photoexcitation on this cell population.

Single pulses of light (20 s intervals) elicited fast onset EPSCs, an effect observed in just over half (55%) of the INs tested (n=59). Slow synaptic responses to single light pulses were not detected. Given the regular occurrence of this effect, and the relative paucity of ionotropic 5-HT_3 receptors in the BLA (Mascagni and McDonald, 2007), a 5-HT mechanism seemed unlikely. Indeed, these light-activated fast EPSCs were completely abolished by the combined application of NBQX (10 μM) and APV (50 μM), selective antagonists of AMPA/kainate and NMDA receptors, respectively [Wilcoxon matched-pairs signed rank test, W=-45, p=0.004, n=9] (Figure 5.2B, C). In contrast, the EPSC amplitude was not altered by the 5-HT_3 receptor antagonist MDL-72222 (20 μM, n=2, data not shown). These results suggest that low-frequency stimulation of 5-HT terminals in the BA preferentially released glutamate over 5-HT to mediate ionotropic glutamate receptor-mediated excitation of BA INs. Consistent with the release of glutamate from BA 5-HT axons, immunohistochemical experiments detected expression of the vesicular glutamate transporter 3 (VGluT3) in ChR2/YFP+ axonal varicosities in the BA, although this co-localisation was relatively sparse (Figure 5.2F, G).

Next, the sensitivity of the glutamate-mediated fast EPSC to increasing stimulation frequencies (1, 10 and 20 Hz) was tested. Greater light pulse number and higher stimulation frequency led to depression of fast EPSC amplitude [repeated-measures two-way ANOVA; main effect of light pulse no. $p<0.001$, main effect of stimulation frequency $p<0.001$; light pulse no. × stimulation frequency interaction $p<0.001$; $n=7$ cells]. Pairwise comparisons revealed that the response amplitude was significantly reduced from the first to the second light pulse at all three stimulation frequencies, but only at 20 Hz was there a decrease from the second to the last light pulse [Bonferroni's *post hoc* comparisons: at 1 Hz stimulation frequency, first vs. second light pulse $p<0.001$, first vs. last light pulse $p<0.001$; at 10 Hz stimulation frequency, first vs. second light pulse $p<0.001$, first vs. last light pulse $p<0.001$; at 20 Hz stimulation frequency, first vs. second light pulse $p<0.001$, second vs. last light pulse $p<0.001$, first vs. last light pulse $p<0.001$]. Pairwise comparisons also showed that the response amplitude at the three stimulation frequencies were significantly different from each other, with the greatest response amplitude at 1 Hz and the lowest at 20 Hz [Bonferroni's *post hoc* comparisons: last light pulse, 20 Hz vs. 10 Hz $p=0.003$, 10 Hz vs. 1 Hz $p=0.001$, 20 Hz vs. 1 Hz $p<0.001$] (Figure 5.2D, E). These data suggest that the strength of glutamate-mediated excitation of INs by 5-HT neurons is greatest at lower firing rates of 5-HT neurons.

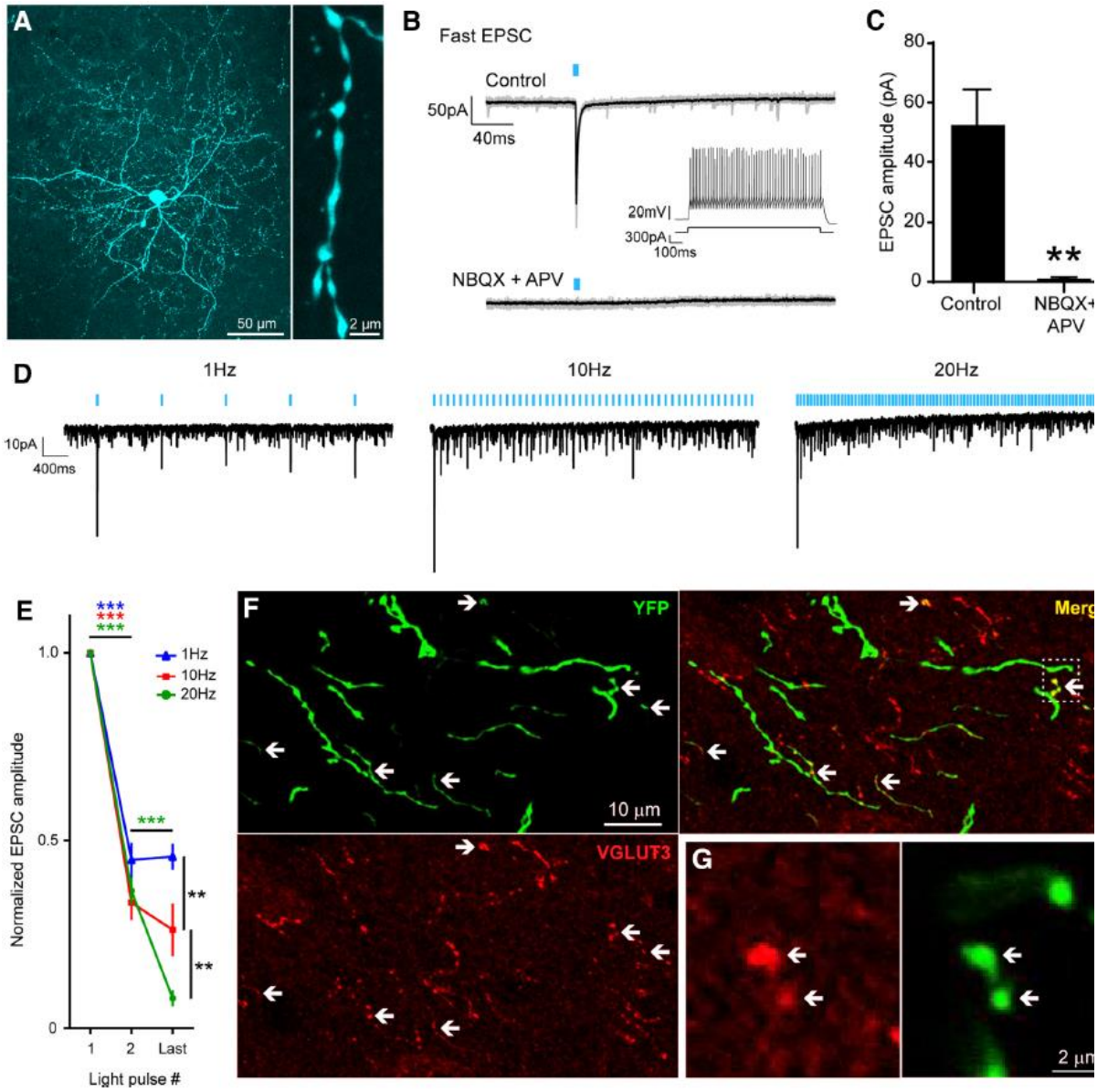


Figure 5.2 - 5-HT neurons release glutamate onto BA INs

A. Representative biocytin-filled BA IN showing a dense local axon (left) and a spiny dendrite (right). **B.** Example of a voltage-clamp (-70 mV) trace from a BA IN showing a fast EPSC evoked by a single light pulse (3 ms) photoexcitation of DRN axons (top); the fast EPSC is blocked by AMPA/kainate and the NMDA receptor antagonists NBQX (10 µM) and APV (50 µM; bottom). Black traces are the average of 10 individual traces, which are shown in gray. Inset, Firing pattern of a BA IN exhibiting the light-evoked fast EPSC. **C.** Fast EPSC evoked in BA INs is blocked by NBQX and APV (n=9). **D.** Example of a voltage-clamp (-70 mV) trace from a BA IN showing frequency-dependent depression of the fast glutamatergic EPSCs evoked by light trains (5 s) at 1 Hz (left), 10 Hz (middle), and 20 Hz (right). Traces shown are an average of five individual traces. **E.** Stimulation frequency-dependent depression of the second and last fast glutamatergic EPSC amplitudes normalised to the first EPSC amplitude for each cell. The depression of the last EPSC increases with higher stimulation frequencies (n=7). **F.** Maximum intensity projection (z-stack: 5.18 µm) showing sparse expression of VGLUT3 in 5-HT neuron axons (YFP+) in the BA. Arrows highlight YFP+/VGLUT3+ boutons. **G.** Magnification of the area framed in *F*. Single optical section (0.43 µm thickness) showing two YFP+boutons immunopositive for VGLUT3. Data are expressed as means ± SEM. *p<0.05; **p<0.01; ***p<0.001.

Since single pulses of light did not evoke any detectable non-glutamate-mediated response in BA INs, further experiments tested the effect of photoexcitation of 5-HT neurons

under conditions when glutamatergic transmission was blocked with kynurenic acid (3 mM). Notably, under these conditions light application at a higher frequency (20 Hz) evoked both excitatory and inhibitory effects in the form of slow EPSCs and IPSCs, which were significantly different from baseline in 53% and 37% of INs tested, respectively (Figure 5.3A, D). The slow EPSC outlasted the duration of the stimulation train, and was blocked by the selective 5-HT_{2A} receptor antagonist MDL-100907 (150 nM) [paired t-test, $t(8)=4.588$, $p=0.002$, $n=9$] (Figure 5.3B). In comparison, the slow IPSC declined before the end of the stimulation train, and was blocked by the selective 5-HT_{1A} receptor antagonist WAY-100635 (1 μM) [paired t-test, $t(6)=0.263$, $p=0.039$, $n=7$] (Figure 5.3E). Thus, light-activated release of 5-HT can both excite and inhibit BA INs, via 5-HT_{2A} and 5-HT_{1A} receptors, respectively.

Next, the sensitivity of these slow 5-HT-mediated responses to stimulation frequency was tested (1, 10 and 20 Hz). The peak amplitudes of both the slow EPSC [repeated measures one-way ANOVA; main effect of frequency, $F(2,10)=2.281$, $p<0.001$; Bonferroni's *post hoc* comparisons: 1Hz vs. 10Hz $p=0.037$, 10 Hz vs. 20 Hz $p=0.014$, 1Hz vs. 20Hz $p=0.002$; $n=6$] and slow IPSC [repeated measures one-way ANOVA; main effect of frequency, $F(2,8)=2.549$, $p=0.004$; Bonferroni's *post hoc* comparisons: 1 Hz vs. 20 Hz $p=0.027$; $n=7$] increased with higher frequencies of stimulation (Figure 5.3C, F), suggesting that, in contrast to glutamate signalling, the strength of 5-HT-mediated signalling onto BA INs is greatest at higher frequency firing of 5-HT neurons.

In a subset of INs demonstrating both fast glutamatergic EPSCs and slow 5-HT_{1A} receptor-mediated IPSCs, 20 Hz photoexcitation was delivered without pharmacological blockade of glutamatergic transmission. This allowed examination of the relationship between glutamate and 5-HT release during the 20 Hz train. While at the beginning of the 20 Hz train glutamatergic EPSCs were predominant, subsequent light pulses resulted in depression of the glutamatergic EPSCs and an increase in amplitude of the 5-HT_{1A} receptor-mediated IPSC, leading to a greater balance between glutamatergic and 5-HT transmission (Figure 5.3G, H). These data suggest that the firing of DRN 5-HT neurons can dynamically shift the balance between glutamatergic and 5-HT modulation of BA INs.

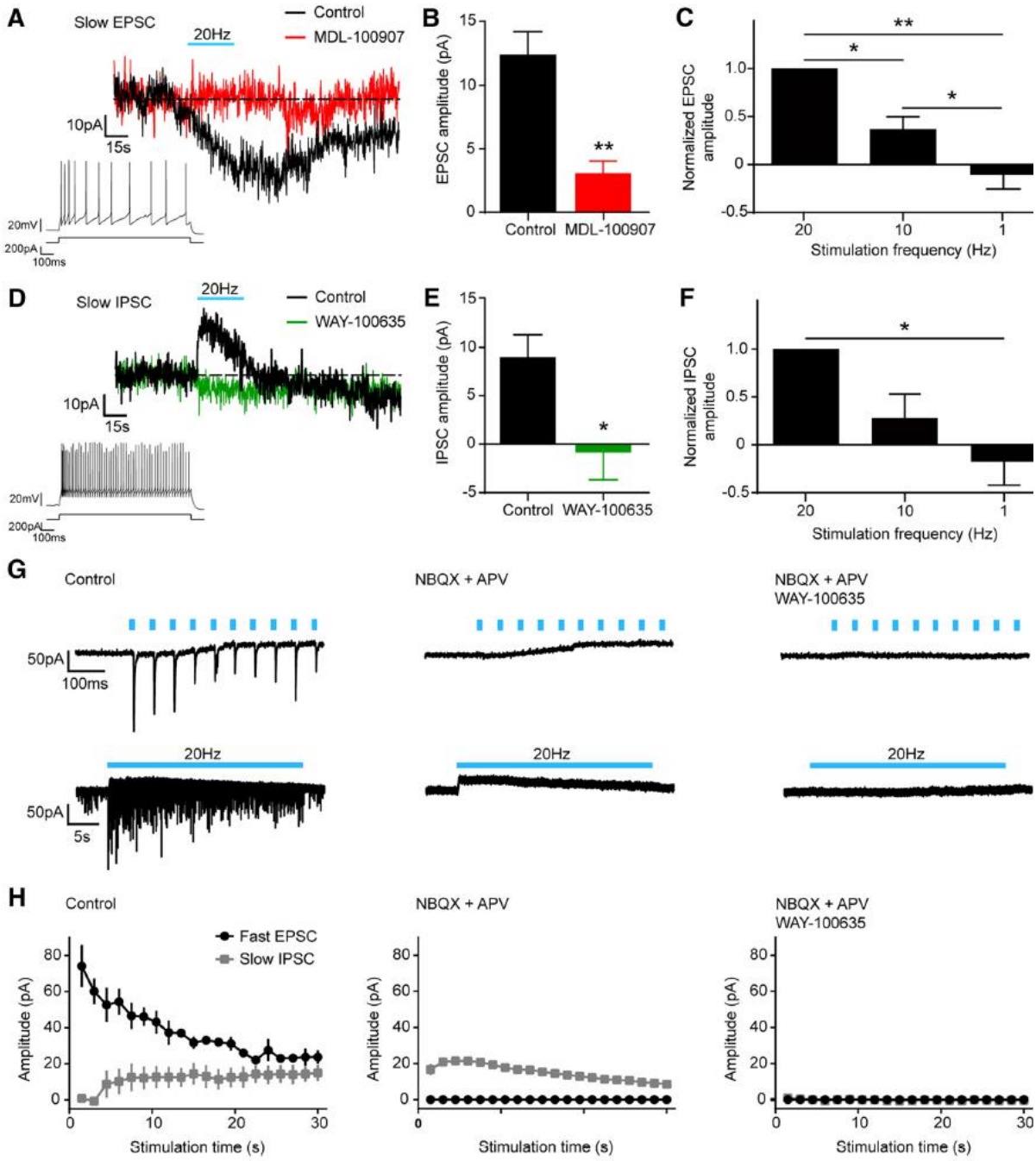


Figure 5.3 - 5-HT neurons modulate BA INs bidirectionally via 5-HT release

A. Example of a voltage-clamp (-70 mV) trace from a BA IN showing a slow EPSC evoked by 30 s photoexcitation at 20 Hz of DRN axons. The slow EPSC is blocked by the 5-HT_{2A} receptor antagonist MDL100907 (150 nM). Recordings were performed in the presence of the generic glutamate receptor blocker kynurenic acid (3 mM) to isolate slow responses. Inset, Example of a firing pattern of a BA IN exhibiting the light-evoked slow EPSC. **B.** Slow EPSC evoked in BA INs is blocked by the 5-HT_{2A} receptor antagonist MDL 100907 (1 µM, n=9). **C.** Slow EPSC amplitude is increased significantly by higher stimulation frequencies. Slow EPSC amplitudes are normalised to the amplitude evoked at 20 Hz stimulation frequency for each cell (n=6). **D.** Example of a voltage-clamp (-70 mV) trace from a BA IN showing a slow IPSC evoked by 30 s photoexcitation at 20 Hz of DRN axons. The slow IPSC is blocked by the 5-HT_{1A} receptor antagonist WAY-100635 (1 µM). Recordings were performed in the presence of the generic glutamate receptor blocker kynurenic acid (3 mM) to isolate slow responses. Inset, Example of a firing pattern of a BA IN exhibiting the light-evoked slow IPSC. **E.** Slow IPSC evoked in BA INs is blocked by the 5-HT_{1A} receptor antagonist WAY-100635 (1 µM, n=7). **F.** Slow IPSC amplitude is significantly increased by higher stimulation frequencies. Slow IPSC amplitudes are normalised to the amplitude evoked at 20 Hz stimulation frequency for each cell (n=5). **G.** Representative voltage-clamp (-70 mV) traces from a BA IN showing simultaneous fast EPSCs and a slow IPSC evoked by photoexcitation at 20 Hz (left), at short (first 10 light pulses, top traces) and long (entire 20 Hz train, bottom

traces) time scales. The fast EPSCs are blocked by AMPA/kainite and NMDA receptor antagonists NBQX (10 μM) and APV (50 μM; middle). Both the fast EPSCs and the slow IPSC are blocked by a combination of NBQX, APV, and WAY-100635 (right). **H.** Light-evoked fast EPSCs and slow IPSC co-occurring in BA INs (left, n=3) are blocked by glutamate receptor (middle, n=2) and 5-HT_{1A} antagonists (right, n=2), respectively. Data are expressed as means ± SEM. *p<0.05; **p<0.01.

5.3.3 Heterogeneity of BA IN responses to photoexcitation of DRN-BA 5-HT projections

Analysis of the response of each cell to photoexcitation of 5-HT neurons revealed that individual BA INs (n=59) displayed different combinations of glutamate-mediated fast EPSC, and 5-HT-mediated slow EPSC and IPSC (Figure 5.4A). Thus, some INs exhibited a response mediated by either glutamate alone (14%) or 5-HT alone (37%), whereas other INs demonstrated a mixture of the two (41%). Overall, the majority (84%) of INs tested were excited by 5-HT neuron activation (glutamate alone, 5-HT alone, or both), while a minority (8%) were solely inhibited (5-HT alone). Interestingly, the amplitude of the slow IPSC positively correlated with the amplitude of the fast EPSC [Pearson correlation coefficient, r^2=0.1727, p=0.001, n=59 cells], whereas the slow EPSC and fast EPSC did not [Pearson correlation coefficient, r^2=0.0439, p=0.111, n=59 cells] (Figure 5.4B). This suggests that those INs strongly excited by glutamate (at low 5-HT neuron firing frequencies) are also strongly inhibited by 5-HT (at high 5-HT neuron firing frequencies).

Interestingly, separation of data obtained from fast-spiking and non-fast-spiking INs revealed evidence of cell-specific effects of 5-HT neuron photoexcitation. Namely, fast-spiking INs showed larger amplitude fast EPSCs than non-fast-spiking INs [Mann Whitney U test, U=233.5, p=0.011, fast-spiking n=21, non-fast-spiking n=36] (Figure 5.4C, E). In addition, fast-spiking INs showed larger amplitude slow IPSCs compared to non-fast-spiking INs [Mann Whitney U test, U=242.5, p=0.009, fast-spiking n=21, non-fast-spiking n=36], whereas the amplitude of slow EPSCs did not differ [Mann Whitney U test, U=338.0, p=0.492, fast-spiking n=21, non-fast-spiking n=36] (Figure 5.4D, E). These data demonstrate that 5-HT neurons are more likely to recruit fast-spiking INs via the release of glutamate at low firing rates. In contrast, high rates of 5-HT neurons' firing appear to trigger primarily

excitation in non-fast-spiking INs and biphasic inhibition-excitation in fast-spiking INs via 5-HT.

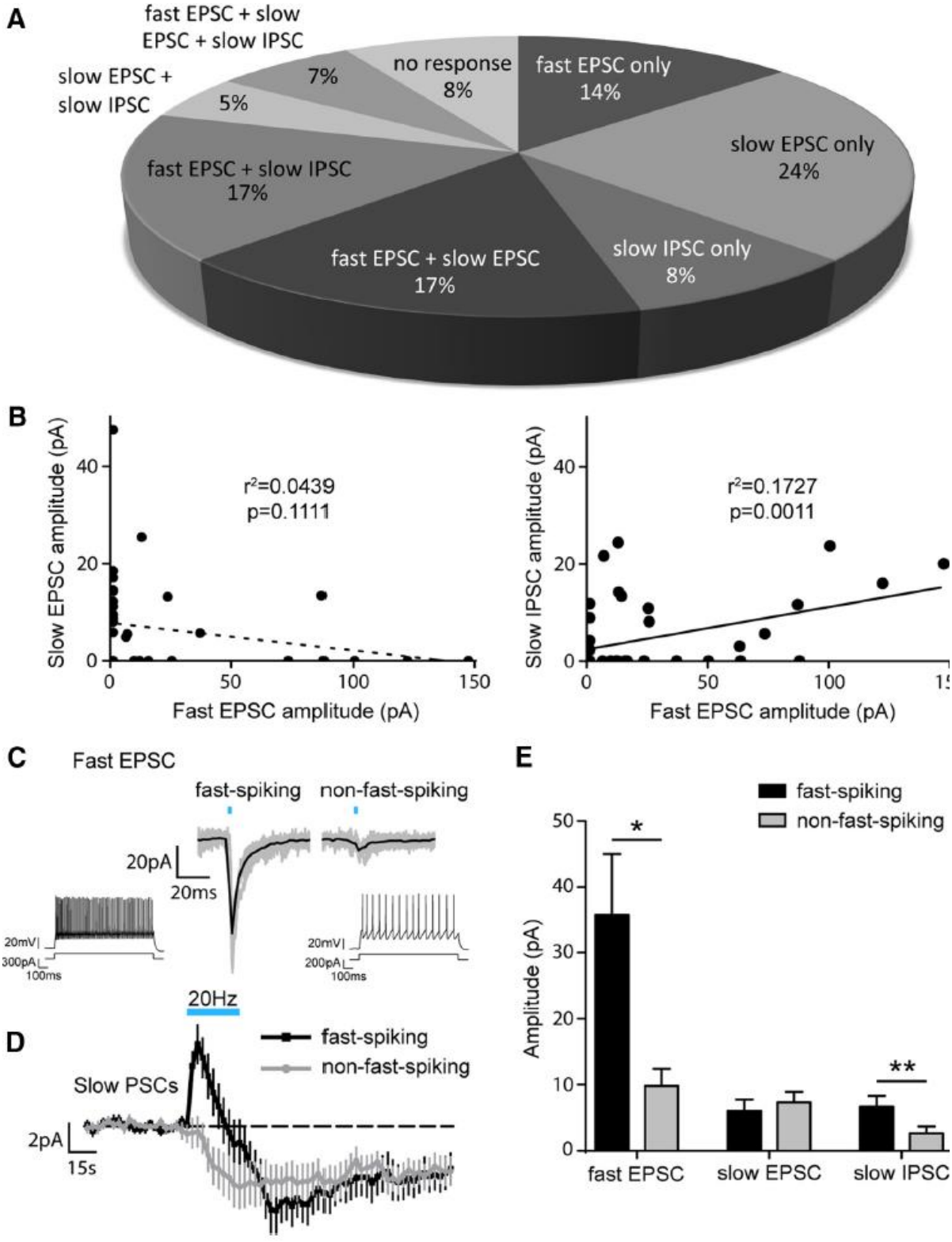


Figure 5.4 - 5-HT neurons differentially modulate BA INs

A. Relative distribution (as a percentage) of response types in BA INs evoked by either single pulses (fast EPSC) or trains (slow EPSC and IPSC) of photoexcitation of DRN axons (n=59). **B.** No correlation between amplitudes of the fast EPSC and slow EPSC responses evoked in BA INs (n=59; left). Positive correlation between amplitudes

of the fast EPSC and slow IPSC responses evoked in BA INs (n=59; right). **C.** Example of voltage-clamp (-70 mV) races showing a larger fast EPSC evoked in a fast-spiking (left) than in a non-fast-spiking (right) BA IN by a single light pulse (3 ms) photoexcitation of DRN axons. Inset, Example of firing patterns of a fast-spiking (left) and a non-fast-spiking (right) BA IN. **D.** Mean voltage-clamp (-70 mV) traces from fast-spiking and non-fast-spiking BA INs showing similar amplitudes of the slow EPSC but different amplitudes of the slow IPSC evoked by 30 s photoexcitation at 20 Hz of DRN axons (fast-spiking n=21, non-fast-spiking n=36). **E.** Amplitudes of the fast EPSC and the slow IPSC, but not the slow EPSC, are greater in fast-spiking than in non-fast-spiking BA INs (fast-spiking n=21, non-fast-spiking n=36). Data are expressed as means ± SEM. *p<0.05; **p<0.01.

5.3.4 Responses evoked in BA PNs upon photoexcitation of DRN-BA 5-HT projections

A final set of experiments tested the influence of optical activation of 5-HT neurons on BA PNs (Figure 5.5A), which form the main output of this nucleus and convey information to other brain structures. In contrast to INs, single pulses of light did not evoke fast EPSCs in PNs (n=18), suggesting that glutamate-releasing 5-HT terminals do not target this cell type. However, as with some INs, a higher stimulation frequency (20 Hz) evoked a slow IPSC in BA PNs (Figure 5.5B). This response to photoexcitation of 5-HT neurons was 5-HT-mediated, since it was reduced by the selective 5-HT_{1A} receptor antagonist WAY-100635 (1 μM) [Wilcoxon matched-pairs signed rank test, W=-26. p=0.031, n=7] (Figure 5.5B, C), whereas combined $GABA_A$ and $GABA_B$ receptor blockade using SR 95531 (50 μM) and CGP54626 (5 μM) had no statistically significant effect [Wilcoxon matched-pairs signed rank test, W=-5. p=0.625, n=5] (Figure 5.5C). In contrast to INs, PNs demonstrated a uniform response to photoexcitation of 5-HT terminals, with 93% of PNs tested exhibiting a slow IPSC and the remainder displaying no response (Figure 5.5D).

Given that high-frequency stimulation of 5-HT terminals elicited 5-HT-mediated EPSCs in BA INs, an increase in sIPSC frequency in PNs was predicted (see also Rainnie, 1999; Jiang et al., 2009; Bocchio et al., 2015). Indeed, photoexcitation at 20 Hz increased sIPSC frequency in PNs [baseline vs. stimulation, Wilcoxon matched-pairs signed rank test, W=43, p=0.025, n=13] (Figure 5.5E, F). This effect was blocked by SR 95531 (50 μM) and CGP54626 (5 μM) [baseline vs. stimulation, Wilcoxon matched-pairs signed rank test, W=1, p>0.999, n=5] (Figure 5.5F), thereby demonstrating the GABAergic and di-synaptic origin of these events. This was confirmed by the action of the 5-HT_{1A} receptor antagonist WAY-

100635 (1 μM) that, as described above, abolished direct slow outward currents in INs. Consistent with this result, WAY-100635 tended to enhance, although not significantly, sIPSC frequency during stimulation compared to baseline [baseline vs. stimulation, paired t-test, t(6)=2.302, p=0.061, n=7] (Figure 5.5F). Increased sIPSC frequency therefore likely arose from 5-HT modulation of BA INs.

Finally, the impact of photoexcitation of 5-HT neurons on the firing of PNs was tested. To elicit firing in baseline conditions, positive rheobase current was injected into PNs in current clamp mode. Under these conditions, photoexcitation at 20 Hz caused a significant reduction in PN firing rate [repeated measures one-way ANOVA; main effect of stimulation time, F(6,42)=34.47, p=0.037; Dunnett's multiple comparisons test, baseline vs. 5 s p=0.026, baseline vs. 10s p=0.046, baseline vs. 15s p=0.041, n=8] (Figure 5.5G). Collectively, these observations suggest that the 5-HT input to the BA (at high firing rates) causes a direct 5-HT-mediated inhibition of PNs, as well as an indirect inhibition through increased GABAergic inputs from INs, leading to an overall decrease in output from the BA.

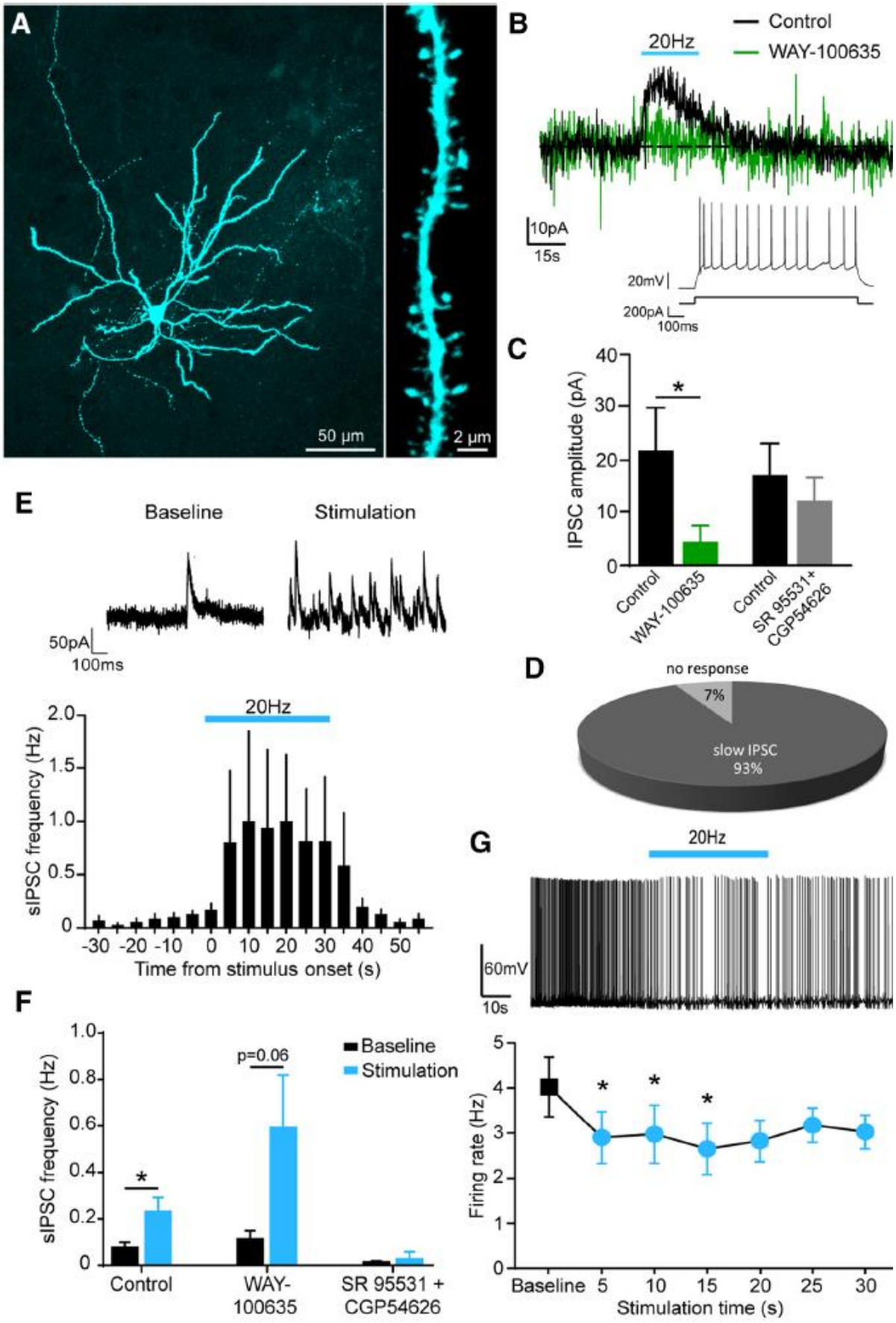


Figure 5.5 - 5-HT neurons inhibit BA PNs via 5-HT$_{1A}$ receptors and enhanced GABA release
A. Representative biocytin-filled PN showing a sparse axon with long-projecting branches (left) and spiny dendrites (right). **B.** Example of a voltage-clamp (-50 mV) trace from a BA PN showing a slow IPSC evoked by

30 s photoexcitation at 20 Hz of DRN axons, blocked by the 5-HT_{1A} receptor antagonist WAY-100635 (1 μM). Inset, Stereotypical firing pattern of a BA PN exhibiting the light-evoked slow IPSC. **C.** Slow IPSC evoked in BA PNs is blocked by the 5-HT_{1A} receptor antagonist WAY-100635 (1 μM; n=7), but not by the $GABA_A$ and $GABA_B$ receptor antagonists SR 95531 (50 μM) and CGP54626 (5 μM; n=5). **D.** Relative distribution (as a percentage) of response types in BA PNs evoked by photoexcitation of 5-HT axons (n =13). **E.** Example of a voltage-clamp (-50 mV) trace from a BA PN showing an increase in sIPSC frequency during 20 Hz photoexcitation of DRN axons (top). Mean PSTH showing an increase in sIPSC frequency in BA PNs during 30 s photoexcitation at 20 Hz of DRN axons (n=14; bottom) is shown. **F.** Increase in sIPSC frequency in BA PNs is blocked by the $GABA_A$ and $GABA_B$ receptor antagonists SR 95531 (50 μM) and CGP54626 (5 μM), but not the 5-HT_{1A} antagonist WAY-100635 (1 μM; control n=13; WAY 100635 n=7; SR 95531 and CGP54626 n=5). **G.** Top, Example of a current-clamp trace from a BA PN. Rheobase-positive current was constantly injected to evoke baseline firing. 30 s of photoexcitation at 20 Hz of 5-HT axons reduced the firing rate. Bottom, Firing rate of BA PNs is significantly reduced by photoexcitation at 20 Hz of 5-HT axons (n=8). Data are expressed as means ± SEM. *p<0.05.

5.4 Discussion

The current study investigated the action of physiologically released 5-HT on BA circuitry using a Cre-dependent construct that allowed selective optogenetic (ChR2) targeting of 5-HT neurons. Photoexcitation of 5-HT neurons elicited marked responses in BA neurons, which pharmacological analysis revealed to be mediated by a combination of 5-HT and ionotropic glutamate receptor-induced effects, suggesting 5-HT and glutamate co-release. Interestingly, this dual-transmitter signalling was separable in terms of stimulus frequency, with glutamate release occurring even at low frequencies, but 5-HT requiring higher frequencies. Furthermore, BA INs and PNs responded differently to 5-HT neuron photoexcitation, suggesting 5-HT and glutamate signals targeted distinct cell types. Overall, the effect of photoexcitation of the 5-HT input to the BA was PN inhibition and thereby dampened BA output.

5.4.1 Optogenetic control of 5-HT release

Expression of ChR2 in 5-HT neurons was achieved by delivering a viral vector carrying floxed ChR2 into the DRN of SERT-Cre mice (Zhuang et al, 2005). DRN ChR2-expressing cells were readily depolarised by pulses of light and were all 5-HT-immunoreactive, verifying the high efficiency and selectivity of this construct, as has been previously reported (Cohen et al., 2015; Li et al., 2016).

Consistent with targeted expression of ChR2 to 5-HT neurons, photoexcitation evoked 5-HT receptor-mediated responses in BA neurons. Specifically, a proportion of BA INs (53%) displayed a slow EPSC blocked by the 5-HT_{2A} antagonist MDL-100907, whereas some INs (37%) responded with a slow IPSC blocked by the 5-HT_{1A} antagonist WAY-100635. Conversely, photoexcitation evoked a 5-HT_{1A}-mediated IPSC in almost all (93%) PNs tested, as well as an increase in indirect GABA-mediated inhibition of PNs, likely caused by depolarisation of INs. Importantly, inhibition of PNs by 5-HT neurons was able to suppress PN firing.

These findings agree with previous pharmacological studies of the effect of bath-applied exogenous 5-HT on BA neurons. Bath-applied 5-HT evoked a 5-HT_{2A}-mediated depolarisation of INs that, in turn, led to increased sIPSC frequency in PNs (Rainnie, 1999; Jiang et al., 2009; Bocchio et al., 2015). Also, exogenous 5-HT evoked hyperpolarisation of a subset of PNs (Rainnie, 1999; Bocchio et al., 2015). In this regard, the main difference between the effect of optically-evoked and bath-applied 5-HT is the 5-HT_{1A}-mediated inhibition of some INs and virtually all PNs observed here using the optogenetic method.

Previous studies have emphasised the difference in time scale between pharmacological and optogenetic approaches, and the potential for activation of non-synaptic receptors by bath-applied transmitter (Unal et al., 2015). Furthermore, prior research has indicated that 5-HT_{1A} autoreceptors are strongly desensitised by pharmacological agonism over a time course of minutes or days (Harrington et al., 1994; Assie et al., 2006), but the current study found that the 5-HT_{1A}-mediated responses showed desensitisation within tens of seconds. Thus, bath application could fail to detect these slow IPSCs, though bath-applied 5-HT_{1A}-mediated effects have been reported in other amygdala regions (Bocchio et al., 2016a).

5.4.2 Release of glutamate from 5-HT neurons

A key finding of our study is that photoexcitation evoked fast EPSCs in BA INs, an effect inhibited by NMDA/AMPA/kainate receptor antagonists. Although earlier immunohistochemical studies report the localisation of ionotropic 5-HT_{3A} receptors on INs in the amygdala (Mascagni and McDonald, 2007), the optically-evoked fast excitation was completely abolished by glutamate receptor blockade, thereby ruling out any involvement of 5-HT. The absence of 5-HT_{3A}-mediated responses is in line with the sparse expression of this receptor in BLA INs (Mascagni and McDonald, 2007).

This is the first study that demonstrates evidence of glutamate and 5-HT co-release in the amygdala. In a recent study combining optogenetics and patch-clamp recordings in the bed nucleus of the stria terminalis (5-HTT-Cre plus ChR2), evidence of glutamate release from 5-HT terminals was not reported (Marcinkiewcz et al., 2016). In contrast, another study reported that photoexcitation of 5-HT neurons (Pet1-Cre plus ChR2) evoked fast glutamate and slow 5-HT receptor-mediated responses in the nucleus accumbens and ventral tegmental area (Liu et al, 2014). Moreover, a previous study reported evidence of 5-HT and glutamate co-release in the hippocampus, albeit using a ChR2 targeting approach that was non-5-HT-selective (Varga et al. 2009). The latter two reports accord with earlier electrophysiological evidence that cultured raphe 5-HT neurons release both 5-HT and glutamate (Johnson, 1994).

This functional evidence of glutamate and 5-HT co-release is supported by molecular evidence for co-localisation of VGLUT3 and 5-HT in DRN neurons in mice (Fu et al., 2010), as well as rats (Gras et al., 2002; Hioki et al., 2004) and humans (Vigneault et al, 2015). Furthermore, the current observation of VGLUT3 localisation in 5-HT (ChR2/YFP+) axons in the BA agrees with similar findings in other regions including cortex, hippocampus and striatum (Shutoh et al, 2008; Gagnon and Parent, 2014; Voisin et al, 2016).

Interestingly, it was observed that some BA INs exhibited responses mediated by either glutamate alone (14%) or 5-HT alone (37%), whereas other INs responded to

photoexcitation with a mixture of glutamate and 5-HT responses (41%). Since only 5-HT neurons were targeted optogenetically, this diversity of responses could arise from two mechanisms. Firstly, this signalling could be coded postsynaptically: Whether the signal is 5-HT- or glutamate-mediated would be determined by the receptors expressed at the postsynaptic target, and 5-HT terminals would release 5-HT and glutamate from the same boutons. Alternatively, this signalling could be coded presynaptically: 5-HT axons could segregate, completely or partially, glutamate- and 5-HT-containing vesicles within distinct boutons. This scenario is consistent with the relatively sparse co-expression of VGLUT3 in DRN 5-HT terminals, and with previous reports of rarely overlapping 5-HTT+ and VGluT3+ boutons in 5-HT axons (Amilhon et al., 2010). The ability to segregate 5-HT- and glutamate-releasing vesicles would be an example of 'co-transmission,' as previously suggested by Vaaga et al. (2014). Interestingly, co-transmission implies different calcium sensitivity for each neurotransmitter released (Ghijsen and Leenders, 2005), which is consistent with the present finding that glutamate- and 5-HT-mediated responses in the BA had differential sensitivity to stimulation frequency. One way to test this would be to photoexcite 5-HT terminals while manipulating external and intracellular calcium concentrations, in an attempt to abolish the 5-HT signal, presumably, while preserving the glutamate.

5.4.3 Frequency-dependent modulation of BA INs by 5-HT

As noted, the response of BA INs to glutamate had a different sensitivity to stimulation frequency compared to 5-HT responses. Specifically, glutamate-mediated fast excitations were observed at low stimulation frequencies (≤1 Hz) and response amplitudes diminished with increased stimulation frequency (10-20 Hz), potentially due to exhaustion of vesicular stores or glutamate receptor desensitisation. In contrast, 5-HT-mediated slow responses only emerged at the higher frequencies.

By examining glutamatergic EPSCs and 5-HT_{1A}-mediated IPSCs concurrently during 20 Hz stimulation trains, it was confirmed that the glutamatergic response was strong at the

beginning of the train, but depressed over time. Conversely, 5-HT responses were absent when initial light pulses were delivered, but increased over time. This suggests that both the firing rate and the duration of firing of 5-HT neurons are critical parameters controlling the balance between glutamate/5-HT transmission in BA INs.

Since many DRN 5-HT neurons fire in a manner that decreases with sleep and increases with arousal (Veasey et al., 1995; Sakai, 2011), 5-HT neurons may signal principally via glutamate during some behavioral states (for instance, sleep), at least in the amygdala. It is important to keep in mind that DRN 5-HT neurons generally fire at slow rates (0.5-5 Hz) (e.g. Allers & Sharp, 2003; Schweimer and Ungless, 2010; Sakai et al. 2011). Thus, prolonged 20 Hz photoexcitation may result in supraphysiological 5-HT accumulation and 5-HT receptor activation. However, significant 5-HT responses in BA neurons also at 10 Hz stimulation were observed. Furthermore, recent opto-tagging studies in awake mice suggest that the firing of DRN 5-HT neurons increases markedly (15-20 Hz, with individual 5-HT neurons firing at up to 60 Hz) in response to punishing or rewarding stimuli (Cohen et al., 2015; Li et al., 2016). The current data argue that 5-HT neurons signal such behaviors in the amygdala, and possibly other regions, via prominent 5-HT release.

Interestingly, fast- and non-fast-spiking BA INs demonstrated a differential response to photoexcitation of 5-HT neurons, suggesting cell-specific targeting; fast-spiking INs displayed greater fast glutamatergic excitation and 5-HT_{1A}-mediated inhibition than non-fast-spiking INs. Hence, slower firing rates (0.5-5 Hz) of 5-HT neurons, for instance during wakefulness, could favour glutamatergic recruitment of fast-spiking BA INs. In contrast, higher firing rates (15-60 Hz), for example during punishment/reward, may lead to more complex glutamate/5-HT modulation of fast- and non-fast-spiking INs. Though not in the scope of this study, future studies could determine how molecularly defined BA INs respond to low/high-frequency stimulation of 5-HT neurons. Importantly, the prominent 5-HT_{1A}-mediated inhibition of fast-spiking INs is in agreement with an immunohistochemical study showing expression of 5-HT_{1A} receptors on parvalbumin-expressing INs (Aznar et al., 2003), some of which are fast-spiking (Rainnie et al., 2006).

The present study did not establish whether similar rules of glutamate/5-HT co-transmission occur in the LA, which receives a sparse 5-HT innervation compared to the BA. Interestingly, VGLUT3 immunoreactivity is abundant in the BA, but not in the LA (Nickerson Poulin et al., 2007), suggesting that glutamate release by DRN 5-HT axons could be less prominent in this area, as also appears to be the case in the bed nucleus of the stria terminalis (Marcinkiewcz et al., 2016).

5.4.4 Functional implications

The vast majority of BA PNs (93%) were inhibited directly by 5-HT release, suggesting that the main effect of 5-HT transmission in the BA is the suppression of its glutamatergic output. The inhibitory action of 5-HT neurons on PN firing could have a profound impact on emotional behavior, because optogenetic inhibition of BLA PNs influences anxiety, fear learning and appetitive learning through different projection targets (Tye et al., 2011; Senn et al., 2014; Namburi et al., 2015).

However, the direct inhibition of PN firing might not be long-lasting, because the 5-HT_{1A}-mediated IPSCs decayed before the end of the photoexcitation, likely due to receptor desensitisation. This suggests that long-lasting modulation of BA PNs by DRN 5-HT neurons can only occur via 5-HT_{2A}-mediated (and potentially glutamate-mediated) depolarisation of INs, which leads to enhanced GABA release onto PNs. Overall, the present study suggests that DRN 5-HT neurons are able to fine-tune populations of BA INs across multiple timescales using firing rate, firing duration, and the different kinetics of glutamate, 5-HT_{1A} and 5-HT_{2A} receptors. This could result in redistribution of GABA release across different subcellular domains of BA PNs, a phenomenon that has been shown to influence emotional learning (Wolff et al., 2014).

5.4.5 Conclusions

In previous chapters, 5-HT projections to the BA have been shown functionally to regulate both fear behaviour and amygdala physiology. Here, evidence has been provided for the co-release of 5-HT and glutamate in the BA from DRN neurons. It is still unclear, however, how the two neurotransmitters might be recruited and whether one is more crucial than the other in fear behaviour. In the next chapter, the modulation of the BA by 5-HT neurons based on their neurochemical characteristics will be investigated.

Chapter 6 Neurochemical characterisation of basal amygdala modulation by 5-HT neurons during fear learning

6.1 Introduction

In earlier chapters, it was shown that 5-HT projections to the BA regulate both fear behaviour and amygdala physiology. In Chapter 5, mechanisms of BA modulation by 5-HT neurons were characterised. Specifically, co-release of 5-HT and glutamate from 5-HT terminals was demonstrated. This finding raised the possibility that 5-HT neurons influence fear through both 5-HT and glutamate transmission. In this chapter, the neurochemical characteristics of BA modulation by DRN projections are explored.

6.1.1 Neurochemical identities of DRN neurons

Neuromodulators such as 5-HT, dopamine, and noradrenaline have been implicated in the physiological regulation of amygdala circuits (Rainnie, 1999; Bissière et al., 2003; Tully et al., 2007; Bocchio et al., 2015). One source that provides neuromodulation to the amygdala is the DRN. Although more than half of DRN neurons produce 5-HT, DRN neurons also express other transmitters and peptides (Wiklund et al., 1981; Vasudeva et al., 2011; Gagnon and Parent, 2014), which remain less well defined, functionally.

The DRN and MRN are medial structures located ventrally to the cerebral aqueduct (Figure 6.1), and cells with distinct neurochemical identities often have particular topographical distributions within these nuclei, as shown in the images below. 5-HT neurons are distributed across the rostro-caudal range of the DRN and MRN (Figure 6.2; Steinbusch, 1981). They are located in all of the subnuclei of the DRN (Descarries et al., 1982), which reflects the fact that most DRN cells are 5-HT+ (Wiklund et al., 1981; Gagnon and Parent, 2014; but see also Descarries et al., 1982). Glutamatergic (VGluT3-expressing) neurons are more localised, extending medially from the dorsal to the ventral subnuclei of the DRN (Figure 6.3), and more highly concentrated in the middle and caudal rather than rostral DRN (Commons, 2009; Hioki et al., 2010). In contrast, GABAergic neurons are less medial, particularly present in the lateral wings and more sparsely distributed than 5-HT cells (Figure 6.4A, B; Stamp and Semba, 1995; Allers and Sharp, 2003; Day et al., 2004; Challis et al., 2013). For their part, dopaminergic (tyrosine hydroxylase- or dopamine transporter (DAT)-expressing) neurons seem to be less localised to certain DRN regions than glutamatergic and GABAergic cells (Figure 6.4C; Hasue and Shammah-Lagnado, 2002; Matthews et al., 2016).

The distributions described above do not take into account the additional factor that some DRN neurons are capable of co-transmission. For instance, medial 5-HT cells produce nitric oxide (Johnson and Ma, 1993) and a small minority co-express 5-HT and GABA (Johnson, 1994; Stamp and Semba, 1995; Day et al., 2004). A number of neuropeptides are also co-expressed in raphe neurons. For example, the neuropeptide substance P co-localises with both GABA and 5-HT (Chan-Palay et al., 1978; Hökfelt et al., 1978; Johansson et al., 1981; Magoul et al., 1986). Leucine-enkephalin, thyrotropin releasing hormone, and galanin are also each expressed in 5-HT cells (Glazer et al., 1981; Johansson et al., 1981; Melander et al., 1986). One study found three transmitters within individual raphe neurons, with co-localised 5-HT, substance P, and thyrotropin releasing hormone (Johansson et al., 1981). The co-expression that has been reported most often is that of 5-HT and VGluT3, markers of 5-

HT and glutamatergic transmission respectively (Gras et al., 2002; Hioki et al., 2004; Mintz and Scott, 2006; Shutoh et al., 2008; Commons, 2009).

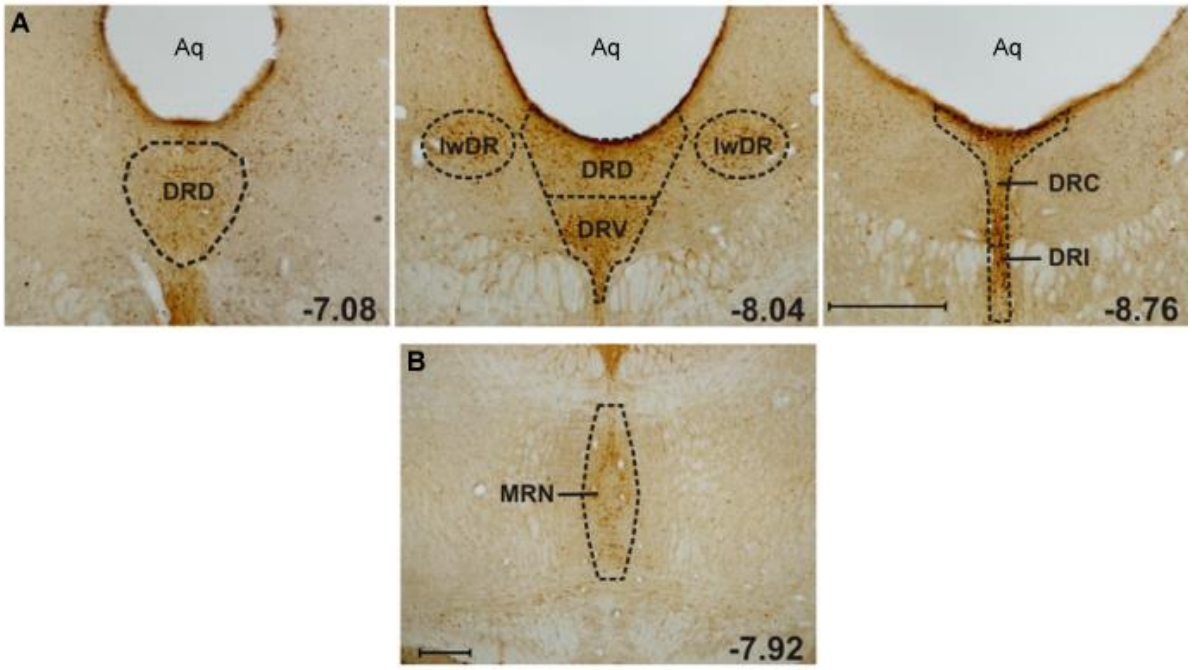


Figure 6.1 – Anatomy of the DRN and MRN
A. DRN (DR) in rostral (left), middle (middle), and caudal (right) coronal sections. **B.** MRN. Scale bars = 300 µm. *Aq* – aqueduct, *DRC* – DR DR caudal subnucleus, *DRD* – DR dorsal subnucleus, *DRI* – DR interfascicular subnucleus, *DRV* – DR ventral subnucleus, *lwDR* – DR lateral wings. Adapted from Spiacci et al. (2012).

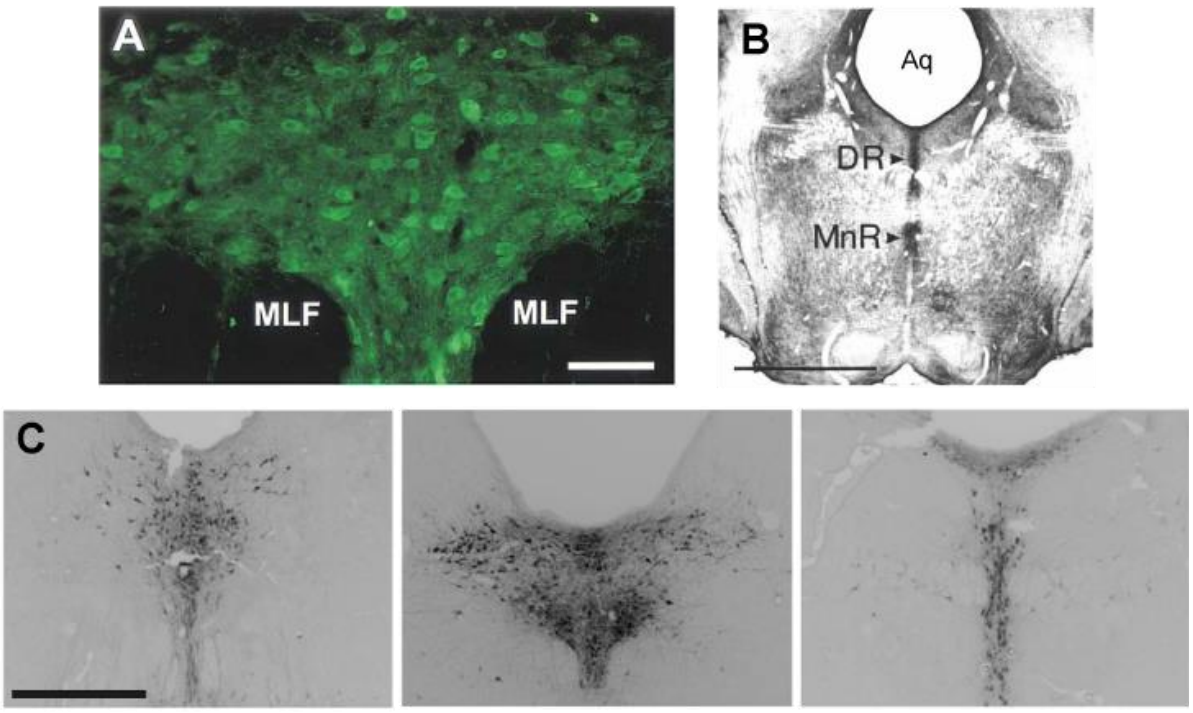


Figure 6.2 – 5-HT neurons in the DRN and MRN
A. 5-HT+ cells (green) in the DRN (DR). Scale bar = 100 µm. **B.** 5-HTT+ cells (black) in the DRN and MRN. Scale bar = 400 µm. **C.** Tph+ cells in the rostral (left), middle (middle), and caudal (right) DR. Scale bar = 1 mm.

Aq – aqueduct, *MLF* – medial longitudinal fasciculus. Adapted from Kirby et al. (2003) (**A**), Sur et al. (1996) (**B**), and Vasudeva et al. (2011) (**C**).

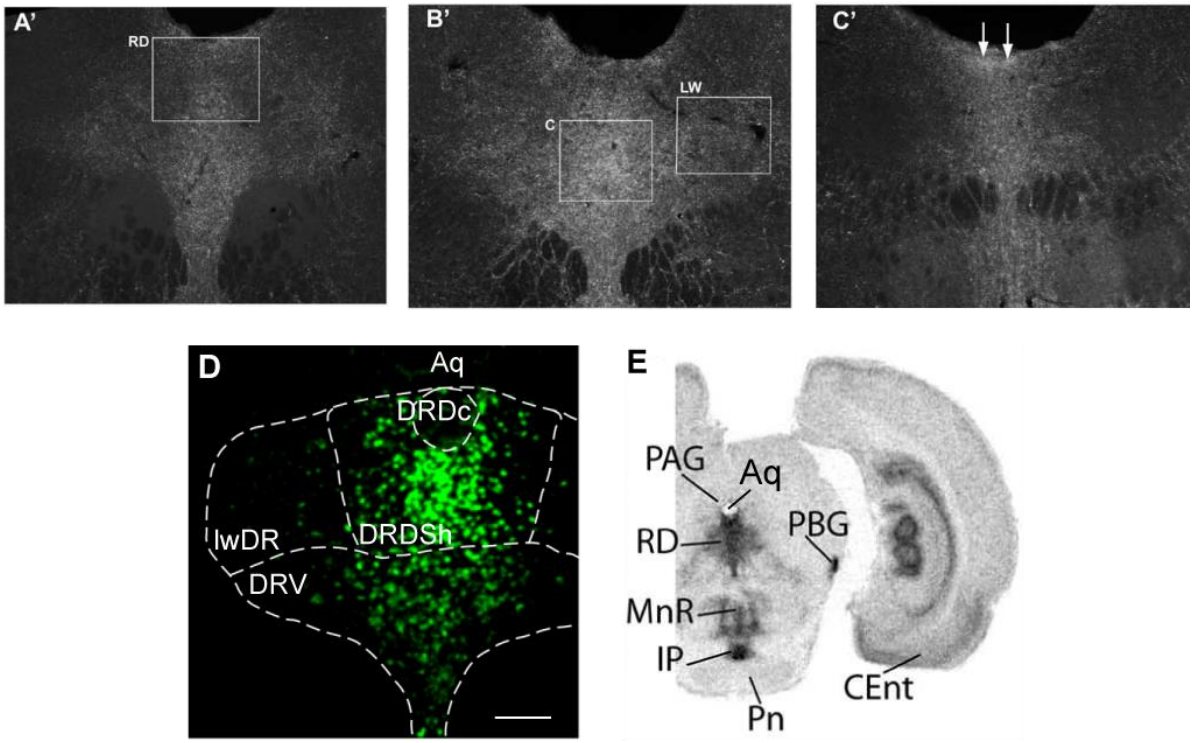


Figure 6.3 – Glutamate neurons in the DRN and MRN
A-C. VGluT3+ cells in the rostral (**A**), middle (**B**), and caudal (**C**) DRN. **D.** VGluT3 mRNA (green) in the DRN. Scale bar = 200 μm. **E.** VGluT3+ cells in the DRN and MRN. *Aq* – aqueduct, *C* – dorsal raphe centre, *CEnt* – entorhinal cortex, *DRDc* – dorsal raphe dorsal subnucleus core, *DRDSh* – dorsal raphe dorsal subnucleus shell, *DRV* – dorsal raphe ventral subnucleus, *lwDR* – dorsal raphe lateral wing, *IP* – interpeduncular nucleus, *LW* – dorsal raphe lateral wings, *MnR* – median raphe nucleus, *PAG* – periaqueductal grey, *PBG* – parabigeminal nucleus, *Pn* – pontine nucleus, *RD* – dorsal raphe nucleus. Adapted from Commons (2009) (**A-C**), Hioki et al. (2010) (**D**), and Herzog et al. (2004) (**E**).

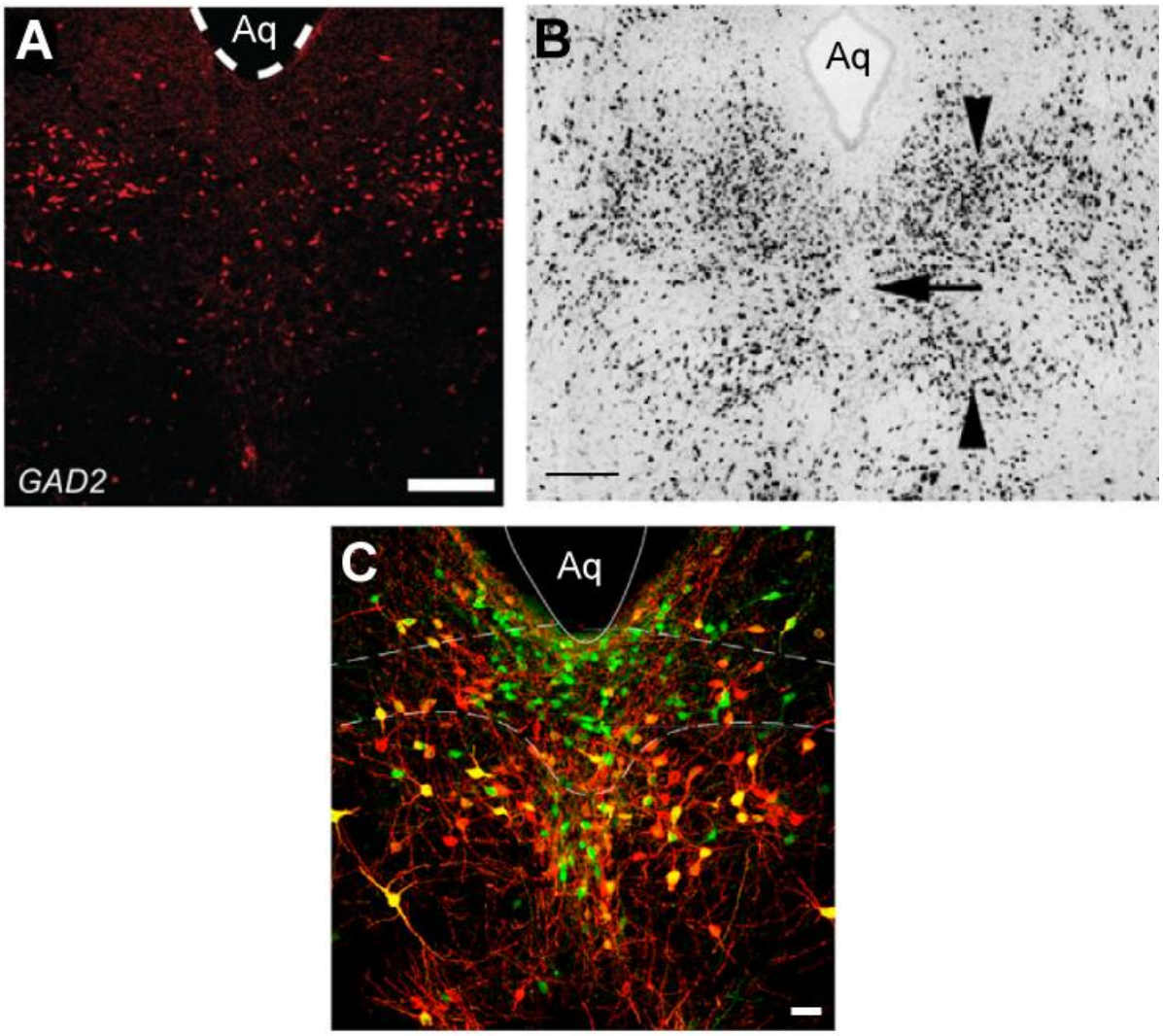


Figure 6.4 – GABA and dopamine neurons in the DRN
A. GAD2-tdTomato (red) cells (GABAergic) in the DRN. Scale bar = 50 μm. **B.** GAD2+ (black) cells (GABAergic) in the DRN. Scale bar = 400 μm. **C.** Tyrosine hydroxylase (TH)-GFP (green) and TH+ (red) cells (dopaminergic) in the DRN. Scale bar = 30 μm. *Aq* – aqueduct. Adapted from Challis et al. (2013) (**A**), Soiza-Reilly and Commons (2011) (**B**), and Matthews et al. (2016) (**C**).

6.1.2 Co-transmission of glutamate from 5-HT neurons

Previous studies have provided functional and molecular evidence for the co-release of glutamate from 5-HT neurons in general. About 60% of 5-HT cells grown in culture form glutamatergic synapses *in vitro* (Johnson, 1994). The proportion of glutamate-releasing neurons does not change over the course of several weeks in culture, suggesting that the co-release phenomenon does not develop in culture. In the previous chapter, glutamate co-transmission from 5-HT projections was observed in the BA. This has also been reported recently in the ventral tegmental area and nucleus accumbens (Liu et al., 2014).

In 5-HT neurons, glutamate is packaged into vesicles by the VGluT3 (Schäfer et al., 2002). VGluT3 shares its functional specificity for glutamate with VGluT1 and VGluT2, but displays an anatomical expression pattern that is highly distinctive. Unlike VGluT1 and VGluT2, which delineate excitatory PNs, VGluT3 is found in discrete GABA/glycinergic INs (Hioki et al., 2004; Gillespie et al., 2005), cholinergic neurons (Gras et al., 2008), and 5-HT neurons (Gras et al., 2002; Fu et al., 2010). In both rodents and humans, VGluT3 reflects a unique excitatory glutamatergic cell phenotype that is entirely separate from and less abundant than VGluT1/2-expressing fibres, and is thought to underlie glutamate co-transmission (Schäfer et al., 2002; Herzog et al., 2004; Hioki et al., 2004; Vigneault et al., 2015). In human brains, VGluT3 also demarcates a sparse population of neurons that is anatomically distinguished from VGluT1/2-expressing cells, as shown by *in situ* hybridisation and immunohistochemistry experiments (Vigneault et al., 2015). The DRN, in particular, expresses VGluT3 but not VGluT1/2. A subpopulation of 5-HTT-expressing neurons is immunoreactive for VGluT3, suggesting potential co-transmission also in human brains.

Although it is well-documented that some DRN neurons co-express VGluT3 and 5-HT markers, the exact degree of overlap is controversial (Soiza-Reilly and Commons, 2011). One *in situ* hybridisation study in rat brain sections observed complete overlap of 5-HTT and VGluT3 expression (Gras et al., 2002), whereas another reported only 80% of Tph2 cells co-expressing VGluT3 (Hioki et al., 2010). Rat immunostaining found almost all 5-HT+ DRN cells to be VGluT3+ in brain sections (Shutoh et al., 2008; Gagnon and Parent, 2014), but only slightly more than 50% in culture (Fremeau et al., 2002). Immunostaining in hamster brain sections showed that almost all 5-HT+ cells contain VGluT3 (Mintz and Scott, 2006). This is corroborated by the expression of glutaminase, a glutamate synthesising enzyme, which was detected in almost all 5-HT+ DRN cells using immunohistochemistry in rat brain sections (Kaneko et al., 1990). In contrast, immunocytochemistry in cultured mouse neurons containing 5-HTT revealed only 4% overlap with VGluT3 (Voisin et al., 2016). In 5-HT terminals, the degree of VGluT3 co-localisation varies across projection targets (Gagnon and Parent, 2014). On the other hand, a rat *in situ* hybridisation study found Tph2 in 80% of

VGluT3+ DRN cells (Hioki et al., 2010), whereas a mouse immunohistochemistry account reported only a small fraction of VGluT3+ cells being 5-HT+ (Kiyasova et al., 2011). Taken together, the evidence points towards some degree of VGluT3 co-expression in DRN 5-HT neurons, but the precise overlap may depend on species, detection method and projection target.

6.1.3 Ascending projections of the DRN

Both anterograde and retrograde tracing experiments have identified the DRN as a source of amygdala innervation (Azmitia and Segal, 1978; Jacobs et al., 1978; Abrams et al., 2005). This pathway, projecting from the DRN to the amygdala, is thought to largely comprise 5-HT neurons because 5-HT lesions significantly reduce the labelling of the pathway (Azmitia and Segal, 1978; Jacobs et al., 1978). This has been verified through retrograde tracing and immunostaining for 5-HT or Tph2, which confirms that the majority of DRN neurons projecting to the amygdala produce 5-HT (Ma et al., 1991; Fernandez et al., 2016).

DRN and MRN neurons expressing VGluT3 project to widespread anatomical targets, including the cortex, hippocampus, amygdala, medial septum, ventral tegmental area, substantia nigra, hypothalamus, suprachiasmatic nucleus, preoptic nuclei, and olfactory bulb (Shutoh et al., 2008; Jackson et al., 2009; Varga et al., 2009; Hioki et al., 2010; Yamakawa and Antle, 2010). In addition, GABAergic raphe projections directly inhibit prefrontal cortex neurons (Puig et al., 2005). Dopaminergic neurons from the DRN modulate the central amygdala and bed nucleus of the stria terminalis (Hasue and Shammah-Lagnado, 2002; Matthews et al., 2016). DRN cells projecting to the central amygdala and bed nucleus of the stria terminalis also contain neuropeptides, including vasoactive intestinal polypeptide, substance P, or leucine-enkephalin (Li et al., 1990; Petit et al., 1995). Thus, the neuromodulation exerted by the raphe nuclei is variegated and target-specific.

Since the neurochemical profiles of DRN projection pathways seem to differ depending on anatomical destinations, BA-projecting neurons may have their own, distinctive characteristics. Although most of the amygdala-projecting cells of the DRN are 5-HT+, a minority are not. Raphe nuclei send ascending non-5-HT projections to various structures across the brain, the amygdala being one of them (Aznar et al., 2004; Halberstadt and Balaban, 2008), but the non-5-HT projections to the BA, specifically, have not yet been characterised. It is known, however, that BA-projecting 5-HT neurons have unique electrophysiological properties that stand apart from those of prefrontal cortex- and hippocampus-targeting 5-HT neurons in the DRN (Fernandez et al., 2016). These characteristics are thought to facilitate rapid and transient neuromodulation of amygdala circuits during salient environmental events. Hence, in addition to outlining the neurochemical nature of BA regulation by DRN neurons, the modulation mechanisms functionally recruited during fear learning need to be dissected in a circuit-specific manner.

6.1.4 Aims of this chapter

In a histological investigation of the DRN to BA projection pathway, the current chapter considered some of the principal neuromodulators known to regulate amygdala circuits. First, neurochemical identities of DRN neurons targeting the BA were characterised using a retrograde tracer, immunohistochemistry (for 5-HT and glutamatergic neurons), and transgenic reporter mouse lines (for GABAergic and dopaminergic neurons). Next, the BA-targeting DRN cell types recruited during fear learning were studied by staining for immediate-early gene (c-fos) expression. Finally, given the glutamate co-transmission described in Chapter 5, optogenetic manipulations were combined with 5-HT receptor antagonism to evaluate the contribution of 5-HT signalling. The main goal was to verify whether DRN neurons can modulate the BA through transmitters other than 5-HT and, if so, whether the predominant regulation of the BA by the DRN during fear was through 5-HT release nonetheless.

6.2 Methods

6.2.1 Experimental animals

Glutamate decarboxylase (GAD2)-GFP mice were generated by crossing Cre-dependent ROSA(EGFP-L10a) males (B6;129S4-Gt(ROSA)26Sor<tm9(EGFP/Rpl10a)Amc>/J; JAX 024750) with GAD2-IRES-Cre+/- females (STOCK Gad2<tm2(cre)Zjh>/J; JAX 010802) to generate a transgenic reporter line in which GABAergic cells were labelled with GFP. DAT-GFP mice were generated by crossing Cre-dependent ROSA(EGFP-L10a) males with DAT-Cre+/- females (B6.SJL-Slc6a3<tm1.1(cre)Bkmn>/J; JAX 006660) to generate a transgenic reporter line in which dopaminergic cells were labelled with GFP. GAD2-GFP, DAT-GFP, and 5-HTT-Cre+/- mice (MMRRC, B6.Cg-Tg(Slc6a4-cre)Et33Gsat, stock number 031028-UCD) were genotyped by Transnetyx (Cordova, TN). Mice of either sex were singly housed after surgeries to facilitate recovery and maintain the integrity of intracranial implants, with *ad libitum* access to food and water in a 12/12 h light/dark cycle (lights on 6am). Experiments were performed in compliance with the National Institutes of Health *Guide for the Care and Use of Laboratory Animals* and approved by the local National Institute on Alcohol Abuse and Alcoholism Animal Care and Use Committee.

6.2.2 Retrograde tracing and immunohistochemistry

6.2.2.1 CTb with 5-HT/VGluT3/c-fos

The retrograde tracer Cholera Toxin B (CTb) conjugated to Alexa Fluor 555 (Invitrogen; 1 µg, 200 nL) was injected into the BA (coordinates (mm) according to bregma; anterior-posterior -1.8; medio-lateral ±3.15; dorso-ventral -5.15) of 5-HTT-Cre-/- mice (3-5 months). On recovery from surgery, mice were administered 5 mg/kg ketoprofen (s.c.) for post-operative analgesia. 7 days following intra-cranial injection, mice were terminally overdosed with pentobarbital 2.5 h after the completion of fear conditioning. Mice were then

transcardially perfused with PBS, followed by 4% PFA. After overnight suspension in 4% PFA at 4°C, 50 µm coronal sections were cut with a vibratome (Classic 1000 model, Vibratome). Brain sections were rinsed 3 times in 0.05 M PBS with 0.3% Triton X-100 (10 mins), and then incubated in blocking solution (1% normal donkey (Jackson ImmunoResearch Laboratories, Inc.) or goat serum (Vector Laboratories) and 0.1% bovine serum albumin (MP Biomedicals) in 0.05 M PBS for 90 min at room temperature and then incubated at 4°C for two nights in rabbit anti-c-fos (1:250 dilution; Cell Signaling Technology, #2250), goat anti-5-HT (1:400 dilution; ImmunoStar, 20079), and guinea pig anti-VGluT3 (1:200 dilution; Frontier Institute, AB_2571855) primary antibodies. Sections were then incubated in donkey anti-rabbit Alexa 488 (1:250 dilution; Life Technologies), donkey anti-goat Alexa 350 (1:200 dilution; Life Technologies), and donkey anti-guinea pig Alexa 647 (1:200 dilution; Life Technologies) secondary antibodies.

6.2.2.2 CTb with GAD2 or DAT

CTb conjugated to Alexa Fluor 555 (Invitrogen; 1 µg, 200 nL) was injected into the BA (coordinates (mm) according to bregma; anterior-posterior -1.8; medio-lateral ±3.15; dorso-ventral -5.15) of GAD2-GFP or DAT-GFP mice (3-5 months). On recovery from surgery, mice were administered 5 mg/kg ketoprofen (s.c.) for post-operative analgesia. 7 days following intra-cranial injection, mice were terminally overdosed with pentobarbital. Mice were then transcardially perfused with PBS, followed by 4% PFA. After overnight suspension in 4% PFA at 4°C, 50 µm coronal sections were cut with a vibratome (Classic 1000 model, Vibratome).

6.2.2.3 Dopamine beta-hydroxylase

Dopamine beta-hydroxylase staining was carried out to identify noradrenaline-producing neurons. 5-HTT-Cre-/- mice (3-5 months) were terminally overdosed with pentobarbital and transcardially perfused with PBS, followed by 4% PFA. After overnight

suspension in 4% PFA at 4°C, 50 µm coronal sections were cut with a vibratome (Classic 1000 model, Vibratome). Brain sections were incubated in blocking solution (1% normal goat serum (Vector Laboratories) and 0.1% bovine serum albumin (MP Biomedicals) in 0.05 M PBS with 0.3% Triton X-100 for 90 min at room temperature and then incubated at 4°C for two nights in rabbit anti-dopamine beta-hydroxylase (DBH) (1:250 dilution; Cell Signaling Technology, #2250) primary antibody. Sections were then incubated in goat anti-rabbit Alexa 488 (1:250 dilution; Life Technologies) secondary antibody.

Brain sections in section 6.2.2 were mounted onto glass slides and coverslipped with Vectashield HardSet mounting medium (Vector Laboratories Inc.). Sections were imaged using an Olympus BX41 microscope (Olympus) and a Zeiss LSM 700 confocal microscope (Carl Zeiss Microscopy).

6.2.3 Quantification of co-localisation with CTb

Coronal sections containing DRN were imaged at 20× magnification with the confocal microscope mentioned above using Zen lite software (Carl Zeiss Microscopy). Images were taken from 5 alternating sections per mouse brain (rostro-caudal coordinates approximately -4.3 to -4.9 mm from bregma; from the Franklin and Watson (2007) atlas). Series of stacked images (10 µm depth) were acquired using a 20× objective lens with 1 µm steps. Counting was performed offline in Zen lite. Counting was performed blind to whether mice were fear conditioned or context controls. Data were pooled on Excel (Microsoft) for further analysis.

6.2.4 Viral transfection and cannulation

To selectively transfect 5-HT neurons with the excitatory light-gated cation channel ChR2, a Cre-inducible recombinant viral vector (AAV-EF1a-DIO-hChR2(E123T/T159C)-

EYFP; UNC Vector Core) carrying a floxed ultrafast (E123T/T159C) ChR2 fused with YFP was stereotaxically injected (1 µl at 100 nL/min) into the DRN (coordinates (mm) according to bregma and the brain surface; anterior-posterior -4.1; dorso-ventral -2.5, -2.2, -1.9) of 5-HTT-Cre mice (2 to 4 months) anaesthetised using 1-2 % isoflurane in oxygen (2 L/min). As a control construct, a Cre-dependent vector (AAV-EF1a-DIO-EYFP; UNC Vector Core) containing only YFP was used. Bilateral opto-fluid cannulae (8 mm; Doric) with affixed ferrules were positioned above the BA (coordinates (mm) according to bregma; anterior-posterior -1.8; medio-lateral ±3.23; dorso-ventral -4) and chronically implanted by attaching to the skull using dental cement (Coralite Dental Products). On recovery from surgery, mice were administered 5 mg/kg ketoprofen (s.c.) for post-operative analgesia. Mice were left undisturbed for 5 to 6 weeks to allow for recovery and virus expression before testing.

6.2.5 Infusions and optogenetic stimulation

Mice were handled for 2 min a day for 6 days and habituated to being connected to optic fibre cables in the home cage for 45 min a day for 3 days before behavioural testing. 15 min prior to testing, mice received bilateral microinjections of vehicle or a drug cocktail of WAY100635 (0.37 nmol) and MDL100907 (0.54 nmol) into the BA (Gomes et al., 2012; Amodeo et al., 2017). Needles (9 mm) connected to a microliter syringe (Hamilton, USA, 2 µL) through a segment of polyethylene tubing were inserted into the guide cannulae. The injection needles extended 1 mm beyond the guide cannulae. The solutions were injected using an infusion pump (Harvard Apparatus PHD 22/2000, Holliston, MA, USA). A 0.3 µL solution volume was injected over 2 min. Following injections, the needles remained in the guide cannulae for an additional 3 mins to ensure diffusion into the BA and minimise reflux.

Optic fibres (8.8 mm length, 200 µm diameter, NA 0.37; Doric) connected to patch cables were inserted into the guide cannulae, extending 0.8 mm beyond the guide cannulae. After inserting the optic fibres, mice were allowed to settle down in their home cages for 15 mins prior to the fear conditioning session. The power of the blue laser was adjusted to 10

mW from the tip of the optic fibre. Laser power was calibrated before insertion into the guide cannulae by measuring the power at the tip of the optic fibre with a PM100D optical power metre with a S120C sensor (Thorlabs, Inc., USA). To excite 5-HT axons in the BA, a blue laser (λ = 473 nm) was bilaterally shone onto ChR2-transfected fibres in the BA. Optogenetic manipulations were made throughout the duration of 30 s CS presentations at 20 Hz during the fear conditioning session.

6.2.6 Behavioural testing

Fear conditioning was conducted in a 30 × 25 × 25 cm chamber with a metal rod floor, metal walls, and a distinctive vanilla olfactory cue (context A). After 180 s acclimation, mice received three pairings (60 to 90 s inter-trial interval) of a 30 s, 80 dB white noise cue (CS) and a co-terminating, 0.5 s, 0.6 mA scrambled footshock (US).

On the next day, fear extinction training was conducted in a different room, in a 27 × 27 × 14 cm chamber with transparent walls, a floor covered with wooden chips, and a distinctive acetic acid olfactory cue (context B). After 180 s acclimation, 50 × 30 s CS presentations (5 s inter-CS interval) were delivered. On the third day, after 180 s of acclimation, extinction retrieval was tested in context B with 5 × 30 s CS presentations (5 s inter-CS interval) (Bukalo et al., 2015).

CS and US presentations were controlled by the Med Associates Video Freeze or MedPC system (Med Associates Inc., St. Albans, VT). Freezing was defined as the absence of visible movement, excluding respiration, and was scored at 5 s intervals by an observer blind to genotype. Freezing was converted to a percentage [(number of freezing observations/total number of observations) × 100] for analysis. On conditioning day, freezing was analysed per CS presentation. On extinction (training) day, CS presentations were grouped into blocks of 5, and the first and last block were compared. On extinction retrieval day, the 5 CS presentations were grouped into one block.

6.2.7 Histology

To verify virus expression, cannulae placements, and infusion sites, mice were terminally overdosed with pentobarbital at the completion of behavioural testing. Mice were then transcardially perfused with PBS, followed by 4% PFA. After overnight suspension in 4% PFA at 4°C, 50 μm coronal sections were cut with a vibratome (Classic 1000 model, Vibratome). Brain sections were incubated in blocking solution (10% normal goat serum (Vector Laboratories) and 2% bovine serum albumin (MP Biomedicals) in 0.05 M PBS with 0.3% Triton X-100] for 90 min at room temperature and then incubated at 4°C overnight in chicken anti-GFP (1:3000 dilution, Abcam cat. no. 13970) primary antibody to enhance visualisation of opsins. The next day, sections were incubated in goat anti-chicken Alexa 488 secondary antibody (1:1000 dilution, Abcam cat. no. 150169). The sections were mounted onto glass slides and coverslipped with Vectashield HardSet mounting medium (Vector Laboratories Inc.). Sections were imaged using an Olympus BX41 microscope (Olympus) and a Zeiss LSM 700 confocal microscope (Carl Zeiss Microscopy).

6.2.8 Drugs

The 5-HT_{1A} antagonist WAY100635 (Tocris, USA, cat. no. 4380) was dissolved in saline (NaCl 0.9%) and stored as a 25 mM stock solution at -20°C for up to 4 weeks. The 5-HT_{2A} antagonist MDL100907 (Tocris, USA, cat. no. 4173) was dissolved in dimethyl sulfoxide (DMSO) and stored as a 100 mM stock solution at -20°C for up to 4 weeks. On the day of behavioural testing, a drug cocktail was prepared by diluting the stock solutions in saline with 1.8% DMSO and 5% polyethylene glycol. The vehicle solution was made up of 1.8% DMSO and 5% polyethylene glycol in saline.

6.2.9 Statistical analysis

Statistical analysis was performed using GraphPad Prism (Graphpad Software, Inc.) and SPSS (IBM) software. Student's unpaired t-tests were used to analyse differences in CTb+ neurons between fear-conditioned and context control mice when data were normally distributed (based on Shapiro-Wilk's test for normality). Otherwise, the non-parametric Mann Whitney U test was used. 2-way ANOVA was used to compare the distribution of neurochemical markers in fear-conditioned and context control mice. The effects of opsin group, drug treatment, and period on freezing were analysed using 3-way ANOVA. Subsequently, Sidak's *post-hoc* pairwise comparisons were made.

6.3 Results

6.3.1 Identification of BA-projecting neurons in the DRN

To label DRN projection neurons targeting the BA, the retrograde tracer CTb was intra-cranially injected into the BA (Figure 6.5A, B). CTb was fused to a fluorescent reporter protein, allowing identification of infected somata in the DRN. Mice were sacrificed 7 days following surgery and their brains sectioned coronally.

CTb-labelled cell bodies were visualised in the raphe nuclei of 23 brains to understand the distribution of BA-projecting neurons. BA-projecting cells were most densely located in the dorsal subnucleus of the DRN (Figure 6.5E), with a greater prevalence in the middle and caudal (Figure 6.5E, F) compared to the rostral (Figure 6.5D) DRN. BA-projecting cells were found to be located medially rather than in the lateral wings. In contrast, the MRN contained very few BA-projecting neurons (Figure 6.5C). Thus, DRN projections to the BA are topographically distinctive in that they are predominant dorsally, arranged near the midline, and more abundant in the middle and caudally.

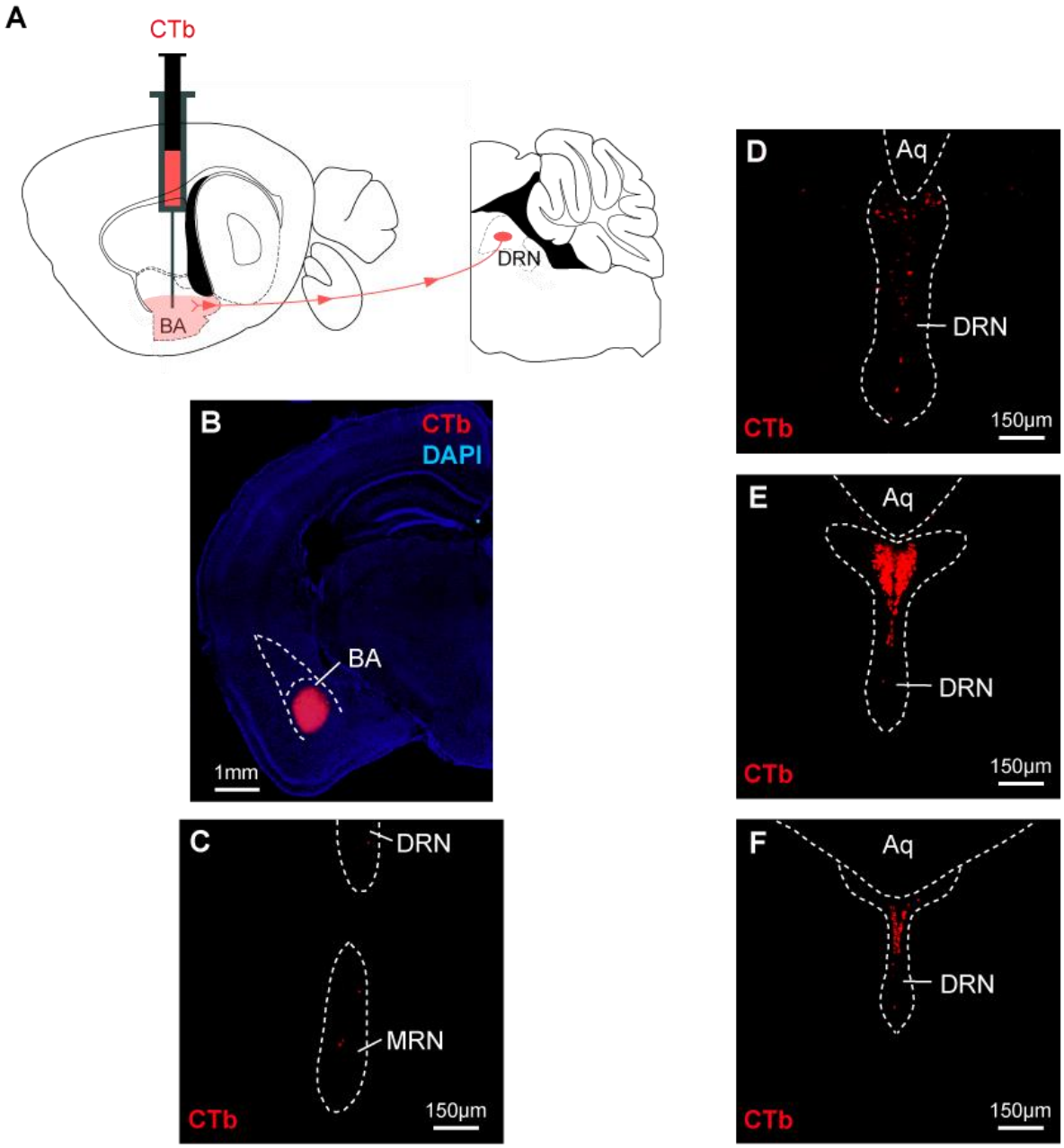


Figure 6.5 – Retrograde labelling of BA-projecting DRN neurons
A. Sagittal schematic showing delivery of retrograde tracerCTb into the BA to label cell neuronal cell bodies in the DRN. **B.** Coronal image of a CTb injection site in the BA. **C.** Coronal image of CTb+ cells in the MRN. **D.** Coronal image of CTb+ cells in the rostral DRN. **E.** Coronal image of CTb+ cells in the middle DRN. **F.** Coronal image of CTb+ cells in the caudal DRN. *Aq* – aqueduct.

6.3.2 Neurochemical identities of BA-projecting DRN neurons

CTb-labelling enabled immunohistochemical analysis of identified BA-projecting neurons in the DRN. 5-HT and VGluT3 antibodies were used on 12 mouse brains to locate 5-HT and glutamate neurons in the DRN, respectively. Notably, CTb+ cells were densely located in an area strongly immunoreactive for both 5-HT and glutamate markers (Figure

6.6A). CTb+, 5-HT+, and VGluT3+ neuron overlap primarily occurred medially in the dorsal subnucleus of the middle to caudal DRN.

To quantify which type of BA-projecting neurons are activated during fear conditioning, mice were sacrificed 2.5 h after fear conditioning and brains were stained for the expression of immediate-early gene c-fos as a marker for neuronal activity (Figure 6.6B, top). CTb+ cells in the DRN were examined for 5-HT, VGluT3, and c-fos immunoreactivity (Figure 6.6B, bottom). 5 DRN sections per mouse were sampled for cell counting, and comparable numbers of CTb+ neurons were found in fear conditioned (50 ± 3 cells per mouse) and context control (50 ± 2 cells per mouse) mice [unpaired t-test, $t(10)=0.08392$, $p=0.935$] (Figure 6.6C, top). Similar distributions of 5-HT+, VGluT3+, and double-positive cells were observed in fear conditioned mice and context controls [2-way ANOVA, main effect of condition $F(1,10)=0.8723$, $p=0.431$; main effect of marker, $F(2,10)=675.3$, $p<0.001$; condition × marker interaction, $F(2,10)=0.1416$, $p=0.869$] (Figure 6.6C, middle). 100% of BA-projecting cells were either 5-HT+ or VGluT3+, with the large majority (84%) co-expressing both markers. 9% of BA-projecting neurons were solely 5-HT+. Only 7% of BA-projecting neurons were non-5-HT, and all of these were VGluT3+. C-fos expression was significantly higher in 5-HT+/VGluT3+ double-positive BA-projecting cells in the fear conditioned mice than in controls [unpaired t-test, $t(10)=4.054$, $p=0.002$], but not in cells solely positive for 5-HT [Mann Whitney U test, $U=14$, $p=0.455$] or VGluT3 [Mann Whitney U test, $U=15$, $p=0.697$] (Figure 6.6C, bottom). This suggests that fear conditioning may have preferentially recruited BA-projecting neurons in the DRN that co-expressed markers for 5-HT and glutamate; however, it should be noted that the 5-HT- and VGluT3-only groups may be underpowered due to their smaller sample sizes.

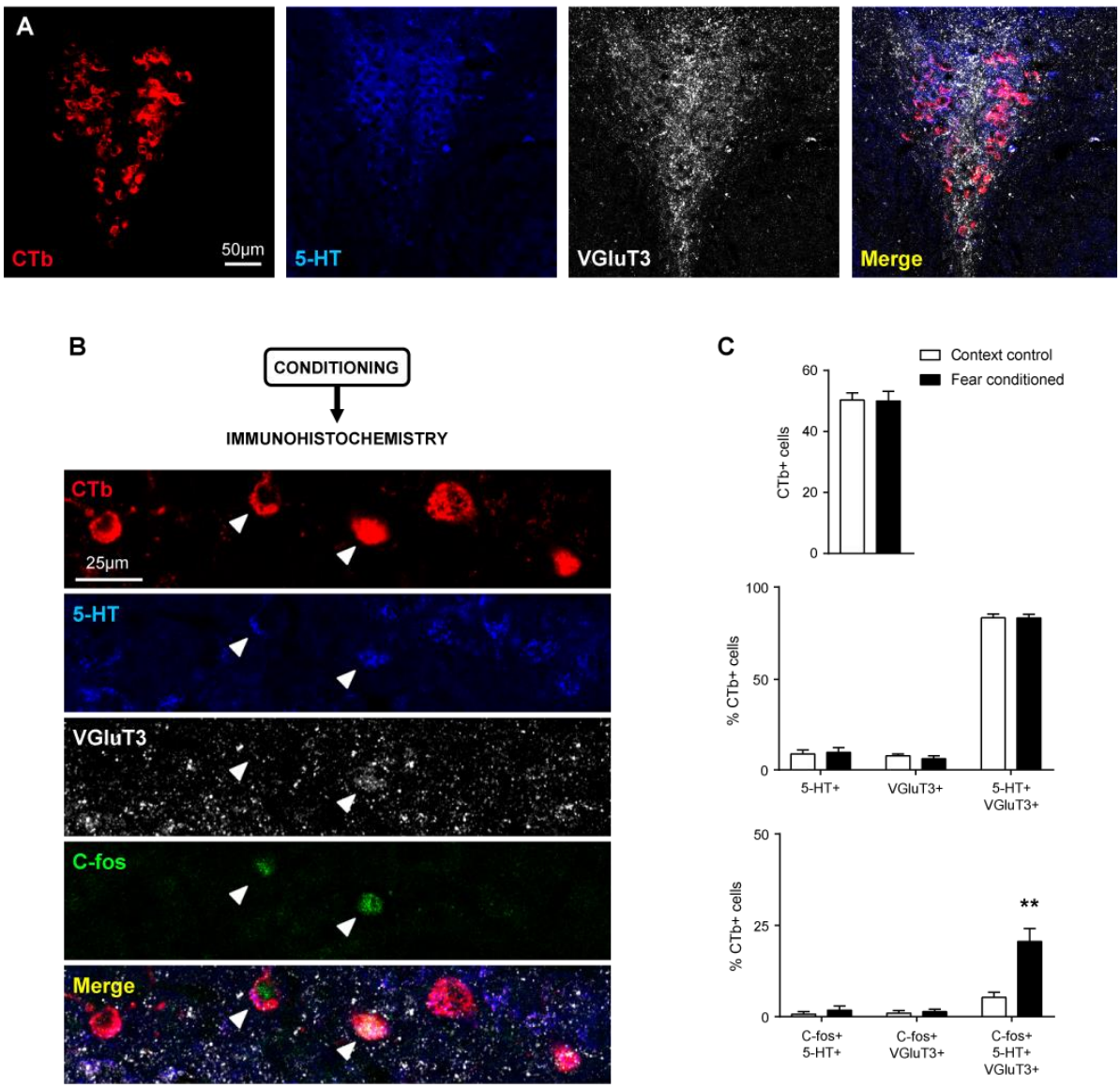


Figure 6.6 – DRN neurons that project to the BA are 5-HT and glutamatergic
A. Coronal image of CTb+, 5-HT+, and VGluT3+ cells in the DRN. **B.** Mice were sacrificed for immunohistochemistry following fear conditioning (top). Example CTb+ cells in the DRN co-expressing 5-HT, VGluT3, and c-fos (single optical section, 1 µm thickness) (bottom). **C.** Mean number of DRN CTb+ cells counted per mouse (top; context control n=6, fear conditioned n=6). Percentage of CTb+ cells expressing 5-HT and/or VGluT3 (middle; context control n=6, fear conditioned n=6). Percentage of CTb+ cells expressing c-fos, 5-HT, and/or VGluT3 (bottom; context control n=6, fear conditioned n=6). Data are expressed as means ± SEM. **p<0.01.

Since DRN cells are known for containing numerous transmitters and for co-transmission, CTb+ cells were also analysed for other neurochemical markers. First, CTb was injected into the BA of GAD2-GFP mice. In 6 mice, GABAergic neurons were sparsely located in the DRN and flanked the medial regions, where CTb+ cells were most dense (Figure 6.7A). Next, CTb was injected into the BA of DAT-GFP mice. In 5 mice, dopaminergic neurons were also sparsely located in the DRN, found more rostrally than the majority of BA-projecting

neurons (Figure 6.7B, C). As a positive control, it was confirmed that the transgenic reporter line was labelling dopamine neurons in the ventral tegmental area (Figure 6.7D). It was also verified, in non-CTb-injected mice, that no DRN neurons were immunoreactive for the enzyme dopamine beta-hydroxylase (DBH), a marker for noradrenaline (Figure 6.7E), whereas cells in the locus coeruleus were immunoreactive for DBH (Figure 6.7F). 6 DRN sections per mouse were sampled for cell counting (67 ± 7 cells per GAD2-GFP mouse, 65 ± 5 cells per DAT-GFP mouse), and virtually no CTb+ neurons expressed GAD2 (0.2%, 1 cell) or DAT (0%). Overall, these data suggest that DRN projections to the BA are 5-HT and glutamatergic, but not GABAergic, dopaminergic, or noradrenergic.

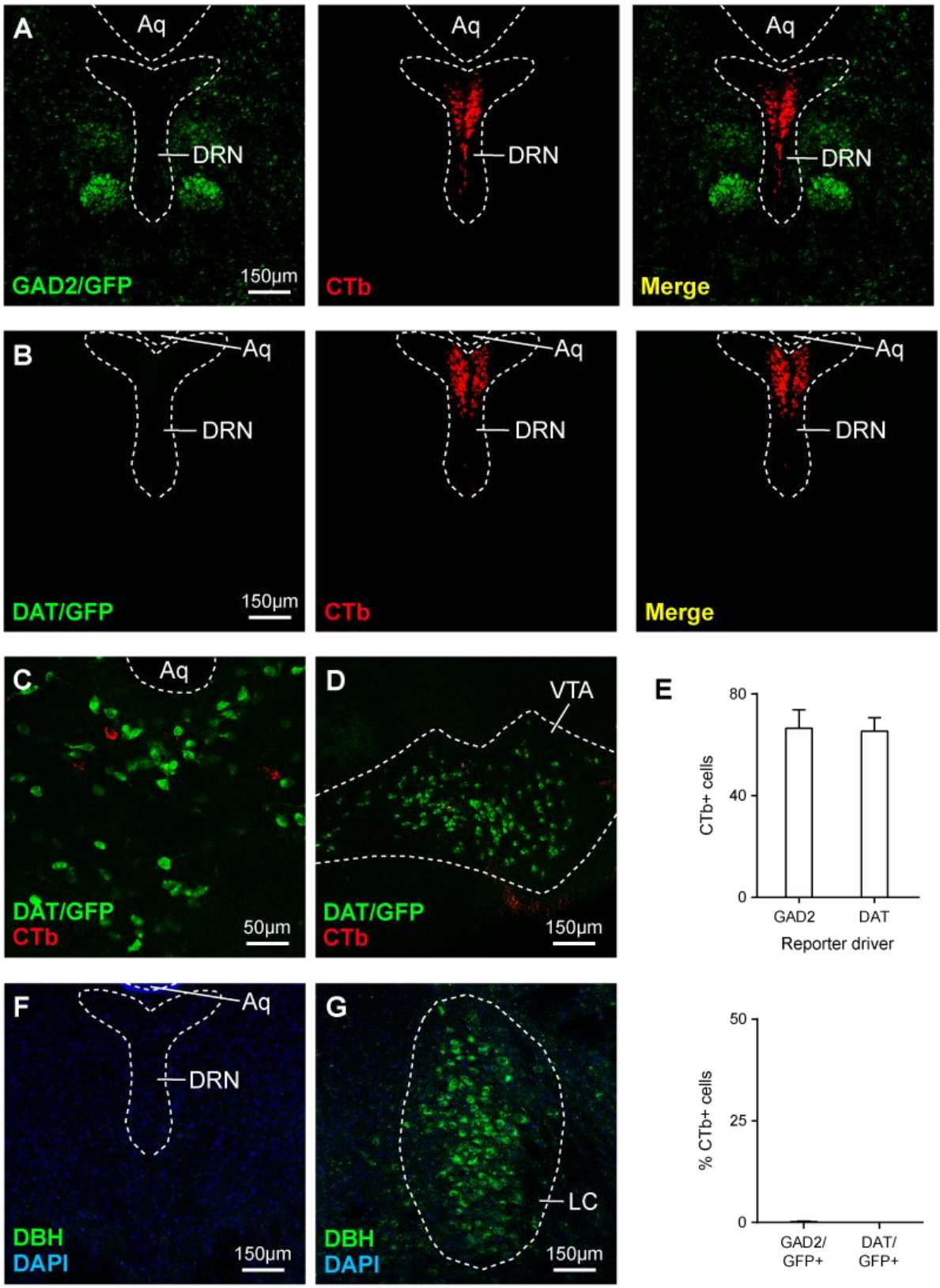


Figure 6.7 – DRN neurons that project to the BA are not GABAergic, dopaminergic, or noradrenergic

Coronal image of GAD2/GFP+ and CTb+ cells in the middle/caudal DRN. **B.** Coronal image of DAT/GFP+ and CTb+ cells in the middle/caudal DRN. **C.** DAT/GFP+ and CTb+ cells in the rostral DRN. **D.** Coronal image of DAT/GFP+ and CTb+ cells in the ventral tegmental area (VTA). **E.** Mean number of DRN CTb+ cells counted per mouse (top; GAD2 n=6, DAT n=5). Percentage of CTb+ cells expressing GAD2 or DAT (bottom; GAD2 n=6, DAT n=5). **F.** Coronal image of DBH+ cells in the DRN. **G.** Coronal image of DBH+ cells in the locus coeruleus (LC). Data are expressed as means ± SEM. *Aq* – aqueduct.

6.3.3 Optogenetic excitation of BA 5-HT projections and pharmacological antagonism of local 5-HT receptors

Since most 5-HT neurons projecting from the DRN to the BA could also be glutamatergic, the behavioural effects of optogenetic photoexcitation in Chapters 3 and 4 may have been driven by either 5-HT or glutamate transmission. To evaluate the specific contribution of 5-HT signalling to fear learning, BA 5-HT projections were optogenetically excited during CS presentations in the fear conditioning session, immediately after 5-HT_{1A} and 5-HT_{2A} antagonists (WAY100635 and MDL100907, respectively) were locally infused into the BA (Figure 6.8A). Antagonism was restricted to 5-HT_{1A} and 5-HT_{2A} receptors because these were identified as physiologically relevant in Chapter 5.

During fear conditioning, ChR2-expressing mice froze significantly more than YFP controls [repeated measures 3-way ANOVA; main effect of opsin $F(1,26)=3.566$, $p=0.070$; main effect of period, $F(3,78)=61.722$, $p<0.001$; opsin × period interaction, $F(3,78)=4.718$, $p=0.004$; Sidak's pairwise comparisons: CS3, YFP vs. ChR2 $p=0.015$]. Irrespective of ChR2-expression, mice administered 5-HT antagonists froze less than mice given vehicle [repeated measures 3-way ANOVA; main effect of drug, $F(1,26)=54.066$, $p<0.001$; opsin × drug interaction, $F(1,26)=1.655$, $p=0.210$; drug × period interaction, $F(3,15)=15.622$, $p<0.001$; opsin × drug × period interaction, $F(2,78)=0.631$, $p=0.597$; Sidak's pairwise comparisons: CS2, vehicle vs. drug $p=0.001$; CS3 vehicle vs. drug $p<0.001$] (Figure 6.8B, left).

When tested in a novel context one day later, ChR2-expressing mice displayed higher freezing to the CS, as compared to YFP controls, and the 5-HT antagonist-administered mice froze less than vehicle mice, regardless of ChR2-expression [repeated measures 3-way ANOVA; main effect of opsin $F(1,26)=4.551$, $p=0.043$; main effect of drug, $F(1,26)=26.325$, $p<0.001$; main effect of period, $F(2,52)=42.667$, $p<0.001$; opsin × drug interaction, $F(1,26)=3.162$, $p=0.087$; opsin × period interaction, $F(2,52)=5.782$, $p=0.005$; drug × period interaction, $F(2,52)=26.450$, $p<0.001$]. Specifically, while vehicle-treated ChR2-expressing mice froze more than vehicle-treated mice expressing YFP, the two virus groups froze to a

similar extent when treated with 5-HT antagonists [repeated measures 3-way ANOVA; opsin × drug × period interaction, $F(2,52)=3.644$, $p=0.033$; Sidak's pairwise comparisons: CS1-5, vehicle, YFP vs. ChR2 $p=0.006$; CS1-5, drug, YFP vs. ChR2 $p=0.754$]. Additionally, the antagonist-treated mice froze less than vehicle-treated counterparts, regardless of the virus they expressed [Sidak's pairwise comparisons: CS1-5, YFP, vehicle vs. drug $p=0.033$; CS1-5, ChR2, vehicle vs. drug $p<0.001$] (Figure 6.8B, middle). Hence, not only did 5-HT antagonism reduce freezing in both YFP- and ChR2-expressing mice, it fully blocked the enhanced fear produced by DRN-BA 5-HT pathway photoexcitation.

On extinction retrieval, the ChR2-expressing group continued to show elevated freezing relative to YFP controls. Moreover, the reduced freezing produced by 5-HT antagonism was also present [repeated measures 3-way ANOVA; main effect of opsin $F(1,26)=18.387$, $p<0.001$; main effect of drug, $F(1,26)=88.445$, $p<0.001$; main effect of period, $F(1,26)=125.430$, $p<0.001$; opsin × drug interaction, $F(1,26)=5.430$, $p=0.028$; opsin × period interaction, $F(1,26)=17.766$, $p<0.001$; drug × period interaction, $F(1,26)=84.195$, $p<0.001$]. More specifically, vehicle-treated ChR2-expressing mice froze more than similarly-treated YFP controls, but the 5-HT antagonist-treated mice from both virus groups froze at similar levels to one another [repeated measures 3-way ANOVA; opsin × drug × period interaction, $F(1,26)=6.764$, $p=0.015$; Sidak's pairwise comparisons: CS1-5, vehicle, YFP vs. ChR2 $p<0.001$; CS1-5, drug, YFP vs. ChR2 $p=0.215$], and less than vehicle-treated counterparts [Sidak's pairwise comparisons: CS1-5, YFP, vehicle vs. drug $p<0.001$; CS1-5, ChR2, vehicle vs. drug $p<0.001$] (Figure 6.8B, right). Thus, 5-HT antagonism produced a reduction in fear and prevented the fear enhancing effects of DRN-BA 5-HT pathway photoexcitation.

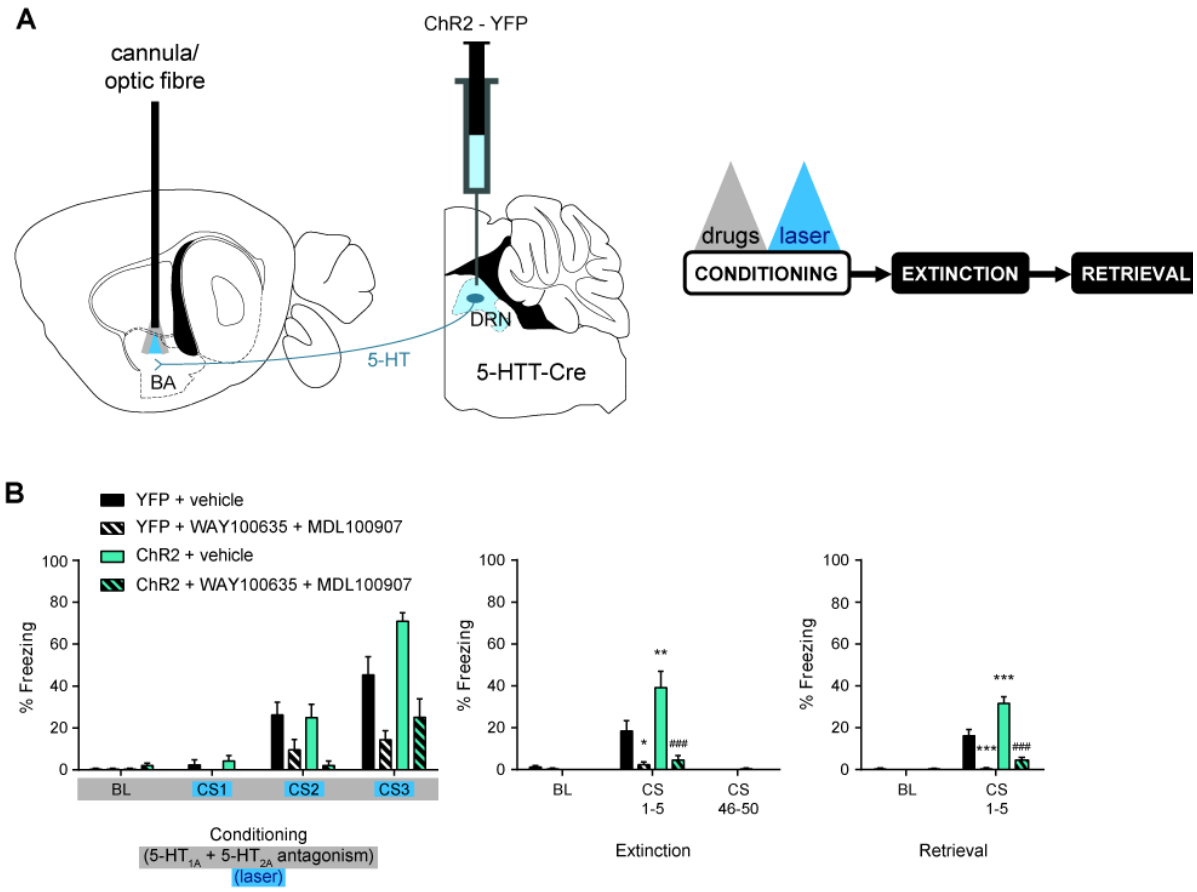


Figure 6.8 - Optogenetic excitation of BA 5-HT projections during fear conditioning enhances fear via 5-HT transmission
A. Sagittal schematic showing delivery of a viral vector containing the ChR2 construct into the DRN under control of the 5-HTT promoter (left). Cannula/optic fibre enables optogenetic excitation of 5-HT projections in the BA through light stimulation following local infusion of 5-HT receptor antagonists. Drugs and light stimulation delivered during the conditioning session of a fear learning task (right). **B.** Optogenetic excitation during the conditioning session of a fear learning task after local infusion of 5-HT_{1A} (WAY100635) and 5-HT_{2A} (MDL100907) antagonists. Percentage time spent freezing in the baseline (BL) period and to the CS during fear conditioning, extinction, and retrieval sessions (YFP + vehicle n=7, YFP + antagonists n=7, ChR2 + vehicle n=8, ChR2 + antagonists n=8). Data are expressed as means ± SEM. *p<0.05, **p<0.01, ***p<0.001 compared to YFP + vehicle. ###p<0.001 compared to ChR2 + vehicle.

6.4 Discussion

This study provides further mechanistic characterisation of the DRN to BA 5-HT pathway. BA-targeting DRN projections were identified using a retrograde tracer, and were all either 5-HT or VGluT3 immunoreactive. The majority of BA-projecting cells in the DRN (84%) co-expressed the markers for both 5-HT and glutamate transmission, and a minority of cells were positive for only 5-HT or VGluT3. C-fos staining showed that the double-positive 5-HT+/VGluT3+ BA-projecting neurons were selectively recruited during fear conditioning. These data, in addition to the results from Chapter 5 demonstrating glutamate co-release *in*

vitro, raised the possibility that 5-HT projections to the BA regulate fear learning via both 5-HT and glutamate transmission. Therefore, in order to isolate the contribution of 5-HT signalling in the BA, DRN 5-HT projections to the BA were optogenetically excited during fear conditioning immediately after local infusion of 5-HT_{1A} and 5-HT_{2A} receptor antagonists. Pharmacological antagonism of BA 5-HT receptors prevented the enhanced fear expression brought about by 5-HT projection excitation, supporting the hypothesis that 5-HT transmission in the BA is necessary for the influence of 5-HT projections on fear.

6.4.1 Fear conditioning preferentially recruits BA-projecting DRN neurons that co-express markers for 5-HT and glutamate

BA-targeting neurons of the DRN that co-express 5-HT and glutamate markers were preferentially activated during fear conditioning. This is in accordance with previous accounts of fear conditioning or inescapable shocks activating 5-HT neurons in the DRN (Grahn et al., 1999; Takase et al., 2004; Spannuth et al., 2011). Previous *in vivo* electrophysiology experiments have also observed, with greater temporal resolution, the excitation of DRN 5-HT neurons evoked by aversive stimuli (Schweimer and Ungless, 2010; Cohen et al., 2015). However, a recent study employing *in vivo* calcium imaging did not reveal an activation of DRN 5-HT neurons elicited by footshock (Li et al., 2016). The current data builds on these earlier findings by clarifying both DRN-BA 5-HT pathway specificity and the VGluT3 co-expression therein, by demonstrating that 5-HT+/VGluT3+ neurons projecting to the BA are selectively recruited during fear conditioning.

BA-projecting neurons appeared to be spatially concentrated to dorsomedial parts of the DRN, with greater abundance in the middle and caudal compared to rostral sections. This concurs with previous reports observing dorsomedial localisation of amygdala-projecting neurons in the middle and caudal rather than rostral DRN (Ma et al., 1991; Asan et al., 2013; Gagnon and Parent, 2014). Although the current study involved bilateral CTb injections, previous research has shown that the unilateral amygdala is innervated predominantly but

not exclusively by the ipsilateral DRN (Li et al., 1990; Ma et al., 1991). Interestingly, reciprocal projections from the amygdala to the DRN are also restricted to the middle and caudal DRN (Vasudeva et al., 2011), potentially forming a critical feedback loop. One caveat of using CTb tracing is that synaptic terminals are not marked, making it difficult to confirm whether BA-projecting DRN neurons also collateralise into other regions, a feature that is known of the widely-projecting 5-HT axons (Gagnon and Parent, 2014). This could be investigated by using alternative tracing techniques (e.g. virally-mediated synaptophysin-fluorescence) to label synaptic terminals in DRN to BA 5-HT projection neurons.

The dorsomedial presence of BA-projecting neurons in the middle to caudal DRN is similar to descriptions of VGluT3 immunoreactivity in the DRN (Commons, 2009; Hioki et al., 2010). Accordingly, the densest 5-HT and VGluT3 overlap occurs in the middle to caudal DRN (Commons, 2009), where most BA-projecting cells were located. According to one study, neurons in the middle to caudal DRN in particular become activated by inescapable shocks (Grahn et al., 1999). Taken together, previous investigations of DRN neurochemistry and anatomy corroborate the current results. Additionally, the data in this chapter identifies the fear-relevant, 5-HT+/VGluT3+ neurons as the projection pathway to the BA.

6.4.2 Co-localisation of neurochemical markers in DRN neurons

A noteworthy observation made in the current study was that a minority of BA-projecting DRN neurons (7%) were not 5-HT+, but solely VGluT3+, which corresponds well with previous findings that some DRN neurons are VGluT3+ and not 5-HT+ (Schäfer et al., 2002; Hioki et al., 2010). Current data are also to some degree in agreement with the findings of Ma et al. (1991) and Fernandez et al. (2016), who respectively reported that 3.4% and 26% of DRN to amygdala projections were non-5-HT. In the central amygdala and bed nucleus of the stria terminalis, non-5-HT innervation from the DRN is dopaminergic (Hasue and Shammah-Lagnado, 2002; Matthews et al., 2016) or peptidergic (Li et al., 1990; Petit et

al., 1995), but the BA seems to be exclusively innervated by 5-HT+ or VGluT3+ DRN projections.

There is disagreement in the literature about the exact degree of 5-HT and VGluT3 overlap in the DRN. While in several cases, almost all 5-HT+ DRN cell bodies also express glutamatergic markers (Kaneko et al., 1990; Gras et al., 2002; Hioki et al., 2004; Mintz and Scott, 2006; Shutoh et al., 2008), other studies reported co-expression ranging widely, from 4-80% (Fremeau et al., 2002; Hioki et al., 2010; Voisin et al., 2016). These discrepancies likely arise from the methodological variations in neurochemical markers studied, protein or mRNA detection approaches, brain section or neuronal culture preparations, species, and age. In fact, some studies have observed little VGluT3 expression in DRN neurons projecting to the amygdala (Hioki et al., 2010; Fernandez et al., 2016). This could be explained by differential neuromodulation of distinct amygdala nuclei, with possibly more dopaminergic innervation of the central nucleus and more glutamatergic innervation of the BA (Hasue and Shammah-Lagnado, 2002; Marcinkiewcz et al., 2016; Matthews et al., 2016). Pertinently, Fernandez et al. (2016), examining 5-HT projections specifically to the BLA, used a Pet1-driver to identify 5-HT neurons. Elimination of Pet1-expressing 5-HT neurons spares much of the BLA 5-HT innervation, which may arise from a different population of 5-HT neurons expressing VGluT3 (Kiyasova et al., 2011).

The current work did not explore the co-expression of neurochemical markers other than 5-HT and VGluT3. Previous research has shed some light on the overlap of other markers. Early studies indicated a possible co-existence of 5-HT and GABAergic neurons in the DRN (Belin et al., 1983; Harandi et al., 1987), but more recent studies confirmed that this overlap was infrequent (Johnson, 1994; Stamp and Semba, 1995; Day et al., 2004). Few cells contain both mRNA for VGluT3 and GAD in the DRN (Hioki et al., 2010). In the current study, only one GABAergic DRN cell was identified as a BA-projection neuron, which may have been one of the rare 5-HT+/GAD+ or VGluT3+/GAD+ cells, though this was not verified using additional techniques. In general, the distribution of GABAergic neurons observed in the current study, flanking the medial DRN and more dense in the lateral wings,

matched previous reports (Stamp and Semba, 1995; Allers and Sharp, 2003; Day et al., 2004; Challis et al., 2013). Lastly, with regards to other classical monoamines, dopaminergic DRN neurons are neither 5-HT+ nor glutamatergic and are located rostrally (Hioki et al., 2010; Matthews et al., 2016), as was observed in this study. Moreover, replicating a previous report (Nagatsu et al., 1979) , noradrenergic neurons were not found in the DRN. The lack of co-localising 5-HT/glutamatergic, GABAergic, and dopaminergic cells suggests spatially discrete neurochemical clusters in the DRN. Given that DRN neurons are topographically organised according to their projection targets (Vasudeva et al., 2011; Fernandez et al., 2016), separate clusters could correspond to differential neuromodulation of distinct neural networks.

6.4.3 5-HT projections to the BA regulate fear via 5-HT transmission

The observation that most 5-HT neurons projecting from the DRN to the BA co-express VGluT3 raised the possibility that both 5-HT and glutamate signalling contribute to fear regulation. Therefore, a multiplexed approach entailing DRN-BA 5-HT neuronal photoexcitation, coupled with selective 5-HT receptor pharmacology, was employed to establish the necessity of 5-HT transmission. The 5-HT_{1A} and 5-HT_{2A} receptor subtypes were targeted because their functional involvement was characterised in Chapter 5. With these 5-HT receptors antagonised in the BA, DRN-5-HT photoexcitation during conditioning failed to produce increased fear on fear retrieval (or subsequent extinction retrieval). This supports the critical downstream contribution of 5-HT transmission, through either or both of these receptor subtypes, to the fear-enhancing effect of DRN-5-HT input to the BA. More generally, these data support the concept that increased 5-HT signalling in the amygdala and bed nucleus of the stria terminalis favours heightened fear states (Macedo et al., 2007; Ruiz Martinez et al., 2007; Zanoveli et al., 2009; Johnson et al., 2015; Baratta et al., 2016; Marcinkiewcz et al., 2016).

Interestingly, mice given 5-HT antagonist treatment during conditioning appeared to display little to no fear retrieval on subsequent days. This matches the low-fear behaviour

observed in 5-HTT OE (Chapter 1) and iC++-expressing (Chapter 3) mice, supporting the fact that reduced 5-HT signalling prevents normal fear learning. It should be noted that this behavioural effect could be specific to the fear learning paradigm used, since 5-HTT OE mice, at least, have shown normal fear expression after experiencing a greater number of CS-US pairings during fear conditioning (Barkus et al., 2014).

The results of this study also suggest that glutamate co-release from 5-HT axons in the BA may not play a crucial a role in fear. This could reflect the finding described in Chapter 5 that 5-HT signalling modulated 78% of INs and 93% of PNs in the BA, while glutamate only influenced 55% of INs and no PNs. Furthermore, Chapter 5 results indicated that 20 Hz laser stimulation of ChR2-expressing BA 5-HT terminals favoured 5-HT over glutamate release. This could explain why the optogenetic excitation of BA 5-HT projections requires 5-HT signalling to exert its effects on fear.

One contradiction between the data from this chapter and Chapter 5 is the observation that in spite of most BA-projecting 5-HT neurons in the DRN containing VGluT3, only a small proportion of postsynaptic BA neurons was modulated by glutamate release from 5-HT terminals. This discrepancy likely arises from the fact that VGluT3 co-localisation in 5-HT cell bodies is greater than in fibres, with axonal overlap varying across different projection targets (Fremeau et al., 2002; Shutoh et al., 2008; Amilhon et al., 2010; Gagnon and Parent, 2014). This may be due to a segregation of glutamate and 5-HT release to distinct terminal boutons, which could explain how glutamate transmission from 5-HT neurons is targeted to particular cell types in the BA (Chapter 5). VGluT3 knockout mice have reduced 5-HT immunoreactivity in neuronal terminals, impaired 5-HT vesicular packaging, and desensitised DRN 5-HT_{1A} autoreceptors, demonstrating that at least constitutive VGluT3 function can impact 5-HT as well as glutamate transmission (Amilhon et al., 2010; Voisin et al., 2016).

It should be made clear that this study did not directly test the necessity of BA glutamate signalling for DRN-BA pathway-mediated fear. One approach would be to

antagonise glutamate receptors in the BA. A problem with this approach is that glutamate receptor antagonism would not exclusively block the effects of glutamate co-release from 5-HT terminals, and signalling from PNs would also be impaired. An alternative, used by other laboratories, is to use VGluT3 knockout mice to evaluate the contribution of glutamate co-transmission to behaviours regulated by 5-HT transmission. Research conducted by Amilhon et al. (2010) demonstrated that VGluT3 knockout mice exhibited increased anxiety-like behaviour. However, global VGluT3 knockout could influence non-5-HT pathways that have VGluT3, such as GABAergic or cholinergic neurons (Hioki et al., 2004; Gillespie et al., 2005; Gras et al., 2008), and alter developmental processes (Gras et al., 2005). More pertinently to the current study, Liu et al. (2014) showed that conditioned place preference and self-stimulation driven by optogenetic photoexcitation of DRN 5-HT neurons were impaired in VGluT3 knockout mice, suggesting that 5-HT neuronal function requires VGluT3 at least for these behaviours. It remains to be definitively established as to whether the same holds true for fear in the DRN-BA 5-HT pathway, but the current data suggest that it might not.

6.4.4 Conclusions

The results in this chapter characterised the molecular expression patterns of the DRN-BA projection pathway and indicated that most DRN 5-HT neurons that project to the BA may have the ability to co-release glutamate. The data further indicated that 5-HT transmission is necessary for BA 5-HT projections to regulate fear. This emphasises the largely undefined functional role of VGluT3 in 5-HT neurons. VGluT3 function and its relationship with 5-HT neurotransmission will be discussed more extensively in Chapter 7.

Chapter 7 General discussion

7.1 Thesis background and aims

5-HT neurotransmission has been strongly implicated in affective disorders that involve maladaptive fear-related behaviour (Nemeroff and Owens, 2002). In spite of this, the mechanisms through which the 5-HT system regulates neural fear circuits are not well-characterised. This is, in part, due to the involvement of anatomically separate 5-HT pathways in widely distinct functions (Graeff et al., 1996; Lucki, 1998). One manifestation of altered 5-HT signalling is amygdala dysfunction, which is associated with changes in fear learning and anxiety traits (Hariri et al., 2002; Bigos et al., 2008; Garfinkel et al., 2014). Notably, fear-related behaviour is differentially affected depending on the time scale and anatomical target of 5-HT manipulations (Li et al., 2006; Cornélio and Nunes-de-Souza, 2007; Ansorge et al., 2008; Karpova et al., 2009; Homberg et al., 2011; Matsuzaki et al., 2011; Rebello et al., 2014), which highlights the need for precise dissection of 5-HT function. This thesis used a translationally-relevant genetic mouse model and an optogenetic approach to respectively probe critical time points of 5-HT transmission and its circuit-specific control of the amygdala in shaping fear behaviour.

7.2 Short summary of results

Although 5-HT neurotransmission has been strongly implicated in fear emotionality, the mechanisms of this modulation are not fully understood. The experiments presented in this thesis make use of a translationally relevant mouse model and an optogenetic approach to dissect temporally- and circuit-specific mechanisms of 5-HT signalling in shaping fear-related behaviours.

The low-fear/anxiety phenotype of adult 5-HTT OE mice was observed in adolescence, indicating a potential neurodevelopmental trajectory. Acute pharmacological inhibition of the 5-HTT via citalopram administration in adolescence at the time of behaviour did not affect the low-fear phenotype, but postnatal citalopram treatment was able to rescue it. *Chapter 2* therefore identified a developmental origin of the fear-related phenotype associated with 5-HTT expression variation.

Next, *in vivo* optogenetic tools were employed to dissect the circuit-specific neuromodulation of the BA by DRN 5-HT neurons during a fear learning task. On the one hand, photoexcitation of DRN-BA 5-HT projections enhanced fear learning and impaired fear extinction. On the other hand, photoinhibition caused a fear learning deficit and facilitated fear extinction. Hence, *Chapter 3* characterised a bidirectional functional role for the BA-targeting 5-HT pathway.

Optogenetic control of the DRN-BA 5-HT pathway was then used while simultaneously recording the activity of BA neurons either *in vivo* during the fear learning task or *ex vivo* in brain slices. In *Chapter 4*, photoexcitation of 5-HT projections during fear learning promoted a physiological state in the BA that has previously been associated with fear expression, both in terms of individual neuron activity and network oscillations. Slice recordings in *Chapter 5* identified glutamate co-transmission, cell type-specific, and frequency-dependent mechanisms of BA circuit control by 5-HT neurons.

Finally, a combination of retrograde tracing and immunohistochemistry was applied to analyse the neurochemical identity of DRN neurons projecting to the BA. The majority co-

expressed markers for 5-HT and glutamate. To evaluate the specific contribution of 5-HT transmission from DRN-BA 5-HT projections, *in vivo* optogenetics was combined with local infusion of 5-HT receptor antagonists. *Chapter 6* thereby demonstrated that the photoexcitation-induced enhancement of fear learning was mediated by 5-HT signalling.

In summary, the results presented in this thesis provide a novel account of circuit-, temporal-, and receptor-specific 5-HT mechanisms that regulate fear-related behaviour. The BA, in particular, was shown to be a key site for 5-HT transmission.

7.3 Summary of main findings

The results presented in this thesis highlight the relationship between 5-HT signalling, amygdala function, and fear behaviour. Both systemically during development and circuit-specifically during aversive experiences, increasing 5-HT transmission enhanced fear behaviour. In particular, a pivotal role for the prominent and specific DRN to BA 5-HT projection pathway was outlined.

Pioneering human gene association and drug studies have reported links between variation in the 5-HTT, functional amygdala reactivity to aversive stimuli, and susceptibility to mood disorders (Lesch et al., 1996; Hariri et al., 2002). These findings solidified the connections between affective psychopathology and the 5-HT system, a known target of first-line drug treatments for depression and anxiety (Nemeroff and Owens, 2002). However, these associations have been questioned more recently (Munafò et al., 2008; Murphy et al., 2013). Human-based research is particularly challenging due to inconsistencies in environmental, demographic, and genetic variables, and transgenic rodent lines have been developed to study connections between the 5-HTT, amygdala, and fear behaviour with greater tractability (Bengel et al., 1998; Jennings et al., 2006; Homberg et al., 2007). While these models have revealed a causal link between altered 5-HTT expression and changes in fear-related behaviour, the underpinning mechanisms that drive the behavioural phenotypes still remain unclear.

In Chapter 2, the characteristic low-anxiety and low-fear phenotypes of 5-HTT OE mice previously reported in adulthood (Line et al., 2011, 2014) were found to be already established in adolescence, indicating that variation in 5-HTT expression likely gives rise to its effects either in an ongoing manner during behaviour, or at a critical earlier time point during development. Interestingly, brain tissue 5-HT levels of adolescent 5-HTT OE mice were reduced, indicating altered 5-HT transmission mechanisms in the DRN and BLA. The reduced fear behaviour of 5-HTT OE mice was rescued by postnatal pharmacological blockade of the 5-HTT, suggesting that variation in 5-HTT expression shapes fear behaviour during a critical neurodevelopmental time window (Gaspar et al., 2003; Ansorge et al., 2004, 2008; Karpova et al., 2009; Homberg et al., 2010; Sarkar et al., 2014; Teissier et al., 2017). Notably, acute systemic 5-HTT inhibition in adolescent WT mice also enhanced fear learning, but this 5-HT-mediated control of fear was absent in OE mice. Therefore, in WT mice, there was a crucial relationship between acute 5-HT signalling in adolescence and fear behaviour. This shows that normal fear behaviour depends on 5-HT mechanisms both during neurodevelopment and at the time of behavioural testing. Experiments in the following chapters aimed to investigate the connection between acute 5-HT transmission and fear learning with circuit specificity and temporal precision.

To this end, an optogenetic approach was used in Chapters 3 to 6 to manipulate the 5-HT pathway projecting from DRN to BA. Evidence shows that aversive stimuli evoke 5-HT release in the BLA (Amat et al., 1998; Zanoveli et al., 2009; Christianson et al., 2010; Baratta et al., 2016), but local antagonism of 5-HT receptors has produced contradictory results in fear behaviour (Li et al., 2006; Matsuzaki et al., 2011; Baratta et al., 2016). To clarify the relationship between 5-HT transmission in the BA and fear learning, the 5-HT afferent pathway from the DRN was selectively controlled using excitatory (ChR2) or inhibitory (iC++) opsins during stimulus presentations in a fear learning task.

It was found that DRN-BA 5-HT projection photoexcitation during either fear conditioning or extinction resulted in enhanced and persistent fear expression. In contrast, DRN-BA 5-HT projection inhibition during either fear conditioning or extinction reduced

fear expression and facilitated extinction. This suggested a bidirectional relationship between BA 5-HT signalling and fear behaviour. Namely, 5-HT inputs to the BA were necessary for normal fear conditioning and impaired fear extinction. Nevertheless, BA 5-HT axon excitation itself was not sufficient for generating a fear memory without footshock presentations, showing that the role of 5-HT transmission is in gating other inputs into the BA. These data clearly indicated that 5-HT neuromodulation is important in regulating fear learning, providing novel BA pathway specificity compared to previous optogenetic investigations (Baratta et al., 2016). To further dissect the neuromodulation of the BA by 5-HT, studies were designed in the next two chapters to explore the influence of 5-HT projections on BA physiology.

Previous research has identified individual BA neurons whose firing rates increase over the course of fear conditioning or extinction (Herry et al., 2008). Furthermore, the amygdala displays theta-frequency network oscillations during fear retrieval that are reduced in low-fear 5-HTT OE mice (Barkus et al., 2014). Chapter 4 aimed to investigate the role of 5-HT inputs in regulating the physiological activity of the BA during fear learning. DRN-BA 5-HT fibres were optogenetically excited during fear conditioning, and BA single unit and network activities were monitored over the course of the fear learning task.

5-HT afferent excitation was found to modulate BA single units of ChR2-expressing mice in a state-dependent manner, with individual BA neuron firing rates increased in the home cage but reduced during fear conditioning CS presentations. This suggests that 5-HT transmission modulates other concurrent inputs to BA circuits, a phenomenon that has been demonstrated *in vitro* (Cheng et al., 1998; Koyama et al., 1999; Yamamoto et al., 2012; Guo et al., 2017). Subsequently, BA single unit firing rates of ChR2-expressing mice were enhanced during salient events in fear and extinction retrieval. BA theta power was also increased in ChR2-expressing mice across all stages of the fear learning task. In addition to displaying both increased BA individual neuron firing and network theta activity, ChR2-expressing mice expressed elevated fear, in accordance with previous reports (Herry et al., 2008; Amano et al., 2011; Barkus et al., 2014; Karalis et al., 2016). These results confirmed that 5-HT

signalling regulates BA activity during fear behaviour. The physiological mechanisms of BA circuit modulation were characterised next.

There is pharmacological evidence for the activation of BLA GABAergic INs via 5-HT_{2A} receptors and this, in turn, inhibits PNs (Rainnie, 1999; Jiang et al., 2009b; Bocchio et al., 2015). The application of optogenetic 5-HT projection excitation in *ex vivo* brain slices enabled the dissection of BA circuit modulation mechanisms in Chapter 5. Specifically, it was shown that DRN 5-HT neurons control BA neurons through 5-HT and glutamate co-transmission in a frequency-dependent and cell type-specific manner (summarised in Figure 7.1). 5-HT actions were mediated via 5-HT_{1A} and 5-HT_{2A} receptors in particular. This raised the possibility that 5-HT projections could regulate fear learning through both 5-HT and glutamate transmission, as has been demonstrated for reward-based tasks (Liu et al., 2014). Further experiments were conducted to clarify the neurochemical nature of BA modulation by DRN 5-HT projections.

DRN neurons have a range of transmitter and neuropeptide identities (Vasudeva et al., 2011). In Chapter 6, BA-projecting cells in the DRN were labelled using a retrograde tracer, the majority containing markers for both 5-HT and glutamate. These co-expressing neurons were preferentially recruited during fear conditioning, consistent with the possibility of fear regulation through both 5-HT and glutamate co-transmission. To evaluate the particular contribution of 5-HT signalling in fear regulation, local 5-HT_{1A} and 5-HT_{2A} receptor antagonism was carried out while BA 5-HT projections were photo-excited during fear conditioning. The optogenetically-induced elevation of fear expression was abolished in the absence of 5-HT transmission, suggesting that 5-HT transmission from DRN-BA 5-HT projections are necessary for enhancing fear learning. Importantly, freezing responses were reduced in both ChR2-expressing and control mice, indicating that normal fear behaviour requires 5-HT signalling in the BA, matching BLA 5-HT terminal lesion data (Izumi et al., 2012; Johnson et al., 2015).

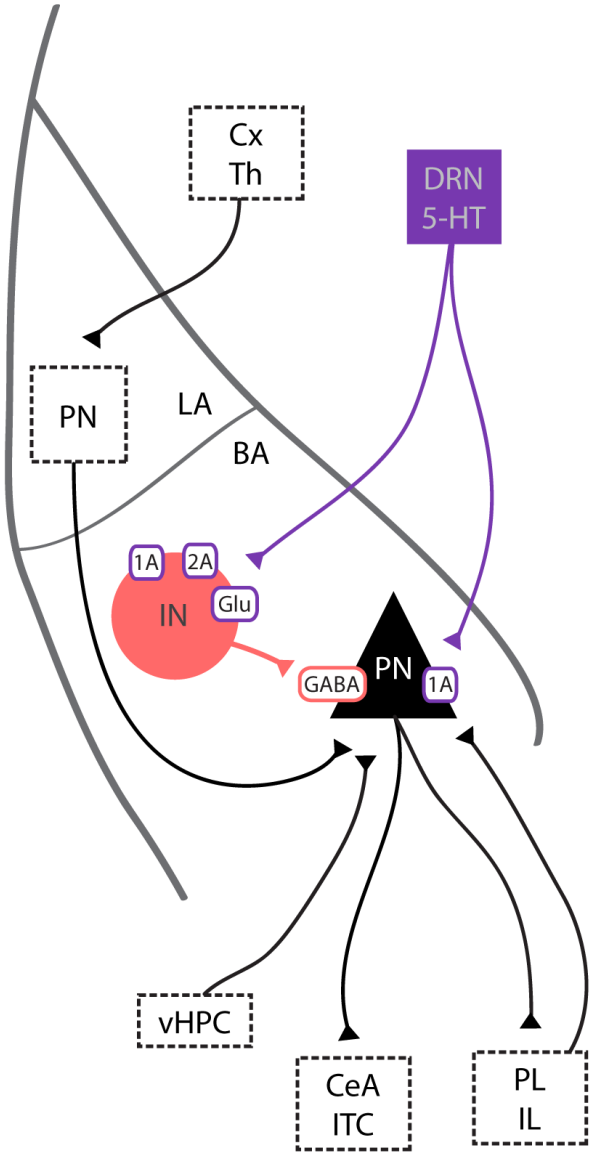


Figure 7.1 – Schematic of DRN-BA 5-HT pathway
Summary of the cell type-specific modulation of BA neurons by DRN 5-HT projections characterised in this thesis. DRN 5-HT projections modulate BA neurons via 5-HT_{1A}, 5-HT_{2A}, and glutamate receptors (shown in purple). Local interneurons inhibit principal neurons through GABAergic signalling (shown in orange). Circuit maps of fear-relevant pathways delineated in dashed boxes are adapted from Herry et al., (2008), Senn et al., (2014), Arruda-Carvalho and Clem (2015), and Bocchio et al., (2016). BA, basal amygdala; CeA, central amygdala; Cx, cortex; IL, infralimbic cortex; IN, interneuron; ITC, intercalated cells; LA, lateral amygdala; PL, prelimbic cortex; PN, principal neuron; Th, thalamus; vHPC, ventral hippocampus.

7.4 Discussion of main findings

7.4.1 Activation of BA-projecting DRN 5-HT neurons during fear conditioning

Fear learning and expression were associated with increased activity of DRN 5-HT projections to the BA. This was evidenced by staining of the immediate-early gene c-fos in

cell bodies (Chapter 6) and optogenetic excitation of axon terminals (Chapters 3, 4, 6). This relationship is in concordance with previous c-fos, electrophysiology, and optogenetic studies reporting enhanced DRN 5-HT neuron activity during aversive stimulus presentations (Grahn et al., 1999; Takase et al., 2004; Schweimer and Ungless, 2010; Spannuth et al., 2011; Cohen et al., 2015; Baratta et al., 2016), but is contested by calcium imaging data (Li et al., 2016). The current experiments isolated the role of DRN 5-HT neurons projecting to the BA in particular. A causal link was established by exciting BA 5-HT projections and consequently enhancing fear learning, showing that a specific circuit is sufficient for driving the 5-HT mediated fear regulation demonstrated with systemic pharmacology in Chapter 2. Moreover, the necessity of BA 5-HT transmission for normal fear learning was demonstrated by impairing fear behaviour through both optogenetic inhibition (Chapter 3) and 5-HT receptor antagonism (Chapter 6). The crucial role of amygdala 5-HT signalling in regulating fear is corroborated by pharmacology and chemical lesion studies (Liang, 1999; Li et al., 2006; Christianson et al., 2010; Matsuzaki et al., 2011; Izumi et al., 2012; Johnson et al., 2015; Baratta et al., 2016).

Importantly, this positive relationship between BA 5-HT transmission and fear held true even during extinction learning (Chapter 3), suggesting that BA 5-HT inputs favour the storage and retrieval of the fear memory in particular rather than facilitating an active learning process. Fear and extinction learning are thought to be mediated by mutually exclusive BA neuronal ensembles (Herry et al., 2008). BA projections to the prelimbic cortex mediate fear learning, whereas BA projections to the infralimbic cortex contribute to extinction learning (Senn et al., 2014). Inputs to DRN 5-HT neurons are also stronger from the prelimbic than the infralimbic cortex (Weissbourd et al., 2014). It is therefore likely that 5-HT differentially modulates these distinct BA cell groups, potentially favouring activation of fear neurons and sustaining fear memories. Although this is not supported by the fact that almost all PNs, the output of the BA, are uniformly modulated via 5-HT_{1A} receptors in acute slices (Chapter 5), the whole-cell patch-clamp experiments did not account for specialised 5-HT modulation of distal dendrites, other inputs, or varied IN dynamics in the BA.

7.4.2 Mechanisms of 5-HT modulation in the BA

One mechanism by which DRN 5-HT projections could influence BA neurons is by gating other inputs to the BA. This is supported by the state-dependent regulation of BA neuron firing rates by 5-HT transmission *in vivo* (Chapter 4) and previous findings *in vitro* (Cheng et al., 1998; Koyama et al., 1999; Yamamoto et al., 2012; Guo et al., 2017). It is also in accordance with the finding that although DRN 5-HT input to the BA enhanced the fearful memory of a noxious stimulus, it was not sufficient for generating a fear memory without the aversive stimulus (Chapter 3). By modulating distinct inputs differentially, 5-HT could selectively favour the storage and retrieval of a fear rather than an extinction memory, as observed in Chapter 3. 5-HT afferents are certainly in a position to modulate other inputs to the BA, because more than half of their terminal boutons in the BLA form triads with the pre- and post-synaptic sites of other synapses (Belmer et al., 2017).

The ability of DRN 5-HT projections to differentially control distinct BA neuron populations is highlighted by their receptor- and cell type-specific modulation mechanisms (Chapter 5). This may appear to contradict the view that 5-HT, due to the extra-synaptic location of the 5-HTT, acts as a volume transmitter (Torres and Amara, 2007), but the specialised nature of modulation could be determined by postsynaptic receptor expression patterns. Additionally, DRN 5-HT neurons signal via glutamate to BA INs exclusively, and to fast-spiking cells in particular (Chapter 5); hence, selective co-release terminals also enable differential regulation of BA neurons (see section 7.4.3 for further discussion). The nature of modulation exerted by distinct GABAergic IN classes is determined by their corresponding sub-cellular target domains, firing patterns, and functional roles. Regulation of BA PNs by local INs during fear learning is diverse and powerful (Ehrlich et al., 2009; Wolff et al., 2014), which means that heterogeneous modulation of INs is another mechanism through which 5-HT can differentially modulate functionally distinct BA outputs (Chapter 5).

The data presented in this thesis did not clarify how DRN 5-HT neurons affect information coding in BA neurons. Given the increased firing rates of BA single units in

ChR2-expressing mice on days following optogenetic excitation (Chapter 4), it can be speculated that 5-HT is involved in plasticity and affects rate coding in BA neurons. 5-HT projection excitation during fear conditioning also likely affected plasticity in a manner that enhanced BA theta power during not only conditioning but also fear and extinction retrieval (Chapter 4). Elevated theta power in the amygdala is associated with fear (Barkus et al., 2014; McHugh et al., 2014; Karalis et al., 2016). Therefore, by increasing theta oscillations, DRN 5-HT neurons could bias BA network activity and animal behaviour towards a fearful state.

7.4.3 5-HT and glutamate co-transmission

Since BA-projecting DRN neurons that co-express 5-HT and glutamate markers were preferentially activated during fear conditioning, it is important to consider the nature of 5-HT and glutamate co-transmission (Chapter 6). Low-frequency excitation of DRN 5-HT projections favoured glutamate transmission, while higher frequency stimulation facilitated 5-HT signalling (Chapter 5). DRN 5-HT neurons are quiescent during sleep and active during emotionally salient events (Allers and Sharp, 2003; Kocsis et al., 2006; Hajós et al., 2007; Schweimer and Ungless, 2010; Sakai, 2011; Cohen et al., 2015; Li et al., 2016). Thus, the activity of DRN 5-HT neurons can functionally dissociate the two transmitters based on the behaviour of the animal, favouring glutamate during rest and 5-HT during arousal. This is supported by the fact that photoexcitation of BA 5-HT projections at 20 Hz during fear conditioning only seemed to enhance fear learning via 5-HT transmission (Chapter 6). It also suggests that glutamate release from 5-HT axons in the BA is not functionally relevant for fear behaviour.

Notably, though the majority of BA-projecting DRN 5-HT neurons contained VGluT3 in their cell bodies, only a minority of BA neurons were modulated by glutamate co-release (Chapters 5, 6). This can be explained by the fact that VGluT3 co-localisation is more prominent in 5-HT somata than fibres, with axonal overlap varying across projection targets (Fremeau et al., 2002; Shutoh et al., 2008; Gagnon and Parent, 2014). Although there is

disagreement over the exact proportion of 5-HT terminals containing VGluT3, several studies have reported some degree of axonal overlap (Fremeau et al., 2002; Hioki et al., 2004; Shutoh et al., 2008; Amilhon et al., 2010; Gagnon and Parent, 2014; Voisin et al., 2016). Varicosities either containing or lacking VGluT3 can be present within the same axonal segments (Shutoh et al., 2008; Gagnon and Parent, 2014), which indicates that glutamatergic transmission may be restricted to certain DRN neuron terminals. Importantly, 5-HTT+ and VGluT3+ boutons are often separate, which means presynaptic segregation of transmitters could contribute to cell type- and subcellular domain-specific mechanisms of BA neuron modulation, as has been demonstrated of co-transmitting dopaminergic afferents in the striatum (Hattori et al., 1991; Amilhon et al., 2010; Voisin et al., 2016).

This study did not directly investigate the necessity or function of VGluT3 in 5-HT neurons. VGluT3 has been shown to enhance 5-HT transmission by assisting in 5-HT vesicular packaging (Amilhon et al., 2010), similar to its function in cholinergic neurons (Gras et al., 2008), indicating that the primary role of VGluT3 in 5-HT axons may not be to mediate glutamate co-release. This is in agreement with the possibility that glutamate co-transmission from BA 5-HT afferents may not be involved in regulating fear learning (Chapter 6). In VGluT3 knockout mice, vesicular 5-HT filling, 5-HT immunoreactivity in 5-HT axons, and 5-HT_{1A} receptor function is deficient without associated changes in the number of total DRN 5-HT neurons (Amilhon et al., 2010; Voisin et al., 2016). Additionally, the high-anxiety phenotype of VGluT3 knockout mice is rescued by reducing 5-HT synthesis, suggesting that the behavioural effects of VGluT3 knockout occur via 5-HT signalling mechanisms (Amilhon et al., 2010). Hence, VGluT3 function, at least when ablated constitutively, affects 5-HT transmission.

In contrast, there is functional evidence that in the nucleus accumbens, ventral tegmental area, and BA, 5-HT fibres are able to co-release glutamate (Liu et al., 2014; Chapter 5). VGluT3, similarly to “classical” glutamate transporters VGluT1 and VGluT2, is highly specific for glutamate, proton-dependent, and stimulated by chloride ions (Schäfer et al., 2002). The presence of VGluT3 confers on neurons the ability to transmit glutamate in

the lateral superior olive, auditory transduction pathway, and hippocampus (Gillespie et al., 2005; Seal et al., 2008; Varga et al., 2009). It should be noted, however, that functional glutamate release has only been demonstrated *in vitro*. There are also DRN neurons containing VGluT3 that are not 5-HT, GABA- or dopaminergic (Hioki et al., 2010), which supports the idea that VGluT3 contributes to glutamatergic transmission. Taken together, the evidence suggests that VGluT3 in 5-HT neurons has dual roles, one in supporting 5-HT transmission and the other in enabling glutamatergic signalling. In the context of fear regulation by BA circuits, the more important function of VGluT3 in 5-HT terminals could be in amplifying 5-HT transmission, making it relevant for 5-HT-based dysfunction in affective disorders.

7.4.4 Neurodevelopmental formation of the 5-HT transmission system

The results in this thesis showed that chronic postnatal 5-HTT blockade reversed the low-fear phenotype of adolescent 5-HTT OE mice, but acute 5-HTT blockade did not have any effect (Chapter 2). This indicated that the critical time of 5-HTT overexpression in shaping fear behaviour was not concurrent with performance on the behavioural task, but rather during early life development. 5-HT transmission during development contributes to the formation of neural fear circuits and of corresponding afferent 5-HT systems (Gaspar et al., 2003; Wellman et al., 2007; Karpova et al., 2009; Homberg et al., 2010; Olivier et al., 2011; Guidotti et al., 2012; Smit-Rigter et al., 2012; Calabrese et al., 2013; Rebello et al., 2014; Teissier et al., 2017). Furthermore, since acute 5-HTT blockade heightened fear learning in adolescent WTs but had no effect on 5-HTT OE mice, the 5-HT transmission system seemed to be disrupted in 5-HTT OE mice (Chapter 2). Similarly, acute tryptophan depletion in human subjects has opposite cognitive effects depending on 5-HTT expression levels (Roiser et al., 2007). These findings are in agreement with the observation that tissue 5-HT levels were lower in the DRN and BLA of 5-HTT OE mice (Chapter 2). Although the

current study demonstrated a reversal of the 5-HTT OE behavioural phenotype by chronic postnatal 5-HTT blockade, it did not test whether the neurochemical phenotype was rescued.

As discussed earlier, the regulation of fear learning by 5-HT projections to the BA could occur through a number of possible modulation mechanisms. These include gating other inputs to the BA (Cheng et al., 1998; Koyama et al., 1999; Yamamoto et al., 2012; Guo et al., 2017; Chapter 4), contributing to plasticity (Chen et al., 2003; Chapter 4), differentially influencing particular BA cell types (Chapter 5), and co-releasing glutamate (Chapter 5). Variation in 5-HTT expression during early life development could disrupt these aspects of 5-HT signalling later in life. Chronic SSRI treatment in adolescence, unlike in adulthood, increases behavioural despair and tends to elevate the expression of neuroplasticity markers in the amygdala (Homberg et al., 2011). Previous research has also reported altered postsynaptic 5-HT receptor function and impaired frequency sensitivity of 5-HT release in 5-HTT OE mice (Jennings et al., 2008, 2010; Bocchio et al., 2015). Moreover, since 5-HT terminals gate other afferents in the BA, (Cheng et al., 1998; Koyama et al., 1999; Yamamoto et al., 2012; Guo et al., 2017), 5-HT innervation needs to form in the proper manner, possibly in synaptic triads (Belmer et al., 2017), to correctly modulate other inputs. 5-HT afferents failing to form appropriately during postnatal development may underlie the inability of acute 5-HTT blockade to affect the low-fear phenotype of 5-HTT OE mice later in life. Therefore, the circuit-specific 5-HT modulation of the BA described in Chapters 3 to 6 might not have the same effects in mice with altered 5-HTT expression, though this was not within the scope of this thesis.

Variation in 5-HTT expression regulates the impact of traumatic life events on negative affect (Caspi et al., 2003). Further evidence of this gene × environment interaction comes from the fact that children and adolescents with lower 5-HTT expression are more sensitive to both negative and positive experiences (Hankin et al., 2011). This possibly arises from the modulatory role of the 5-HT system in adjusting stimulus-representing cellular inputs to neural fear circuits, such as to the BA. The interaction with environment is also reflected in 5-HT neuron function; in a mouse model of fear learning, 5-HT neuron

photoexcitation in the DRN only enhanced fear learning in animals pre-exposed to stress (Baratta et al., 2016). These findings together suggest that previous emotional experiences moderate the ability of 5-HT to affect fear. As discussed above, 5-HT afferents may be established ectopically during neurodevelopment depending on 5-HTT expression, and this could impair the regulation of emotionally salient experiences encoded heterosynaptically.

Interestingly, 5-HTT OE mice, which are associated with diminished 5-HT signalling, display reduced sensitivity to both negative and positive reinforcers (Jennings et al., 2010; Line et al., 2014). In contrast, specifically in the BA, enhanced 5-HT transmission appears to favour only fear but not extinction learning (Chapter 3). This discrepancy is likely due to the distinctive functions of 5-HT modulation in different brain circuits (Graeff et al., 1996). For example, 5-HT signalling in the nucleus accumbens or ventral tegmental area seems to regulate reward-based learning (Liu et al., 2014; McDevitt et al., 2014), while this thesis found that 5-HT transmission in the BA mediates fear learning in particular (Chapters 3 to 6).

7.5 Technical limitations and future directions

Multiple chapters in this thesis employed an optogenetic approach to reversibly and selectively manipulate the activity of DRN 5-HT projections to the BA. While this technique makes use of endogenously produced transmitters, it is not wholly physiological. First, 5-HT pathways are involved in critical feedback loops (Bosker et al., 2001) whose influence may become disrupted during photo-manipulation of 5-HT neurons. Second, laser stimulation trains can evoke unnatural firing patterns in ChR2-expressing and postsynaptic cells. One way to avoid this it to design more physiological stimulation protocols that match the natural activity of relevant circuits (Royer et al., 2010). DRN 5-HT neurons spontaneously fire over a wide range of frequencies (Allers and Sharp, 2003; Kocsis et al., 2006; Hajós et al., 2007). In the current study, 20 Hz laser stimulation trains were intended to emulate the firing rate of

DRN 5-HT neurons during emotionally salient experiences (Cohen et al., 2015; Li et al., 2016).

7.5.1 Achieving temporally precise measurements of BA 5-HT projection activity

The majority of experiments utilised optogenetic manipulations of DRN 5-HT projections to the BA, but the natural activation induced by fear conditioning was only measured in Chapter 6 using c-fos immunoreactivity. However, immunostaining of immediate-early genes lacks the temporal precision to monitor the real-time activity of 5-HT neurons during fear behaviour. In particular, the ability to record BA-projecting 5-HT neuron activity could shed light on whether the contribution of 5-HT transmission changes over the course of fear or extinction learning.

In vivo electrophysiology and calcium imaging studies have monitored the activity of DRN 5-HT neurons with temporal detail during reward-based and aversive learning tasks (Cohen et al., 2015; Li et al., 2016; Matias et al., 2017; Weixin et al., 2017). In these studies, 5-HT neurons have been targeted using Cre-dependent optogenetic constructs or calcium indicators. 5-HT neurons are identified either by "photo-tagging" (based on reliably evoked neuronal responses to light stimulation) or visually (based on fluorescent indicators). DRN 5-HT neurons are known to display non-uniform electrophysiological properties and functional responses (Kocsis et al., 2006; Cohen et al., 2015). It would be interesting to test whether DRN 5-HT neurons display less heterogeneous behaviour when they share a common projection target. Therefore, BA-projecting DRN neurons could be specifically targeted by delivering Cre-recombinase in a retrograde transducing CAV2 viral vector into the BA while introducing Cre-driven opsins or genetically encoded indicators to the DRN for photo-tagging or imaging experiments (Gore et al., 2013). The rapidly progressing imaging techniques offer increasingly sensitive and precise approaches to monitor neuronal activity;

the imaging quality of recent miniature microscopy facilitates capturing hundreds of cells within a single experiment (Ghosh et al., 2011).

The causal role of DRN 5-HT projections to the BA was investigated through optogenetic interventions, but the natural activity of BA 5-HT terminals was not directly measured during fear learning. Thus, similar to c-fos staining, these experiments were unable to dissect the temporally precise behaviour of BA 5-HT projections during the fear learning and extinction processes. Recent technological advances have overcome challenges of imaging deep brain structures such as the BA using microendoscopes (Hamel et al., 2015). For a detailed read-out of 5-HT projection activity during the fear learning task, calcium imaging of DRN 5-HT axons in the BA could be achieved by implanting an optic fibre sensitive enough to detect activity changes in neuronal fibres (Gunaydin et al., 2014).

7.5.2 Probing modulation of BA information processing by 5-HT transmission

In addition to elucidating the activity of DRN 5-HT projection activity in the BA during fear learning, the influence of 5-HT transmission on information processing and storage in the BA needs to be investigated. Earlier, it was discussed that 5-HT signalling in the BA likely affects BA rate coding. The potential 5-HT impact on a temporal code cannot be evaluated without analysing the phase-locking of BA single unit firing to network oscillations. The long-term effects of 5-HT projection photo-excitation on BA physiology and fear behaviour indicate that, among other mechanisms, 5-HT inputs to the BA mediate plasticity. In addition, 5-HT regulates other afferents in the BA (Cheng et al., 1998; Koyama et al., 1999; Yamamoto et al., 2012; Guo et al., 2017). Slice electrophysiology experiments should be carried out to characterise the actions of 5-HT on the synaptic strength of other BA inputs. Optogenetic excitation of 5-HT terminals during behaviour could be followed by *ex vivo* whole-cell recordings of BA neurons to test the influence of 5-HT on BA synapses during fear learning. 5-HT afferents could also be photo-excited at different frequencies in slices, in the

presence or absence of specific receptor antagonists. This approach would enable a detailed study of plastic events and the mechanisms through which 5-HT moderates them.

Importantly, 5-HT mediated plasticity can occur both perisomatically and at BA distal dendrites (McDonald and Mascagni, 2007). While whole-cell electrophysiology detects electrical changes predominantly in the soma, imaging with voltage indicators allows recording of activity changes in subcellular compartments including dendrites. Another advantage of imaging is that it can be conducted *in vivo* with a high degree of spatial resolution. Recent developments in the speed and dynamic range of genetically encoded voltage indicators provide the means to monitor dendritic voltage changes in awake, behaving mice (Gong et al., 2015). In addition, a novel "all-optical" approach combines optogenetics with imaging techniques, instead of with electrophysiological techniques, to manipulate neurons while simultaneously recording activity without optical cross-talk (Emiliani et al., 2015). In fact, this new approach possesses single cell-specificity, enabling the testing of BA circuit-specific 5-HT mechanisms *in vivo* that were previously identified *in vitro*; photo-excitation of DRN 5-HT terminals could be combined with calcium or voltage imaging of postsynaptic BA neurons (Rajasethupathy et al., 2015).

An advantage of *in vivo* miniature microscopy over microelectrode electrophysiology is that network dynamics can be spatially visualised across the BA over several days. Calcium imaging has thus been used to characterise BA neuronal ensembles over the course of fear learning and extinction (Grewe et al., 2017). A similar approach could be used to investigate the dynamic effects of 5-HT transmission during behaviour. Indeed, immediate-early gene-driven optogenetic control could be used to specifically capture control of DRN 5-HT projections to the BA that are naturally activated during fear learning (Gore et al., 2015). Additionally, voltage indicators can be used to record field potentials, allowing visualisation of oscillatory activity shaped by 5-HT transmission across the BA (Gong et al., 2015). This would be particularly intriguing in the amygdala, which lacks the laminar organisation of the hippocampus or cortex and would therefore be unlikely to generate oscillations through the sources and sinks described in the hippocampus (Buzsáki, 2002). Voltage dyes can even be

genetically directed to certain neurons to monitor the field potentials evoked by particular BA cell types during behaviour (Marshall et al., 2016). This could, for example, help clarify whether parvalbumin INs generate theta oscillations in the BA, as they do in the prefrontal cortex and hippocampus (Courtin et al., 2013; Amilhon et al., 2015), and whether 5-HT projections modulate this mechanism.

7.5.3 Achieving precise manipulation of VGluT3 function

Previous studies have made use of global, constitutive VGluT3 knockout mice to probe the role of the atypical glutamate transporter (Amilhon et al., 2010; Liu et al., 2014; Voisin et al., 2016). However, this approach cannot truly isolate glutamatergic signalling of 5-HT neurons, and may have off-target effects that give rise to the findings reported in those studies. First, VGluT3 is expressed in non-5-HT neurons and in brain regions other than the DRN (Gras et al., 2002, 2008; Hioki et al., 2004; Gillespie et al., 2005). Second, early postnatal VGluT3 expression patterns differ from adulthood, and may serve a unique developmental function (Gras et al., 2005). Third, long-term knockout may lead to compensatory mechanisms that alter aspects of both glutamatergic and 5-HT transmission mechanisms that do not simply reflect the absence of VGluT3.

To address these challenges, a Cre-driven RNA interference strategy can be employed (Ventura et al., 2004). In this approach, a viral vector with a Cre-dependent construct encoding RNA designed to disrupt VGluT3 expression could be delivered into the DRN of 5-HTT-Cre mice. This would allow cell type-specific VGluT3 knockdown in DRN 5-HT neurons. Alternatively, the retrograde CAV2-Cre construct could be introduced into the BA to only knockdown VGluT3 in BA-projecting DRN neurons in a pathway-specific manner. These mice could be analysed through a battery of behavioural tests, neurochemical 5-HT measurements, *ex vivo* slice electrophysiology, and vesicular filling assays.

7.5.4 Towards a study of circuit dysfunction in psychopathology

As discussed earlier, 5-HT transmission during postnatal development seems to be crucial in shaping fear-related neural circuits and behaviours (Gaspar et al., 2003; Ansorge et al., 2008; Karpova et al., 2009; Homberg et al., 2010; Calabrese et al., 2013; Rebello et al., 2014; Teissier et al., 2017). Although the low-fear and low-anxiety phenotypes of 5-HTT OE mice were both reversed by chronic postnatal 5-HTT blockade, the neurochemical phenotype was not investigated following postnatal SSRI treatment. It should be verified whether, similar to the behavioural phenotype, the low-tissue 5-HT levels of 5-HTT OE mice are restored by chronic postnatal SSRI administration. If the neurochemical phenotype were restored, it would support the idea that postnatal 5-HTT is responsible for setting up neural fear circuits and their 5-HT afferent pathways. In addition, it could be tested whether 5-HTT OE mice postnatally treated with SSRI have restored 5-HT function by checking if acute 5-HTT inhibition in the same animals in adolescence elevates fear learning in the same manner as in WTs. Such experiments could shed light on why individuals respond differently to SSRI treatment in later life; variation in 5-HTT expression could underlie some of the discrepant effects of pharmacotherapy for mood disorders.

In a similar way, it could also be investigated whether 5-HTT OE mice fail to exhibit the relationship between BA 5-HT transmission and fear behaviour that was demonstrated in Chapters 3 to 6. This would require crossing the 5-HTT OE and 5-HTT-Cre transgenic mouse lines to enable optogenetic dissection of circuit-specific 5-HT pathways in the translationally relevant 5-HTT OE model. If photoexcitation of BA 5-HT fibres failed to produce the same effects reported in this thesis, a rescue of the normal role of 5-HT afferents could be attempted through chronic postnatal 5-HTT blockade. In addition, local field potentials could be simultaneously recorded in the prefrontal cortex and BA to explore how top-down entrainment of network activity is affected by the 5-HT system, as has been demonstrated in 5-HTT KO mice (Narayanan et al., 2011).

Although cell-type specific tools may not be easily translated at present, using them to gather data about relevant neural circuits is important for understanding the aetiology of affective disorders. This could be particularly informative about mechanisms that become dysregulated in animal models of psychopathology. This thesis focussed on 5-HT transmission in the amygdala, but 5-HT projections are known to collateralise and target multiple brain regions (Gagnon and Parent, 2014). After verifying whether 5-HT inputs to the BA are altered by 5-HTT expression variation, other circuits innervated by the same 5-HT neurons could be identified and studied. BA-projecting DRN neurons could be labelled by using the retrograde transducing CAV2-Cre vector in the BA (Gore et al., 2013). Different Cre-dependent constructs could then be delivered to the DRN, such as fluorescently-tagged synaptophysin to visualise synaptic terminals across the brain (Herman et al., 2016), calcium or voltage indicators to record projection activity during fear behaviour (Gunaydin et al., 2014), or opsins to control fibre activity in target regions other than the BA. 5-HT projection pathways to distinct anatomical targets are thought to mediate different functions (Deakin and Graeff, 1991), but it is unclear whether this is true for axonal branches within individual neurons. Analysis of BA projection collaterals to other circuits would help resolve the potentially multifaceted role of DRN neurons and address whether certain functions over others become disrupted in affective disorder models.

As the major source of 5-HT innervation in the brain, the DRN can be regarded as part of a larger circuit involved in regulating fear behaviour. Therefore, to understand how 5-HTT expression variation and altered 5-HT transmission can impact neural fear circuits, it would be helpful to map DRN efferent and afferent connectivity and study its function in models of psychopathology. Anterograde trans-synaptic labelling with Cre-dependent herpes simplex viral vectors can be used to identify cells in different brain regions that are postsynaptic to DRN 5-HT neurons (Lo and Anderson, 2011). These targets can be compared across models of 5-HTT expression variation, based on quantity, morphology, electrophysiological properties, and molecular expression profiles, among other features. In the BA in particular, functional output pathways can be distinguished by retrograde beads in

the prelimbic and infralimbic cortices (Senn et al., 2014). As mentioned earlier, prelimbic projector cells in the BA seem to mediate fear learning, whereas infralimbic projectors underlie extinction learning. Thus, acute slice electrophysiology experiments could compare whether 5-HT modulation of these mutually exclusive BA subpopulations differs after mice undergo fear learning tasks and, if so, becomes altered in 5-HTT expression variation models. Inputs should also be taken into account when considering the function of DRN 5-HT neurons. In three extensive tracing studies, monosynaptic inputs to DRN 5-HT neurons were labelled using a Cre-dependent retrograde rabies viral strategy (Ogawa et al., 2014; Pollak Dorocic et al., 2014; Weissbourd et al., 2014). Such tracing studies can be used to design circuit-based optogenetic, electrophysiology, or imaging studies that can investigate functional changes in inputs to DRN 5-HT neurons as a result of 5-HTT expression variation.

7.6 Conclusions

In summary, the data presented in this thesis highlight the BA as a key site for 5-HT signalling during fear and extinction learning, using neurophysiology, behaviour, and a translationally relevant transgenic mouse model. It was shown, either systemically or in the BA, that 5-HT modulates temporally-specific phenomena that have previously been identified as crucial for fear behaviour (Herry et al., 2008; McHugh et al., 2014; Sarkar et al., 2014). Namely, 5-HT transmission during neurodevelopment is critical in establishing neural circuits and 5-HT innervation that underlie aversive learning later in life. Hence, normal fear learning relies on 5-HT mechanisms during both development and behaviour. Furthermore, 5-HT inputs to the BA favour fear learning and retrieval by biasing BA information representation towards a high-fear state via circuit- and cell type-specific mechanisms.

This thesis provided a novel contribution to the knowledge of how the 5-HT neuromodulatory system regulates fear behaviour, particularly through its actions on BA circuits. Given the widespread projection pathways of 5-HT neurons and their multifaceted functions, it is necessary to investigate the circuit-specific roles of 5-HT to gain a mechanistic

understanding of emotional control in health and disease. This is particularly important because systemic pharmacological therapies often have inconsistent results in patients (Vasa et al., 2006). The work conducted in this thesis was intended as an acknowledgment of the complexity of 5-HT transmission and a preliminary attempt at disentangling some of its precise actions. A meticulous dissection of circuit-, temporal-, and receptor-specific 5-HT mechanisms could clarify the individual differences observed in human patients, leading the way for improved and personalised therapies in the future.

To conclude this thesis, perhaps I might take heed of Salvador Dali's apt advice to extinguish some of my own fears: "Have no fear of perfection; you'll never reach it."

References

Abrams JK, Johnson PL, Hay-Schmidt A, Mikkelsen JD, Shekhar A, Lowry CA (2005) Serotonergic systems associated with arousal and vigilance behaviors following administration of anxiogenic drugs. Neuroscience 133:983–997.

Adolphs R (1997) Fear and the human amygdala. Neurocase 3:267–274.

Aghajanian GK, Bloom FE (1967) Localization of tritiated serotonin in rat brain by electron-microscopic autoradiography. J Pharmacol Exp Ther 156:23–30.

Alexandre C, Popa D, Fabre V, Bouali S, Venault P, Lesch K, Hamon M, Adrien J (2006) Early Life Blockade of 5-Hydroxytryptamine 1A Receptors Normalizes Sleep and Depression-Like Behavior in Adult Knock-Out Mice Lacking the Serotonin Transporter. J Neurosci 26:5554–5564.

Allers KA, Sharp T (2003) Neurochemical and anatomical identification of fast- and slow-firing neurones in the rat dorsal raphe nucleus using juxtacellular labelling methods in vivo. Neuroscience 122:193–204.

Alvarez RP, Biggs A, Chen G, Pine DS, Grillon C (2008) Contextual Fear Conditioning in Humans: Cortical-Hippocampal and Amygdala Contributions. J Neurosci 28:6211–6219.

Amano T, Duvarci S, Popa D, Paré D (2011) The fear circuit revisited: contributions of the basal amygdala nuclei to conditioned fear. J Neurosci 31:15481–15489.

Amat J, Matus-Amat P, Watkins LR, Maier SF (1998) Escapable and inescapable stress differentially alter extracellular levels of 5-HT in the basolateral amygdala of the rat. Brain Res 812:113–120.

Amilhon B, Lepicard E, Renoir T, Mongeau R, Popa D, Poirel O, Miot S, Gras C, Gardier AM, Gallego J, Hamon M, Lanfumey L, Gasnier B, Giros B, El Mestikawy S (2010) VGLUT3 (Vesicular Glutamate Transporter Type 3) Contribution to the Regulation of Serotonergic Transmission and Anxiety. J Neurosci 30:2198–2210.

Amilhon B, Huh CYL, Manseau F, Ducharme G, Nichol H, Adamantidis A, Williams S (2015) Parvalbumin Interneurons of Hippocampus Tune Population Activity at Theta Frequency. Neuron 86:1277–1289.

Amodeo DA, Rivera E, Cook EH, Sweeney JA, Ragozzino ME (2017) 5HT2A receptor blockade in dorsomedial striatum reduces repetitive behaviors in BTBR mice. Genes, Brain Behav 16:342–351.

Anglada-Figueroa D, Quirk G (2005) Lesions of the Basal Amygdala Block Expression of Conditioned Fear But Not Extinction. J Neurosci 25:9680–9685.

Ansorge MS, Morelli E, Gingrich JA (2008) Inhibition of serotonin but not norepinephrine transport during development produces delayed, persistent perturbations of emotional behaviors in mice. J Neurosci 28:199–207.

Ansorge MS, Zhou M, Lira A, Hen R, Gingrich JA (2004) Early-life blockade of the 5-HT transporter alters emotional behavior in adult mice. Science 306:879–881.

Arruda-Carvalho M, Clem RL (2014) Pathway-Selective Adjustment of Prefrontal-Amygdala Transmission during Fear Encoding. J Neurosci 34:15601–15609.

Arruda-Carvalho M, Clem RL (2015) Prefrontal-amygdala fear networks come into focus. Front Syst Neurosci 9:145.

Asan E, Steinke M, Lesch KP (2013) Serotonergic innervation of the amygdala: Targets, receptors, and implications for stress and anxiety. Histochem Cell Biol 139:785–813.

Ascoli GA et al. (2008) Petilla terminology: nomenclature of features of GABAergic interneurons of the cerebral cortex. Nat Rev Neurosci 9:557–568.

Asede D, Bosch D, Lüthi A, Ferraguti F, Ehrlich I (2015) Sensory inputs to intercalated cells provide fear-learning modulated inhibition to the basolateral amygdala. Neuron 86:541–554.

Ashby CR, Edwards E, Wang RY (1992) Action of serotonin in the medial prefrontal cortex-mediation by serotonin 3-like receptors. Synapse 10:7–15.

Assie M-B, Lomenech H, Ravailhe V, Faucillon V, Newman-Tancredi A (2006) Rapid desensitization of somatodendritic 5-HT 1A receptors by chronic administration of the high- efficacy 5-HT 1A agonist, F13714: a microdialysis study in the rat. Br J Pharmacol 149:170–178.

Atasoy D, Aponte Y, Su HH, Sternson SM (2008) A FLEX Switch Targets Channelrhodopsin-2 to Multiple Cell Types for Imaging and Long-Range Circuit Mapping. J Neurosci 28:7025–7030.

Azmitia C, Segal M (1978) An Autoradiographic Analysis of the Differential Ascending Projections of the Dorsal and Median Raphe Nuclei in the Rat. J Comp Neurol 179:641–668.

Aznar S, Qian ZX, Knudsen GM (2004) Non-serotonergic dorsal and median raphe projection onto parvalbumin- and calbindin-containing neurons in hippocampus and septum. Neuroscience 124:573–581.

Aznar S, Qian Z, Shah R, Rahbek B, Knudsen GM (2003) The 5-HT1A serotonin receptor is located on calbindin- and parvalbumin-containing neurons in the rat brain. Brain Res 959:58–67.

Bannerman DM, Deacon RMJ, Offen S, Friswell J, Grubb M, Rawlins JNP (2002) Double dissociation of function within the hippocampus: Spatial memory and hyponeophagia. Behav Neurosci 116:884–901.

Baratta M V., Kodandaramaiah SB, Monahan PE, Yao J, Weber MD, Lin PA, Gisabella B, Petrossian N, Amat J, Kim K, Yang A, Forest CR, Boyden ES, Goosens KA (2016) Stress Enables Reinforcement-Elicited Serotonergic Consolidation of Fear Memory. Biol Psychiatry 79:814–822.

Barkus C, Line SJ, Huber A, Capitao L, Lima J, Jennings K, Lowry J, Sharp T, Bannerman DM, McHugh SB (2014) Variation in serotonin transporter expression modulates fear-evoked hemodynamic responses and theta-frequency neuronal oscillations in the amygdala. Biol Psychiatry 75:901–908.

Barnes NM, Sharp T (1999) A review of central 5-HT receptors and their function. Neuropharmacology 38:1083–1152.

Bazelot M, Bocchio M, Kasugai Y, Fischer D, Dodson PD, Ferraguti F, Capogna M (2015) Hippocampal Theta Input to the Amygdala Shapes Feedforward Inhibition to Gate Heterosynaptic Plasticity. Neuron 87:1290–1303.

Bechara A, Tranel D, Damasio H, Adolphs R, Rockland C, Damasio A (1995) Double dissociation of conditioning and declarative knowledge relative to the amygdala and hippocampus in humans. Science 269:1115–1118.

Belin MF, Nanopoulos D, Didier M, Aguera M, Steinbusch H, Verhofstad A, Maitre M, Pujol JF (1983) Immunohistochemical evidence for the presence of gamma-aminobutyric acid and serotonin in one nerve cell. A study on the raphe nuclei of the rat using antibodies to glutamate decarboxylase and serotonin. Brain Res 275:329–339.

Belmer A, Klenowski PM, Patkar OL, Bartlett SE (2017) Mapping the connectivity of serotonin transporter immunoreactive axons to excitatory and inhibitory neurochemical synapses in the mouse limbic brain. Brain Struct Funct 222:1297–1314.

Benekareddy M, Vadodaria KC, Nair AR, Vaidya VA (2011) Postnatal serotonin type 2 receptor blockade prevents the emergence of anxiety behavior, dysregulated stress-induced immediate early gene responses, and specific transcriptional changes that arise following early life stress. Biol Psychiatry 70:1024–1032.

Bengel D, Murphy DL, Andrews AM, Wichems CH, Feltner D, Science C, Maryland DB (1998) Altered Brain Serotonin Homeostasis and Locomotor Insensitivity to 3 , 4-Methylenedioxymethamphetamine (“Ecstasy”) in Serotonin Transporter-Deficient Mice. Mol Pharmacol 655:649–655.

Bergado JA, Lucas M, Richter-Levin G (2011) Emotional tagging-A simple hypothesis in a complex reality. Prog Neurobiol 94:64–76.

Bernstein JG, Boyden ES (2011) Optogenetic tools for analyzing the neural circuits of behavior. Trends Cogn Sci 15:592–600.

Bienvenu TCM, Busti D, Magill PJ, Ferraguti F, Capogna M (2012) Cell-Type-Specific Recruitment of Amygdala Interneurons to Hippocampal Theta Rhythm and Noxious Stimuli In Vivo. Neuron 74:1059–1074.

Bigos KL, Pollock BG, Aizenstein HJ, Fisher PM, Bies RR, Hariri AR (2008) Acute 5-HT reuptake blockade potentiates human amygdala reactivity. Neuropsychopharmacology 33:3221–3225.
Bissière S, Humeau Y, Lüthi A (2003) Dopamine gates LTP induction in lateral amygdala by suppressing feedforward inhibition. Nat Neurosci 6:587–592.
Bisson J, Roberts N, Andrew M, Cooper R, Lewis C (2013) Psychological therapies for chronic post-traumatic stress disorder (PTSD) in adults. Cochrane Database Syst Rev.
Blakely RD, De Felice LJ, Hartzell HC (1994) Molecular physiology of norepinephrine and serotonin transporters. J Exp Biol 196:263–281.
Blakely RD, Berson HE, Fremeau RT, Caron MG, Peek MM, Prince HK, Bradley CC (1991) Cloning and expression of a functional serotonin transporter from rat brain. Nature 354:66–70.
Bocchio M, Fisher SP, Capogna M, Unal G, Ellender TJ, Vyazovskiy V V (2016) Sleep and Serotonin Modulate Paracapsular Nitric Oxide Synthase Expressing Neurons of the Amygdala. eNeuro 3.
Bocchio M, Fucsina G, Oikonomidis L, McHugh SB, Bannerman DM, Sharp T, Capogna M (2015) Increased Serotonin Transporter Expression Reduces Fear and Recruitment of Parvalbumin Interneurons of the Amygdala. Neuropsychopharmacology 40:3015–3026.
Bocchio M, McHugh SB, Bannerman DM, Sharp T, Capogna M (2016) Serotonin, Amygdala and Fear: Assembling the Puzzle. Front Neural Circuits 10:24.
Bocchio M, Nabavi S, Capogna M (2017) Synaptic Plasticity, Engrams, and Network Oscillations in Amygdala Circuits for Storage and Retrieval of Emotional Memories. Neuron 94:731–743.
Boll S, Gamer M, Gluth S, Finsterbusch J, Büchel C (2013) Separate amygdala subregions signal surprise and predictiveness during associative fear learning in humans. Eur J Neurosci 37:758–767.
Bonn M, Schmitt A, Lesch KP, Van Bockstaele EJ, Asan E (2013) Serotonergic innervation and serotonin receptor expression of NPY-producing neurons in the rat lateral and basolateral amygdaloid nuclei. Brain Struct Funct 218:421–435.
Bosker FJ, Cremers TIFH, Jongsma ME, Westerink BHC, Wikström H V., Den Boer JA (2001) Acute and chronic effects of citalopram on postsynaptic 5-hydroxytryptamine1A receptor-mediated feedback: A microdialysis study in the amygdala. J Neurochem 76:1645–1653.
Bosker FJ, Klompmakers A, Westenberg HGM (1997) Postsynaptic 5-HT(1A) receptors mediate 5-hydroxytryptamine release in the amygdala through a feedback to the caudal linear raphe. Eur J Pharmacol 333:147–157.
Bosker F, Vrinten D, Klompmakers A, Westenberg H (1997) The effects of A 5-HT1A receptor agonist and antagonist on the 5-hydroxytryptamine release in the central nucleus of the amygdala: a microdialysis study with flesinoxan and WAY 100635. Naunyn Schmiedebergs Arch Pharmacol 355:347–53.
Bowker RM, Westlund KN, Sullivan MC, Wilber JF, Coulter JD (1982) Transmitters of the raphe-spinal complex: Immunocytochemical studies. Peptides 3:291–298.
Bremner JD, Staib LH, Kaloupek D, Southwick SM, Soufer R, Charney DS (1999) Neural correlates of exposure to traumatic pictures and sound in Vietnam combat veterans with and without posttraumatic stress disorder: A positron emission tomography study. Biol Psychiatry 45:806–816.
Brocke B, Armbruster D, Muller J, Hensch T, Jacob CP, Lesch K-P, Kirschbaum C, Strobel A (2006) Serotonin transporter gene variation impacts innate fear processing: acoustic startle response and emotional startle. Mol Psychiatry 11:1106–1112.
Büchel C, Morris J, Dolan RJ, Friston KJ (1998) Brain systems mediating aversive conditioning: An event-related fMRI study. Neuron 20:947–957.
Bukalo O, Pinard CR, Silverstein S, Brehm C, Hartley ND, Whittle N, Colacicco G, Busch E, Patel S, Singewald N, Holmes A (2015) Prefrontal inputs to the amygdala instruct fear extinction memory formation. Sci Adv 1:e1500251.
Burghardt NS, Sullivan GM, McEwen BS, Gorman JM, Ledoux JE (2004) The selective serotonin reuptake inhibitor citalopram increases fear after acute treatment but reduces fear with chronic treatment: A comparison with tianeptine. Biol Psychiatry 55:1171–1178.
Burnham KE (2009) Investigating the role of 5-HT6 receptors in prefrontal cortical function. PhD thesis. In: Department of Pharmacology, University of Oxford.

Buzsáki G (2002) Theta oscillations in the hippocampus. Neuron 33:325–340.
Calabrese F, Guidotti G, Middelman A, Racagni G, Homberg J, Riva M a (2013) Lack of serotonin transporter alters BDNF expression in the rat brain during early postnatal development. Mol Neurobiol 48:244–256.
Campbell BM, Merchant KM (2003) Serotonin 2C receptors within the basolateral amygdala induce acute fear-like responses in an open-field environment. 993:1–9.
Caspi A, Hariri AR, Holmes A, Uher R, Moffitt TE (2010) Genetic sensitivity to the environment: the case of the serotonin transporter gene and its implications for studying complex diseases and traits. Am J Psychiatry 167:509–527.
Cassell MD, Gray TS (1989) Morphology of peptide-immunoreactive neurons in the rat central nucleus of the amygdala. J Comp Neurol 281:320–333.
Challis C, Boulden J, Veerakumar A, Espallergues J, Vassoler FM, Pierce RC, Beck SG, Berton O (2013) Raphe GABAergic Neurons Mediate the Acquisition of Avoidance after Social Defeat. J Neurosci 33:13978–13988.
Chan-Palay V, Jonsson G, Palay SL (1978) Serotonin and substance P coexist in neurons of the rat's central nervous system. Proc Natl Acad Sci 75:1582–1586.
Chen A, Hough CJ, Li H (2003) Serotonin type II receptor activation facilitates synaptic plasticity via n-methyl-D-aspartate-mediated mechanism in the rat basolateral amygdala. Neuroscience 119:53–63.
Cheng L, Wang S, Gean P (1998) Serotonin depresses excitatory synaptic transmission and depolarization-evoked Ca 2+ influx in rat basolateral amygdala via 5-HT 1A receptors. Eur J Neurosci 10:2163–2172.
Cheriyan J, Kaushik MK, Ferreira AN, Sheets PL (2016) Specific targeting of the basolateral amygdala to projectionally defined pyramidal neurons in prelimbic and infralimbic cortex. eNeuro 3:2–16.
Chiu CQ, Lur G, Morse TM, Carnevale NT, Ellis-Davies GCR, Higley MJ (2013) Compartmentalization of GABAergic Inhibition by Dendritic Spines. Science 340:759–762.
Cho JH, Deisseroth K, Bolshakov VY (2013) Synaptic encoding of fear extinction in mPFC-amygdala circuits. Neuron 80:1491–1507.
Christianson JP, Ragole T, Amat J, Greenwood BN, Strong P V., Paul ED, Fleshner M, Watkins LR, Maier SF (2010) 5-Hydroxytryptamine 2C Receptors in the Basolateral Amygdala Are Involved in the Expression of Anxiety After Uncontrollable Traumatic Stress. Biol Psychiatry 67:339–345.
Ciocchi S, Herry C, Grenier F, Wolff SBE, Letzkus JJ, Vlachos I, Ehrlich I, Sprengel R, Deisseroth K, Stadler MB, Müller C, Lüthi A (2010) Encoding of conditioned fear in central amygdala inhibitory circuits. Nature 468:277–282.
Cohen JY, Amoroso MW, Uchida N (2015) Serotonergic neurons signal reward and punishment on multiple timescales. Elife 4:1–25.
Commons KG (2009) Locally collateralizing glutamate neurons in the dorsal raphe nucleus responsive to substance P contain vesicular glutamate transporter 3 (VGLUT3). J Chem Neuroanat 38:273–281.
Cornélio AM, Nunes-de-Souza RL (2007) Anxiogenic-like effects of mCPP microinfusions into the amygdala (but not dorsal or ventral hippocampus) in mice exposed to elevated plus-maze. Behav Brain Res 178:82–89.
Costall B, Kelly ME, Naylor RJ, Onaivi ES, Tyers MB (1989) Neuroanatomical sites of action of 5-HT3 receptor agonist and antagonists for alteration of aversive behaviour in the mouse. Br J Pharmacol 96:325–332.
Courtin J, Chaudun F, Rozeske RR, Karalis N, Gonzalez-Campo C, Wurtz H, Abdi A, Baufreton J, Bienvenu TCM, Herry C (2013) Prefrontal parvalbumin interneurons shape neuronal activity to drive fear expression. Nature 505:92–96.
Dahlström A, Fuxe K (1964) Localization of monoamines in the lower brain stem. Experientia 20:398–399.

Dannlowski U, Ohrmann P, Bauer J, Deckert J, Hohoff C, Kugel H, Arolt V, Heindel W, Kersting A, Baune BT, Suslow T (2008) 5-HTTLPR biases amygdala activity in response to masked facial expressions in major depression. Neuropsychopharmacology 33:418–424.

Davis M (1992) The role of the amygdala in fear and anxiety. Annu Rev Neurosci 15:353–375.

Davis M, Rainnie D, Cassell M (1994) Neurotransmission in the rat amygdala related to fear and anxiety. Trends Neurosci 17:208–214.

Davis P, Zaki Y, Maguire J, Reijmers LG (2017) Cellular and oscillatory substrates of fear extinction learning. Nat Neurosci 20:1624–1633.

Day HEW, Greenwood BN, Hammack SE, Watkins LR, Fleshner M, Maier SF, Campeau S (2004) Differential expression of 5HT-1A, alpha 1b adrenergic, CRF-R1, and CRF-R2 receptor mRNA in serotonergic, gamma-aminobutyric acidergic, and catecholaminergic cells of the rat dorsal raphe nucleus. J Comp Neurol 474:364–378.

De Mello Cruz AP, Pinheiro G, Alves SH, Ferreira G, Mendes M, Faria L, Macedo CE, Motta V, Landeira-Fernandez J (2005) Behavioral effects of systemically administered MK-212 are prevented by ritanserin microinfusion into the basolateral amygdala of rats exposed to the elevated plus-maze. Psychopharmacology (Berl) 182:345–354.

De Oca BM, DeCola JP, Maren S, Fanselow MS (1998) Distinct regions of the periaqueductal gray are involved in the acquisition and expression of defensive responses. J Neurosci 18:3426–3432.

Deakin JFW, Graeff FG (1991) 5-HT and mechanisms of defence. J Psychopharmacol 5:339–341.

Dejean C, Courtin J, Rozeske RR, Bonnet MC, Dousset V, Michelet T, Herry C (2015) Neuronal Circuits for Fear Expression and Recovery: Recent Advances and Potential Therapeutic Strategies. Biol Psychiatry 78:298–306.

Delgado MR, Olsson A, Phelps EA (2006) Extending animal models of fear conditioning to humans. Biol Psychol 73:39–48.

Descarries L, Watkins KC, Garcia S, Beaudet A (1982) The serotonin neurons in nucleus raphe dorsalis of adult rat: a light and electron microscope radioautographic study. J Comp Neurol 207:239–254.

Descarries L, Alain B, Watkins KC (1975) Serotonin nerve terminals in adult rat neocortex. Brain Res 100:563–588.

Domschke K, Braun M, Ohrmann P, Suslow T, Kugel H, Bauer J, Hohoff C, Kersting A, Engelien A, Arolt V, Heindel W, Deckert J (2006) Association of the functional -1019C/G 5-HT1A polymorphism with prefrontal cortex and amygdala activation measured with 3 T fMRI in panic disorder. Int J Neuropsychopharmacol 9:349–355.

Duvarci S, Pare D (2014) Amygdala microcircuits controlling learned fear. Neuron 82:966–980.

Duxon MS, Kennett GA, Lightowler S, Blackburn TP, Fone KC (1997) Activation of 5-HT2B receptors in the medial amygdala causes anxiolysis in the social interaction test in the rat. Neuropharmacology 36:601–608.

Ehrlich I, Humeau Y, Grenier F, Ciocchi S, Herry C, Lüthi A (2009) Amygdala Inhibitory Circuits and the Control of Fear Memory. Neuron 62:757–771.

Eichhammer P, Langguth B, Wiegand R, Kharraz A, Frick U, Hajak G (2003) Allelic variation in the serotonin transporter promoter affects neuromodulatory effects of a selective serotonin transporter reuptake inhibitor (SSRI). Psychopharmacology (Berl) 166:294–297.

Eidelberg E, Goldstein GP, Deza L (1967) Evidence for serotonin as a possible inhibitory transmitter in some limbic structures. Exp Brain Res 4:73–80.

Emiliani V, Cohen AE, Deisseroth K, Hausser M (2015) All-Optical Interrogation of Neural Circuits. J Neurosci 35:13917–13926.

Erickson JD, Schafer MK, Bonner TI, Eiden LE, Weihe E (1996) Distinct pharmacological properties and distribution in neurons and endocrine cells of two isoforms of the human vesicular monoamine transporter. Proc Natl Acad Sci 93:5166–5171.

Esaki T, Cook M, Shimoji K, Murphy DL, Sokoloff L, Holmes A (2005) Developmental disruption of serotonin transporter function impairs cerebral responses to whisker stimulation in mice. Proc Natl Acad Sci 102:5582–5587.

Fanselow MS (2010) From contextual fear to a dynamic view of memory systems. Trends Cogn Sci 14:7–15.

Fendt M, Fanselow MS (1999) The neuroanatomical and neurochemical basis of conditioned fear. Neurosci Biobehav Rev 23:743–760.

Feng J, Cai X, Zhao J, Yan Z (2001) Serotonin receptors modulate GABA(A) receptor channels through activation of anchored protein kinase C in prefrontal cortical neurons. J Neurosci 21:6502–6511.

Fernandez SP, Cauli B, Cabezas C, Muzerelle A, Poncer J-C, Gaspar P (2016) Multiscale single-cell analysis reveals unique phenotypes of raphe 5-HT neurons projecting to the forebrain. Brain Struct Funct 221:4007–4025.

File SE, James TA, MacLeod NK (1981) Depletion in amygdaloid 5-hydroxytryptamine concentration and changes in social and aggressive behaviour. J Neural Transm 50:1–12.

Flores Á, Herry C, Maldonado R, Berrendero F (2017) Facilitation of Contextual Fear Extinction by Orexin-1 Receptor Antagonism Is Associated with the Activation of Specific Amygdala Cell Subpopulations. Int J Neuropsychopharmacol 20:654–659.

Fremeau RT, Burman J, Qureshi T, Tran CH, Proctor J, Johnson J, Zhang H, Sulzer D, Copenhagen DR, Storm-Mathisen J, Reimer RJ, Chaudhry F a, Edwards RH (2002) The identification of vesicular glutamate transporter 3 suggests novel modes of signaling by glutamate. Proc Natl Acad Sci 99:14488–14493.

Freund N, Thompson BS, Denormandie J, Vaccarro K, Andersen SL (2013) Windows of vulnerability: Maternal separation, age, and fluoxetine on adolescent depressive-like behavior in rats. Neuroscience 249:88–97.

Fu W, Le Maître E, Fabre V, Bernard JF, Xu ZQD, Hökfelt T (2010) Chemical neuroanatomy of the dorsal raphe nucleus and adjacent structures of the mouse brain. J Comp Neurol 518:3464–3494.

Fujimiya M, Kimura H, Maeda T (1986) Postnatal development of serotonin nerve fibers in the somatosensory cortex of mice studied by immunohistochemistry. J Comp Neurol 246:191–201.

Furmark T, Tillfors M, Garpenstrand H, Marteinsdottir I, Långström B, Oreland L, Fredrikson M (2004) Serotonin transporter polymorphism related to amygdala excitability and symptom severity in patients with social phobia. Neurosci Lett 362:189–192.

Gagnon D, Parent M (2014) Distribution of VGLUT3 in highly collateralized axons from the rat dorsal raphe nucleus as revealed by single-neuron reconstructions. PLoS One 9:e87709.

Gandolfi O, Dall'Olio R, Roncada P, Montanaro N (1990) NMDA antagonists interact with 5-HT-stimulated phosphatidylinositol metabolism and impair passive avoidance retention in the rat. Neurosci Lett 113:304–308.

Garcia-Garcia AL, Meng Q, Richardson-Jones J, Dranovsky A, Leonardo ED (2016) Disruption of 5-HT1A function in adolescence but not early adulthood leads to sustained increases of anxiety. Neuroscience 321:210–221.

Garcia-Garcia AL, Meng Q, Canetta S, Gardier AM, Guiard BP, Kellendonk C, Dranovsky A, Leonardo ED (2017) Serotonin Signaling through Prefrontal Cortex 5-HT1A Receptors during Adolescence Can Determine Baseline Mood-Related Behaviors. Cell Rep 18:1144–1156.

Garfinkel SN, Abelson JL, King AP, Sripada RK, Wang X, Gaines LM, Liberzon I (2014) Impaired Contextual Modulation of Memories in PTSD: An fMRI and Psychophysiological Study of Extinction Retention and Fear Renewal. J Neurosci 34:13435–13443.

Garpenstrand H, Annas P, Ekblom J, Oreland L, Fredrikson M (2001) Human fear conditioning is related to dopaminergic and serotonergic biological markers. Behav Neurosci 115:358–364.

Gaspar P, Cases O, Maroteaux L (2003) The developmental role of serotonin: news from mouse molecular genetics. Nat Rev Neurosci 4:1002–1012.

Geracitano R, Kaufmann WA, Szabo G, Ferraguti F, Capogna M (2007) Synaptic heterogeneity between mouse paracapsular intercalated neurons of the amygdala. J Physiol 585:117–134.

Ghijsen WEJM, Leenders MAG (2005) Differential signaling in presynaptic neurotransmitter release. Cell Mol Life Sci 62:937–954.

Ghosh KK, Burns LD, Cocker ED, Nimmerjahn A, Ziv Y, Gamal A El, Schnitzer MJ (2011) Miniaturized integration of a fluorescence microscope. Nat Methods 8:871–878.

Gillespie DC, Kim G, Kandler K (2005) Inhibitory synapses in the developing auditory system are glutamatergic. Nat Neurosci 8:332–338.

Glazer E, Steinbusch H, Verhofstad A, Basbaum A (1981) Serotonin neurons in nucleus raphe dorsalis and paragigantocellularis of the cat contain enkephalin. J Physiol (Paris) 77:241–245.

Glover LR, Schoenfeld TJ, Karlsson R, Bannerman DM, Cameron HA (2017) Ongoing neurogenesis in the adult dentate gyrus mediates behavioral responses to ambiguous threat cues. PLoS Biol 15:e2001154.

Gobbi G, Murphy DL, Lesch K, Blier P (2001) Modifications of the serotonergic system in mice lacking serotonin transporters: an in vivo electrophysiological study. J Pharmacol Exp Ther 296:987–995.

Gomes F V, Reis DG, Alves FH, Corrêa FM, Guimarães FS, Resstel LB (2012) Cannabidiol injected into the bed nucleus of the stria terminalis reduces the expression of contextual fear conditioning via 5-HT 1A receptors. J Psychopharmacol 26:104–113.

Gong Y, Huang C, Li JZ, Grewe BF, Zhang Y, Eismann S, Schnitzer MJ (2015) High-speed recording of neural spikes in awake mice and flies with a fluorescent voltage sensor. Science 350:1361–1366.

Gonzalez LE, Andrews N, File SE (1996) 5-HTIA and benzodiazepine receptors in the basolateral amygdala modulate anxiety in the social interaction test, but not in the elevated plus-maze. BRAIN Res BrainResearch732 732:145–153.

Gore BB, Soden ME, Zweifel LS (2013) Manipulating gene expression in projection-specific neuronal populations using combinatorial viral approaches. Curr Protoc Neurosci 1:1–20.

Gore F, Schwartz EC, Brangers BC, Aladi S, Stujenske JM, Likhtik E, Russo MJ, Gordon JA, Salzman CD, Axel R (2015) Neural Representations of Unconditioned Stimuli in Basolateral Amygdala Mediate Innate and Learned Responses. Cell 162:134–145.

Graeff FG, Guimariies FS, de Andrade TGCS, Deakins JFW (1996) Role of 5-HT in Stress, Anxiety, and Depression. Pharmacol Biochem Behav 54:129–141.

Grahn RE, Will MJ, Hammack SE, Maswood S, McQueen MB, Watkins LR, Maier SF (1999) Activation of serotonin-immunoreactive cells in the dorsal raphe nucleus in rats exposed to an uncontrollable stressor. Brain Res 826:35–43.

Gras C, Herzog E, Bellenchi GC, Bernard V, Ravassard P, Pohl M, Gasnier B, Giros B, Mestikawy S (2002) A third vesicular glutamate transporter expressed by cholinergic and serotoninergic neurons. J Neurosci 22:5442–5451.

Gras C, Amilhon B, Lepicard ÈM, Poirel O, Vinatier J, Herbin M, Dumas S, Tzavara ET, Wade MR, Nomikos GG, Hanoun N, Saurini F, Kemel M-L, Gasnier B, Giros B, Mestikawy S El (2008) The vesicular glutamate transporter VGLUT3 synergizes striatal acetylcholine tone. Nat Neurosci 11:292–300.

Gras C, Vinatier J, Amilhon B, Guerci A, Christov C, Ravassard P, Giros B, El Mestikawy S (2005) Developmentally regulated expression of VGLUT3 during early post-natal life. Neuropharmacology 49:901–911.

Greenberg BD, Tolliver TJ, Huang SJ, Li Q, Bengel D, Murphy DL (1999) Genetic variation in the serotonin transporter promoter region affects serotonin uptake in human blood platelets. Am J Hum Genet 88:83–87.

Grewe BF, Gründemann J, Kitch LJ, Lecoq JA, Parker JG, Marshall JD, Larkin MC, Jercog PE, Grenier F, Li JZ, Lüthi A, Schnitzer MJ (2017) Neural ensemble dynamics underlying a long-term associative memory. Nature 543:670–675.

Griebel G (1995) 5-Hydroxytryptamine-interacting drugs in animal models of anxiety disorders: more than 30 years of research. Pharmacol Ther 65:319–395.

Gross C, Zhuang X, Stark K, Ramboz S, Oosting R, Kirby L, Santarelli L, Beck S (2002) Serotonin 1A receptor acts during development to establish normal anxiety-like behaviour in the adult. Nature 416:396–400.

Guidotti G, Calabrese F, Auletta F, Olivier J, Racagni G, Homberg J, Riva MA (2012) Developmental Influence of the Serotonin Transporter on the Expression of Npas4 and GABAergic Markers: Modulation by Antidepressant Treatment. Neuropsychopharmacology 37:746–758.

Gunaydin LA, Grosenick L, Finkelstein JC, Kauvar I V., Fenno LE, Adhikari A, Lammel S, Mirzabekov JJ, Airan RD, Zalocusky KA, Tye KM, Anikeeva P, Malenka RC, Deisseroth K (2014) Natural neural projection dynamics underlying social behavior. Cell 157:1535–1551.

Guo J-D, O'Flaherty BM, Rainnie DG (2017) Serotonin gating of cortical and thalamic glutamate inputs onto principal neurons of the basolateral amygdala. Neuropharmacology 126:224–232.

Hajós M, Allers KA, Jennings K, Sharp T, Charette G, Sík A, Kocsis B (2007) Neurochemical identification of stereotypic burst-firing neurons in the rat dorsal raphe nucleus using juxtacellular labelling methods. Eur J Neurosci 25:119–126.

Halladay LR, Blair HT (2015) Distinct ensembles of medial prefrontal cortex neurons are activated by threatening stimuli that elicit excitation vs. inhibition of movement. J Neurophysiol 114:793–807.

Hamel EJO, Grewe BF, Parker JG, Schnitzer MJ (2015) Cellular level brain imaging in behaving mammals: An engineering approach. Neuron 86:140–159.

Hamon M, Glowinski J (1974) Regulation of serotonin synthesis. Life Sci 15:1533–1548.

Handley SL, Mithani S (1984) Effects of alpha-adrenoceptor agonists and antagonists in a maze-exploration model of "fear"-motivated behaviour. Naunyn Schmiedebergs Arch Pharmacol 327:1–5.

Hankin BL, Nederhof E, Oppenheimer CW, Jenness J, Young JF, Abela JRZ, Smolen A, Ormel J, Oldehinkel AJ (2011) Differential susceptibility in youth: evidence that 5-HTTLPR x positive parenting is associated with positive affect "for better and worse". Transl Psychiatry 1:e44.

Hannon J, Hoyer D (2008) Molecular biology of 5-HT receptors. Behav Brain Res 195:198–213.

Hansen HH, Sánchez C, Meier E (1997) Neonatal administration of the selective serotonin reuptake inhibitor Lu 10-134-C increases forced swimming-induced immobility in adult rats: a putative animal model of depression? J Pharmacol Exp Ther 283:1333–1341.

Harada K, Yamaji T, Matsuoka N (2008) Activation of the serotonin 5-HT 2C receptor is involved in the enhanced anxiety in rats after single-prolonged stress. 89:11–16.

Harandi M, Aguera M, Gamrani H, Didier M, Maitre M, Calas A, Belin M (1987) gamma-Aminobutyric acid and 5-hydroxytryptamine interrelationship in the rat nucleus raphe dorsalis: combination of radioautographic and immunocytochemical techniques at light and electron microscopy levels. Neuroscience 21:237–251.

Hariri AR, Drabant EM, Munoz KE, Kolachana BS, Mattay VS, Egan MF, Weinberger DR (2005) A susceptibility gene for affective disorders and the response of the human amygdala. Arch Gen Psychiatry 62:146–152.

Hariri AR, Mattay VS, Tessitore A, Kolachana B, Fera F, Goldman D, Egan MF, Weinberger DR (2002) Serotonin transporter genetic variation and the response of the human amygdala. Science 297:400–403.

Harrington MA, Shaw K, Zhong P, Ciaranello RD (1994) Agonist-induced desensitization and loss of high-affinity binding sites of stably expressed human 5-HT 1A receptors. J Pharmacol Exp Ther 268:1098–1106.

Hartley CA, McKenna MC, Salman R, Holmes A, Casey BJ, Phelps EA, Glatt CE (2012) Serotonin transporter polyadenylation polymorphism modulates the retention of fear extinction memory. Proc Natl Acad Sci 109:5493–5498.

Hashimoto S, Inoue T, Koyama T (1997) Effects of the co-administration of 5-HT(1A) receptor antagonists with an SSRI in conditioned fear stress-induced freezing behavior. Pharmacol Biochem Behav 58:471–475.

Hasue RH, Shammah-Lagnado SJ (2002) Origin of the dopaminergic innervation of the central extended amygdala and accumbens shell: A combined retrograde tracing and immunohistochemical study in the rat. J Comp Neurol 454:15–33.

Hattori T, Takada M, Moriizumi T, Van Der Kooy D (1991) Single dopaminergic nigrostriatal neurons form two chemically distinct synaptic types: possible transmitter segregation within neurons. J Comp Neurol 309:391–401.

Haydon P, McCobb D, Kater S (1984) Serotonin selectively inhibits growth cone motility and synaptogenesis of specific identified neurons. Science 226:561–564.

Heils A, Teufel A, Petri S, Stöber G, Riederer P, Bengel D, Lesch KP (1996) Allelic variation of human serotonin transporter gene expression. J Neurochem 66:2621–2624.
Herman AM, Ortiz-Guzman J, Kochukov M, Herman I, Quast KB, Patel JM, Tepe B, Carlson JC, Ung K, Selever J, Tong Q, Arenkiel BR (2016) A cholinergic basal forebrain feeding circuit modulates appetite suppression. Nature 538:253–256.
Herry C, Ciocchi S, Senn V, Demmou L, Müller C, Lüthi A (2008) Switching on and off fear by distinct neuronal circuits. Nature 454:600–606.
Herry C, Ferraguti F, Singewald N, Letzkus JJ, Ehrlich I, Lüthi A (2010) Neuronal circuits of fear extinction. Eur J Neurosci 31:599–612.
Herry C, Johansen JP (2014) Encoding of fear learning and memory in distributed neuronal circuits. Nat Neurosci 17:1644–1654.
Herzog E, Gilchrist J, Gras C, Muzerelle A, Ravassard P, Giros B, Gaspar P, El Mestikawy S (2004) Localization of VGLUT3, the vesicular glutamate transporter type 3, in the rat brain. Neuroscience 123:983–1002.
Higgins GA, Jones BJ, Oakley NR, Tyers MB (1991) Evidence that the amygdala is involved in the disinhibitory effects of 5-HT3 receptor antagonists. Psychopharmacology (Berl) 104:545–551.
Hioki H, Fujiyama F, Nakamura K, Wu SX, Matsuda W, Kaneko T (2004) Chemically specific circuit composed of vesicular glutamate transporter 3- and preprotachykinin B-producing interneurons in the rat neocortex. Cereb Cortex 14:1266–1275.
Hioki H, Nakamura H, Ma YF, Konno M, Hayakawa T, Nakamura KC, Fujiyama F, Kaneko T (2010) Vesicular glutamate transporter 3-expressing nonserotonergic projection neurons constitute a subregion in the rat midbrain raphe nuclei. J Comp Neurol 518:668–686.
Hjorth S, Westlin D, Bengtsson HJ (1997) WAY100635-induced augmentation of the 5-HT-elevating action of citalopram: Relative importance of the dose of the 5-HT(1A) (Auto)receptor blocker versus that of the 5-HT reuptake inhibitor. Neuropharmacology 36:461–465.
Hodges H, Green S, Glenn B (1987) Evidence that the amygdala is involved in benzodiazepine and serotonergic effects on punished responding but not on discrimination. Psychopharmacology (Berl) 92:491–504.
Hökfelt T, Ljungdahl Å, Steinbusch H, Verhofstad A, Nilsson G, Brodin E, Pernow B, Goldstein M (1978) Immunohistochemical evidence of substance P-like immunoreactivity in some 5-hydroxytryptamine-containing neurons in the rat central nervous system. Neuroscience 3:517–538.
Hökfelt T, Arvidsson U, Cullheim S, Millhorn D, Nicholas AP, Pieribone V, Seroogy K, Ulfhake B (2000) Multiple messengers in descending serotonin neurons: localization and functional implications. J Chem Neuroanat 18:75–86.
Holmes A (2008) Genetic variation in cortico-amygdala serotonin function and risk for stress-related disease. Neurosci Biobehav Rev 32:1293–1314.
Holmes A, Murphy DL, Crawley JN (2003a) Abnormal behavioral phenotypes of serotonin transporter knockout mice: parallels with human anxiety and depression. Biol Psychiatry 54:953–959.
Holmes A, Yang RJ, Lesch K-P, Crawley JN, Murphy DL (2003) Mice lacking the serotonin transporter exhibit 5-HT(1A) receptor-mediated abnormalities in tests for anxiety-like behavior. Neuropsychopharmacology 28:2077–2088.
Homberg JR, Olivier JDA, Smits BMG, Mul JD, Mudde J, Verheul M, Nieuwenhuizen OFM, Cools AR, Ronken E, Cremers T, Schoffelmeer ANM, Ellenbroek BA, Cuppen E (2007) Characterization of the serotonin transporter knockout rat: A selective change in the functioning of the serotonergic system. Neuroscience 146:1662–1676.
Homberg JR, Olivier JDA, Blom T, Arentsen T, van Brunschot C, Schipper P, Korte-Bouws G, van Luijtelaar G, Reneman L (2011) Fluoxetine exerts age-dependent effects on behavior and amygdala neuroplasticity in the rat. PLoS One 6:1–10.
Homberg JR, Schubert D, Gaspar P (2010) New perspectives on the neurodevelopmental effects of SSRIs. Trends Pharmacol Sci 31:60–65.
Hopkins DA, Holstege G (1978) Amygdaloid projections to the mesencephalon, pons and medulla oblongata in the cat. Exp brain Res 32:529–547.

Hoyer D, Hannon JP, Martin GR (2002) Molecular, pharmacological and functional diversity of 5-HT receptors. Pharmacol Biochem Behav 71:533–554.
Hu XZ, Rush AJ, Charney D, Wilson AF, Sorant AJ, Papanicolaou GJ, Fava M, Trivedi MH, Wisniewski SR, Laje G, Paddock S, McMahon FJ, Manji H, Lipsky RH (2007) Association between a functional serotonin transporter promoter polymorphism and citalopram treatment in adult outpatients with major depression. ArchGenPsychiatry 64:783–792.
Humphrey PPA, Hartig P, Hoyer D (1993) A proposed new nomenclature for 5-HT receptors. Trends Pharmacol Sci 14:233–236.
Inoue T, Li XB, Abekawa T, Kitaichi Y, Izumi T, Nakagawa S, Koyama T (2004) Selective serotonin reuptake inhibitor reduces conditioned fear through its effect in the amygdala. Eur J Pharmacol 497:311–316.
Invernizzi R, Belli S, Samanin R (1992) Citalopram's ability to increase the extracellular concentrations of serotonin in the dorsal raphe prevents the drug's effect in the frontal cortex. Brain Res 584:322–324.
Invernizzi R, Bramante M, Samanin R (1995) Extracellular concentrations of serotonin in the dorsal hippocampus after acute and chronic treatment with citalopram. Brain Res 696:62–66.
Ipser J, Seedat S, Stein DJ (2006) Pharmacotherapy for post-traumatic stress disorder - A systematic review and meta-analysis. South African Med J 96:1088–1096.
Iversen LL (1971) Role of transmitter uptake mechanisms in synaptic neurotransmission. Br J Pharmacol 41:571–591.
Izumi T, Ohmura Y, Futami Y, Matsuzaki H, Kubo Y, Yoshida T, Yoshioka M (2012) Effects of serotonergic terminal lesion in the amygdala on conditioned fear and innate fear in rats. Eur J Pharmacol 696:89–95.
Jackson J, Bland B, Antle M (2009) Nonserotonergic projection neurons in the midbrain raphe nuclei contain the vesicular glutamate transporter VGLUT3. Synapse 63:31–41.
Jacobs BL, Foote SL, Bloom FE (1978) Differential projections of neurons within the dorsal raphe nucleus of the rat: a horseradish peroxidase (HRP) study. Brain Res 147:149–153.
Janak PH, Tye KM (2015) From circuits to behaviour in the amygdala. Nature 517:284–292.
Jennings KA, Sheward WJ, Harmar AJ, Sharp T (2008) Evidence that genetic variation in 5-HT transporter expression is linked to changes in 5-HT2A receptor function. Neuropharmacology 54:776–783.
Jennings KA, Loder MK, Sheward WJ, Pei Q, Deacon RMJ, Benson MA, Olverman HJ, Hastie ND, Harmar AJ, Shen S, Sharp T (2006) Increased expression of the 5-HT transporter confers a low-anxiety phenotype linked to decreased 5-HT transmission. J Neurosci 26:8955–8964.
Jennings KA, Lesch KP, Sharp T, Cragg SJ (2010) Non-linear relationship between 5-HT transporter gene expression and frequency sensitivity of 5-HT signals. J Neurochem 115:965–973.
Jiang X, Xing G, Yang C, Verma A, Zhang L, Li H (2009) Stress impairs 5-HT2A receptor-mediated serotonergic facilitation of GABA release in juvenile rat basolateral amygdala. Neuropsychopharmacology 34:410–423.
Jiang X-Z, Liu Y-Q, Zhang Y-Z, Zhang L-M, Li J, Li Y-F (2009) [Neonatal fluoxetine exposure induced depression-like behaviors in adult Kunming mice and the antidepressant-like effect of agmatine]. Yao xue xue bao 44:716–721.
Johansen JP, Tarpley JW, LeDoux JE, Blair HT (2010) Neural substrates for expectation-modulated fear learning in the amygdala and periaqueductal gray. Nat Neurosci 13:979–986.
Johansson O, Hökfelt T, Pernow B, Jeffcoate SL, White N, Steinbusch HWM, Verhofstad AAJ, Emson PC, Spindel E (1981) Immunohistochemical support for three putative transmitters in one neuron: Coexistence of 5-hydroxytryptamine, substance p- and thyrotropin releasing hormone-like immunoreactivity in medullary neurons projecting to the spinal cord. Neuroscience 6:1857–1881.
Johnson MD, Ma PM (1993) Localization of NADPH diaphorase activity in monoaminergic neurons of the rat brain. J Comp Neurol 332:391–406.
Johnson MD (1994) Synaptic glutamate release by postnatal rat serotonergic neurons in microculture. Neuron 12:433–442.

Johnson PL, Molosh A, Fitz SD, Arendt D, Deehan GA, Federici LM, Bernabe C, Engleman EA, Rodd ZA, Lowry CA, Shekhar A (2015) Pharmacological depletion of serotonin in the basolateral amygdala complex reduces anxiety and disrupts fear conditioning. Pharmacol Biochem Behav 138:174–179.

Jolkkonen E, Pitkänen A (1998) Intrinsic connections of the rat amygdaloid complex: Projections originating in the central nucleus. J Comp Neurol 395:53–72.

Kaneko T, Akiyama H, Nagatsu I, Mizuno N (1990) Immunohistochemical demonstration of glutaminase in catecholaminergic and serotoninergic neurons of rat brain. Brain Res 507:151–154.

Karalis N, Dejean C, Chaudun F, Khoder S, Rozeske RR, Wurtz H, Bagur S, Benchenane K, Sirota A, Courtin J, Herry C (2016) 4-Hz oscillations synchronize prefrontal–amygdala circuits during fear behavior. Nat Neurosci 19:605–612.

Karpova NN, Pickenhagen A, Lindholm J, Tiraboschi E, Kulesskaya N, Agustsdottir A, Antila H, Popova D, Akamine Y, Sullivan R, Hen R, Drew LJ, Castren E (2011) Fear Erasure in Mice Requires Synergy Between Antidepressant Drugs and Extinction Training. Science 334:1731–1734.

Karpova NN, Lindholm J, Pruunsild P, Timmusk T, Castrén E (2009) Long-lasting behavioural and molecular alterations induced by early postnatal fluoxetine exposure are restored by chronic fluoxetine treatment in adult mice. Eur Neuropsychopharmacol 19:97–108.

Kawahana M, Yoshida M, Yokoo H, Nishi M, Tanaka M (1993) Psychological stress increases serotonin release in the rat amygdala and prefrontal cortex assessed by in vivo microdialysis. Neurosci Letts 162:81–84.

Kim DK, Tolliver TJ, Huang SJ, Martin BJ, Andrews AM, Wichems C, Holmes A, Lesch KP, Murphy DL (2005) Altered serotonin synthesis, turnover and dynamic regulation in multiple brain regions of mice lacking the serotonin transporter. Neuropharmacology 49:798–810.

Kim JJ, Fanselow MS (1992) Modality-specific retrograde amnesia of fear. Science 256:675–677.

Kim JJ, Jung MW (2006) Neural circuits and mechanisms involved in Pavlovian fear conditioning: A critical review. Neurosci Biobehav Rev 30:188–202.

Kim W Bin, Cho J-H (2017) Encoding of Discriminative Fear Memory by Input-Specific LTP in the Amygdala. Neuron 95:1129–1146.e5.

Kirby LG, Pernar L, Valentino RJ, Beck SG (2003) Distinguishing characteristics of serotonin and non-serotonin-containing cells in the dorsal raphe nucleus: Electrophysiological and immunohistochemical studies. Neuroscience 116:669–683.

Kiyasova V, Fernandez SP, Laine J, Stankovski L, Muzerelle A, Doly S, Gaspar P (2011) A genetically defined morphologically and functionally unique subset of 5-HT neurons in the mouse raphe nuclei. J Neurosci 31:2756–2768.

Knight DC, Smith CN, Stein E a, Helmstetter FJ (1999) Functional MRI of human Pavlovian fear conditioning: patterns of activation as a function of learning. Neuroreport 10:3665–3670.

Kocsis B, Varga V, Dahan L, Sik A (2006) Serotonergic neuron diversity: Identification of raphe neurons with discharges time-locked to the hippocampal theta rhythm. Proc Natl Acad Sci 103:1059–1064.

Koyama S, Kubo C, Rhee JS, Akaike N (1999) Presynaptic serotonergic inhibition of GABAergic synaptic transmission in mechanically dissociated rat basolateral amygdala neurons. J Physiol 518:525–538.

Krettek JE, Price JL (1978) A description of the amygdaloid complex in the rat and cat with observations on intra-amygdaloid axonal connections. J Comp Neurol 178:255–279.

Krettek JE, Price JL (1977) Projections from the amygdaloid complex to the cerebral cortex and thalamus in the rat and cat. J Comp Neurol 172:687–722.

Krettek JE, Price JL (1978) Amygdaloid projections to subcortical structures within the basal forebrain and brainstem in the rat and cat. J Comp Neurol 178:225–253.

LaBar KS, LeDoux JE, Spencer DD, Phelps EA (1995) Impaired fear conditioning following unilateral temporal lobectomy in humans. JNeurosci 15:6846–6855.

LaBar KS, Gatenby CJ, Gore JC, LeDoux JE, Phelps EA (1998) Human amygdala activation during conditioned fear acquisition and extinction: a mixed-trial fMRI study. Neuron 20:937–945.

LaLumiere RT, Nguyen LT, McGaugh JL (2004) Post-training intrabasolateral amygdala infusions of dopamine modulate consolidation of inhibitory avoidance memory: Involvement of noradrenergic and cholinergic system. Eur J Neurosci 20:2804–2810.
Lau JYF, Goldman D, Buzas B, Fromm SJ, Guyer AE, Hodgkinson C, Monk CS, Nelson EE, Shen P-H, Pine DS, Ernst M (2009) Amygdala function and 5-HTT gene variants in adolescent anxiety and major depressive disorder. Biol Psychiatry 65:349–355.
Lauder JM (1990) Ontogeny of the Serotonergic System in the Rat: Serotonin as a Developmental Signal. Ann N Y Acad Sci 600:297–314.
Le Poul E, Boni C, Hanoun N, Laporte AM, Laaris N, Chauveau J, Hamon M, Lanfumey L (2000) Differential adaptation of brain 5-HT(1A) and 5-HT(1B) receptors and 5-HT transporter in rats treated chronically with fluoxetine. Neuropharmacology 39:110–122.
Lebrand C, Cases O, Adelbrecht C, Doye A, Alvarez C, El Mestikawy S, Seif I, Gaspar P (1996) Transient uptake and storage of serotonin in developing thalamic neurons. Neuron 17:823–835.
Lebrand C, Cases O, Wehrle R, Blakely RD, Edwards RH, Gaspar P (1998) Transient Developmental Expression of Monoamine Transporters in the Rodent Forebrain. J Comp Neurol 401:506–524.
LeDoux JE, Iwata J, Cicchetti P, Reis DJ (1988) Different projections of the central amygdaloid nucleus mediate autonomic and behavioral correlates of conditioned fear. J Neurosci 8:2517–2529.
LeDoux J (2003) The emotional brain, fear, and the amygdala. Cell Mol Neurobiol 23:727–738.
Lee HJ, Lee MS, Kang RH, Kim H, Kim SD, Kee BS, Kim YH, Kim YK, Kim JB, Yeon BK, Oh KS, Oh BH, Yoon JS, Lee C, Jung HY, Chee IS, Paik IH (2005) Influence of the serotonin transporter promoter gene polymorphism on susceptibility to posttraumatic stress disorder. Depress Anxiety 21:135–139.
Lee S, Amir A, Haufler D, Pare D (2017) Differential Recruitment of Competing Valence-Related Amygdala Networks during Anxiety. Neuron 96:81–88.
Lee S, Kim K, Zhou ZJ (2010) Role of ACh-GABA Cotransmission in Detecting Image Motion and Motion Direction. Neuron 68:1159–1172.
Lesch KP, Bengel D, Heils A, Sabol SZ, Greenberg BD, Petri S, Benjamin J, Müller CR, Hamer DH, Murphy DL (1996) Association of anxiety-related traits with a polymorphism in the serotonin transporter gene regulatory region. Science 274:1527–1531.
Li Q, Wichems C, Heils A, Lesch KP, Murphy DL (2000) Reduction in the density and expression, but not G-protein coupling, of serotonin receptors (5-HT1A) in 5-HT transporter knock-out mice: gender and brain region differences. J Neurosci 20:7888–7895.
Li X, Inoue T, Abekawa T, Weng S, Nakagawa S, Izumi T, Koyama T (2006) 5-HT1A receptor agonist affects fear conditioning through stimulations of the postsynaptic 5-HT1A receptors in the hippocampus and amygdala. Eur J Pharmacol 532:74–80.
Li Y, Zhong W, Wang D, Feng Q, Liu Z, Zhou J, Jia C, Hu F, Zeng J, Guo Q, Fu L, Luo M (2016) Serotonin neurons in the dorsal raphe nucleus encode reward signals. Nat Commun 7:10503.
Li YQ, Jia HG, Rao ZR, Shi JW (1990) Serotonin-, substance P- or leucine-enkephalin-containing neurons in the midbrain periaqueductal gray and nucleus raphe dorsalis send projection fibers to the central amygdaloid nucleus in the rat. Neurosci Lett 120:124–127.
Liang KC (1999) Pre- or post-training injection of buspirone impaired retention in the inhibitory avoidance task: Involvement of amygdala 5-HT(1A) receptors. Eur J Neurosci 11:1491–1500.
Liberzon I, Taylor SF, Amdur R, Jung TD, Chamberlain KR, Minoshima S, Koeppe RA, Fig LM (1999) Brain activation in PTSD in response to trauma-related stimuli. Biol Psychiatry 45:817–826.
Likhtik E, Pelletier JG, Popescu AT, Paré D (2006) Identification of basolateral amygdala projection cells and interneurons using extracellular recordings. J Neurophysiol 96:3257–3265.
Likhtik E, Stujenske JM, A Topiwala M, Harris AZ, Gordon JA (2013) Prefrontal entrainment of amygdala activity signals safety in learned fear and innate anxiety. Nat Neurosci 17:106–113.
Line SJ, Barkus C, Rawlings N, Jennings K, Mchugh S, Sharp T, Bannerman DM (2014) Reduced sensitivity to both positive and negative reinforcement in mice over-expressing the 5-hydroxytryptamine transporter. Eur J Neurosci 40:3735–3745.

Line SJ, Barkus C, Coyle C, Jennings KA, Deacon RM, Lesch KP, Sharp T, Bannerman DM (2011) Opposing alterations in anxiety and species-typical behaviours in serotonin transporter overexpressor and knockout mice. Eur Neuropsychopharmacol 21:108–116.

Linnman C, Rougemont-Bücking A, Beucke JC, Zeffiro TA, Milad MR (2011) Unconditioned responses and functional fear networks in human classical conditioning. Behav Brain Res 221:237–245.

Lira A, Zhou M, Castanon N, Ansorge MS, Gordon JA, Francis JH, Bradley-Moore M, Lira J, Underwood MD, Arango V, Kung HF, Hofer MA, Hen R, Gingrich JA (2003) Altered depression-related behaviors and functional changes in the dorsal raphe nucleus of serotonin transporter-deficient mice. Biol Psychiatry 54:960–971.

Liu Z, Zhou J, Li Y, Hu F, Lu Y, Ma M, Feng Q, Zhang J en, Wang D, Zeng J, Bao J, Kim JY, Chen ZF, Mestikawy S El, Luo M (2014) Dorsal raphe neurons signal reward through 5-HT and glutamate. Neuron 81:1360–1374.

Lo L, Anderson DJ (2011) A cre-dependent, anterograde transsynaptic viral tracer for mapping output pathways of genetically marked neurons. Neuron 72:938–950.

Lonsdorf TB, Weike AI, Nikamo P, Schalling M, Hamm AO, Ohman A (2009) Genetic Gating of Human Fear Learning and Extinction. Psychol Sci 20:198–206.

Lopez de Armentia M, Sah P (2004) Firing properties and connectivity of neurons in the rat lateral central nucleus of the amygdala. J Neurophysiol 92:1285–1294.

Lovett-Barron M, Turi GF, Kaifosh P, Lee PH, Bolze F, Sun X-H, Nicoud J-F, Zemelman B V, Sternson SM, Losonczy A (2012) Regulation of neuronal input transformations by tunable dendritic inhibition. Nat Neurosci 15:423–430.

Lucki I (1998) The spectrum of behaviors influenced by serotonin. Biol Psychiatry 44:151–162.

Ma QP, Yin GF, Ai MK, Han JS (1991) Serotonergic projections from the nucleus raphe dorsalis to the amygdala in the rat. Neurosci Lett 134:21–24.

Macedo CE, Ruiz Martinez RC, Albrechet-Souza L, Molina VA, Brandão ML (2007) 5-HT2- and D1-mechanisms of the basolateral nucleus of the amygdala enhance conditioned fear and impair unconditioned fear. Behav Brain Res 177:100–108.

Mahn M, Prigge M, Ron S, Levy R, Yizhar O (2016) Biophysical constraints of optogenetic inhibition at presynaptic terminals. Nat Neurosci 19:554–556.

Malison RT, Price LH, Berman R, van Dyck CH, Pelton GH, Carpenter L, Sanacora G, Owens MJ, Nemeroff CB, Rajeevan N, Baldwin RM, Seibyl JP, Innis RB, Charney DS (1998) Reduced brain serotonin transporter availability in major depression as measured by [123I]-2 beta-carbomethoxy-3 beta-(4-iodophenyl)tropane and single photon emission computed tomography. Biol Psychiatry 44:1090–1098.

Mann JJ, Huang YY, Underwood MD, Kassir S a, Oppenheim S, Kelly TM, Dwork a J, Arango V (2000) A serotonin transporter gene promoter polymorphism (5-HTTLPR) and prefrontal cortical binding in major depression and suicide. Arch Gen Psychiatry 57:729–738.

Marcinkiewcz CA, Mazzone CM, D'Agostino G, Halladay LR, Hardaway JA, DiBerto JF, Navarro M, Burnham N, Cristiano C, Dorrier CE, Tipton GJ, Ramakrishnan C, Kozicz T, Deisseroth K, Thiele TE, McElligott ZA, Holmes A, Heisler LK, Kash TL (2016) Serotonin engages an anxiety and fear-promoting circuit in the extended amygdala. Nature 537:97–101.

Maren S, Quirk GJ (2004) Neuronal signalling of fear memory. Nat Rev Neurosci 5:844–852.

Marowsky A, Yanagawa Y, Obata K, Vogt KE (2005) A specialized subclass of interneurons mediates dopaminergic facilitation of amygdala function. Neuron 48:1025–1037.

Marshall JD, Li JZ, Zhang Y, Gong Y, St-Pierre F, Lin MZ, Schnitzer MJ (2016) Cell-Type-Specific Optical Recording of Membrane Voltage Dynamics in Freely Moving Mice. Cell 167:1650–1662.

Mascagni F, McDonald AJ (2007) A novel subpopulation of 5-HT type 3A receptor subunit immunoreactive interneurons in the rat basolateral amygdala. Neuroscience 144:1015–1024.

Mathews TA, Fedele DE, Coppelli FM, Avila AM, Murphy DL, Andrews AM (2004) Gene dose-dependent alterations in extraneuronal serotonin but not dopamine in mice with reduced serotonin transporter expression. J Neurosci Methods 140:169–181.

Mathur BN, Capik NA, Alvarez VA, Lovinger DM (2011) Serotonin Induces Long-Term Depression at Corticostriatal Synapses. J Neurosci 31:7402–7411.

Matias S, Lottem E, Dugué GP, Mainen ZF (2017) Activity patterns of serotonin neurons underlying cognitive flexibility. Elife 6:1–24.
Matsuzaki H, Izumi T, Horinouchi T, Boku S, Inoue T, Yamaguchi T, Yoshida T, Matsumoto M, Togashi H, Miwa S, Koyama T, Yoshioka M (2011) Juvenile stress attenuates the dorsal hippocampal postsynaptic 5-HT 1A receptor function in adult rats. Psychopharmacology (Berl) 214:329–337.
Matthews GA, Nieh EH, Vander Weele CM, Halbert SA, Pradhan R V., Yosafat AS, Glober GF, Izadmehr EM, Thomas RE, Lacy GD, Wildes CP, Ungless MA, Tye KM (2016) Dorsal Raphe Dopamine Neurons Represent the Experience of Social Isolation. Cell 164:617–631.
McCormick DA, Wang Z, Huguenard JR (1993) Neurotransmitter control of neuronal activity and excitability. Cereb Cortex 3:387–398.
McDevitt RA, Tiran-Cappello A, Shen H, Balderas I, Britt JP, Marino RAM, Chung SL, Richie CT, Harvey BK, Bonci A (2014) Serotonergic versus nonserotonergic dorsal raphe projection neurons: Differential participation in reward circuitry. Cell Rep 8:1857–1869.
McDonald AJ, Mascagni F (2007) Neuronal localization of 5-HT type 2A receptor immunoreactivity in the rat basolateral amygdala. Neuroscience 146:306–320.
McDonald AJ (1998) Cortical pathways to the mammalian amygdala. Prog Neurobiol 55:257–332.
McDonald AJ (1982) Cytoarchitecture of the central amygdaloid nucleus of the rat. J Comp Neurol 208:401–418.
McDonald AJ (1984) Neuronal organization of the lateral and basolateral amygdaloid nuclei in the rat. J Comp Neurol 222:589–606.
McDonald AJ (1982) Neurons of the lateral and basolateral amygdaloid nuclei: A golgi study in the rat. J Comp Neurol 212:293–312.
McHugh SB, Deacon RMJ, Rawlins JNP, Bannerman DM (2004) Amygdala and ventral hippocampus contribute differentially to mechanisms of fear and anxiety. Behav Neurosci 118:63–78.
McHugh SB, Barkus C, Huber A, Capitao L, Lima J, Lowry JP, Bannerman DM (2014) Aversive Prediction Error Signals in the Amygdala. J Neurosci 34:9024–9033.
McHugh SB, Barkus C, Lima J, Glover LR, Sharp T, Bannerman DM (2015) SERT and uncertainty: Serotonin transporter expression influences information processing biases for ambiguous aversive cues in mice. Genes, Brain Behav 14:330–336.
McKernan MG, Shinnick-Gallagher P (1997) Fear conditioning induces a lasting potentiation of synaptic currents in vitro. Nature 390:607–611.
McNally GP, Pigg M, Weidemann G (2004) Opioid Receptors in the Midbrain Periaqueductal Gray Regulate Extinction of Pavlovian Fear Conditioning. J Neurosci 24:6912–6919.
Melander T, Hökfelt T, Rökaeus A, Cuello AC, Oertel WH, Verhofstad A, Goldstein M (1986) Coexistence of galanin-like immunoreactivity with catecholamines, 5-hydroxytryptamine, GABA and neuropeptides in the rat CNS. J Neurosci 6:3640–3654.
Miceli S, Negwer M, van Eijs F, Kalkhoven C, van Lierop I, Homberg J, Schubert D (2013) High serotonin levels during brain development alter the structural input-output connectivity of neural networks in the rat somatosensory layer IV. Front Cell Neurosci 7:88.
Milad MRR, Quirk GJJ (2002) Neurons in medial prefrontal cortex signal memory for fear extinction. Nature 420:70–74.
Milad MR, Pitman RK, Ellis CB, Gold AL, Shin LM, Lasko NB, Zeidan MA, Handwerger K, Orr SP, Rauch SL (2009) Neurobiological Basis of Failure to Recall Extinction Memory in Posttraumatic Stress Disorder. Biol Psychiatry 66:1075–1082.
Milad MR, Quirk GJ (2012) Fear Extinction as a Model for Translational Neuroscience: Ten Years of Progress. Annu Rev Psychol 63:129–151.
Milad MR, Wright CI, Orr SP, Pitman RK, Quirk GJ, Rauch SL (2007) Recall of Fear Extinction in Humans Activates the Ventromedial Prefrontal Cortex and Hippocampus in Concert. Biol Psychiatry 62:446–454.
Millhouse OE (1986) The intercalated cells of the amygdala. J Comp Neurol 247:246–271.
Mintz EM, Scott TJ (2006) Colocalization of serotonin and vesicular glutamate transporter 3-like immunoreactivity in the midbrain raphe of Syrian hamsters (Mesocricetus auratus). Neurosci Lett 394:97–100.

Moret C, Briley M (1996) Effects of acute and repeated administration of citalopram on extracellular levels of serotonin in rat brain. Eur J Pharmacol 295:189–197.
Muller J, Corodimas KP, Fridel Z, LeDoux JE (1997) Functional inactivation of the lateral and basal nuclei of the amygdala by muscimol infusion prevents fear conditioning to an explicit conditioned stimulus and to contextual stimuli. Behav Neurosci 111:683–691.
Muller JF, Mascagni F, McDonald AJ (2007) Serotonin-immunoreactive Axon Terminals Innervate Pyramidal Cells and Interneurons in the Rat Basolateral Amygdala. J Comp Neurol 505:314–335.
Munafò MR, Brown SM, Hariri AR (2008) Serotonin transporter (5-HTTLPR) genotype and amygdala activation: a meta-analysis. Biol Psychiatry 63:852–857.
Murphy DL, Fox MA, Timpano KR, Moya PR, Ren-Patterson R, Andrews AM, Holmes A, Lesch KP, Wendland JR (2008) How the serotonin story is being rewritten by new gene-based discoveries principally related to SLC6A4, the serotonin transporter gene, which functions to influence all cellular serotonin systems. Neuropharmacology 55:932–960.
Murphy DL, Lesch K-P (2008) Targeting the murine serotonin transporter: insights into human neurobiology. Nat Rev Neurosci 9:85–96.
Murphy DL, Moya PR (2011) Human serotonin transporter gene (SLC6A4) variants: their contributions to understanding pharmacogenomic and other functional G x G and G x E differences in health and disease. Curr Opin Pharmacol 11:3–10.
Murphy SE, Norbury R, Godlewska BR, Cowen PJ, Mannie ZM, Harmer CJ, Munafò MR (2013) The effect of the serotonin transporter polymorphism (5-HTTLPR) on amygdala function: a meta-analysis. Mol Psychiatry 18:512–520.
Murphy SE, Norbury R, O'Sullivan U, Cowen PJ, Harmer CJ (2009) Effect of a single dose of citalopram on amygdala response to emotional faces. Br J Psychiatry 194:535–540.
Muzerelle A, Scotto-Lomassese S, Bernard JF, Soiza-Reilly M, Gaspar P (2016) Conditional anterograde tracing reveals distinct targeting of individual serotonin cell groups (B5–B9) to the forebrain and brainstem. Brain Struct Funct 221:535–561.
Nagatsu I, Inagaki S, Kondo Y, Karasawa N, Nagatsu T (1979) Immunofluorescent studies on the localization of tyrosine hydroxylase and dopamine-β-hydroxylase in the mes-, di-, and telencephalon of the rat using unperfused fresh frozen sections. Acta Histochem Cytochem 12:20–37.
Namburi P, Beyeler A, Yorozu S, Calhoon GG, Halbert SA, Wichmann R, Holden SS, Mertens KL, Anahtar M, Felix-Ortiz AC, Wickersham IR, Gray JM, Tye KM (2015) A circuit mechanism for differentiating positive and negative associations. Nature 520:675–678.
Narayanan V, Heiming RS, Jansen F, Lesting J, Sachser N, Pape H-C, Seidenbecher T (2011) Social defeat: impact on fear extinction and amygdala-prefrontal cortical theta synchrony in 5-HTT deficient mice. PLoS One 6:e22600.
Nelson N (1998) The Family of Na + / Cl Neurotransmitter Transporters. J Neurochem 71:1785–1803.
Nemeroff CB, Owens MJ (2002) Treatment of mood disorders. Nat Neurosci 5:1068–1070.
Nickerson Poulin A, Guerci A, El Mestikawy S, Semba K (2007) Vesicular Glutamate Transporter 3 Immunoreactivity Is Present in Cholinergic Basal Forebrain Neurons Projecting to the Basolateral Amygdala in Rat. J Comp Neurol 504:287–297.
Nonkes LJP, de Pooter M, Homberg JR (2012) Behavioural therapy based on distraction alleviates impaired fear extinction in male serotonin transporter knockout rats. J Psychiatry Neurosci 37:224–230.
Nonkes LJP, van de Vondervoort IIGM, Homberg JR (2014) The attribution of incentive salience to an appetitive conditioned cue is not affected by knockout of the serotonin transporter in rats. Behav Brain Res 259:268–273.
Norcross M, Poonam M, Enoch AJ, Karlsson RM, Brigman JL, Cameron HA, Harvey-White J, Holmes A (2008) Effects of adolescent fluoxetine treatment on fear-, anxiety- or stress-related behaviors in C57BL/6J or BALB/cJ mice. Psychopharmacology (Berl) 200:413–424.
Ogawa SK, Cohen JY, Hwang D, Uchida N, Watabe-Uchida M (2014) Organization of monosynaptic inputs to the serotonin and dopamine neuromodulatory systems. Cell Rep 8:1105–1118.
Oh SW et al. (2014) A mesoscale connectome of the mouse brain. Nature 508:207–214.

Olivier JDA, Akerud H, Kaihola H, Pawluski JL, Skalkidou A, Högberg U, Sundström-Poromaa I (2013) The effects of maternal depression and maternal selective serotonin reuptake inhibitor exposure on offspring. Front Cell Neurosci 7:73.

Olivier JDA, Cools AR, Olivier B, Homberg JR, Cuppen E, Ellenbroek BA (2008a) Stress-induced hyperthermia and basal body temperature are mediated by different 5-HT1A receptor populations: A study in SERT knockout rats. Eur J Pharmacol 590:190–197.

Olivier JDA, Vallès A, Van Heesch F, Afrasiab-Middelman A, Roelofs JJPM, Jonkers M, Peeters EJ, Korte-Bouws GAH, Dederen JP, Kiliaan AJ, Martens GJ, Schubert D, Homberg JR (2011) Fluoxetine administration to pregnant rats increases anxiety-related behavior in the offspring. Psychopharmacology (Berl) 217:419–432.

Olivier JDA, Van Der Hart MGC, Van Swelm RPL, Dederen PJ, Homberg JR, Cremers T, Deen PMT, Cuppen E, Cools AR, Ellenbroek BA (2008b) A study in male and female 5-HT transporter knockout rats: An animal model for anxiety and depression disorders. Neuroscience 152:573–584.

Pampallona S, Bollini P, Tibaldi G, Kupelnick B, Munizza C (2004) Combined pharmacotherapy and psychological treatment for depression: a systematic review. Arch Gen Psychiatry 61:714–719.

Pape HC, Driesang RB (1998) Ionic mechanisms of intrinsic oscillations in neurons of the basolateral amygdaloid complex. J Neurophysiol 79:217–226.

Paré D, Smith Y (1993) Distribution of GABA immunoreactivity in the amygdaloid complex of the cat. Neuroscience 57:1061–1076.

Patel PD, Pontrello C, Burke S (2004) Robust and tissue-specific expression of TPH2 versus TPH1 in rat raphe and pineal gland. Biol Psychiatry 55:428–433.

Pellow S, Chopin P, File SE, Briley M (1985) Validation of open : closed arm entries in an elevated plus-maze as a measure of anxiety in the rat. J Neurosci Methods 14:149–167.

Petit J-M, Luppi P-H, Peyron C, Rampon C, Jouvet M (1995) VIP-like immunoreactive projections from the dorsal raphe and caudal linear raphe nuclei to the bed nucleus of the stria terminalis demonstrated by a double immunohistochemical method in the rat. Neurosci Lett 193:77–80.

Phelps EA, Delgado MR, Nearing KI, Ledoux JE (2004) Extinction learning in humans: Role of the amygdala and vmPFC. Neuron 43:897–905.

Phillips RG, LeDoux JE (1992) Differential contribution of amygdala and hippocampus to cued and contextual fear conditioning. Behav Neurosci 106:274–285.

Phillips R, LeDoux J (1992) Differential contribution of amygdala and hippocampus to cued and contextual fear conditioning. Behav Neurosci 106:274–285.

Pitkänen A, Pikkarainen M, Nurminen N, Ylinen A (2000) Reciprocal connections between the amygdala and the hippocampal formation, perirhinal cortex, and postrhinal cortex in rat. A review. Ann N Y Acad Sci 911:369–391.

Pitkänen A, Savander V, LeDoux JE (1997) Organization of intra-amygdaloid circuitries in the rat: An emerging framework for understanding functions of the amygdala. Trends Neurosci 20:517–523.

Pluess M, Velders FP, Belsky J, van IJzendoorn MH, Bakermans-Kranenburg MJ, Jaddoe VW V, Hofman A, Arp PP, Verhulst FC, Tiemeier H (2011) Serotonin transporter polymorphism moderates effects of prenatal maternal anxiety on infant negative emotionality. Am J Psychiatry 69:520–525.

Pollak Dorocic I, Fürth D, Xuan Y, Johansson Y, Pozzi L, Silberberg G, Carlén M, Meletis K (2014) A Whole-Brain Atlas of Inputs to Serotonergic Neurons of the Dorsal and Median Raphe Nuclei. Neuron 83:663–678.

Popa D, Lena C, Alexandre C, Adrien J (2008) Lasting Syndrome of Depression Produced by Reduction in Serotonin Uptake during Postnatal Development: Evidence from Sleep, Stress, and Behavior. J Neurosci 28:3546–3554.

Portas CM, Bjorvatn B, Fagerland S, GrØnli J, Mundal V, SØrensen E, Ursin R (1998) On-line detection of extracellular levels of serotonin in dorsal raphe nucleus and frontal cortex over the sleep/wake cycle in the freely moving rat. Neuroscience 83:807–814.

Price JL, Amaral DG (1981) An autoradiographic study of the projections of the central nucleus of the monkey amygdala. J Neurosci 1:1242–1259.

Puig MV, Artigas F, Celada P (2005) Modulation of the activity of pyramidal neurons in rat prefrontal cortex by raphe stimulation in vivo: Involvement of serotonin and GABA. Cereb Cortex 15:1–14.

Rainnie DG (1999) Serotonergic modulation of neurotransmission in the rat basolateral amygdala. J Neurophysiol 82:69–85.

Rainnie DG, Mania I, Mascagni F, McDonald AJ (2006) Physiological and Morphological Characterization of Parvalbumin- Containing Interneurons of the Rat Basolateral Amygdala. J Comp Neurol 498:142–161.

Rajasethupathy P, Sankaran S, Marshel JH, Kim CK, Ferenczi E, Lee SY, Berndt A, Ramakrishnan C, Jaffe A, Lo M, Liston C, Deisseroth K (2015) Projections from neocortex mediate top-down control of memory retrieval. Nature 526:653–659.

Rauch SL, Whalen PJ, Shin LM, McInerney SC, Macklin ML, Lasko NB, Orr SP, Pitman RK (2000) Exaggerated amygdala response to masked facial stimuli in posttraumatic stress disorder: a functional MRI study. Biol Psychiatry 47:769–776.

Rebello TJ, Yu Q, Goodfellow NM, Caffrey Cagliostro MK, Teissier A, Morelli E, Demireva EY, Chemiakine A, Rosoklija GB, Dwork AJ, Lambe EK, Gingrich JA, Ansorge MS (2014) Postnatal day 2 to 11 constitutes a 5-HT-sensitive period impacting adult mPFC function. J Neurosci 34:12379–12393.

Ribas VR, Aniceto HKR, Martins HADL, Ribas KH dos S, Guerra-Ribas RDM, Fraga SDN, Ribeiro-Ribas V, Vasconcelos CMM, Viana MT, Manhaes-de-Castro R (2008) Neonatal administration of fluoxetine did not alter the anxiety indicators, but decreased the locomotor activity in adult rats in the elevated plus-maze. Arq Neuropsiquiatr 66:844–847.

Richmond MA, Murphy CA, Pouzet B, Schmid P, Rawlins JNP, Feldon J (1998) A computer controlled analysis of freezing behaviour. J Neurosci Methods 86:91–99.

Risch N, Herrell R, Lehner T, Liang K-Y, Eaves L, Hoh J, Griem A, Kovacs M, Ott J, Merikangas KR (2009) Interaction between the serotonin transporter gene (5-HTTLPR), stressful life events, and risk of depression: a meta-analysis. JAMA 301:2462–2471.

Rogan MT, Stäubli U V, LeDoux JE (1997) Fear conditioning induces associative long-term potentiation in the amygdala. Nature 390:604–607.

Roiser JP, Müller U, Clark L, Sahakian BJ (2007) The effects of acute tryptophan depletion and serotonin transporter polymorphism on emotional processing in memory and attention. Int J Neuropsychopharmacol 10:449.

Royer S, Martina M, Paré D (1999) An inhibitory interface gates impulse traffic between the input and output stations of the amygdala. J Neurosci 19:10575–10583.

Royer S, Zemelman BV, Barbic M, Losonczy A, Buzsáki G, Magee JC (2010) Multi-array silicon probes with integrated optical fibers: light-assisted perturbation and recording of local neural circuits in the behaving animal. Eur J Neurosci 31:2279–2291.

Ruiz Martinez RC, Oliveira AR, Brandão ML (2007) Serotonergic mechanisms in the basolateral amygdala differentially regulate the conditioned and unconditioned fear organized in the periaqueductal gray. Eur Neuropsychopharmacol 17:717–724.

Sah P, Faber ES, Lopez DA, Power J (2003) The amygdaloid complex: anatomy and physiology. Physiol Rev 83:803–834.

Sakai K (2011) Sleep-waking discharge profiles of dorsal raphe nucleus neurons in mice. Neuroscience 197:200–224.

Sarkar A, Chachra P, Vaidya VA (2014) Postnatal fluoxetine-evoked anxiety is prevented by concomitant 5-HT2A/C receptor blockade and mimicked by postnatal 5-HT2A/C receptor stimulation. Biol Psychiatry 76:858–868.

Schäfer MKH, Varoqui H, Defamie N, Weihe E, Erickson JD (2002) Molecular cloning and functional identification of mouse vesicular glutamate transporter 3 and its expression in subsets of novel excitatory neurons. J Biol Chem 277:50734–50748.

Schipper P, Nonkes LJP, Karel P, Kiliaan AJ, Homberg JR (2011) Serotonin transporter genotype x construction stress interaction in rats. Behav Brain Res 223:169–175.

Schweimer JV, Ungless MA (2010) Phasic responses in dorsal raphe serotonin neurons to noxious stimuli. Neuroscience 171:1209–1215.

Seal RP, Akil O, Yi E, Weber CM, Grant L, Yoo J, Clause A, Kandler K, Noebels JL, Glowatzki E, Lustig LR, Edwards RH (2008) Sensorineural Deafness and Seizures in Mice Lacking Vesicular Glutamate Transporter 3. Neuron 57:263–275.

Seidenbecher T, Laxmi TR, Stork O, Pape HC (2003) Amygdalar and Hippocampal Theta Rhythm Synchronization During Fear Memory Retrieval. Science 301:846–850.

Senn V, Wolff SBE, Herry C, Grenier F, Ehrlich I, Gründemann J, Fadok JP, Müller C, Letzkus JJ, Lüthi A (2014) Long-range connectivity defines behavioral specificity of amygdala neurons. Neuron 81:428–437.

Seo D, Carillo MA, Chih-Hsiung Lim S, Tanaka KF, Drew MR (2015) Adult Hippocampal Neurogenesis Modulates Fear Learning through Associative and Nonassociative Mechanisms. J Neurosci 35:11330–11345.

Serretti A, Benedetti F, Zanardi R, Smeraldi E (2005) The influence of Serotonin Transporter Promoter Polymorphism (SERTPR) and other polymorphisms of the serotonin pathway on the efficacy of antidepressant treatments. Prog Neuro-Psychopharmacology Biol Psychiatry 29:1074–1084.

Shan L, Schipper P, Nonkes LJP, Homberg JR (2014) Impaired fear extinction as displayed by serotonin transporter knockout rats housed in open cages is disrupted by IVC cage housing. PLoS One 9:5–9.

Shephard RA, Broadhurst PL (1982) Effects of diazepam and picrotoxin on hyponeophagia in rats. Neuropharmacology 21:771–773.

Shin LM, Wright CI, Cannistraro PA, Wedig MM, McMullin K, Martis B, Macklin ML, Lasko NB, Cavanagh SR, Krangel TS, Orr SP, Pitman RK, Whalen PJ, Rauch SL (2005) A Functional Magnetic Resonance Imaging Study of Amygdala and Medial Prefrontal Cortex Responses to Overtly Presented Fearful Faces in Posttraumatic Stress Disorder. Arch Gen Psychiatry 62:273.

Shin LM, Orr SP, Carson MA, Rauch SL, Macklin ML, Lasko NB, Peters PM, Metzger LJ, Dougherty DD (2014) Regional Cerebral Blood Flow in the Amygdala and Medial Prefrontal Cortex During Traumatic Imagery in Male and Female Vietnam Veterans With PTSD. 61.

Shutoh F, Ina A, Yoshida S, Konno J, Hisano S (2008) Two distinct subtypes of serotonergic fibers classified by co-expression with vesicular glutamate transporter 3 in rat forebrain. Neurosci Lett 432:132–136.

Sierra-Mercado D, Padilla-Coreano N, Quirk GJ (2011) Dissociable Roles of Prelimbic and Infralimbic Cortices, Ventral Hippocampus, and Basolateral Amygdala in the Expression and Extinction of Conditioned Fear. Neuropsychopharmacology 36:529–538.

Sigurdsson T, Doyère V, Cain CK, LeDoux JE (2007) Long-term potentiation in the amygdala: A cellular mechanism of fear learning and memory. Neuropharmacology 52:215–227.

Smith GS, Lotrich FE, Malhotra AK, Lee AT, Ma Y, Kramer E, Gregersen PK, Eidelberg D, Pollock BG (2004) Effects of serotonin transporter promoter polymorphisms on serotonin function. Neuropsychopharmacology 29:2226–2234.

Smith Y, Paré D (1994) Intra-amygdaloid projections of the lateral nucleus in the cat: PHA-L anterograde labeling combined with postembedding GABA and glutamate immunocytochemistry. J Comp Neurol 342:232–248.

Smit-Rigter LA, Noorlander CW, von Oerthel L, Chameau P, Smidt MP, van Hooft JA (2012) Prenatal fluoxetine exposure induces life-long serotonin 5-HT3 receptor-dependent cortical abnormalities and anxiety-like behaviour. Neuropharmacology 62:865–870.

Smits BMG, Mudde JB, van de Belt J, Verheul M, Olivier J, Homberg J, Guryev V, Cools AR, Ellenbroek BA, Plasterk RHA, Cuppen E (2006) Generation of gene knockouts and mutant models in the laboratory rat by ENU-driven target-selected mutagenesis. Pharmacogenet Genomics 16:159–169.

Soiza-Reilly M, Commons KG (2011) Glutamatergic drive of the dorsal raphe nucleus. J Chem Neuroanat 41:247–255.

Soiza-Reilly M, Goodfellow NM, Lambe EK, Commons KG (2015) Enhanced 5-HT1A receptor-dependent feedback control over dorsal raphe serotonin neurons in the SERT knockout mouse. Neuropharmacology 89:185–192.

Sosulina L, Meis S, Seifert G, Steinhäuser C, Pape HC (2006) Classification of projection neurons and interneurons in the rat lateral amygdala based upon cluster analysis. Mol Cell Neurosci 33:57–67.

Sotres-Bayon F, Sierra-Mercado D, Pardilla-Delgado E, Quirk GJ (2012) Gating of Fear in Prelimbic Cortex by Hippocampal and Amygdala Inputs. Neuron 76:804–812.

Spannuth BM, Hale MW, Evans AK, Lukkes JL, Campeau S, Lowry CA (2011) Investigation of a central nucleus of the amygdala/dorsal raphe nucleus serotonergic circuit implicated in fear-potentiated startle. Neuroscience 179:104–119.

Spiacci A, Coimbra NC, Zangrossi H (2012) Differential involvement of dorsal raphe subnuclei in the regulation of anxiety- and panic-related defensive behaviors. Neuroscience 227:350–360.

Stamp JA, Semba K (1995) Extent of colocalization of serotonin and GABA in the neurons of the rat raphe nuclei. Brain Res 677:39–49.

Steinbusch HWM, Verhofstad AAJ, Joosten HWJ (1978) Localization of serotonin in the central nervous system by innunohistochemistry: description of a specific and sensitive technique and some applications. Neurosci78; 3:811-819 3:811–819.

Steinbusch HWM, Nieuwenhuys R (1983) The raphe nuclei of the rat brainstem: a cytoarchitectonic and immunohistochemical study. Chem Neuroanat:131–207.

Steinbusch H (1981) Distribution of serotonin-immunoreactivity in the central nervous system of the rat—Cell bodies and terminals. Neuroscience 6:557–618.

Stutzmann GE, LeDoux JE (1999) GABAergic antagonists block the inhibitory effects of serotonin in the lateral amygdala: a mechanism for modulation of sensory inputs related to fear conditioning. J Neurosci 19:RC8.

Sun N, Cassell MD (1993) Intrinsic GABAergic neurons in the rat central extended amygdala. J Comp Neurol 330:381–404.

Sur C, Betz H, Schloss P (1996) Immunocytochemical detection of the serotonin transporter in rat brain. Neuroscience 73:217–231.

Sylvers P, Lilienfeld SO, LaPrairie JL (2011) Differences between trait fear and trait anxiety: Implications for psychopathology. Clin Psychol Rev 31:122–137.

Takase LF, Nogueira MI, Baratta M, Bland ST, Watkins LR, Maier SF, Fornal CA, Jacobs BL (2004) Inescapable shock activates serotonergic neurons in all raphe nuclei of rat. Behav Brain Res 153:233–239.

Tamir H, Gershon MD (1990) Serotonin-storing secretory vesicles. Ann N Y Acad Sci 600:53–66.

Teissier A, Soiza-Reilly M, Gaspar P (2017) Refining the Role of 5-HT in Postnatal Development of Brain Circuits. Front Cell Neurosci 11:1–9.

Thakker DR, Natt F, Hüsken D, van der Putten H, Maier R, Hoyer D, Cryan JF (2005) siRNA-mediated knockdown of the serotonin transporter in the adult mouse brain. Mol Psychiatry 10:782–789.

Törk I (1990) Anatomy of the serotonergic system. Ann N Y Acad Sci 600:9-34-5.

Torres GE, Amara SG (2007) Glutamate and monoamine transporters: new visions of form and function. Curr Opin Neurobiol 17:304–312.

Torres GE, Gainetdinov RR, Caron MG (2003) Plasma membrane monoamine transporters: structure, regulation and function. Nat Rev Neurosci 4:13–25.

Tran L, Lasher BK, Young K a, Keele NB (2013) Depletion of serotonin in the basolateral amygdala elevates glutamate receptors and facilitates fear-potentiated startle. Transl Psychiatry 3:e298.

Tritsch NX, Granger AJ, Sabatini BL (2016) Mechanisms and functions of GABA co-release. Nat Rev Neurosci 17:139–145.

Trudeau LÉ (2004) Glutamate co-transmission as an emerging concept in monoamine neuron function. J Psychiatry Neurosci 29:296–310.

Tully K, Li Y, Tsvetkov E, Bolshakov VY (2007) Norepinephrine enables the induction of associative long-term potentiation at thalamo-amygdala synapses. Proc Natl Acad Sci 104:14146–14150.

Turner BH, Herkenham M (1991) Thalamoamygdaloid projections in the rat: A test of the amygdala's role in sensory processing. J Comp Neurol 313:295–325.

Tye KM, Prakash R, Kim S-Y, Fenno LE, Grosenick L, Zarabi H, Thompson KR, Gradinaru V, Ramakrishnan C, Deisseroth K (2011) Amygdala circuitry mediating reversible and bidirectional control of anxiety. Nature 471:358–362.

Uher R, Caspi A, Houts R, Sugden K, Williams B, Poulton R, Moffitt TE (2011) Serotonin transporter gene moderates childhood maltreatment's effects on persistent but not single-episode depression: Replications and implications for resolving inconsistent results. J Affect Disord 135:56–65.

Uhlhaas PJ, Singer W (2006) Neural Synchrony in Brain Disorders: Relevance for Cognitive Dysfunctions and Pathophysiology. Neuron 52:155–168.

Unal CT, Paré D, Záborszky L (2015) Impact of Basal Forebrain Cholinergic Inputs on Basolateral Amygdala Neurons. J Neurosci 35:853–863.

Vaaga CE, Borisovska M, Westbrook GL (2014) Dual-transmitter neurons: Functional implications of co-release and co-transmission. Curr Opin Neurobiol 29:25–32.

van der Doelen RHA, Calabrese F, Guidotti G, Geenen B, Riva MA, Kozicz T, Homberg JR (2014) Early life stress and serotonin transporter gene variation interact to affect the transcription of the glucocorticoid and mineralocorticoid receptors, and the co-chaperone FKBP5, in the adult rat brain. Front Behav Neurosci 8:1–11.

Varga V, Losonczy A, Zemelman B V, Borhegyi Z, Nyiri G, Domonkos A, Hangya B, Holderith N, Magee JC, Freund TF (2009) Fast synaptic subcortical control of hippocampal circuits. Science 326:449–453.

Vasa RA, Carlino AR, Pine DS (2006) Pharmacotherapy of Depressed Children and Adolescents: Current Issues and Potential Directions. Biol Psychiatry 59:1021–1028.

Vasudeva RK, Lin RCS, Simpson KL, Waterhouse BD (2011) Functional organization of the dorsal raphe efferent system with special consideration of nitrergic cell groups. J Chem Neuroanat 41:281–293.

Veasey SC, Fornal CA, Metzler CW, Jacobs BL (1995) Response of serotonergic caudal raphe neurons in relation to specific motor activities in freely moving cats. J Neurosci 15:5346–5359.

Ventura A, Meissner A, Dillon CP, McManus M, Sharp PA, Van Parijs L, Jaenisch R, Jacks T (2004) Cre-lox-regulated conditional RNA interference from transgenes. Proc Natl Acad Sci 101:10380–10385.

Vidal-Gonzalez I, Vidal-Gonzalez B, Rauch SL, Quirk GJ (2006) Microstimulation reveals opposing influences of prelimbic and infralimbic cortex on the expression of conditioned fear. Learn Mem 13:728–733.

Vigneault É, Poirel O, Riad M, Prud'homme J, Dumas S, Turecki G, Fasano C, Mechawar N, Mestikawy S El (2015) Distribution of vesicular glutamate transporters in the human brain. Front Neuroanat 9:23.

Vlachos I, Herry C, Lüthi A, Aertsen A, Kumar A (2011) Context-dependent encoding of fear and extinction memories in a large-scale network model of the basal amygdala. PLoS Comput Biol 7:e1001104.

Voisin AN, Mnie-Filali O, Giguère N, Fortin GM, Vigneault E, El Mestikawy S, Descarries L, Trudeau L-É (2016) Axonal Segregation and Role of the Vesicular Glutamate Transporter VGLUT3 in Serotonin Neurons. Front Neuroanat 10:1–17.

Weissbourd B, Ren J, DeLoach KE, Guenthner CJ, Miyamichi K, Luo L (2014) Presynaptic Partners of Dorsal Raphe Serotonergic and GABAergic Neurons. Neuron 83:645–662.

Zhong W, Li Y, Feng Q, Luo M (2017) Learning and Stress Shape the Reward Response Patterns of Serotonin Neurons. J Neurosci 37:8863–8875.

Wellman CL, Izquierdo A, Garrett JE, Martin KP, Carroll J, Millstein R, Lesch K-P, Murphy DL, Holmes A (2007) Impaired Stress-Coping and Fear Extinction and Abnormal Corticolimbic Morphology in Serotonin Transporter Knock-Out Mice. J Neurosci 27:684–691.

West MJ (1999) Stereological methods for estimating the total number of neurons and synapses: Issues of precision and bias. Trends Neurosci 22:51–61.

Wiegert JS, Mahn M, Prigge M, Printz Y, Yizhar O (2017) Silencing Neurons: Tools, Applications, and Experimental Constraints. Neuron 95:504–529.

Wiklund L, Léger L, Persson M (1981) Monoamine cell distribution in the cat brain. A fluorescence histochemical study with quantification of indolamine and locus coeruleus cell groups. J Comp Neur 203:613–647.

Wilensky AE, Schafe GE, Kristensen MP, LeDoux JE (2006) Rethinking the Fear Circuit: The Central Nucleus of the Amygdala Is Required for the Acquisition, Consolidation, and Expression of Pavlovian Fear Conditioning. J Neurosci 26:12387–12396.

Wolff SBE, Gründemann J, Tovote P, Krabbe S, Jacobson GA, Müller C, Herry C, Ehrlich I, Friedrich RW, Letzkus JJ, Lüthi A (2014) Amygdala interneuron subtypes control fear learning through disinhibition. Nature 509:453–458.

Yamakawa GR, Antle MC (2010) Phenotype and function of raphe projections to the suprachiasmatic nucleus. Eur J Neurosci 31:1974–1983.

Yamamoto R, Ueta Y, Sugai T, Kato N (2012) A serotonergic discrimination favoring synaptic inputs that accompany robust spike firing in lateral amygdala neurons. Neuroscience 220:119–130.

Yamamoto R, Hatano N, Sugai T, Kato N (2014) Serotonin induces depolarization in lateral amygdala neurons by activation of TRPC-like current and inhibition of GIRK current depending on 5-HT 2C receptor. Neuropharmacology 82:49–58.

Yamauchi M, Miyara T, Matsushima T, Imanishi T (2006) Desensitization of 5-HT2A receptor function by chronic administration of selective serotonin reuptake inhibitors. Brain Res 1067:164–169.

Yamauchi M, Tatebayashi T, Nagase K, Kojima M, Imanishi T (2004) Chronic treatment with fluvoxamine desensitizes 5-HT2C receptor-mediated hypolocomotion in rats. Pharmacol Biochem Behav 78:683–689.

Yang RJ, Mozhui K, Karlsson R-M, Cameron HA, Williams RW, Holmes A (2008) Variation in mouse basolateral amygdala volume is associated with differences in stress reactivity and fear learning. Neuropsychopharmacology 33:2595–2604.

Yokoyama M, Suzuki E, Sato T, Maruta S, Watanabe S, Miyaoka H (2005) Amygdalic levels of dopamine and serotonin rise upon exposure to conditioned fear stress without elevation of glutamate. Neurosci Lett 379:37–41.

Zanoveli JM, Carvalho MC, Cunha JM, Brandão ML (2009) Extracellular serotonin level in the basolateral nucleus of the amygdala and dorsal periaqueductal gray under unconditioned and conditioned fear states: An in vivo microdialysis study. Brain Res 1294:106–115.

Zhao S, Edwards J, Carroll J, Wiedholz L, Millstein RA, Jaing C, Murphy DL, Lanthorn TH, Holmes A (2006) Insertion mutation at the C-terminus of the serotonin transporter disrupts brain serotonin function and emotion-related behaviors in mice. Neuroscience 140:321–334.

Zhuang X, Masson J, Gingrich JA, Rayport S, Hen R (2005) Targeted gene expression in dopamine and serotonin neurons of the mouse brain. J Neurosci Methods 143:27–32.